

Interactive comment on “Numerical experiments on isotopic diffusion in polar snow and firn using a multi-layer energy balance model” by Alexandra Touzeau et al. A. Kerkweg kerkweg@uni-bonn.de Received and published: 7 November 2017

Dear authors, In my role as Executive editor of GMD, I would like to bring to your attention our Editorial version 1.1: <http://www.geosci-model-dev.net/8/3487/2015/gmd-8-3487-2015.html> This highlights some requirements of papers published in GMD, which is also available on the GMD website in the ‘Manuscript Types’ section: http://www.geoscientific-model-development.net/submission/manuscript_types.html.

In particular, please note that for your paper, the following requirements have not been met in the Discussions paper:

- "The main paper must give the model name and version number (or other unique identifier) in the title."

- "If the model development relates to a single model then the model name and the version number must be included in the title of the paper. If the main intention of an article is to make a general (i.e. model independent) statement about the usefulness of a new development, but the usefulness is shown with the help of one specific model, the model name and version number must be stated in the title. The title could have a form such as, "Title outlining amazing generic advance: a case study with Model XXX (version Y)".

- "All papers must include a section, at the end of the paper, entitled 'Code availability'. Here, either instructions for obtaining the code, or the reasons why the code is not available should be clearly stated. It is preferred for the code to be uploaded as a supplement or to be made available at a data repository with an associated DOI (digital object identifier) for the exact model version described in the paper. Alternatively, for established models, there may be an existing means of accessing the code through a particular system. In this case, there must exist a means of permanently accessing the precise model version described in the paper. In some cases, authors may prefer to put models on their own website, or to act as a point of contact for obtaining the code. Given the impermanence of websites and email addresses, this is not encouraged, and authors should consider improving the availability with a more permanent arrangement. After the paper is accepted the model archive should be updated to include a link to the GMD paper."

Thus please add the models name (SURFEX/Crocus ?) and the version number to the title of your article. Additionally, it would be good if the explicit version described in this article would be archived in a permanent archive providing a DOI (e.g. Zenodo). Yours, Astrid Kerkweg

We apologize for not including the model references in the article title. We will add the relevant information to the title:

1. 1: 'Numerical experiments on **vapor diffusion** in polar snow and firn and **its impact on isotopes** using **the multi-layer energy balance model Crocus in SURFEX V8.0**'

We will also update our code availability section. The model SURFEX is open-source and available online after free registration through the platform cnrm-game-meteo.fr. Therefore, it is not necessary to provide a copy on Zenodo.

We have updated the code availability section:

I. 768: 'The code used in the manuscript is a **development of the open source code for SURFEX/ISBA-Crocus model based on version V8.0, hosted on an open git repository at CNRM (https://opensource.umr-cnrm.fr/projects/surfex_git2)**. Before downloading the code, you must register as a user at <https://opensource.umr-cnrm.fr/>. You can then obtain the code used in the present study by downloading the revision tagged 'Touzeau_jan2018' of the branch touzeau_dev (last access: January 2018). The meteorological forcing required to perform the runs is available as a supplement.'

***** Interactive comment on Geosci. Model Dev. Discuss.,
<https://doi.org/10.5194/gmd-2017-217>, 2017.

Interactive comment on “Numerical experiments on isotopic diffusion in polar snow and firn using a multi-layer energy balance model” by Alexandra Touzeau et al. Anonymous Referee #1 Received and published: 30 November 2017

Touzeau et al. presents a detailed study in implementing isotopes into a semi-complex one-dimensional snow pack model. Unfortunately it is my opinion that the authors still need a little bit more work to allow this publication to become a significant contribution to the community. I am though positive that the manuscript will be publishable after my major comments have been taken into account.

Major comments:

(The following list of comments are not ordered in accordance with importance as they are more or less equally important)

- The use of parentheses throughout the manuscript is not in accordance with good practice. It makes reading the manuscript difficult. Please rewrite relevant sentences.

Most of the parentheses will be removed in the revised manuscript.

- The term ‘oriented vapor transport’ seems to complicate the reading. The model has already been defined as 1D and hence no need to include the word ‘oriented’. Please remove throughout paper.

We used the term ‘oriented vapor transport’ to stress that vapor diffusion was not only driven by isotope gradients but also by temperature gradients. Diffusion induced by temperature gradient do not lead to homogeneous repartition of isotopes in contrast to the diffusion along isotopic gradient and this was the reason why we chose the term “oriented”. We agree that this may not be obvious, and we have thus replaced ‘oriented vapor transport’ by ‘thermally induced vapor transport’ in the manuscript.

- ‘Vapor density gradients’. Please change to ‘vapor pressure gradients’ throughout the paper. The use of vapor pressure is the normal term used i.e Merlivat and Jouzel 1979 and Jouzel and Merlivat 1984 etc.

“Density” was indeed probably not the best term (see also reviewer 3 comments). Because the unit of this term is kg.m^{-3} , we have chosen to use the term “concentration” as suggested by reviewer 3.

- If a sentence is longer than 2 lines, it is most likely too long. Please refrain from using extremely long sentence that complicates the understanding of the manuscript. This is seen at several instances through out the manuscript, but my favorite example is section 2.1 L106-109 where I really have no idea what is being described.

We have rephrased the introduction of Section 2.1. using shorter sentences.

l. 117-121: **'Here we describe first processes leading only to attenuation of the original amplitude (Sect. 2.1.1.). Then we describe processes which lead to other types of signal modifications (Sect. 2.1.2.). These modifications include transporting and accumulating isotopes in some layers without consideration of the original isotopic signal. They also comprise processes taking isotopes away from the snow, and therefore shifting the mean $\delta^{18}\text{O}$ value of the snow deposited.'**

- Rephrase 'mean local pluriannual value' or describe what you mean.

Here we define 'mean local pluriannual value' as the average isotopic composition in the precipitation taken over several years (~10 years). This value averages seasonal variations and synoptic variations in the precipitation. It may be different from the average value in the snow layers that corresponds to the same period of time due to post-deposition processes.

- Rephrase 'oriented processes' or describe what you mean

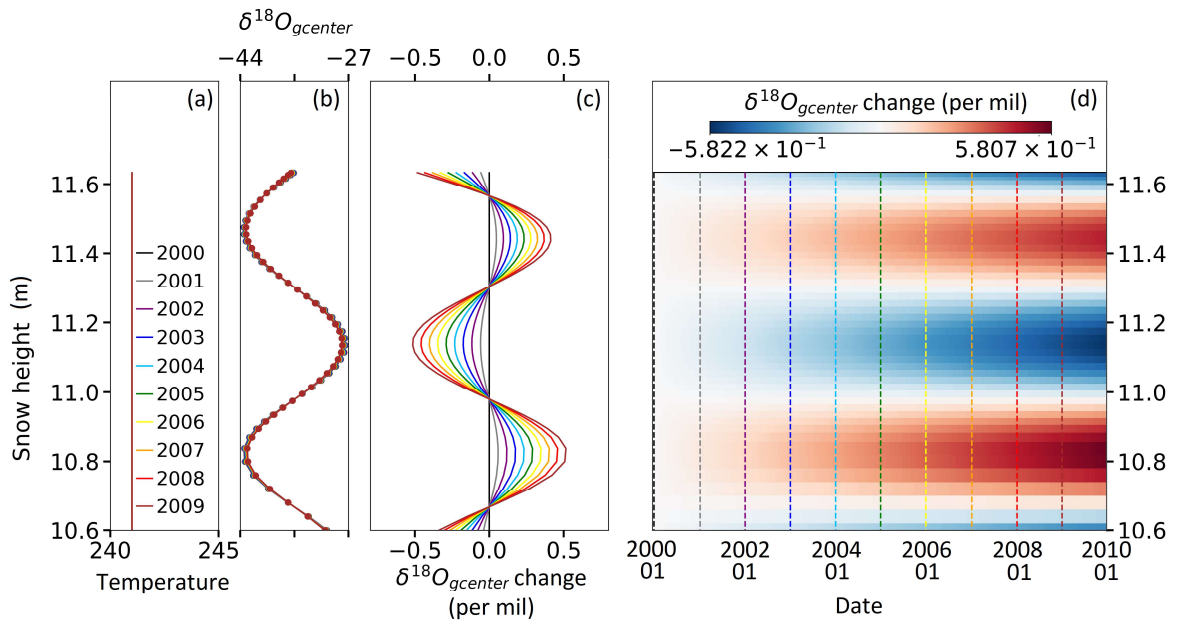
Here we mean dynamical processes of vapor transport that are forced by atmospheric pressure or temperature variations. We used the term 'oriented' in opposition to 'random', in the sense 'forced' or 'pushed' or 'driven'. Maybe we should have said instead 'orienting' processes, as it is the vapor molecules which get 'oriented', not the processes themselves.

We propose to keep the term 'oriented' for the water molecules themselves, and to replace 'oriented processes' by 'processes leading to oriented vapor transport'. We also add a line in the text to stress that 'oriented' is used in opposition to 'random agitation', and not in the sense of 'unidimensional' or 'vertical'.

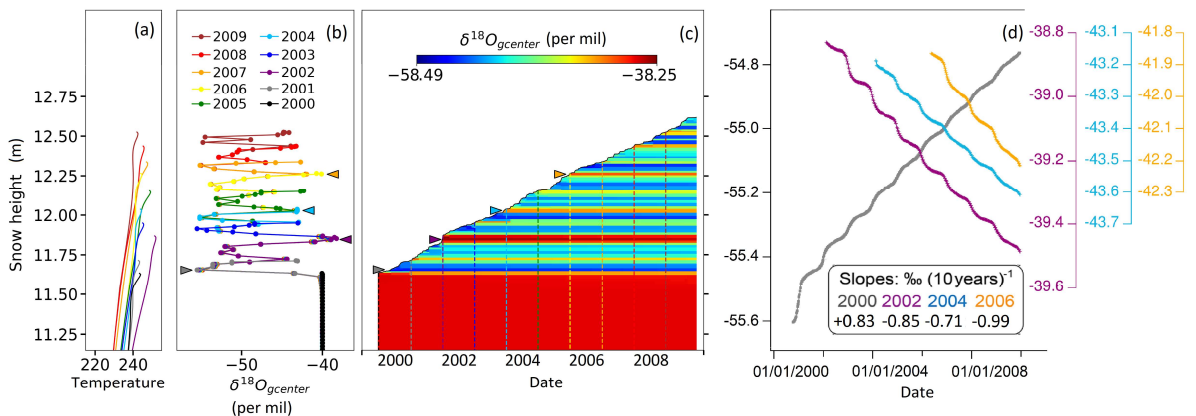
l. 142-143: **'We use the term 'oriented' here to describe an overall movement of water molecules that is different from their molecular agitation, and externally forced.'**

- In L113 you write "Indeed, higher temperatures correspond to higher vapor densities, and also higher diffusivities in the vapor and the solid phase". This is correct, but then you line 260 define the vapor diffusivity in air to be a constant despite that it is depending on both temperature and pressure. This needs to be corrected. You need to allow for a temperature and pressure dependence on the diffusivity.

The reviewer is perfectly right. We have run the two main simulations again with varying D_{v0} (function of atmospheric air pressure and snow temperature using the formula of Johnsen et al., 2000), and found some differences in the attenuation compared to the initial simulations. For the 10 years simulation at Dome C, the attenuation increases by 2-5%, and for the 10 years simulation at GRIP (with fixed temperature) it increases by 9-16%. Therefore, we will replace the corresponding figures in the manuscript by the new ones and modify the values of attenuation given in the text.



New Figure 2. Simulation 1: 10 years at GRIP with fixed temperature (240 K), with D_{v0} function of the temperature.



New Figure 11: Simulation 6: 10 years at Dome C with precipitation with varying $\delta^{18}\text{O}$; with temperature evolution throughout the year; with D_{v0} function of temperature.

- I have a problem with your first sentence in the introduction “Ice is a key archive for past climate reconstruction, which preserves . . . indications relevant to the temperature of formation of the snow precipitation. . . variations of the isotopic ratio of oxygen and deuterium”. This sentence is problematic because you have co-authors who have published papers documenting in both Greenland and Antarctica how the isotopic composition of the deposited precipitation is changed through exchange with the atmospheric water vapor isotopes. You cite 8 publications to document your statement, but they are between 10 and 30 years old. You thereby disregard published research for the last five years. Please update.

We do not see a contradiction here, as a climatic signal may persist even after post-deposition

processes have occurred. Therefore, information regarding temperature may still be present, even if exchange with vapor isotope has taken place. Nevertheless, we will update the bibliography and soften these statements.

I. 28: 'The isotopic ratios of oxygen or deuterium measured in ice cores have been used for a long time to reconstruct the evolution of temperature over the Quaternary (EPICA comm. members, 2004; Johnsen et al., 1995; Jones et al., 2018; Jouzel et al., 2007; Kawamura et al., 2007; Lorius et al., 1985; Petit et al., 1999; Schneider et al., 2006; Stenni et al., 2004; Stenni et al., 2011; Uemura et al., 2012; WAIS-Divide members, 2013). They are however subject to alteration during post-deposition through various processes. As a consequence, even if the link between temperature and isotopic composition of the precipitations is quantitatively determined from measurements and modelling studies (Stenni et al., 2016; Goursaud et al., TCD, 2017), it cannot faithfully be applied to reconstruction of past temperature.'

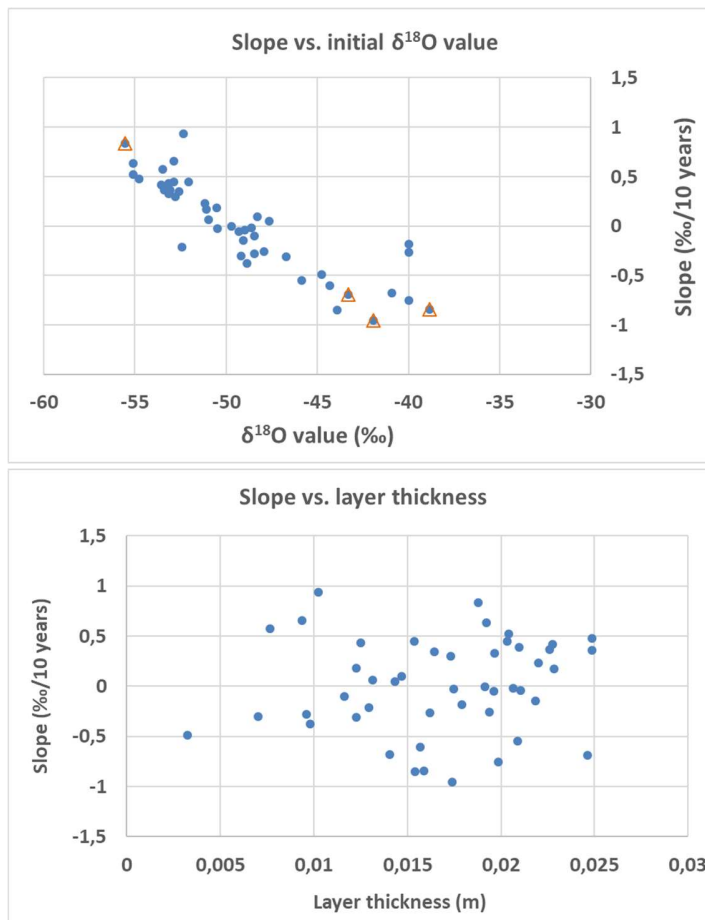
- In L 17: Why not study the influence of temperature and not only temperature gradients? What is the difference between "compaction" and "Wind compaction"? Do you study the effect of amount of precipitation or the isotopes of the precipitation?

- Physically, higher temperatures lead to increased diffusion through increased molecular agitation and also through increased vapor content in the air. In the first case, the control is a power function, while in the second case the control is exponential. Thus, we considered in a first approximation that molecular agitation was of second order and could be neglected. Still, in this new version, we will also consider the direct influence of temperature since the dependency of diffusivity on temperature is added.

- There are two possible types of compaction implemented in the model (see Vionnet et al., 2012, for more details):

- 1) Compaction caused by the weight of overlying layers ("compaction"),
- 2) Compaction caused by wind reworking of the snow, which leads to increased density in the top layers (« wind compaction »).

- We did not study specifically the effect of precipitation amount, as we used only one set of precipitation data coming from ERA-Interim. We did not vary this parameter to see how diffusion would be modified but it would be easy for future users to make such a study with the available code. Still, over the course of 10 years, variability of the precipitation amounts did occur. We followed 48 layers which were maintained for one year at least, and up to 10 years. For these layers, the thickness was ranging from 3 mm to 2.5 cm, and the slope was ranging from -0.137 to +0.133 ‰/10 years. Based on these layers, the slope does not seem to be related to the layer thickness. However, it appears that the slope is related to the original $\delta^{18}\text{O}$ value in the layer.



- Regarding the isotopic composition in the precipitation we have run a zero-simulation with constant $\delta^{18}\text{O}$ in the precipitation. We wanted to see how vapor transport could possibly generate $\delta^{18}\text{O}$ variations, based on temperature gradients, in the absence of initial signal (Figure 6 and Figure 8). For the first layer, the $\delta^{18}\text{O}$ changes by about 1‰ in one year, whereas for the deeper layers, the change is about 0.1‰ during the same period. We then used the air temperature to compute $\delta^{18}\text{O}$ variations in the precipitation, to evaluate attenuation based on a realistic $\delta^{18}\text{O}$ signal (Figure 10 and Figure 11).

- L 52: Use another word than “Mechanical shuffling”

We replaced this term by “mechanical reworking”.

- L119: You write that the annual cycles generally disappear at sites with accumulation lower than 200 kg/m²/year – but does that not depend on time scales – please be more precise.

It is true that thinning will also have an effect on the disappearance of annual cycles at deep depths. We will thus modify the statement saying that annual cycles disappeared at shallower depths (100 m deep) for sites with accumulation lower than 200 kg/m²/year.

I. 135: ‘In Greenland, Johnsen et al. (1977) indicate that annual cycles generally disappear at depths shallower than 100 m for sites with accumulation lower than 200 kg m⁻² yr⁻¹.’

- L120: You write that the diffusion is more intense in the upper layers – but don't the diffusion depend on the isotopic gradient and would you not expect that to be larger further down in the snow? Please be precise! Also the word 'intense' might not be the best to use in this case

Indeed, theoretically, if diffusion was initially very low, and no other processes were active, the effect of compaction could increase $\delta^{18}\text{O}$ gradients downward by reducing layer thicknesses. In that case, the diffusion based on isotopic gradients would indeed increase downward. Our model is indeed able to study such effect. It may be the purpose of a future application through a much longer run of the model than those presented here.

Our aim here was to take the diffusion effect from the beginning, i.e. from the upper layer where porosity is large and temperature gradient huge hence enabling a strong diffusion. This will be clearly written in the revised version since it was not clear enough here.

I. 136: 'Diffusion **along** isotopic gradients exists throughout the entire snow/ice column. It occurs **mainly in the vapor phase in the firn, especially in the upper layers with larger porosities. After pore closure, it takes place mostly in the solid phase, at a much slower rate.**'

- Section 3.1.2: Describe why the new vapor transport subroutine is inserted after module 5 but before module 6? What are the thoughts behind this?

The steps of the model first describe changes in the snow structure and microstructure (new layers, densification, metamorphism, wind drift) and later the energy exchanges. Because vapor diffusion is closely associated with metamorphism, and lead to changes in the layer density, it seems natural to put it within this first series of modules that describe snow structure. Furthermore, its effect on the temperature profile is probably limited.

- L251: "... is the effective diffusivity of water vapor in the snow at the interface". Do you mean effective diffusivity of water vapor in the air between the snow grains?

There is a first step where we indeed compute "effective diffusivity" for each layer (from diffusivity in air and taking into account the size of the porosity, Equation (5)).

$$\frac{D_{eff}(t,n)}{D_v} = \frac{3}{2} \left(1 - \frac{\rho_{sn}(t,n)}{\rho_{ice}} \right) - \frac{1}{2} \quad (5)$$

Then, what we name "interfacial diffusivity" ($D_{eff}(t,n \rightarrow n+1)$) is the average of two "effective diffusivities" from two adjacent layers ($D_{eff}(t,n)$ and $D_{eff}(t,n+1)$, Equation (6)). The "interface" here is the limit between the two layers.

$$D_{eff}(t, n \rightarrow n + 1) = \frac{1}{\frac{1}{D_{eff}(t,n)} + \frac{1}{D_{eff}(t,n+1)}} \quad (6)$$

This explanation is already present in the text.

I. 270: "flux of vapor at the interface between two layers"

I. 277: "The effective diffusivity at the interface is obtained in two steps: first the effective diffusivities ($D_{eff}(t,n)$ and $D_{eff}(t,n+1)$) in each layer are calculated (Eq. (5)), second, the interfacial diffusivity is computed as their harmonic mean (Eq. (6)). "

To facilitate reading, we will add an indication line 270:

l. 269: **'In this section, the term 'interface' is used for the horizontal surface of exchange between two consecutive layers.'**

- Equation 6: I am not sure, but isn't a layer thickness missing from this formula as you might not have the same layer thickness in layer n and n+1?

Assessing interfacial effective transport properties in the case where layer thicknesses are different is a classical, yet, critical issue (e. g. D'Amboise et al., 2017 GMD), especially if the contrast in layer thickness is too large. Here we ensure that the contrast in layer thickness remains as small as possible to limit the impact of this effect, and under such a situation we make the simplifying assumption that the interfacial diffusivity depends equally on the values of the two layers concerned.

- Equation 7: Why do you use an analytical approximation of Clausius-Clapeyron around zero and not a more precise empirical formula?

We are not aware that this formulation would provide worse results than empirical formulae.

- L 313 : "Long time" – what do you mean – please be precise

Original text:

'Equilibrium fractionation is a hypothesis that is correct in layers where the air has been standing still for a long time in the porosity and where vapor has reached equilibrium with ice grains, physically and chemically.'

We implied here that the equilibrium fractionation hypothesis was a reasonable hypothesis in our case. Indeed, the equilibrium situation is limited by the water vapor - snow mass transfer whose associated speed is of the order of 0.09 m.s^{-1} (Albert and McGilvary, 1992). In our case, we are dealing with centimetric scale layers thickness and recalculate the isotopic composition every second so that we consider that the speed of the mass transfer is not limiting the equilibrium situation at the water vapor - snow interface.

We have thus reformulated the text accordingly:

l. 336: 'Equilibrium fractionation is a hypothesis that is correct in layers where vapor has reached equilibrium with ice grains, physically and chemically. This process is limited by the water vapor - snow mass transfer whose associated speed is of the order of 0.09 m.s^{-1} (Albert and McGilvary, 1992). In our case, we are dealing with centimetric scale layers thickness and recalculate the isotopic composition every second so that we consider that the speed of the mass transfer is not limiting the equilibrium situation at the water vapor - snow interface.'

- L334: What vapor are you referencing to? H₂O in general or H₂¹⁶O?

Here we refer to H₂O. We propose to add this precision in the text:

l. 3624: 'When the vapor concentration is the same in two adjacent layers, the total flux of vapor is null. But we still have isotopic diffusion because of the isotopic concentration gradients (Eq. (13)), as long as they are non-zero.'

- L335: I believe you meant to write "we will still have diffusion of heavy water isotopes during conditions where the water isotopic gradient is non-zero."

This is very close to our meaning yes. We forgot to mention that in that case, diffusion is driven by isotopic gradients, only if they themselves are non-zero. Thanks for this precision. However, both heavy and light isotopes will diffuse. Therefore, we propose this correction:

I. 363: “But we still have isotopic diffusion because of the isotopic concentration gradients (Eq. (13)), as long as they are non-zero.”

- L335-336: The sentence is very convoluted. I believe you could also have zero flux of H216O but a flux of H218O in one direction and HD16O in another direction.

We will remove this sentence, to simplify the reading.

- L353: “Here the condensation of excess vapor occurs without additional fractionation”. Why do you make this assumption? Whenever you have a phase change due to condensation you will have isotopic fractionation. I think this is something that needs to be updated in your code.

We take this fractionation into account **earlier** in the model. We define our interstitial vapor as being **at equilibrium** with the solid phase (all the time) due to permanent sublimation/condensation in the porosity. This is why we write “without any additional fractionation”. We do not want to apply this fractionation twice.

Kinetic fractionation due to supersaturation is also taken into account during the diffusion of the different isotopes, each with their associated diffusion coefficient.

Still, we understand that this aspect was not very clear in the initial manuscript and propose the following revision:

I.380: “Here the condensation of excess vapor occurs without additional fractionation **because (1) there is a permanent isotopic equilibrium between surface snow and interstitial vapor (each first step of the sub-routine) and (2) kinetic fractionation associated with diffusion is taken into account during diffusion of the different isotopic species along the isotopic gradients**”

- L356: “The transfer of isotopes takes place from the grain surface toward the vapor without fractionation” If you assume this then the interstitial vapor will not be in isotopic equilibrium with the snow surface. This would then correct itself. Hence I think that your code needs to be set-up such that the interstitial vapor is in isotopic equilibrium with the snow surface at all time.

Yes, temporarily, after this sublimation the vapor is no longer at equilibrium with the solid phase. But this is corrected immediately, as both are merged again before the next step (each step has a duration of one second). At the beginning of the next step, vapor isotopic composition is defined again at equilibrium with snow surface.

It is mathematically difficult to predict the composition of the sublimated vapor needed to have equilibrium in the end, and much easier to merge the two compartments and recreate later an equilibrium.

- Please note that you throughout the paper are mixing up GRIP and Summit. They are two different geographical places in Greenland albeit being close to each other.

We are sorry for this mixing, this will be corrected. Still, the climatic characteristics of these neighbour two sites are very similar so that this does not affect the results presented here.

- I am surprised to read that there are no density measurements for neither GRIP nor Summit and that you therefore use NGRIP. Please double-check this.

Indeed, GRIP density measurements are available as listed in Bréant et al. (2017) and reference therein (http://gcmd.nasa.gov/r/d/LSSU_PSU_Firn_data and Schwander et al., 1997; Lizuka et al., 2008). The density profile is close to the NGRIP profile. We ran the model with the correct density profile and found that the new profile did not change the results. Still, the new version will include the correct data.

- You do not give a relationship for the isotope-temperature relationship for GRIP. Please correct.

This is because the simulations at GRIP do not include precipitation, so the isotopic composition in the precipitation (and its relationship to temperature) is not useful here.

We have added a sentence in the text to clarify this point:

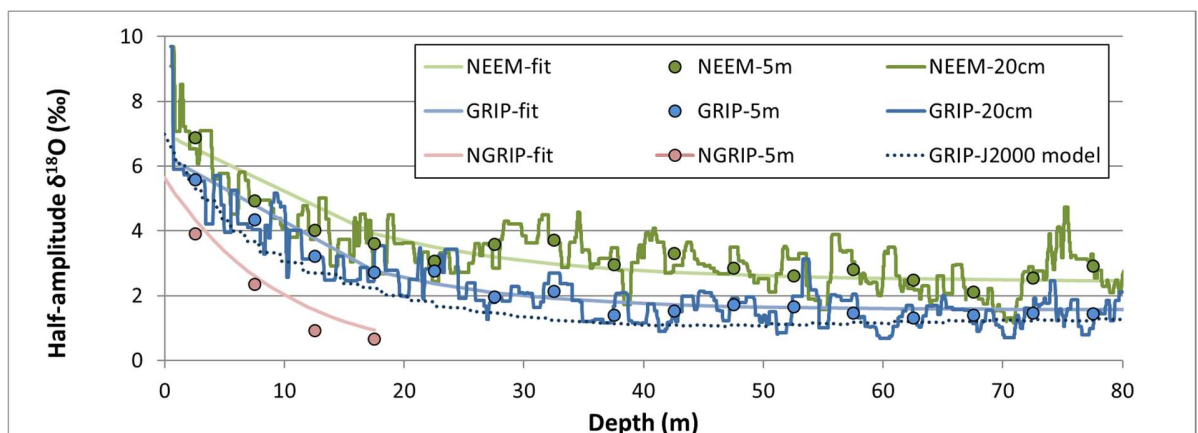
L. 481: "following Eq. (15) to link $\delta^{18}\text{O}$ in the snowfall to the local temperature (T_{air} , in K):

$$\delta^{18}\text{O}_{\text{sf}} = 0.45 \times (T_{\text{air}} - 273.15) - 31.5$$

(16)

We do not provide an equivalent expression for GRIP, Greenland, because the simulations run here (see Sect. 3.1.1) do not include precipitation."

- Figure 2: You should include a comparison with the model of Johnsen et al. 2000



New figure 4 with the model of Johnsen et al. (2000).

We have added a curve (GRIP-J2000 model) on this figure corresponding to the model of Johnsen et al. (2000) for GRIP. We have used their equation 4 (amplitude as a function of *diffusion length* σ and *wavelength* λ) as well as Figure 2 for the evolution of diffusion length with depth. We then obtained the wavelength evolution with depth on the Eurocore data by detection of maxima and minima.

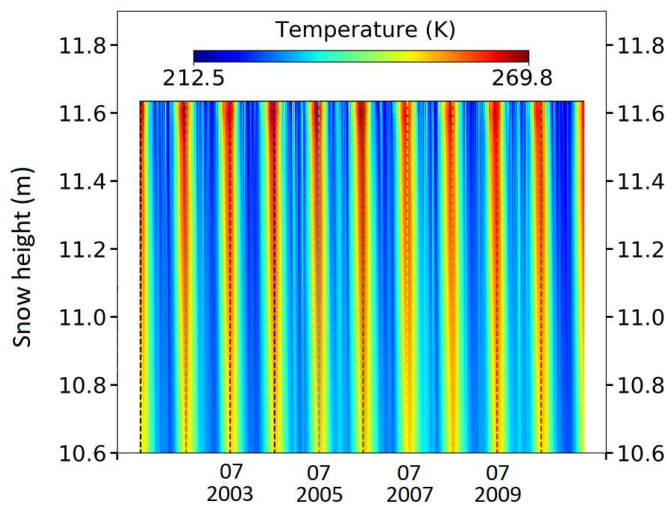
- Figure 3: You write in the manuscript that the temperature is varying but on the figure you only show temperatures for the summer. Does this mean that you only use summer temperatures? I would expect you would use varying temperatures through the whole year.

The temperature indeed varies the whole year but we have chosen to show only one

temperature profile per year, to limit the number of curves on the graph. We chose January, because we considered that this month was one of the warmest, and likely to produce strong temperature gradients and strong vapor diffusion.

We will include a figure showing weekly temperature evolution in the Supplement. We will also add a note in the Figure 3 caption to clarify this point.

I. 1110: “(a) Vertical temperature profile for each summer; (b) $\delta^{18}\text{O}_{\text{gcenter}}$ profile for each summer; (c) Deviation of the $\delta^{18}\text{O}$ relative to the original profile, for each summer; (d) Evolution of the deviation to the original profile of $\delta^{18}\text{O}_{\text{gcenter}}$. **Note that temperature varies during the whole year (see Fig. S1).**”



- I am surprised to find that your model does not show an influence of temperature gradients at GRIP as you would normally assume that temperature gradients would force vapor to be transported between layers due to the vapor pressure gradient?

There is indeed an effect of temperature gradient at GRIP. This can be seen on the two figures 2 and 3. When temperature gradients are active, attenuation is stronger in upper layers, while under constant temperature, the attenuation is the same at 15 cm depth and at 70 cm depth. Moreover, thermally induced vapor diffusion does not only attenuate original sinusoidal variations, but also seems to accumulate heavy or light isotopes in certain layers. We have modified this section of the manuscript to better describe these two effects.

I. 529: ‘Figure 3 shows the result of **Simulation 2**, i.e. with varying temperature in the snowpack. **The attenuation is stronger than the one observed in the previous simulation. The minima at 11.46 m increases by 1.03 ‰ over ten years, and the maxima at 11.15 m decreases by 0.84 ‰. Thus, the total attenuation for the range of heights is ~1.9 ‰. This corresponds to an attenuation by 11.7 %. For the layers below, the attenuation is smaller, with a total attenuation of only 6 % for heights between 10.54 and 10.85 m. If we compare attenuation for heights 11.46 and 11.56 m in the 1st and 2nd simulation, we note that including temperature gradients leads to an attenuation increased by half.**

Between 11.46 m and 11.56 m, the $\delta^{18}\text{O}_{\text{gcenter}}$ values increase over ten years by 1 to 4 ‰. This increase is not caused only by attenuation of the original sinusoidal signal. Indeed, at h=11.60 m, the values get higher than the initial maxima which was -36 ‰ at 11.64 m. There is therefore a local accumulation of heavy isotopes in this

layer as a result of vapor transport. This maxima corresponds to a local maxima in temperature and is coherent with departure of ^{18}O -depleted water vapor from this layer. Thus, thermally induced vapor transport does not only result into signal attenuation, but can also shift the $\delta^{18}\text{O}$ value, regardless of the initial sinusoidal variations.

Lastly, in the first 2-3 cm of the snowpack, **strong** depletion is observed over the period, **with a decrease by 2 to 3 ‰ instead of 0.5 ‰ previously**. This depletion probably results from arrival of ^{18}O -depleted water vapor from warmer layers below. **This shows again** the influence of temperature gradients which were absent from the previous simulation. However, **note that in this simulation we neglect precipitation** and exchange of vapor with the atmosphere. **Thus**, the depletion observed here may not occur **in natural settings** when these processes **are active**.

In conclusion, at GRIP, the diffusion of vapor as a result of temperature gradients has a double impact on isotopic compositions. It increases the attenuation in the first 60 cm of snow, because of higher vapor fluxes. And it also creates local isotopic maximas and minimas, in a pattern corresponding to temperature gradients in the snowpack, but disconnected from the original $\delta^{18}\text{O}$ sinusoidal signal.'

- L503: Is the attenuation at GRIP significant larger than NEEM? 86% and 90% seems very similar.

The reviewer is right, we will replace "greater" by "**slightly higher**" in the text.

- L511: Why don't you calculate the attenuation using Johnsen at GRIP such that you can compare with Bolzan and Pohjola?

A comparison with the Johnsen model will be included in the revised version (cf. comment above)

- L526: It is unclear how Denux in 1996 can indicate that a study by Johnsen et al. in 2000 overestimates the attenuation. Time travel hasn't really been possible yet. You might write that "A study by Denux (1996). . ."

Sorry for that, of course he was referring to the study published by Johnsen in 1977, and dealing with the same model. We have corrected the error:

I. 591: 'Denux (1996) and van der Wel et al. (2015) indicate that the model **developed by Johnsen (1977) and used in Johnsen et al. (2000)** overestimates the attenuation compared to observed values. For Denux (1996), the model of **Johnsen (1977)** should take into account the presence of ice crusts and the temperature gradients in the surface snow to get...'

- L528: You write that Johnsen et al. should take into considerations temperature gradients in order to not overestimate the attenuation. But would you not expect that temperature gradients would increase the attenuation due the vapor transport driven by vapor pressure gradients?

It is not clear yet if including temperature gradients would indeed increase the attenuation of the isotopic signal. This process might move the signal downward or upward without altering it much. It could also produce local isotope accumulation originally not present in the signal (see Figure 6). By creating these local isotope maximas the original signal could in the end 'gain' variability, instead of being smoothed.

However, the presence of ice crusts proposed in Denux (1996) is a more straightforward explanation, and should be tested first.

It is also possible that the discrepancy come from the 'isotopic diffusivity' used by Johnsen et al. (2000), which oversimplify a series of processes into one single equation. Introducing temperature gradients would necessarily imply a rewriting of this equation which might be the occasion to make the model more detailed and accurate.

We will slightly modify our sentence to enlighten which explanation is the most likely:

I. 592: 'For Denux (1996), the model of Johnsen (1977) should take into account the presence of ice crusts, and maybe also the temperature gradients in the surface snow, to get closer to the real attenuation at remote Antarctic sites.'

- I strongly suggest that you set up an experiment with Crocus that allow you compare as closely as possible the simulated attenuation with the calculated attenuation using the model of Johnsen et al. 2000.

This was exactly the aim of section 3.3.1 where indeed, temperature gradient were removed. We have added the comparison of the attenuation from Johnsen model in the figure (see above).

- Section 4.2.1: I suggest to remove the detailed description of simulation of density at Dome C to a supplementary material as it influences the flow of the manuscript which should be focusing on the evolution of isotopes in the snow pack.

OK, this will be moved.

- L 604: You suggest that the higher diffusion at GRIP compared to Dome C could be explained by higher temperatures – but in line 260 you assume that the diffusivity is constant and not influenced by temperature.

This will be corrected in the revised version (see comments above on the dependency of the diffusivity on temperature and pressure).

- In general for all the figures you need to adjust the values for the color bar such that you don't have too many digits. For example in Figure 2 the color bar should go from -0.6 to 0.6 and in figure 3 it should be -1.9 to 0.8.

The limits are computed automatically as the maximum and minimum values of the variable over the first 60 layers. These values are then used in the text as a point of comparison between the different simulations. If we choose/ascribe the limits, this comparison will not be possible anymore.

- Figure S1: Why not combine panel b, c, and d

We are not sure what the reviewer expects here. We can of course remove the blank spaces. However, if the reviewer was meaning to use only one window, then we prefer not to make the modification. With just one window, we will not be able to show all the information, because of the differences in horizontal scales. Especially, the very small shift caused by compaction on panel (c) would not be visible anymore.

Minor comments

L14 “The isotopes . . . resolution” should not be in abstract

OK

L16 “condensation is realized” – what does this mean

This sentence means that the vapor density is brought back to its initial value by condensing excess vapor or sublimating snow. This step thus corresponds to solid/vapor exchanges, after vapor transport. We propose the following correction:

I. 17 “2) a kinetic fractionation is applied during transport, and 3) vapor is condensed or snow is sublimated to compensate deviation to vapor pressure at saturation.”

L21: “model underestimates” -> modeled attenuation due to diffusion is underestimated, or that other processes, such as ventilation influences attenuation

We have modified the text according to the reviewer suggestion.

L24-25: should be moved to conclusion

OK

L42: Randomness in the core stratigraphy -> stratigraphic noise

We have modified the text according to the reviewer suggestion.

L45: series of snow pits -> series of records from snowpits

OK

L53: ice microstructure at solid state -> snow grains due to solid diffusion

OK

L58-61: Cite Ebner et al. 2016 and 2017

OK

L87 Missing parenthesis after Brun et al. 2011

OK

L99: Quick survey-> brief overview

OK

L118: Wavelength of what?

It was the wavelength of the seasonally periodic isotopic signal. However, the text has been modified and wavelength no longer appear.

L178: What do you mean by “Permanent cycles”

We mean that the snow grain is never fully stable, and always undergoes sublimation and condensation at its borders. Depending on the balance of these two processes, its size may increase or decrease. When the two effects are balanced its size is constant. However, even in that case, its isotopic composition is still subject to evolution as sublimation and condensation are both active.

The term “cycle” does not convey our meaning correctly, as both processes are active at the same time. We propose the following correction:

L. 201: “Indeed each grain experiences **continuous recycling through** sublimation/condensation”

L184: to get an -> to obtain an

OK

L185: Remove the content of the parenthesis.

OK

L224: What does this mean: “and taken to compensate yearly accumulation

Sorry for this complicated formulation. When we apply compaction we decrease the height of the firm column, while keeping its mass constant. Its total density is thus increased. We do this to make space for the deposition of a new snow layer at the top while keeping the surface level constant.

Using an accumulation at Dome C of 0.001 kg m^{-2} per 15 min, and considering that total snow column (over 12 meters) weights about 4461 kg, the compaction rate is: $2.2 \cdot 10^{-7}$ per 15 min. For a layer of 330 kg m^{-3} , the density increase is: $+7.4 \cdot 10^{-5} \text{ kg m}^{-3}$ per 15 min. Per year, the total accumulation would be 35 kg m^{-2} and the density change, for the selected layer would be $+2.59 \text{ kg m}^{-3}$.

L240: What about the influence of absorption of radiation energy in layers below the surface layer?

It increases the heat of the layer, and therefore its temperature.

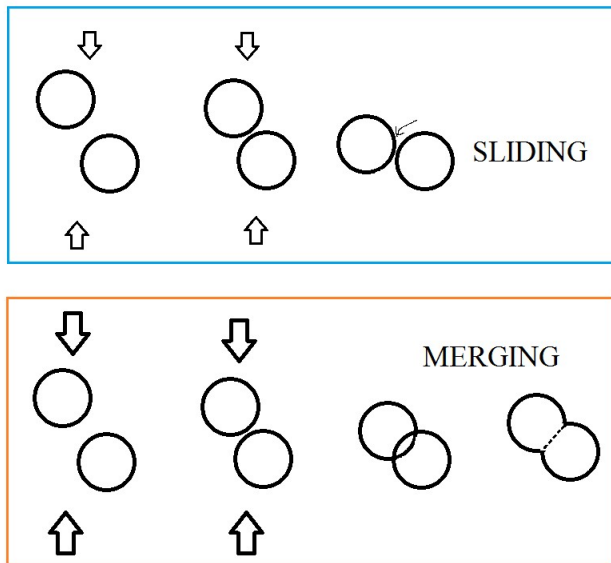
L254: “Interface”: Please be more precise on defining what interface you are referring to

We have added a sentence to define the interface between two layers.

L. 269: ‘In this section, the term ‘interface’ is used for the horizontal surface of exchange between two consecutive layers. The flux of vapor at the interface between two layers is obtained using the Fick’s law of diffusion (Eq. (4)).’

L258: “interpenetrate”: What do you mean?

When two grains are strongly pressed one against the other, the boundary between them becomes flat, and the two grains are merged together to make only one grain. ‘Interpenetration’ is the step when their limits cross each other during the merging. If the pressure is not strong enough, the shape of the grain is not modified; they slide one upon another without merging.



We have rephrased the sentence to facilitate understanding:

I. 279: ‘Effective diffusivity can be expressed as a function of the snow density using the relationship proposed by Calonne et al. (2014), for layers **with relatively low density**. **In these circumstances**, the compaction occurs by ‘boundary sliding’, meaning that the grains slide on each other, but that their shape is not modified. It is **therefore applicable to our study** where density is always below 600 kg m^{-3} .

L296: “that are” -> being

OK

L304: Have you defined kinetic fractionation previously?

No. We have added a sentence to define kinetic fractionation in the Introduction.

I. 156: ‘It becomes the main process of vapor transport when air is stagnant in the porosity.

During diffusion, lighter molecules move more quickly in the porosity, leading to kinetic fractionation of the various isotopologues.’

EQ 12: typo in $D_{\text{eff},n,n}$

Thanks, we have replaced the notation $D_{\text{eff},n,n+1}$ by the symbol used before $D_{\text{eff}}(t, n \rightarrow n + 1)$, in order to keep homogeneous notations.

L486: “Amplitude decrease by -1.3 o/oo” – do you mean amplitude increase by 1.3 o/oo

No, we mean decrease (the amplitude is reduced because of attenuation).

We have corrected the text:

I. 527: ‘Over 10 years (2000-2009), the amplitude decreases **by 1.2 ‰** which corresponds to a 7.3 % variation.’

Interactive comment on Geosci. Model Dev. Discuss., <https://doi.org/10.5194/gmd-2017-217>,

2017.

Interactive comment on “Numerical experiments on isotopic diffusion in polar snow and firn using a multi-layer energy balance model” by Alexandra Touzeau et al. Anonymous Referee #2 Received and published: 1 December 2017

The post-depositional modification is an important but poorly understood part of the "isotopic paleo-thermometer". After the solid precipitation is deposited on the top of the polar ice sheet snow surface, its isotopic content is changed drastically due to the water and mass exchange with the atmospheric water vapor and due to molecular diffusion in snow. These processes disturb or even completely erase the initial climatic signal recorded in the isotopic content of the precipitation. To solve this problem, different approaches are applied including modeling of the snow pack evolution during snow metamorphism. This manuscript is an attempt to simulate the snow isotopic content of the polar snow in the course of the post-depositional processes. For the first time the snow-pack Crocus model is applied for this purpose. The authors clearly understand that this work is a small step towards the full description of the isotopic post-depositional modifications. A lot of efforts still has to be done. However, this attempt deserves to be published as a separate paper in "Geoscientific Model Development" journal.

The manuscript is nicely structured and provides a good review of literature on the formation of the climatic signal in the snow isotopic composition. The authors make a nice attempt to describe in simple way a rather complicated process of the isotopic modifications in the snow thickness. I do not have major corrections, only a few minor comments or questions:

In your model you do not take into account the mechanical snow mixing by wind. This mixing erases the initial climatic signal (shorter than few years) in central Antarctica, and makes the vertical isotopic profiles in the upper part of snow thickness similar to white noise. Recent study by Thomas Laepple (<https://www.the-cryospherediscuss.net/tc-2017-199/>) showed that the filtering of this noise by isotopic diffusion can create false cycles in the isotopic profiles. So, I suggest that in the further versions of your model you introduce random component of the initial isotopic composition of the precipitation (or of the upper snow layer if you wish) in parallel to the regular component given by precipitation events. You might mention this in section 4.4. and conclusion.

We agree with the reviewer that wind mixing should be included in the model somehow as it is an important process in Antarctica.

Libois et al. (2014) already paved the way to do it. They proposed to run the Crocus model in parallel (50 snow columns for the same site) and to exchange snow between these columns. This method is called 'stochastic snow redistribution scheme'. However, because the vapor transport scheme is run at a 1 s time-step, it is slowing down the model. Thus, running 50 simulations in parallel might be very time-consuming in our case.

Other solutions could be proposed, such as taking the first centimeters of snow away (wind ablation), store it temporarily in an atmospheric reservoir and letting it fall again. If several layers are

eroded, they could fall down in a different order, or maybe be mixed together while still in the atmosphere. We will also consider the reviewer suggestion, to add a random component to the signal in precipitation. This could be the simplest way to simulate this process.

We have modified the text in two places to stress the importance of this process to be taken into account in future work:

I. 717: 'The next step for Crocus-iso development is thus to implement ventilation. **Finally, we are also aware that in Antarctic central regions, the wind reworking of the snow has a strong effect in shaping the isotopic signal. A combination of stratigraphic noise and diffusion could indeed be responsible for creating isotopic cycles of non-climatic origin in the firn (Laepplé et al., 2017). Wind reworking may also contribute to attenuation, by mixing together several layers deposited during different seasons.'**

L. 753: 'Second, in low accumulation sites like Dome C, wind scouring has probably an important effect on the evolution of the $\delta^{18}\text{O}$ signal in depth through a reworking of the top snow layers (Libois et al., 2014). This effect has not been considered here **but could be implemented in the model in the next years.'**

Other minor comments:

line 33 - better to write "1950s"

OK

lines 352-353 - why condensation is without additional fractionation?

See above (same comment by the first reviewer).

lines 502-503: the values (86% and 90%) are the remaining amplitudes, right?

Yes, we made a mistake. After the correction, the new sentence is:

I. 565: 'The 2.5 m attenuation is slightly higher at GRIP, leading to a remaining amplitude of 86 %, **than at NEEM where the remaining amplitude is 90 % (Fig. 4).'**

section 4.2.3: how much snowfall have you added to the snow thickness in this simulation?

The total cumulated precipitation was 37 kg/m² for year 2001 (11 cm of fresh snow, 4 cm i.e.). In average for the period 2000-2010, the annual total of precipitation was 29 kg/m²/year. 2001 is the year with the highest accumulation.

lines 582-583: this gives 10 cm / year, but above you said that the accumulation rate at DC is 8 cm / year (snow equiv.).

Sorry for this discrepancy. The '8 cm' value comes from glaciological analysis, and corresponds to long time scales, whereas the '10 cm' value is the one measured for recent years (see Landais et al., 2017). Our forcing data has an accumulation of 29 kg/year, corresponding to 9.6 cm of fresh snow, and therefore coherent with measured accumulation for the last 10 years.

We will modify the text to remove this ambiguity.

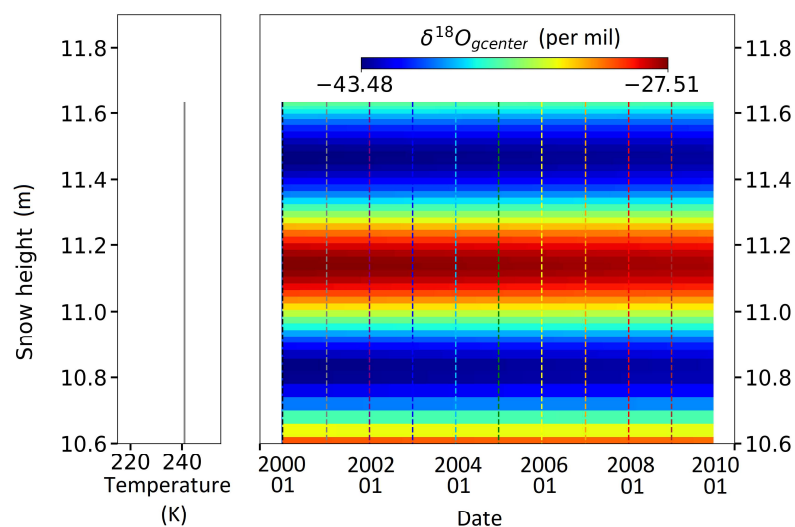
I. 439: 'About **10 cm of fresh snow** are deposited every year (Genthon et al., 2016; Landais et al.,

2017), which implies that in order to keep seasonal information, at least one point every 4 cm is required in the first meter...'

Figure 2d is a bit misleading. From the first glance a reader may think that the seasonal amplitude is increasing with time. Then, it becomes clear that it is actually $\delta^{18}\text{O}$ change that is increasing with time. It would be nicer to show here the $\delta^{18}\text{O}$ values themselves (instead of $\delta^{18}\text{O}$ changes), so that the colors would nicely illustrate the fading isotopic variability. The same comment is for Figures 3 and 12.

We are aware that our figure is not easy to understand at first glance and we apologize for that.

We hesitated between this 'difference' figure and the original one with the true values of $\delta^{18}\text{O}$ (see below). However, the attenuation is not much easier to see in the original figure (shown below).



An attenuation by 0.5‰ over a half-amplitude of 8 ‰ is barely visible for the maxima (dark red becoming lighter) and no at all for the minima (shades of blue difficult to distinguish).

We therefore prefer to keep the 'difference' figure in the manuscript. Moreover, since the caption clearly states that we are plotting the deviation to the original profile, we do not see our figure as misleading.

line 1055: December 2001.

OK. Thanks.

Interactive comment on Geosci. Model Dev. Discuss., <https://doi.org/10.5194/gmd-2017-217>, 2017.

Interactive comment on “Numerical experiments on isotopic diffusion in polar snow and firn using a multi-layer energy balance model” by Alexandra Touzeau et al. Anonymous Referee #3 Received and published: 4 December 2017

1 Overview

Firn isotope diffusion is a process that affects the $\delta^{18}\text{O}$ signal of polar snow from the time of deposition until pore close-off. Taking place in the vapor phase within the porous medium of the firn and driven by the apparent seasonal, annual and multiannual isotopic gradients it results in an attenuation of the $\delta^{18}\text{O}$ signal, often obliterating its annual component.

Assuming a good estimate of the diffusive rates in firn is obtained, a “reverse calculation” of diffusion can be possible that allows the (almost) complete reconstruction of the initial signal. Additionally, knowledge of the diffusive rates offers valuable information on past firn temperatures and as a result can be used as a paleothermometry tool if ice core data of sufficient resolution and precision are available.

Previous studies have looked into the description and characterisation of these effects and part of these studies suggests that post depositional processes different to purely fickian diffusion of water isotopes can also be at play acting supplementary to the signal attenuation affects or even introducing biases (Town et al., 2008). These processes are mostly of advective nature caused by the bulk movement of air and vapor in the snow, driven by pressure and temperature variations.

In this work titled “Numerical Experiments on isotopic diffusion in polar snow and firn using a multi-layer balance model”, Touzeau et al attempt to build and test a water isotope module on top of the Crocus snowpack model. In particular, the authors focus on trying to simulate post-depositional effects that cause changes of the initial $\delta^{18}\text{O}$ signal in polar snow and firn. Processes related to snow/firn isotope diffusion as well as diffusive vapor transport due to temperature gradients in the firn are modelled assuming various scenarios. The study focuses on two different regimes that are representative of conditions typical for deep ice coring sites on Greenland and East Antarctica. Ice core data sets are also used in order to evaluate the performance of the model and the results are also compared to existing firn isotope diffusion modelling approaches. This is a very welcome contribution and it most certainly points to the correct direction with respect to future modelling efforts. The study also fits very well the description and scope of the GMD journal and the overall quality of the research conducted is of high level. Thus I would recommend it for publication in GMD after the following points are carefully considered by the authors.

2 General comments

1. Unfortunately the language of the manuscript requires a significant revision. In particular there are examples in the text where technical/physical terms are used wrongly and many definitions appear to be loose. This is particularly problematic for a manuscript of this type, where

modelling approaches and physical processes are described. The most notable example is the description of the transport mechanisms in snow in sections 2.1.1 and 2.1.2. Diffusion is a very well defined process and unfortunately the term is used falsely several times in sections 2.1.1 and 2.1.2 (and elsewhere in the manuscript). After reading these two sections I feel confused about the meaning of many of the terms used here and as a result about the kind of methods followed and the assumptions made in this study.

In this paper, we distinguish 3 types of diffusion:

- solid diffusion (limited effect in the first meters of snow, because it is very slow);
- diffusion in vapor phase caused by isotopic gradients (gradients present originally in the solid phase, but transmitted to the vapor);
- diffusion in vapor phase caused by temperature gradients (which produce vapor pressure gradients in the porosity).

The first two processes are not **oriented** (=externally forced), they result from random movement of molecules in vapor phase or of ions in solid phase. The last process is **oriented** (=externally forced) as it is forced by an external variable which is the atmospheric temperature. While the two first types of diffusion can only attenuate the original signal, the last type can add 'noise' to the original signal. When diffusion due to temperature gradients is active, original information is not only damped, but even replaced. Thus contrary to the first two processes, it will not be possible to 'reverse' the phenomenon in that case.

Thus we class the 'solid diffusion' and 'diffusion caused by isotopic gradients' within the category of 'processes' leading **only to signal smoothing** in an homogeneous way (Section 2.1.1). And we class 'diffusion caused by temperature gradients' as a process leading to **oriented vapor transport** (Section 2.1.2.), and therefore much more difficult to deconvolute. In this Section 2.1.2., we present other processes also leading to **oriented vapor transport** such as convection and ventilation. Note that we have not included convective processes (convection, and advection due to the vertical gradient of air pressure) in the model yet. Only diffusive processes are present.

The processes we describe are the same as described by others, and the only novelty here is in the way we split the processes. The classical way to do it is to separate convective processes (ventilation and convection) from diffusive processes (the three types of diffusion described). Here, we prefer to split them based on their effect on the original isotopic signal. Is it possible to deconvolute the signal stored in ice cores, because only smoothing is active? Or is the isotopic composition modified more strongly, in particular through the accumulation of heavy isotopes in a specific layer?

We are aware that this splitting may surprise people, as it is not based on the physics of the process, but on its effects. However, it has interest for people who are working at the interface between physical description of processes and interpretation of 'noisy' geochemical data. Moreover, we did not invent this splitting. It was first proposed by Ekaykin et al. in 2009.

In order to help the reader to follow our line of thinking, we have modified the introduction to this section 2.1:

l. 117: 'Several studies address the evolution of the isotopic compositions in the snow column after deposition. Here we describe first processes leading only to attenuation of the original amplitude (Sect. 2.1.1.). Then we describe processes which lead to other types of signal modifications (Sect. 2.1.2.). These modifications include transporting and accumulating isotopes in some layers without

consideration of the original isotopic signal. They also comprise processes taking isotopes away from the snow, and therefore shifting the mean $\delta^{18}\text{O}$ value of the snow deposited.'

Also in relation with a comment made by reviewer 1, we have replaced the term 'oriented processes', which was too vague, by the more precise expression '**processes of oriented vapor transport**' all other the section.

And we define these 'processes of oriented vapor transport' at the beginning of Section 2.1.2:

I. 141: 'We consider here the **oriented movement** of water molecules forced by external variables such as temperature or pressure. We use the term '**oriented**' here to describe an overall movement of water molecules that is different from their molecular agitation, and externally forced.'

What is an "oriented process" for example? In page7line73 the sentence "We focus on the impact of oriented vapor transport caused by vapor density gradients in the snow..." is very untechnical and unfortunately creates a lot of confusion about what the authors have done.

'Oriented process': See above.

Line 73: The sentence was modified based on this comment as well as on the first reviewer comment.

I. 78: 'We focus on the movement of water isotopes in the vapor phase in the porosity, in the absence of macroscopic air movement. In that situation, the movement of vapor molecules in the porosity is caused by vapor pressure gradients, or by diffusion along isotopic gradients. Note that in the first case, the vapor transport is 'thermally induced' i.e. the vapor pressure gradients directly result from temperature gradients within the snowpack.'

Here we focus on two out of the three diffusion processes presented above:

- a) the diffusion in vapor phase *caused by isotopic gradients*;
- b) and the diffusion in vapor phase *caused by temperature gradients*.

If the term "vapor density" indeed refers to "vapor (molar?) concentration" as I assume then the process described here is a vapor diffusion process.

It is not a molar concentration, but a **massic concentration (its unit is kg/m^3)**. And yes, the concentration gradients drive the diffusion in our model (Fick's law).

We agree that this term leads to confusion. The first reviewer suggested to replace this term by '**vapor pressure**' which is more commonly used. However, this is not coherent with our unit, and therefore not applicable for when we are describing the symbols in equations. Using the term '**concentration**' is probably a better option in these cases.

Therefore, we have replaced 'vapor density gradients' by '**vapor concentration gradients**' as much as possible in the paper. For equations, we have also used the term '**mass concentration**' which is more accurate.

After having read the text several times and tried to infer what the authors try to describe in sections 2.1.1 and 2.1.2 I conclude that they split the processes under consideration in two kinds.

Thanks for trying to understand this section, despite our particular way of splitting processes. We apologize for not being clear enough. We hope that after adjustments, this section of the manuscript will be easier to follow for the reader.

○ The first, what they call “signal attenuation on a vertical profile”, is a the combination of two processes, (a) solid isotope diffusion and (b) firn isotope diffusion in the vapor phase.

(a) The first is extremely slow and can easily be neglected in this study. I find it important that the authors point out in the text that solid diffusion affects all isotopes equally.

We have added a sentence in the text as a reminder:

l. 138: ‘**Note that in the solid phase, all isotopes have the same diffusion coefficient.**’

(b) The second is a diffusive process taking place in the porous medium of the firn driven by the isotopic gradients.

Both processes introduced here follow the same physical principle ie transport of mass due to concentration gradients of a substance. The transport occurs along (or down) the concentration gradients and not “against” as often described in the text.

As suggested, we have replaced ‘against’ by ‘along’ in the manuscript.

○ The second category of processes outlined in section 2.1.2 and termed as “oriented processes”. My interpretation of the text is that this type processes are “bulk motion” processes either due to pressure or temperature gradients.

The reviewer is right. The processes described in this second section indeed correspond to an overall movement of vapor molecules resulting from temperature or pressure gradients. Thus, they are not limited to ventilation and convection.

The first case is a typical example of advective transport.

NB: The first case (l. 145) was wind-pumping, which we agree to be convective by nature.

The second is a bit more complicated however the term diffusion used by the authors is incomplete. Temperature gradients in the snow will eventually cause vapor concentration gradients. The latter, will drive a diffusion process for the vapor as a whole. However this cannot be seen as an isotope diffusion process due to the fact that the diffusive transport of vapor has nothing to do with isotopic gradients. Eventually of course the diffusive transport of water vapor will very likely bring vapor molecules in layers of the snow with different isotopic composition where subsequently an isotope diffusion process will occur locally.

NB2: The second case (l. 147) was thermally induced vapor diffusion.

There has never been any confusion in our mind between diffusion driven by isotopic gradients and diffusion driven by temperature gradients. Indeed, we have separated strictly diffusion in vapor phase caused **by isotopic gradients** in the first section, from **thermal diffusion of vapor** in the second section. We agree with the reviewer that the second one affects isotopes only indirectly.

Although thermal induced diffusion is certainly a diffusion process, it is indeed a shortcut to call it an ‘isotope diffusion’ process, and a better expression would be ‘vapor diffusion process **with**

consequences for isotopes’.

We will modify instances in the text where ‘isotope diffusion’ or ‘isotopic diffusion’ were appearing. We will clarify every time if we were talking about *diffusion along isotopic gradients* or about *thermally induced diffusion of vapor... and its consequences on isotopes*.

L. 1: ‘Numerical experiments on **vapor diffusion** in polar snow and firn **and its impact on isotopes** using a multi-layer energy balance model’

L. 20: ‘We also run complete simulations of **vapor diffusion along isotopic gradients** and of **vapor diffusion driven by temperature gradients** at GRIP, Greenland and at Dome C, Antarctica over’

L. 363: ‘... the total flux of vapor is null. But **diffusion along isotopic gradients still occurs if the isotopic gradients are non-zero**(Eq. (13)).’

L. 726: ‘The main process implemented here to explain post-deposition isotopic variations is diffusion. We have implemented **two types of diffusion in vapor phase: 1) water vapor diffusion along isotopic gradients, and 2) thermally induced vapor diffusion**. The vapor diffusion between layers was realized at the centimetric scale. **The consequences of the two vapor diffusion processes on isotopes in the solid phase were investigated. The solid phase was modelled as snow grains divided in two sub-compartments: a grain surface sub-compartment in equilibrium with interstitial water vapor and an inner grain only exchanging slowly with the surface compartment. We parameterized the’**

This was only an example of how the loose use of technical terms and faulty language creates unnecessary confusion to the reader already from the introduction, leading possibly to confusion and misunderstandings of the methods and principles used in this study. I find it essential that the authors look into the manuscript carefully and revise the text accordingly. In the “Specific Comments” section I include more of these examples as they appear in the text.

We have made our best to modify the terms in order to make the sentences and our meaning clearer. We will check the use of the term ‘diffusion’ and remove the term ‘isotope diffusion’ as stated above.

2. There is an unclear situation regarding the vapor diffusivity parametrization and value used in this study. It is not exactly clear if there is a temperature dependency of the effective diffusivity D_v to temperature. Based on equation 5 in the manuscript and the comment on the value of D_v I conclude that the value of D_v is taken constant and reflects a temperature of 263 K. If this is indeed the case I would be inclined to question the validity of many of the statements found in the manuscript that concern the comparison of this model with other models of diffusion or results from ice core data. The diffusivity coefficient is heavily dependent on temperature and thus a constant value is an oversimplification for such a study. I would strongly prefer a version of the manuscript where the diffusivity is allowed to depend on temperature. However, if the authors indeed choose to follow the approach of constant diffusivity they will need to stress out very clearly in the manuscript that the comparisons presented here are essentially between different things. This should be even more prominent for the case of the Dome C modelling experiments due to the very large difference between the site temperature and the temperature used for the diffusivity coefficient value (almost 40K).

Indeed, this has to be addressed, see answer to this question in the first review.

3. Despite my belief that the work performed by the authors is of high quality I need to point out that several elements of the manuscript feel opaque not allowing the reader to judge for herself on the quality of the work and the significance of the results. I find this a fundamental weakness of the manuscript that needs to be addressed. In particular:

- The authors claim that the model is evaluated for the top 10 m of snow. However only the top 50-60 cm are presented.

We do not present results downwards simply because the layers are too thick (~20 cm). Therefore no seasonal pattern is visible in these layers and the attenuation by diffusion is impossible to evaluate. But we can easily print a window of the whole snowpack for those interested.

- The authors do not provide any information about neither the ice core data used nor the method used to calculate peak-amplitudes. The latter is not a straight forward procedure and can have a significant influence on the result of such model-data comparisons for diffusion. Information about the depth interval the data originate from, the temperature, accumulation and pressure conditions of the sites as well as the resolution of the data are pieces of information a thorough reader needs to have access to. Present the ice core data.

We are particularly sensitive to this remark, as we encountered exactly the same problem while looking at previous publications where these ice core data were published and used for diffusion study. While the attenuation (%) was given, we were unable to find the original signal nor the methodology used to calculate the attenuation.

We propose to give in the appendix of the revised manuscript the methodology that we followed to compute the attenuation.

1) We define 'half-amplitude' as: $\text{abs}(\delta^{18}\text{O} - \text{mean}(\delta^{18}\text{O}))$. Thus, we first compute the mean $\delta^{18}\text{O}$ in the core, and then for each depth compute the absolute difference to the mean. Following a suggestion by Reviewer 3, we will replace 'half-amplitude' by the more common term 'semi-amplitude' in the manuscript.

2) We then look for maximas in this series of half-amplitudes. In the first version of the manuscript, we used 20-cm windows at this step. However, this is not well adapted for NEEM. In the revised version we will present results obtained with a 30-cm window for the first 10 meters of the core. Indeed, in this shallow part of the firn the density is about 400 kg m³. Using accumulation rates of 0.23 m i.e. at GRIP, and 0.22 m i.e. at NEEM, the expected length for the cycles is 52 and 55 cm respectively. Since we are looking at half-cycles, a window of 30 cm should allow to get all the maximas present in the record. Deeper in the firn we will use **a window of only 20 cm** coherent with higher snow density downward.

This has been clarified in the text:

l. 558: 'For NEEM the values of the four cores are taken together. For NEEM and GRIP, the **semi-amplitude** is computed along the core. **In the first 10 meters, the maximum value every 30 cm is retained, and deeper in the firn, the maximum value every 20 cm is retained (Fig. 4).** Maximum'

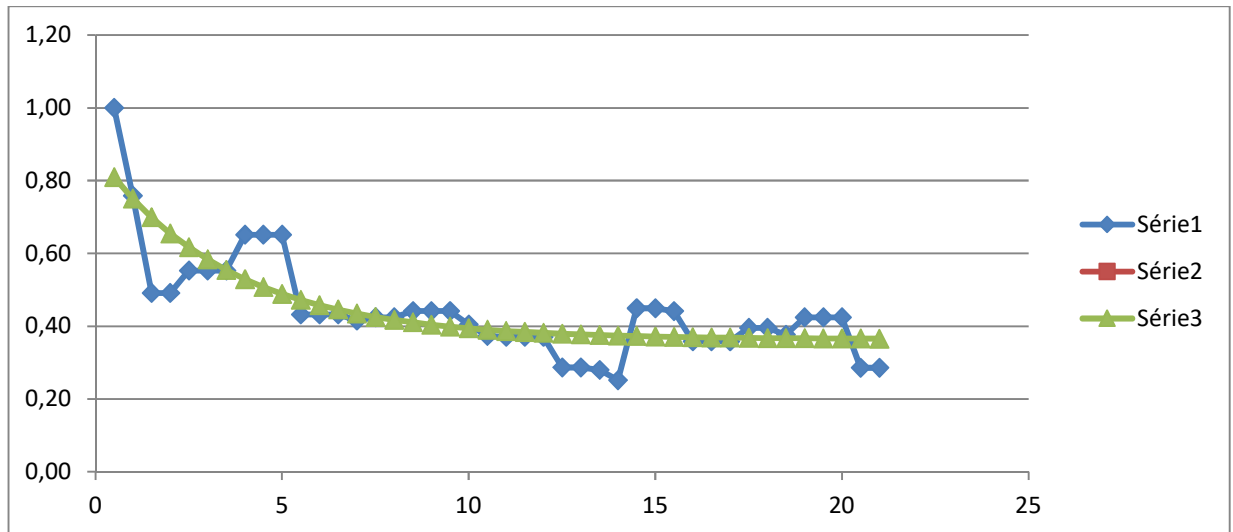
3) Then over this series of maxima, we keep the maximum value for **each meter of the core** (see Figure below). We use this larger window for the fitting, because we prefer to evaluate attenuation based on the larger (well-defined) maxima. We use the value obtained in the first meter as our 'initial

half-amplitude'. All other maximas are expressed relative to this first meter “maxima of maximas”, even if the maximas downward happened to be larger.

We add two sentences in the text to clarify this step:

I. 562: ‘**Consequently, from this first series of maxima, a second series of maxima is computed, with a larger window of 1 meter. The ‘remaining amplitude’ is then defined as the ratio between any of these 1-meter maxima and the initial 1-meter maxima. Maximum semi-amplitudes every 5 m are also computed and displayed on Figure 4.**

4) Lastly, we apply an exponential fit to these values:



- The initial $\delta^{18}\text{O}$ profile as well as snapshots of some layers should be plotted. The difference plots with the plethora of colors do not add anything neither for the case of density nor for the case of $\delta^{18}\text{O}$. The colormaps of these plots are unfortunately very ambiguous to read and despite having the max and min values it looks to me that some of these colormaps are non linear. In combination with the very small difference values for both the density and the $\delta^{18}\text{O}$ these color plots leave me guessing. There is very little valuable information I can extract from them.

The omni-present 2D colored graph is the most common way to present Crocus outputs. The script to make this graph is indeed delivered with the model.

However, we are aware of its limitations, which is why we decided to add **on the side of most figures** a series of 1D profiles, that are often more explicit than the traditional 2D Figure. We plot in particular **the original profile of $\delta^{18}\text{O}$ on Figure 2, 3 and 11**. We also plot the deviation to the original **as 1D profiles (depth) on Figure 2 and 3 and as 1D (time) profiles on Figure 11** for a selection of layers.

Although these 1D profiles are often more explicit, we also keep the traditional 2D figure in the article, because people might be interested to see the whole picture and not only what we select.

For instance, we hesitated to insert a 2D figure of temperature evolution when submitting this manuscript. We decided against, as we had already a lot of figures to display. This was an error: because we extracted only summer vertical profiles, the first reviewer asked for profiles in winter which were not apparent. So even if they are difficult to read, the 2D plots remain necessary.

Regarding the color bar, the reviewer is right in thinking that it is non-linear. We have two

different (linear) scales for positive and negative change. Positive change is in level of red and negative change in levels of blue. Thus, when negative change is ten times smaller than positive change, it is still visible in the graph. Of course, white color corresponds to zero change. This color convention (red-white-blue, two linear scales both sides of zero) is used everywhere in the paper (except for Figure 11, which will be modified).

l. 453: **'The white color corresponds to an absence of change of the variable.'**

We hope our explanation will make the figure easier to understand.

• **The study considers all three isotopologues of water ($\delta^{18}\text{O}$, $\delta^{17}\text{O}$ and δD) however the authors choose to present only the results for $\delta^{18}\text{O}$. Based on (Johnsen et al., 2000) the diffusive attenuation is expected to be stronger for $\delta^{18}\text{O}$ compared to δD . Can the model produce this differential signal? This is a very simple test.**

This is a good question. We did not look at the attenuation of δD signal simply because this variable never appear (we use $\delta^{18}\text{O}$, dex and $^{17}\text{O}_{\text{ex}}$). However δD can of course be deduced from the other parameters.

For winter 2000, the slope for δD is $-5.64\text{‰}/10\text{years}$. Divided by 8, this would correspond to 0.71‰ attenuation per 10 years in $\delta^{18}\text{O}$ which is indeed less than the value of $0.82\text{‰}/10\text{years}$ obtained for the $\delta^{18}\text{O}$ slope. We thus indeed find that attenuation is larger for $\delta^{18}\text{O}$ than for δD .

4. The discussion about the comparison with GRIP data feels incomplete and not thorough. The actual data set is never shown in the manuscript while there is very little information about how diffusion is estimated for this data set. Measuring peak-to-peak amplitudes on ice core $\delta^{18}\text{O}$ data can be very misleading as the initial $\delta^{18}\text{O}$ value is unknown and most likely it has been variable through the time.

We have already answered above about our methods. We are acutely aware of the lack of a reliable method to estimate attenuation from an ice core dataset.

One technically correct way to estimate diffusion on data is to look into the spectral domain and estimate diffusion length values. Either way the reader had practically no access to information about how diffusion is estimated from the GRIP data.

Looking at the spectral domain was not possible in our case because the longest simulation was run for 10 years and this is much too short for this approach. For such short record, looking at the spectral domain (and at the diffusion length) would be efficient only if the ice record was perfect (no wind, no stratigraphic noise). **Then (in that case only)** we can expect periodicity and amplitude to decrease jointly in a predictable way.

Additionally, it should be noted that the GRIP data set, originating from a certain depth interval in the ice core (that is not given in the manuscript) it may have experienced a combination of temperature and accumulation different from the modern one. Does the comparison presented here take this into account?

We are presenting a figure (3) that goes **down to 80 meters from the surface**. Thus, the core considered comes from **a depth interval that is 0 to 80 meters**, hence directly comparable to modern

conditions. We will precise it in the text since it appears to be confusing.

We have added two sentences to clarify this point:

I. 556: published in White et al., 1997. **For the GRIP core, only the first 80 meters are considered. Therefore, the data presented corresponds to deposition and densification conditions similar to the modern ones.**

In particular if the CROCUS model only uses a fixed diffusivity value for 263 K, there is no doubt that there will be a discrepancy with the data deduced diffusion. These are very important elements of such a study and are notably absent in the manuscript.

We made a mistake in keeping the diffusivity constant with temperature. However, as indicated above, the direct effect of temperature (molecular agitation) is much less than its indirect effect through vapor concentration and vapor concentration gradients.

When using the formula provided by Johnsen et al. for temperature control on diffusivity, we find that the main difference compared to diffusivity in our simulation **comes not** from the temperature component but from the **atmospheric pressure** component. Indeed, we used air diffusivity at 263 K and 1 atm before and therefore just adding the pressure component (1/0.650) almost double the diffusivity because air is less dense and molecules have more space to move. Again compared to this effect, the temperature effect is limited.

5. Plots and captions need to be reworked. There are several stylistic inconsistencies that should not be allowed for a publication of this quality. A mixture of different font types, missing measurement units from axes, different approaches in presenting measurement units (using either parentheses or a / sign) and a %sign presented in two ways. I think that many of the captions are too long while in the same time they miss one important piece of information that is the number of the experiment and maybe the ice core site under consideration. I do not think it is the job of a reviewer to go through every single detail and problem with the plots thus I will trust that the authors are certainly able to carefully go through the presented plots and make the necessary changes.

We will take these remarks into consideration for improving the figures in the revised version of the manuscript.

6. Regarding the references given, I think that for the introduction section there is probably an overwhelming number of works cited and a small clean-up is possible. More importantly though, some of the works cited are not peer reviewed belonging to the "Discussions" versions of some of the Copenicus publications journals. I believe that the authors should consider these cases and preferably either omit them or update their references list in case some of the papers in question have reached a post peer-review status.

This will be taken into account in the revised version.

3 Specific comments

Here some more specific comments for the authors.

P2L45 "and then only stacking...". As one looks in higher depths in a core this is less of an issue.

Yes.

P3L57 Make sure the reader understands this is vapor-solid exchange in the porous medium of the firn.

We have added a precision.

I. 56: 'Second, within the porosity, the vapor isotopic composition can change due to: 1) diffusion along isotopic gradients in gaseous state, 2) thermally induced vapor transport caused by vapor pressure gradients, 3) ventilation in gaseous state, or 4) exchanges between the gas phase and the solid phase i.e. sublimation and condensation. In the porosity, the combination of diffusion along isotopic gradients in the vapor and of exchange between vapor and the solid phase has been suggested to be the main explanation to the smoothing of the isotopic signal in the solid phase (Johnsen et al., 2000; Gkinis et al., 2014; Ebner et al., 2016, 2017).'

P3L67 Diffusion length mentioned here but no definition given.

In Johnsen et al. (1977) the diffusion length is defined as the **mean displacement of a water molecule during its time of presence in the porosity**. More precisely:

$$(\Delta L_f)^2 = 2 D \tau_v \left(\frac{2}{\pi}\right)^2$$

With D the diffusivity of water molecules, τ_v , the residence time of vapor in the porosity and ΔL_f the diffusion length.

We have added this definition in the text.

L. 71: were able to simulate and deconvolute the influence of diffusion along isotopic gradients in the vapor at GRIP and NGRIP using a numerical model. To do this, they define a quantity named 'diffusion length' which is the mean displacement of a water molecule during its residence time in the porosity. Using a thinning model and an equation of diffusivity of the water isotopes in snow, they compute this diffusion length as a function of depth. It is then used to compute the attenuation ratio (A/Ao), and in the end retrieve the original amplitude (Ao).

P3L74 "...and of diffusion against isotopic gradients" Is this vapor firn diffusion or solid?

We are focusing on vapor diffusion, because solid diffusion plays only a minor role.

We propose the following modification to the manuscript:

I. 78: 'We focus on the movement of water isotopes in the vapor phase in the porosity, in the absence of macroscopic air movement. In that situation, the movement of vapor molecules in the porosity is caused by vapor pressure gradients, or by diffusion along isotopic gradients. Note that in the first case, the vapor transport is 'thermally induced' i.e. the vapor pressure gradients directly result from temperature gradients within the snowpack.'

P5L117 For an informative plot on the matter see Gkinis et al 2014. Higher accumulation rates also result in increased densification rates and therefore reduced diffusivities.

Thanks for this complement of information. We will add it to the text:

I.132: 'high accumulation rates ensure a greater separation between seasonal $\delta^{18}\text{O}$ peaks (Ekaykin et al., 2009; Johnsen et al., 1977) thereby limiting the impact of diffusion. They also result in

increased densification rates, and therefore reduced diffusivities (Gkinis et al., 2014). Because sites with high accumulation'

P5L120 Diffusion indeed takes place in the ice column but with rates orders of magnitude lower than that of firn. You want to be more specific about it in the text as you often mix the terms vapor and solid diffusion without being specific about the process taking place in the porous of the firn or in the solid ice.

Again, our aim here was to separate "smoothing" processes from "building/shifting" processes. Diffusion **along isotopic gradients**, in the vapor phase **AND** in the solid phase will only lead to smoothing. This is why we do not distinguish between the two processes in this early section of the manuscript: they have the same effect.

But we are aware that they act at different time scales and at different depths. We are also aware that the solid diffusion is much slower (as indicated in section 2.2.1.).

We will modify the last sentence to clarify our meaning:

l. 137: 'Diffusion along isotopic gradients exists throughout the entire snow/ice column. **It occurs mainly in the vapor phase in the firn, especially in the upper layers with larger porosities. After pore closure, it takes place mostly in the solid phase, at a much slower rate.'**

P6L143 It would be helpful to add even one sentence where you explain why and how the spherical ice elements approach is too simplistic (is it?).

Approximating snow microstructure by a monodisperse collection of spherical ice elements has been carried out in several studies in the past (Legagneux and Domine, 2005, Flanner and Zender, 2006). This makes it possible to perform explicit calculations, for a medium featuring the same surface area/volume ratio, without accounting for the complex microstructure of snow. Several limitations arise, related to the requirement to better account for the full distribution of curvature of the ice/air interface, which is critical for snow metamorphism (Flin and Brzoska, 2008). Furthermore, the ice sphere geometry modifies the distribution of ice chord distances, i.e. the mean ice path which is relevant for ice diffusion. Such effects would better be accounted for using a more comprehensive description of the snow microstructure, although the level of complexity would make it untractable using the current generation of multilayer snowpack models.

P7L161 "...the transfer of molecules from the grain boundary towards the center of the grain is very slow" Solid diffusion at the temperatures we are talking about is indeed slow. However this sentence gives a false impression that there is a 1-way motion from boundary to center. This is wrong for two reasons. Firstly, any diffusion process would not result in a 1-way motion of molecules. Secondly and more important, solid diffusion in ice seems to be a self-diffusion process following a vacancy mechanism. This means that there is no isotope effect and diffusion affects all isotopologues equally or in other words molecular transport does not take place along and due to the isotopic gradients in ice (therefore there is no index denoting isotopic species in Eq. 1 - ice diffusivity concerns water molecules in the solid phase regardless of their isotopic composition). As a result the model used here of an isotopically heterogeneous material with internal and external layers does not cause any isotope diffusion in the solid phase due to the radial gradients. In a perfectly homogeneous

material you should be expecting the same magnitude of diffusive mixing in the solid phase as in the heterogeneous material assumed in the text. It would be good to correct these errors in section 2.2.2 and clarify the presence of the self-diffusion mechanism. The calculations of characteristic times in this section look correct and are relevant though. Just make sure that you clearly explain that this characteristic time concerns not only movement of the different isotopologues along a specific path (surface to center of grain) but of ALL water molecules towards all directions in the grain and across the grains.

We are sorry for this mistake and will correct the text.

I. 182: 'The grain center isotopic composition may change either as a result of crystal growth/sublimation or as a result of solid diffusion within the grain. **For solid diffusion, water molecules move in the crystal lattice through a vacancy mechanism, in a process of self-diffusion that has no particular direction, and that is very slow.** The diffusivity of water molecules in solid ice...'

I. 192: 'Therefore the solid diffusion ~~between the surface of the grain and the inner part of~~ **within** the grain, at the time'

section 3.1.1 I was wondering if it would be possible to outline the components of the Crocus model in a summarising table and shorten this section significantly?

We feel that, while possible, it is not necessary to shorten this section, given that this manuscript is a model description paper submitted to GMD. It is preferable that the manuscript is a little long, at place, rather than cutting apparently unnecessary details which may hamper the comprehension of some readers. We suggest to keep this part as it is, given that it does not include confusing or misleading information, and rather describes how the isotopic modules are incorporated in the overall Crocus structure.

P10L221 There does not seem to be any dependence of the densification rate to temperature or accumulation rate. Neither is there a two or three stage densification process as done usually in some other densification models. Can you elaborate on this? Would this model be suitable for modelling the full firn profile from surface to firn-ice transition?

The parametrization that we use for densification is very simplified, and would not work for a deeper snowpack or the entire firn column. Indeed, we 'compensate' the annual accumulation falling on top of the snow by densifying only the first 10 meters in order to keep the level of the surface steady. And we apply homogeneous compaction, not differentiating between layers with small or large crystal grains or made of resistant hoar.

The original scheme present in Crocus is much better by any regard, and should lead to density predictions much closer to reality. However, it will lead to stable surface level only if the entire snowpack is present within the model. Since we decided to study only the first meters of the snowpack, the original scheme was leading to a permanent increase in the surface level (the compaction below ten meters was absent, as were these layers). We therefore decided to modify the scheme to remove this side-effect.

We will add this precision to the text:

I. 240: '**Layer thickness decreases, and layer density increases** under the burden of the overlying layers and resulting from metamorphism. **In the original module,** snow viscosity is parameterized using

the layer density and also using information on the presence of hoar or liquid water. However, this parameterization of the viscosity was designed for alpine snowpack (Vionnet et al., 2012) and may not be adapted to polar snow packs. **Moreover, since we are considering only the first 12 m of the snowpack in the present simulations, the compaction in the considered layers does not compensate the yearly accumulation, leading to rising snow level with time. To maintain a stable surface level in our simulations, we used a simplified'**

Eq.4 I think the right term for the quantity p_v should be mass concentration instead of vapor density (this term is wrongly used in more places in the manuscript). Density refers to the ratio of mass to volume of the same substance whereas what you use here is the mass of vapor divided by the volume of air in the open porosity of the layer under consideration. Accordingly I think you should change the symbol from p_v to C_v or similar.

We have replaced 'vapor density' by '**vapor concentration**' or by '**vapor mass concentration**' everywhere in the manuscript.

I may be missing something but if I use Fick's first law and a forward difference differentiation scheme I do not get the factor of 2 as in Eq. 4. Can you elaborate please?

We are looking at the diffusion between the middle of the lower layer and the middle of the upper layer. Therefore, the water molecules travel along a total distance that is $dz_{\text{low}}/2 + dz_{\text{up}}/2$. Half the thickness of the lower layer and half the thickness of the upper layer. So this factor comes from the denominator.

P11L260 D_v is a function of temperature and pressure. How significant is the fact that you are using a fixed value?

See above.

Eq.5 The fact that the diffusivity used here is independent of temperature and site pressure seems problematic to me. Can you comment on this and add a line in the manuscript about the effect of this approach?

See above.

Eq. 7 Again strictly speaking the quantity you need here is a concentration and not a density. Change the symbols as well.

We have modified the text according to the reviewer suggestion. Vapor density was replaced by **vapor concentration** and p_v by **C_v** , in the text, equations and tables. We also modified the definition of $c_{vap\ ini}^x$, to stress that it is not the same type of concentration as C_v . C_v has a unit (kg m^{-3}) whereas $c_{vap\ ini}^x$ is a ratio of mass and has no unit.

I. 1060:

$c_{vap\ ini}^x$ Ratio between the mass of a given isotopologue in the initial vapor (x is ^{18}O , ^{17}O , ^{16}O , ^1H or D) and the total mass of vapor (no unit). The mass balance is made separately

and independently for H and O (i.e.: $c_{vap\ ini}^{18} + c_{vap\ ini}^{17} + c_{vap\ ini}^{16} = 1$ and $c_{vap\ ini}^{1H} + c_{vap\ ini}^D = 1$).

P14L312 Consider using the term rare isotope instead of heavy isotope. Also using an index i is more appropriate than a * sign as later on in Eq. 8 and 9 you use “17”, “18” and “D” in the position of the * sign.

For the isotopes considered here, ‘heavy’ and ‘rare’ are interchangeable, without harm, but it is not necessarily the case for other isotopes. We will add a note on this matter in the manuscript.

We will also replace * by i in the equations as suggested by the reviewer.

Eq. 8 and 9

The term C_{vap}^i needs to be clarified both here and in Table 1. What I understand is that C_{vap}^i refers to isotope concentration as

$$C_{vap}^{16} = \frac{[H_2^{16}O]}{[H_2^{18}O] + [H_2^{17}O] + [H_2^{16}O]} = \frac{{}^{16}R}{{}^{18}R + {}^{17}R + {}^{16}R} = \frac{1}{{}^{18}R + {}^{17}R + 1} \quad (1)$$

(again (Mook , 2000) is a good source for definitions).

However later in Eq. 11 you seem to be using the same quantity for something slightly different, this time the masses ratio and not the abundancies ratio. Can you comment on that and make sure the definitions are clear to the reader? If needed add a definition equation in Table 1.

It is true that we make an approximation here. In the traditional equation to define the ratio of two isotopologues, molar concentrations are used. Here we approximate this ratio of molar concentrations by a ratio of masses. We thus neglect the molecular mass term ($g\ mol^{-1}$).

$$R^{18} = \frac{[H_2^{18}O]}{[H_2^{16}O]} \approx \frac{m_{vap}^{18}}{m_{vap}^{16}} = \frac{c_{vap\ ini}^{18} m_{vap}}{c_{vap\ ini}^{16} m_{vap}}$$

Our $c_{vap\ ini}^{18}$ is therefore also a mass ratio. It is the mass of the studied isotopologue in the porosity relative to the total mass of vapor in the porosity. We will modify the definition in Table 1 to make this clearer.

$c_{vap\ ini}^x$ **Ratio between the mass of a given isotopologue in the initial vapor (x is ^{18}O , ^{17}O , ^{16}O , 1H or D) and the total mass of vapor (no unit). The mass balance is made separately and independently for H and O (i.e.: $c_{vap\ ini}^{18} + c_{vap\ ini}^{17} + c_{vap\ ini}^{16} = 1$ and $c_{vap\ ini}^{1H} + c_{vap\ ini}^D = 1$).**

We will also add a remark in the text about this approximation:

I. 346: ‘The equilibrium fractionation coefficients (α_{subi}) are obtained using the temperature-based parameterization from Ellehoj et al. (2013). **Note that we make a slight approximation here, by replacing molar concentrations by massic concentrations in our mass balance formulas (see Table 1 for symbol definitions).**’

P14L319 I would be very interested to know why you have used the fractionation factors from (Ellehoj et al., 2013)

We used them because they are recent.

P14I329 This note concerns the use of the term kinetic fractionation throughout the whole manuscript. Kinetic effects refer to anything that is non-equilibrium. And indeed fractionation due to the different diffusivity coefficients for the different isotopologues is a type of kinetic fractionation. Though it is an overstatement to claim that you have included all possible kinetic fractionation processes by only using the ratio of the diffusivities. Fractionation effects related to different binding energies of the molecules for example can also be affected by a non-equilibrium/kinetic regime and this is something that is not addressed by the D^*/D term. I would suggest that you go through the manuscript and clarify this (term kinetic is used in pages 1, 13, 14, 16, 30, 42 and 43). I would also refer the authors to the sections 3.1 to 3.5 in vol. 1 of (Mook, 2000). Even though some of these definitions sound trivial I think the manuscript can benefit greatly by getting these small details right, thus avoiding misconceptions.

We will check the manuscript to make sure that this term is used correctly.

When only the ratio of diffusivity is taken into account, we will use the term 'a' before kinetic fractionation, to underline the fact that it is only one aspect of kinetic fractionation. Alternatively we will precise kinetic fractionation 'during diffusion' or 'during transport', to distinguish this from the kinetic fractionation associated for instance to binding.

Eq. 12 See previous comment on Eq. 4

The factor 2 comes from the distance between the center of the two considered layers (see above).

P15I353 "Here the condensation of excess vapor occurs without additional fractionation". Is this not unphysical. Can you comment?

Please see above.

P18I407 Rephrase the sentence. The term "oriented processes" (also used in 2.1.2) is not a technical term. From what I understand your use of the term "oriented processes" refers to advection-based processes that bias the isotopic signal. Diffusion is not such a process, it attenuates the isotopic signal and is driven by isotopic composition gradients as opposed to for example ventilation that is driven by a bulk motion of air in the open porosity. Additionally diffusion takes place for much longer than 12 m (depending on close-off depth) whereas the extent to which ventilation is apparent in polar firn can be debated.

We apologize for being unclear.

However, we **do** include diffusion driven by temperature gradients in the '**processes of oriented vapor transport**', which are **not necessarily** driven by advection. Here, diffusion is driven by the gradients of vapor concentration, and ultimately by the temperature gradients.

As already indicated above, 'oriented vapor transport' means that it is **forced by an external variable** (temperature, pressure) and not resulting from random molecular agitation.

Because temperature gradients are particularly strong in the upper part of the snowpack, and because the porosity is also larger at shallow depths, this **thermally induced diffusion** is mostly effective in the top meters of the snow.

We will amend the sentence to precise that we are talking here about thermally induced diffusion, and not diffusion along isotopic gradients.

l. 435: Typically, **processes of oriented vapor transport** such as **thermally induced diffusion** and ventilation occur mainly in the first meters of snow. **Therefore**, the model starts with an initial snowpack of about 12 m.

P18I414 “Thus the diffusion process can only be studied in the first 2 m of the model snowpack” Can you elaborate on this? Is it a computation time issue that does not allow for thinner layers below the top 2 m. How do the calculations look like below this depth?

Yes, we have set an upper limit to the number of layers (100) to limit computational time. However, splitting 12 meters of snow into equal pieces would have led to layers of 12 cm. These thick layers would not have been very useful to quantify attenuation of annual cycles which have shorter wavelength.

The various modules are still active in the next 10 meters, and vapor transport occurs, but the density changes and isotopic changes are much reduced because of the low temperature gradients, larger distances, and larger masses of the layers.

P19I432 Stick to one name for GRIP/Summit throughout the manuscript.

See above.

P19I445 Citing a published work (Bréant et al., 2017) dealing with the density studies at Dome C and GRIP is of course acceptable though the density profile here is of great importance for the diffusion calculations, therefore giving some more information and possibly figures would be appreciated.

See above.

Additionnally you give the density as a function of n and t where t (the model time) is an independent variable to z. Can you explain this a little bit better? How do Eq. 16 and 17 give you an evolution of the column density and the densification rates? Please also update the reference to the one past the review process, published in the Climate of the Past

- In the Crocus model, t and z are orthogonal (as observed on the various 2D graphs in the manuscript). ‘t’ corresponds to time evolution forward, over a few months or years. ‘z’ corresponds to the depth of a given layer (layer number is n). Of course, the depth ‘z’ of a given layer n will change with time because of compaction and deposition of new snow layers. Therefore, z depends on both n and t.

- The **initial density profile** is defined as a function of depth, but only at a given time $t=0$. So, in the equations (17) and (18), the density varies only with depth z, and depth varies only with layer number n, as t is fixed. We will amend the equations to make this clearer:

The initial density profile in the snowpack is obtained from fitting density measurements from Greenland and Antarctica (Bréant et al., 2016). Over the first 12 m of snow, we obtain the following

evolution (Eq. (17) and Eq. (18)) for GRIP and Dome C respectively:

$$\rho_{sn}(t=0, n) = 17.2 \cdot z(t=0, n) + 310. \quad (N=22; R^2=0.95) \quad (17)$$

$$\rho_{sn}(t=0, n) = 12.41 \times z(t=0, n) + 311.28 \quad (N=293; R^2=0.50)$$

(18)

- Equations (17) and (18) are not used elsewhere in the model (only at model initiation).
For $t > 0$, densification occurs based on Equations (3) and (4).

- NB: The NGRIP profile will be replaced by the GRIP profile in the revised version of the manuscript.

- We have updated the reference for Bréant et al., 2017.

P19I450 Earlier in the manuscript you mentioned that all diffusivity values are for a temperature of 263K. Does the isothermal profile at 241 K affect this and if yes how?

Please see above.

P20I457 In Table 2 you refer to a different work for the value of accumulation at GRIP. Be consistent and use only one reference.

We will keep the value of Dahl-Jensen et al. (1993) which was the original reference.

P20I457 You can be a bit more specific and call it “peak to peak amplitude”.

OK.

P20I461 Please refer to general comment nr. 1 with respect to the difference between “isotope firn diffusion” due to isotopic gradients in the snow/firn and signal attenuation/alteration because of air or vapor “bulk motion” driven by pressure or temperature gradients in the snow.

We have rephrased the sentence, and replaced ‘isotopic diffusion’ by ‘transport of isotopes’. Isotopes are indeed transported in both cases, either through diffusion along isotopic gradients or through the overall movement of water vapor forced by temperature gradients.

I. 502: ‘The second simulation is run with evolving temperature in the snowpack (computed by the model, using meteorological forcing from ERA-Interim, see Table 4). In that case, the **transport of isotopes** in the vapor phase results both from **diffusion along isotopic gradients** and from **vapor concentration gradients**. The initial snowpack’

P20I471 What does the term “densities” refer to here? Vapor densities (use term water vapor concentration instead) or firn densities. If it refers to firn densities can you be more specific about how your densification rates depend on temperature?

We are talking about the snow densities.

As already indicated above the compaction scheme is very simple here and taken to compensate yearly accumulation. It does not depend at all on the temperature.

However, the temperature and temperature gradients control the intensity of water vapor diffusion in the snowpack. Thus, layers with higher temperature will lose water and therefore density, because their thicknesses will not be modified during water vapor transport. Oppositely, colder layers will

receive more water vapor and their density will increase. This is really a result of the vapor transport module, and has nothing to do with compaction. It is not exactly a densification process, since layers can gain or lose mass.

Section 3.3.3 In my view this section is unnecessary, and its sole sentence can be included in the previous section.

OK. We moved the sentence to line 475, right after the section title.

P21I486 Is this peak to peak amplitude?? Also writing that maxima and minima are reduced sounds inaccurate. Attenuation would result in reduced maxima and increased minima, or in the difference between the two being lower. Lack of visual examples makes this type of language errors quite critical as they can be very confusing for the reader.

The reviewer is right, our sentence was imprecise. What we meant to say was that the amplitude was reduced, with the maximas decreasing and the minimas increasing. This attenuation is visible on panel (b) of the Figure 2.

This is the revised sentence:

l. 527: 'As expected **the peak to peak amplitude of $\delta^{18}\text{O}$ cycles is reduced** as a result of diffusion.'

P21I490 The description of the model in the previous sections suggests that the diffusivity coefficient is independent of temperature. It is not clear though if there is some dependancy of the diffusivity to temperature for your model experiments. One possible cause of the increased depletion for the upper few cm could also be that the firn appears to be quite warmer, something that would result in enhanced diffusion rates for these few cm of the firn column thus attenuating this part more compared to the layers below. I also miss some info on the density profile here and specifically the surface density.

- The uppermost millimeters of the snowpack are indeed warm, but a little colder than the layers around 2 cm depth. The fact that the temperature is high implies large vapor concentration and therefore effective vapor transport and reinforced attenuation. So, we agree with the reviewer that this elevated temperature facilitates vapor transport and attenuation. The reverse temperature gradient that we describe will act on top of the previous phenomenon, by moving vapor preferentially upwards, and therefore bringing also preferentially light isotopes to the very first layer. Both mechanisms could produce the depletion observed, and therefore, we consider the two explanations valid.

- The initial density profile is the same as in the previous simulation. See text:

l. 446: The initial density profiles are defined for each site specifically (see Sect. 3.2.).

l. 483: **The initial density** profile in the snowpack is obtained from fitting density measurements from Greenland and Antarctica (**Bréant et al., 2017**). Over the first 12 m of snow, we obtain the following evolution (**Eq. (17)** and **Eq. (18)**) for GRIP and Dome C respectively:

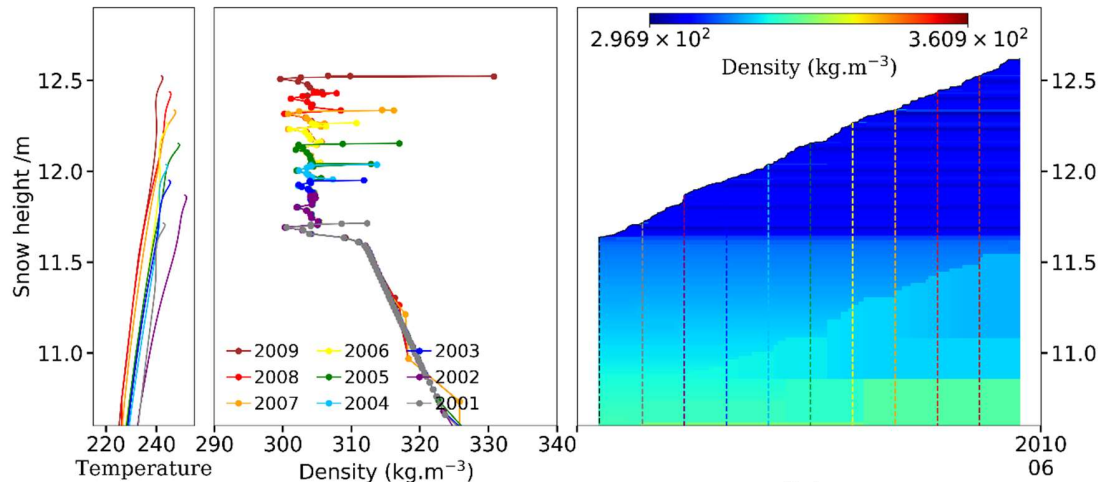
$$\rho_{sn}(t = 0, n) = 17.2 \cdot z(t = 0, n) + 310.3 \quad (N=22; R^2=0.95)$$

(17)

$$\rho_{sn}(t = 0, n) = 12.41 \times z(t = 0, n) + 311.28 \quad (N=293; R^2=0.50)$$

(18)

The first layer has therefore initially a density of 310.3 kg m^{-3} (or very close, depending on its thickness).



Supp. Figure: Evolution of snow density with time (Dome C, **Simulation 6**, D_{v0} varies). Initial density profile linear (black line). New layers deposited with a density of 304 kg m^{-3} . They gain mass due to vapor transfer as long as they are exposed. After burial, their density decreases again, as they are subject to alternating vapor fluxes (and the overall density is still close to 304 kg m^{-3}).

Section 4.1.2 This section lacks a proper description of the methods used in order to estimate the amplitude of the isotopic signal for the cores presented. In Johnsen et al. the amplitude of the annual signal is computed using a rather sophisticated modification of the Maximum Entropy Method where the annual signal spectral peak is integrated to give a value in permille. This of course is an estimate dependent on the initial isotopic signature (some years have a greater amplitude than others) and for this reason 5m intervals are considered in Johnsen et al. How is this analysis performed here? Can a 20cm interval produce satisfactory results when the layer thickness for these depths at NEEM is in the order of 50-60 cm? Also the term half-amplitude should be peak-amplitude or semi-amplitude.

The reviewer is right, using a 20-cm interval is not adapted at NEEM. For layers below 10 meters at this site, using this window is ok, because then the cycles have a period smaller than 40 cm, therefore the half-period between a given maxima and the following minima is smaller than 20 cm. For layers shallower than 10 meters a window of 30 cm would be better. We will update our methodology and Figure n°4, to correct this mistake: the window will be changed to 30 cm for layers above 10 meters, at NEEM and at GRIP.

I. 558: 'For NEEM the values of the four cores are taken together. For NEEM and GRIP, the semi-amplitude is computed along the core. **In the first 10 meters, the maximum value every 30 cm is retained, and deeper in the firn, the maximum value every 20 cm is retained (Fig. 4).** Maximum semi-amplitudes every 5 m are also computed.'

Note nonetheless that the ‘remaining amplitude’ was computed based on maximas obtained with a 1-meter window. Thus, updating the size of the smaller window should not modify our results and conclusions.

We will replace the term half-amplitude by semi-amplitude as suggested.

P22I513 GRIP is also slightly colder.

OK. But the temperature difference is quite small.

P22I520 This is a very good point. Temperature has a strong impact on the diffusivity coefficient. It is certainly relevant to consider various other processes that can be the cause to these discrepancies though a very simple test you could do here is to apply the Johnsen et al diffusivity parametrization in Crocus and compare the results.

This has been done, following the reviewer suggestion, and the results are presented above and will be integrated into the manuscript. The main impact on the diffusivity is not through the temperature, but through the pressure.

I am puzzled by the values that are given here for the firn diffusivity. These are much closer to air diffu values. Firn diffusivity values for $p = 350\text{kgm}^{-3}$ around the temperature of 241 K are orders of magnitude lower. I attach a plot of the Johnsen et al diffusivity for a range of temperatures. What is the reason for such a large difference? Fig. 1. Diffusivity in firn for O18 at $p = 350\text{kgm}^{-3}$

Unfortunately, we cannot see the Figure 1 mentioned.

However, we suppose that the reviewer is comparing our diffusivity in vapor phase D_{eff} to Johnsen et al.’s *isotopic* diffusivity in the ensemble {vapor + solid}, Ω_{fi} . The values are indeed very different, because the ensemble considered is not the same. It is much easier to move molecules around in the porosity, and homogenize it, than to move molecules around in the crystal lattice and homogenize it. Johnsen’s diffusivity integrates not only the diffusivity in vapor phase (which is very close to ours), but also an exchange step between vapor and solid, and evaluates in the end the timing of snow homogenization, not of vapor transport.

P23I530 It should be mentioned here that the van der Wel (Van der Wel et al., 2015) study is made by spraying a layer of isotopically spiked artificial snow on top of the natural Summit snow. Such experiments are extremely challenging and the approach of using artificial snow can potentially introduce artifacts with respect to the diffusion processes.

This is right. As stated by the authors themselves, the artificial snow obtained by snow gun may have different diffusivity properties compared to natural snow. However, the spike layer was only 2 cm thick and the diffusion process later continued into the natural snowpack, both downward and upward. So, at some distance from the artificial layer, the diffusion properties are probably back to natural.

The authors discuss this at length in the paper, and conclude that the discrepancy between their data and the Johnsen’s et al. model prediction cannot be explained by reduced diffusion in the artificial layer. Indeed, they systematically remove the data from this layer from their computations. And while looking at the time evolution of diffusion length, the discrepancy increases, even if the layers considered

are further and further away from the artificial layer region. So, it is not the artificial layer that is responsible for the discrepancy.

We will however add a note in the manuscript regarding this question, as recommended by the reviewer.

I. 594: ‘**Van der Wel et al. (2015) have compared the model results to a spike-layer experiment realized at Summit. Because an artificial snow layer cannot be representative of natural diffusion, they took care to evaluate diffusion based only on the natural layers present above and below the artificial layer.**’

P23I548 Perhaps you can slightly rephrase as “..are required to observe significant change in densities due to vapor transport at the seasonal cycle”.

We have modified the text according to the reviewer suggestion.

P24-25 The numbers of the experiments should be stated for clarity in the subsection titles or very soon after in the main body of each subsection.

OK.

P25I585 It is a little bit unclear here why and how the precipitation intermittency results in a biasing of the isotopic signal (from -53.2 ‰ to -49.8 ‰). I can see how the winter precipitation events are biased towards warmer temperatures and more enriched $\delta^{18}\text{O}$ values but cannot understand how this creates an additional bias in the isotopic composition of the snow.

We were imprecise here. What we call (wrongly) initial signal in the precipitation is the expected values in the precipitation if precipitation was falling every day at the same rate. It is based on the temperature data, and not on the actual precipitation amount.

This is what we meant by ‘constant precipitation throughout the year’, I. 622.

We will correct the sentence to clarify our meaning:

I. 638: ‘**Based on the atmospheric temperature variations only, the isotopic composition in the precipitation should vary around an average value of -53.2 ‰, with a semi-amplitude of 8.6 ‰. The main reason for this difference is the precipitation amounts: large precipitation events in winter are associated with relatively high $\delta^{18}\text{O}$ values. The vertical resolution chosen for the model of 2.5 cm may also contribute to the decrease of the semi-amplitude. Indeed, light snowfall events do not result in the production of a new surface layer, but are integrated into the old surface layer.**’

P25I590 “As expected the maxima and the minima of $\delta^{18}\text{O}$ are further reduced as a result...”
A more precise and careful writing would be very much appreciated. What does this sentence mean? Is this a decrease of the whole $\delta^{18}\text{O}$ signal, a decrease in the peak to peak amplitude of the signal or a decrease in only the minimum and the maximum of the signal?

As above, what we meant was that the amplitude decreases, because minimas are increasing and maximas are decreasing. We will correct the sentence to clarify our meaning.

I. 643: ‘**As expected, the peak to peak amplitude of $\delta^{18}\text{O}$ variations is further reduced...**’

Additionally (see also general comments) you can technically not have isotopic diffusion because of temperature gradients. The latter can indeed create water vapor concentration gradients that will result in diffusive transport of all water vapor molecules. This is though not the same process as isotope diffusion.

Here, both vapor diffusion **caused by temperature gradients** and vapor diffusion **caused by isotopic gradients** are active. While diffusion along isotopic gradients will certainly lead to attenuation, the influence of the second process is more difficult to predict. It is possible that this process contributes to the observed attenuation, at least partially, as is the case for Greenland. The global effect of the two vapor diffusion processes seems to be an attenuation of the original signal.

We will modify the sentence to remove ambiguity here:

l. 643: 'As expected, the **peak to peak amplitude of $\delta^{18}\text{O}$ variations** is further reduced as a result of the **two vapor diffusion processes and of associated vapor/solid exchanges.**'

P26l600 It is very difficult for the reader to follow the discussion of this paragraph when no access is given to the $\delta^{18}\text{O}$ profiles pre and after diffusion. The approach of using contour plots or tracking single layers does not give a good picture of the initial conditions and the evolution of the simulation experiments. Even when those plots are presented they only cover the top 40-50 cm of the studied snow-firn column. As a result, referring to gradients of for example 24 ‰/m feels as an irrelevant piece of information.

It is not clear to us what should be modified here.

1) The initial $\delta^{18}\text{O}$ profile at the beginning of the simulation is without interest, since the initial snowpack has an homogeneous $\delta^{18}\text{O}$ value of -40 ‰.

2) Moreover, vertical profiles of $\delta^{18}\text{O}$ are presented at the beginning of each new year on panel (b). By comparing these profiles together, it is already apparent that the maximas are reduced from one year to the next (and that the minimas are increased). Therefore, we ARE presenting profiles before and after diffusion. We also think that including the panel (d) help to better visualize this attenuation.

3) Another possibility would be to present profiles that follow a diagonal on the 2D graph. For instance, we could present a diagonal profile for the isotopic composition over the first week after precipitation, for all the layers, to present 'original' isotopic composition, and then a second one, for the layer composition after say 5 years of existence. Is this what the reviewer is aiming at?

4) Again, presenting what is happening downwards (below 40 cm) has no interest since the layers are isotopically homogeneous (so attenuation is unlikely).

5) We can indeed convert the gradient into another unit, such as ‰/cm, to be more coherent with our layer thicknesses.

l. 658: 'low vertical gradients of $\delta^{18}\text{O}$ of the order of **0.24 ‰ cm⁻¹**, much smaller than the typical $\delta^{18}\text{O}$ gradients at Dome C (**1.10 ‰ cm⁻¹**).'

As stated above we will add in the Supplement a 2D plot of the temperature over the same period. This could help the reader to understand the conditions of the simulation.

P26l605 Indeed lower temperatures will slow down diffusive fluxes. This though can only be modelled if the diffusivity coefficient is temperature dependent something that is not the case for this study. Can you comment on this?

As explained above, the temperature also acts on diffusion by increasing the amount of water vapor available, and not only through diffusivity.

P26I607 Which other parameters are loosely estimated? When the term “large uncertainty” is used it is only logical for the reader to ask how large is the uncertainty.

The two parameters that are loosely estimated are τ and $\Delta t_{\text{surf/center}}$. We will clarify this in the text.

In this section we explore a range of possible values for both parameters, to evaluate how they affect the results and especially the attenuation. It was an error to state in advance that these parameters bring large uncertainty, because the situation is different for Dome C and GRIP, and because for GRIP the attenuation is increased only by one third. Thus, we will remove this assertion from the text, and simply say that these parameters lead to uncertainty on the simulation result. The rest of the section brings answers on this uncertainty.

I. 662: ‘In parallel, the parameters of the model associated to grain renewal (τ and $\Delta t_{\text{gsurf/center}}$), could only loosely be estimated leading to uncertainty in the attenuation modeling.’

P28I644 Replace badly with poorly.

OK.

P28I645 Being able to implement more processes in a model sounds in principle as a step forward. However I think that a discussion on improving on the knowledge, assumptions and parameters used in the more dominating processes of diffusion is missing here. Integration of more processes that are poorly implemented can be misleading and give the false impression of an improved approach for the description of the problem. With this in mind I think that a comment on proposed improvements, measurements and proper tests with real data would be most welcome in this manuscript especially if it focuses on the more dominating processes of the problem.

Before testing them, it is difficult to decide which aspect of the problem is dominant. It may indeed be diffusion but we cannot be sure of that, especially since the model simulation falls short of reproducing attenuation observed in the data. Therefore, listing other processes potentially active (and maybe even dominant) seems logical here.

The present article aimed only at presenting the model modifications and its possible applications. But comparisons to real data is of course a necessary follow-up to the present paper. For instance, it would be nice to compare model results to on-site experiments on diffusion, such as the one by van der Wel et al. (2015).

We will add a remark on this in section 4.4, stating that the model should be improved not only by adding more processes but also by better constraining diffusion with real data.

I. 702: ‘To improve the model compatibility with data, two kinds of approaches are possible. On the one hand, it would be useful to realize simulations adapted to on-site experiments such as the one by van der Wel et al. (2015). This would allow to verify how diffusion can be improved in the model. For instance, previous studies have suggested that water vapor diffusivity within the snow porosity may be underestimated by a factor of 5 (Colbeck, 1983), but this is debated (Calonne et al., 2014). On the other hand, we also believe that other processes...’

P28I660 The top 10 m of snow may have been modelled in this study but results only the top 0.5 m are presented here. Thus I think this sentence should be rephrased in order to reflect the actual results presented in the study.

We will modify the sentence:

I. 723: 'Water vapor transport and water isotopes have been implemented in the Crocus snow model enabling depicting the temporal $\delta^{18}\text{O}$ variations in the **top 50 cm** of the snow in response to new precipitation, evolution of temperature gradient in the snow and densification.'

P29I675 Refer to my general comments on the GRIP case.

See above.

4 Comments on figures

Figures of experiments results

The experiment number should be included in the captions and titles of all relevant figures.

We added the information in the captions. Our figures do not have a title, only axes titles, which will not be modified.

Color maps of figures The color maps of the density and $\delta^{18}\text{O}$ change plots can become more readable if there is also some information about where the zero value is. I assume it is the white but cannot tell with certainty.

Yes, this is right. We have added a line to clarify this point.

I. 453: 'The variations of the considered variable are displayed as color levels. **The white color corresponds to an absence of change of the variable. As'**

Density and O18 change plots I find these plots confusing and not intuitive. The meaning of the term "density change" and " $\delta^{18}\text{O}$ change" appears only in the caption of fig. 7 and 8. It is very hard for the reader to understand what this change refers to. My impression until I reached figure 7 and 8 was that these were rates ie change per time. Please clarify in the main text and on the legends of the figures.

For Figure 2 and 3, the term ' $\delta^{18}\text{O}$ change' is already defined in the caption: it is the **deviation to the original profile of $\delta^{18}\text{O}$** .

For Figure 5: We indicated that the density change was 'cumulative'. This may not be very explicit for the reader. We will complete the explanation with the following sentence:

(in supplement) '**Here, 'density change' stands for the difference between density at t and at the beginning of the simulation for the selected layer.'**

We do the same for $\delta^{18}\text{O}$ on Figure 6:

I. 1127: '**Here, ' $\delta^{18}\text{O}$ change' stands for the difference between $\delta^{18}\text{O}$ at t and at the beginning of the simulation for the selected layer.'**

For Figure 7 to 10, the caption already contained the necessary information.

Figure 11: The original figure was indeed difficult to apprehend. Here, the initial profile was homogeneous, with $\delta^{18}\text{O}$ values of -40 ‰ at all depths. We had decided to use this value as reference and plot ' $\delta^{18}\text{O}$ change' simply as the simulated value of $\delta^{18}\text{O}$ minus -40 ‰. Thus, the values of -18 and -2 present on the colorbar corresponded to $\delta^{18}\text{O}$ values of -58 ‰ and -42 ‰.

To make this figure easier to understand, we will remove the term ' $\delta^{18}\text{O}$ change' and replace it by ' $\delta^{18}\text{O}$ '. We will therefore change the values to -58 ‰ and -42 ‰ on the colorbar.

The caption will be modified accordingly:

I. 1147: **Simulation 6: Evolution of $\delta^{18}\text{O}_{\text{gcenter}}$ values as a result of snowfall and vapor transport over 10 years (compaction is inactive; merging between layers is allowed but limited). (a) Temperature profiles at mid-January for each year. (b) $\delta^{18}\text{O}_{\text{gcenter}}$ profile at mid-January for each year. (c) Repartition of $\delta^{18}\text{O}_{\text{gcenter}}$ values as a function of time and depth. d) Evolution of $\delta^{18}\text{O}_{\text{gcenter}}$**

C20 Figure 11 It is odd that while the slope for the 2000 winter layer is opposite to the other summer layers and you choose to comment on this, the scale of the axis for these data is inverted thus visually "masking" the event. I would really not mind if the lines end up crossing each other if all axes are plotted in the same way.

OK, we will modify the Figure 11 as suggested.

References

C. Bréant, P. Martinerie, A. Orsi, L. Arnaud, and A. Landais. Modelling firn thickness evolution during the last deglaciation: constraints on sensitivity to temperature and impurities. *Clim. Past*, 13(7):833–853, July 2017.

M. D. Ellehoj, H. C. Steen-Larsen, S. J. Johnsen, and M. B. Madsen. Ice-vapor equilibrium fractionation factor of hydrogen and oxygen isotopes: Experimental investigations and implications for stable water isotope studies. *Rapid Commun. Mass Spectrom.*, 27(19):2149–2158, 2013.

S. J. Johnsen, H. B. Clausen, K. M. Cuffey, G. Hoffmann, J. Schwander, and T. Creyts. Diffusion of stable isotopes in polar firn and ice. the isotope effect in firn diffusion. In T. Hondoh, editor, *Physics of Ice Core Records*, pages 121–140, Sapporo, 2000. Hokkaido University Press. W. Mook. *Environmental Isotopes in the Hydrological Cycle: Principles and Applications*, vol. I, IAEA. Unesco and IAEA, 2000.

M. S. Town, S. G. Warren, V. P. Walden, and E. D. Waddington. Effect of atmospheric water vapor on modification of stable isotopes in near-surface snow on ice sheets. *Journal of Geophysical Research-atmospheres*, 113:D24303, December 2008.

L. G. van der Wel, H. A. Been, R. S. W. van de Wal, C. J. P. P. Smeets, and H. A. J. Meijer. Constraints on the D_h diffusion rate in firn from field measurements at summit, Greenland. *The Cryosphere*, 9(3):1089–1103, May 2015.

Albert, M. R., & McGilvary, W. R. (1992). Thermal effects due to air flow and vapor transport in dry snow. *Journal of Glaciology*, 38(129), 273–281

Flin, F. and J.-B. Brzoska, 2008. The temperature gradient metamorphism of snow : vapour diffusion model and application to tomographic images, *Ann. Glaciol.*, 49, 17–21, doi :

10.3189/172756408787814834.

Landais, A., Casado, C., Prié, F., Magand, O., Arnaud, L., Ekaykin, A., Petit, J.-R., Picard, G., Fily, M., Minster, B., Touzeau, A., Goursaud, S., Masson-Delmotte, V., Jouzel, J., Orsi, A., 2017. Surface studies of water isotopes in Antarctica for quantitative interpretation of deep ice core data, *Comptes Rendus Géosciences*, 349, 139-150.

Numerical experiments on vapor diffusion in polar snow and firn and its impact on isotopes using the multi-layer energy balance model Crocus in SURFEX V8.0

Alexandra Touzeau¹, Amaëlle Landais¹, Samuel Morin², Laurent Arnaud³, Ghislain Picard³

¹LSCE, CNRS UMR8212, UVSQ, Université Paris-Saclay, Gif-sur-Yvette, 91191, France

²Météo-France - CNRS, CNRM UMR3589, Centre d'Etudes de la Neige, Grenoble, France

³IGE, CNRS UMR5183, Université Grenoble Alpes, Grenoble, France

Correspondence to: Alexandra Touzeau (alexandra.touzeau@uib.no)

Abstract.

To evaluate the impact of vapor diffusion onto isotopic composition variations in the snow pits and then in ice cores, we introduced water isotopes in the detailed snowpack model Crocus. At each step and for each snow layer, 1) the initial isotopic composition of vapor is taken at equilibrium with solid phase, 2) a kinetic fractionation is applied during transport, and 3) vapor is condensed or snow is sublimated to compensate deviation to vapor pressure at saturation.

We study the different effects of temperature gradient, compaction, wind compaction and precipitation on the final vertical isotopic profiles. We also run complete simulations of vapor diffusion along isotopic gradients and of vapor diffusion driven by temperature gradients at GRIP, Greenland and at Dome C, Antarctica over periods of 1 or 10 years. The vapor diffusion tends to smooth the original seasonal signal, with an attenuation of 7 % to 12 % of the original signal over 10 years at GRIP. This is smaller than the observed attenuation in ice cores, indicating that the model attenuation due to diffusion is underestimated or that other processes, such as ventilation, influence attenuation. At Dome C, the attenuation is stronger (18 %), probably because of the lower accumulation and stronger $\delta^{18}\text{O}$ gradients.

1 Introduction

The isotopic ratios of oxygen or deuterium measured in ice cores have been used for a long time to reconstruct the evolution of temperature over the Quaternary (EPICA comm. members, 2004; Johnsen et al., 1995; Jones

et al., 2018; Jouzel et al., 2007; Kawamura et al., 2007; Lorius et al., 1985; Petit et al., 1999; Schneider et al., 2006; Stenni et al., 2004; Stenni et al., 2011; Uemura et al., 2012; WAIS-Divide members, 2013). They are however subject to alteration during post-deposition through various processes. Consequently, even if the link between temperature and isotopic composition of the precipitations is quantitatively determined from measurements and modelling studies (Stenni et al., 2016; Goursaud et al., 2017), it cannot faithfully be applied to reconstruction of past temperature. Nevertheless, ice cores remain a primary climatic archive for the Southern Hemisphere where continental archives are rare (Mann and Jones, 2003). In Antarctica, where meteorological records only started in the 1950s (Genthon et al., 2013), they provide useful information for understanding climate variability (e.g. EPICA comm. members, 2006; Shaheen et al., 2013; Steig, 2006; Stenni et al., 2011) and recent climate change (e.g. Altnau et al., 2015; Schneider et al., 2006). When using ice cores for past climate reconstruction, other parameters than temperature at condensation influence the isotopic compositions and must be considered. Humidity and temperature in the region of evaporation (Landais et al., 2008; Masson-Delmotte et al., 2011), or the seasonality of precipitation (Delmotte et al., 2000; Sime et al., 2008; Laepple et al., 2011) should be taken into account. In addition, uneven accumulation in time and space introduces **stratigraphic noise** (Ekaykin et al., 2009). Indeed, records from adjacent snow pits have been shown to be markedly different, under the influence of decameter-scale local effects **such as** wind redeposition of snow, erosion, compaction, **and** metamorphism (Ekaykin et al., 2014; Petit et al., 1982). These local effects reduce **the signal/noise** ratio. Then only stacking **a series of records from snow pits** can eliminate this local variability and yield information relevant to recent climate variations (Fisher and Koerner, 1994; Hoshina et al., 2014; Ekaykin et al., 2014; Altnau et al., 2015). This concern is particularly significant in central regions of east Antarctica characterized by accumulation rates **lower than** 100 mm **water equivalent** per year (van de Berg et al., 2006). **There**, strong winds can scour and erode snow layer over depths larger than the annual accumulation (Frezzotti et al., 2005; Morse et al., 1999; Libois et al., 2014). There is thus a strong need to study post-deposition effects in these cold and dry regions.

Additionally to **mechanical reworking** of the snow, the isotopic compositions are further modified in the snowpack. First, diffusion **along** isotopic gradients can occur within **the snow grains due to solid diffusion** (Ramseier et al., 1967). Second, within the porosity, the vapor isotopic composition can change due to: **1) diffusion along** isotopic gradients **in gaseous state**, **2) thermally induced** vapor transport caused by **vapor pressure gradients**, **3) ventilation**

in gaseous state, or 4) exchanges between the gas phase and the solid phase i.e. sublimation and condensation. In the porosity, the combination of diffusion along isotopic gradients in the vapor and of exchange between vapor and the solid phase has been suggested to be the main explanation to the smoothing of the isotopic signal in the solid phase (Ebner et al., 2016, 2017; Gkinis et al., 2014; Johnsen et al., 2000). The isotopic compositions in the solid phase is also modified by ‘dry metamorphism’ and ‘ventilation’ but in a less predictable way. In both cases, the vapor transport exerts an influence on the isotopic compositions in the solid phase because of permanent exchanges between solid and vapor. During ‘dry metamorphism’ (Colbeck et al., 1983), vapor transport is driven by vapor pressure gradients, themselves caused by temperature gradients. During ventilation (Town et al., 2008), vapor moves as part of the air in the porosity, because of pressure variations at the surface. Last, at the top of the snowpack, the isotopic composition of snow may also be modified through direct exchange with atmospheric vapor (Ritter et al., 2016).

To elucidate the impact of these various post-deposition processes on the snow isotopic compositions, numerical models are powerful tools. They allow one to discriminate between processes and test their impact one at a time. Indeed, Johnsen et al. (2000) were able to simulate and deconvolute the influence of diffusion along isotopic gradients in the vapor at two Greenland ice-core sites, GRIP and NGRIP, using a numerical model. To do this, they define a quantity named ‘diffusion length’ which is the mean displacement of a water molecule during its residence time in the porosity. Using a thinning model and an equation of diffusivity of the water isotopes in snow, they compute this diffusion length as a function of depth. It is then used to compute the attenuation ratio A/A_0 , and in the end retrieve the original amplitude A_0 . Additionally, the effect of forced ventilation was investigated by Neumann (2003) and Town et al. (2008) using similar multi-layer numerical models. In these models, wind-driven ventilation forces atmospheric vapor into snow. There, the vapor is condensed especially in layers colder than the atmosphere. We focus on the movement of water isotopes in the vapor phase in the porosity, in the absence of macroscopic air movement. In that situation, the movement of vapor molecules in the porosity is caused by vapor pressure gradients, or by diffusion along isotopic gradients. Note that in the first case, the vapor transport is ‘thermally induced’ i.e. the vapor pressure gradients directly result from temperature gradients within the snowpack. Thus, the first prerequisite of our model is to correctly simulate macroscopic energy transfer within the snowpack and energy exchange at the surface.

The transport of vapor molecules will affect the isotopic composition in the solid phase only if exchanges between vapor and solid are also implemented. Thus, the second prerequisite is that the model includes a description of the snow microstructure, and of its evolution in time. Snow microstructure is typically represented by its emerging scalar properties such as density, specific surface area and higher order terms often referred to as “shape parameters” (e.g. Krol and Löwe, 2016). While the concept of “grain” bears ambiguity, it is a widely used term in snow science and glaciology which we here employ as a surrogate for “elementary microstructure element”, without explicit reference to a formal definition, be it crystallographic or geometrical.

Crocus is a unidimensional multi-layer model of snowpack with a typically centimetric resolution initially dedicated to the numerical simulation of snow in temperate regions (Brun et al., 1992). It describes the evolution of the snow microstructure driven by temperature and temperature gradients during dry snow metamorphism, using semi-empirical variables and laws. It has been used for ice-sheets conditions in polar regions, both Greenland and Antarctica (Brun et al., 2011; Lefebvre et al., 2003; Fréville et al., 2013; Libois et al., 2014, 2015). In these regions, it gives realistic predictions of density and snow type profiles (Brun et al., 1992; Vionnet et al., 2012), snow temperature profile (Brun et al., 2011) and snow specific surface area and permeability (Carmagnola et al., 2014; Domine et al., 2013). It has been recently optimized for application to conditions prevailing at Dome C, Antarctica (Libois et al., 2014). This was necessary to account for specific conditions such as high snow density values at the surface and low precipitation amounts.

The Crocus model has high vertical spatial resolution and also includes interactive simulation of snow metamorphism in near-surface snow and firn. Therefore, it is a good basis for the study of post-deposition effects in low accumulation regions. For the purpose of this study, we thus implemented vapor transport resulting from temperature gradients and the water isotopes dynamics into the Crocus model. This article presents this double implementation, and a series of sensitivity tests. A perfect match of observations is not anticipated, in part because not all relevant processes are represented in the model. This study represents thus a first step towards better understanding the impact of diffusion driven by temperature gradients on the snow isotopic composition.

2 Physical basis

The isotopic composition of the snow can evolve after deposition due to several processes. Here, we first **give a brief overview** of such processes at the macroscopic level. **Section 2.1 thus deals** with modification of the isotopic composition of a centimetric/decametric snow layer after exchanges with the other **layers**. Second, we consider the evolution of the isotopic composition at the microscopic level, i.e. at the level of the microstructure. Indeed, the macroscopic change of the isotopic composition results from both large scale and small-scale processes. For instance, dry metamorphism includes both vapor transport from one layer to another, and vapor/ice grain exchange inside a layer.

2.1 Evolution of the snow layers composition at the macroscopic scale

Several studies address the evolution of the isotopic compositions in the snow column after deposition. **Here we describe first processes leading only to attenuation of the original amplitude (Sect. 2.1.1). Then we describe processes which lead to other types of signal modifications (Sect. 2.1.2). These modifications result from transportation and accumulation of heavy or light isotopes in some layers without any link to the original isotopic signal. In some cases, the mean $\delta^{18}\text{O}$ value of the snow deposited can also be modified.**

2.1.1 Signal attenuation on a vertical profile: smoothing

In this Section we consider processes leading only to attenuation of the original amplitude of the $\delta^{18}\text{O}$ signal by smoothing. We define the mean local pluriannual value as the average isotopic composition in the precipitation taken over 10 years. The smoothing processes, which act only on signal variability, do not modify this average value. Within the snow layers, the smoothing of isotopic compositions is caused by diffusion **along** isotopic gradients in vapor phase and in solid phase. The magnitude of smoothing depends on site temperature, and on accumulation. Indeed, higher temperatures correspond to higher **vapor concentrations**, and higher diffusivities in the vapor and solid phases. Oppositely, high accumulation rates ensure a greater separation between seasonal $\delta^{18}\text{O}$ peaks (Ekaykin et al., 2009; Johnsen et al., 1977) thereby limiting the impact of diffusion. **They also result in increased densification rates, and therefore reduced diffusivities (Gkinis et al., 2014).** Because sites with high accumulation rates also usually have higher temperatures, the resulting effect on diffusion is still unclear. These two competing effects should be thoroughly investigated and Johnsen et al. (2000) displays the damping amplitude of a periodic signal depending

on wavelength and on diffusion length, strongly driven by temperature.

In Greenland, Johnsen et al. (1977) indicate that **annual cycles generally disappear at depths shallower than 100 m for sites with accumulation lower than 200 kg m⁻² yr⁻¹**. Diffusion **along** isotopic gradients exists throughout the entire snow/ice column. **It occurs mainly in the vapor phase in the firn, especially in the upper layers with larger porosities. After pore closure, it takes place mostly in the solid phase, at a much slower rate. Note that in the solid phase, all isotopes have the same diffusion coefficient.**

2.1.2 Signal shift caused by processes leading to oriented vapor transport

We consider here the **oriented movement** of water molecules forced by external variables such as temperature or pressure. **We use the term ‘oriented’ here to describe an overall movement of water molecules that is different from their molecular agitation, and externally forced.** Three processes can contribute to **oriented vapor transport** and hence possible isotopic modification within the snowpack: diffusion, convection, and ventilation (Albert et al., 2002). **Brun et Touvier (1987) have demonstrated that convection of dry air within the snow occurs only in case of very low snow density of the order of ~100 kg/m³. These conditions are generally not encountered in Antarctic snow and therefore convection is not considered here.** Bartelt et al. (2004) also indicate that energy transfer by advection is negligible compared to energy transfer by conduction in the first meters of the snowpack. The two other processes, ventilation and diffusion are forced respectively by variations of the surface pressure and surface temperature. In the first case, the interaction between wind and surface roughness is responsible for wind-pumping, i.e. renewal of the air of the porosity through macroscopic air movement (Albert et al., 2002; Colbeck, 1989, Neumann et al., 2004). In the second case, air temperature diurnal or seasonal variations generate vertical temperature gradients within the snow (Albert and McGilvary, 1992; Colbeck, 1983). **They result into vertical vapor pressure gradients,** responsible for vapor diffusion. These two processes are largely exclusive (Town et al., 2008) because strong ventilation homogenize the air and vapor in the porosity and therefore prevents diffusion. Diffusion as a result of temperature gradients can coexist with ventilation only at very low air velocities (Calonne et al., 2015). It becomes the main process of vapor transport when air is stagnant in the porosity. **During diffusion, lighter molecules move more quickly in the porosity, leading to a kinetic fractionation of the various isotopologues.**

2.2 Evolution of the isotopic composition at the microscopic scale

2.2.1 Conceptual representation of snow microstructure as spherical grains

The term “snow grain” as used classically is an approximation. In reality, ‘snow grains’ are very diverse in size, shape, degree of metamorphism and may also be made of several snow crystals agglomerated. Moreover, they are often connected to each other, forming an ice matrix, **or ‘snow microstructure’**. However, several studies addressing snow metamorphism physical processes have relied on spherical ice elements to represent snow grains and snow microstructure (Legagneux and Domine, 2005; Flanner and Zender, 2006). Here, we consider that the snow grains are made of two concentric layers, **one internal and one external**, with different isotopic compositions. In terms of snow microstructure, this could correspond to inner vs. outer regions of the snow microstructure.

Indeed, the snow grain **or microstructure** is not necessarily homogeneous in terms of isotopic composition. On the one hand, the central part of the grain **or of** the microstructure is relatively insulated. **This central part** becomes even more insulated as the grain grows, **or as** the structure gets coarser. On the other hand, outer layers are not necessarily formed at the same **time as the central part**, or in the same environment (Lu and DePaolo, 2016). They are prone to subsequent sublimation or condensation of water molecules, implying that their composition **varies more frequently than for** the inner layers. Of course, only the bulk $\delta^{18}\text{O}$ value of the snow grain can be measured by mass spectrometry. **But** considering the heterogeneity of the grain may be required to get a fine understanding of the processes. In the following, we propose to split the ice grain compartment into two sub-compartments: grain surface and grain center. Thus, the grain surface isotopic composition **evolves** because of exchange **with two compartments**: 1) with vapor in the **porosity through** sublimation or condensation, and 2) with grain center **through solid diffusion**, or grain center translation. The grain center composition evolves at the time scale of week/month, as opposed to the grain surface, where the composition **changes** at the time scale of the vapor diffusion, i.e. over minutes.

2.2.2 Solid diffusion within snow grains

The grain center isotopic composition may change either as a result of crystal growth/sublimation or as a result of solid diffusion within the grain. **For solid diffusion, water molecules move in the crystal lattice through a vacancy mechanism, in a process of self-diffusion that has no particular direction, and that is very slow.** The diffusivity of water molecules in solid ice D_{ice} in $\text{m}^2\cdot\text{s}^{-1}$ follows Arrhenius **law. Thus, it** can be expressed as a

function of ice temperature T (Gkinis et al., 2014; Johnsen et al., 2000; Ramseier, 1967) using Eq. (1):

$$D_{ice} = 9.2 \cdot 10^{-4} \times \exp\left(\frac{-7186}{T}\right) \quad (1)$$

where symbols are listed in Table 1.

Thus at 230 K, the diffusivity is $2.5 \times 10^{-17} \text{ m}^2 \cdot \text{s}^{-1}$. **Gay et al. (2002) indicate that in the first meter at Dome C, a typical snow grain has a radius of 0.1 mm. Across this typical snow grain, the characteristic time for diffusion is given by Eq. (2):**

$$\Delta t_{sol} = \frac{R_{moy}^2}{D_{ice}} = 4.03 \times 10^8 \text{ s, or } \sim 13 \text{ years} \quad (2)$$

Therefore, the solid diffusion **within** the grain is close to zero at the time scales considered in the model. For Dome C, **if we use the average temperature T of 248 K for the summer months (Dec. to Jan., Table 2),** the characteristic time becomes 15 months. **Thus, within a summer period, the snow grain is only partially refreshed through this process.** At Summit the grain size is typically larger, **from 0.2 to 0.25 mm** in wind-blown and wind pack and **from 0.5 to 2 mm** in the depth hoar layer (Albert and Shultz, 2002). The summer temperature is also higher, with an average value **T of 259 K at Summit from July to Sept,** after Shuman et al. (2001). **Using a grain size of 0.25 mm, the resulting characteristic time is of the order of 30 months.**

2.2.3 Snow grain recrystallization

During snow metamorphism, the number of snow grains tends to decrease with time, while the snow grain size tends to increase (Colbeck, 1983). Indeed, each grain experiences **continuous recycling through** sublimation/condensation, but the small grains are more likely to disappear completely. **Then,** there is no more nucleus for condensation at the grain initial position. Oppositely, the bigger grains do not disappear and accumulate the vapor released by the smaller ones. Concurrently to this change of grain size, the grain shape also tends to evolve. In conditions of maintained/stable temperature gradient, facets appear at the condensing end of snow grains, while the sublimating end becomes rounded (Colbeck, 1983). In that case, the center of the grain moves toward the warm air region. This migration causes a renewal of the grain center, on a proportion that can be estimated from the apparent grain displacement (Pinzer et al., 2012). Pinzer et al. (2012) use this method to **obtain** an estimation of vapor fluxes.

The asymmetric recrystallization of snow grains implies that the surface layer of the snow grain is eroded at one end and buried at the other end. Therefore, the composition of the grain center changes more often than if the surface layer

was **thickening through condensation or thinning through sublimation** homogeneously over the grain surface. This means that the ‘inner core’ of the grain gets exposed more often. Implementing this process is thus very important to have a real-time evolution of the snow grain center isotopic composition. Here, we reverse the method of Pinzer et al. (2012). Therefore, we use the fluxes of isotopes in vapor phase computed by the model to assess the renewal of the grain center (Sect. 3.1.3.).

3 Material and Methods

3.1 Description of the model **SURFEX/Crocus V8.0**

We first present the model structure and second describe the new module of vapor transport (diffusion forced by temperature gradients). Third, we present the integration of water isotopes in the model.

3.1.1 Model structure

The Crocus model is a one-dimensional detailed snowpack model, consisting of a series of snow layers with variable and evolving thicknesses. Each layer is characterized by its density, heat content, and by parameters describing snow **microstructure such as** sphericity and specific surface area (Vionnet et al., 2012, Carmagnola et al., 2014). In the model, the profile of temperature evolves with time in response to 1) surface temperature and 2) energy fluxes at the surface **and at the base of** the snowpack. To correctly compute energy balance, the model integrates albedo calculation, deduced from surface microstructure and impurity content (Brun et al., 1992, Vionnet et al., 2012).

The successive components of the Crocus model have been described by Vionnet et al. (2012). Here we only list them to describe those modified to include water stable isotopes and water vapor transfer. Note that the Crocus model has a typical internal time step of 900 s (15 min), corresponding to the update frequency of layers properties. We only refer here to processes occurring in dry snow.

1) Snow fall: The presence/absence of precipitation at a given time is determined from the atmospheric forcing inputs. When there is precipitation, a new layer of snow may be **formed. Its thickness** is deduced from the precipitation amount.

2) Update of snow layering: At each step, the model may split one layer into two or merge two layers together to get closer to a target vertical profile for optimal calculations. **This target profile has high** resolution in the first

layers to correctly simulate heat and matter exchanges. The layers that are merged together are the closest in terms of microstructure variables.

3) Metamorphism: The microstructure variables evolution follows empirical laws. These laws describe the change of grain parameters as a function of temperature, temperature gradient, snow density and liquid water content.

4) Snow compaction: **Layer thickness decreases, and layer density increases** under the burden of the overlying layers and resulting from metamorphism. **In the original module, snow** viscosity is parameterized using the layer density and also using information on the presence of hoar or liquid water. However, this parameterization of the viscosity was designed for alpine snowpack (Vionnet et al., 2012) and may not be adapted to polar snow packs.

Moreover, since we are considering only the first 12 m of the snowpack in the present simulations, the compaction in the considered layers does not compensate the yearly accumulation, leading to rising snow level with time. To maintain a stable surface level in our simulations, we used a simplified compaction scheme, **where the compaction rate ε is the same for all the layers. The compaction rate is obtained by dividing the accumulation rate at the site (see Sect. 3.3) by the total mass of the snow column (Eq. 3). It is then applied to all layers to obtain the density change per time step using Eq. 4.**

$$\varepsilon = \frac{dm_{sn}}{dt} / \sum_1^{nmax} (\rho_{sn}(t, n) \times dz(t, n)) \quad (3)$$

$$\frac{\rho_{sn}(t+dt, n) - \rho_{sn}(t, n)}{dt} = \varepsilon \times \rho_{sn}(t, n) \quad (4)$$

5) Wind drift events: They modify the properties of the snow grains which tend to become more rounded. They also increase the density of the first layers through **compaction**. An option allows snow to be partially sublimated during these wind drift events (Vionnet et al., 2012).

6) Snow albedo and transmission of solar radiation: **In the first 3 cm of snow**, snow albedo and absorption coefficient are computed from snow microstructure properties and impurity **content. The average albedo value in the first 3 cm is used to determine the part of incoming** solar radiation reflected at the surface. **The** rest of the radiation penetrates into the snowpack. Then, **the absorption coefficient is used to describe the rate of decay of the radiation as it is progressively absorbed by the layers downward, following an exponential law.**

7) Latent and sensible surface energy and mass fluxes: The sensible heat flux and the latent heat flux are computed using the aerodynamic resistance and the turbulent exchange coefficients.

- 8) Vertical snow temperature profile: It is deduced from the heat diffusion equation, using the snow conductivity, as well as the energy balance at the top **and at the** bottom of the snowpack.
- 9) Snow sublimation and condensation at the surface: The amount of snow sublimated/condensed is deduced from the latent heat flux, and the thickness of the first layer is updated. Other properties of the first layer **such as density and SSA** are kept constant.

3.1.2 Implementation of water transfer

The new vapor transport subroutine has been inserted after the compaction (4) and wind drift (5) modules, and before the solar radiation module (6). **In this section, the term ‘interface’ is used for the horizontal surface of exchange between two consecutive layers.** The flux of vapor at the **interface** between two layers is obtained using the Fick’s law of diffusion (Eq. (5)):

$$F(n + 1 \rightarrow n) = \frac{-2 D_{eff}(t, n \rightarrow n+1)(C_v(t, n) - C_v(t, n+1))}{dz(t, n) + dz(t, n+1)} \quad (5)$$

where $dz(t, n)$ and $dz(t, n+1)$ are the thicknesses of the two layers considered in meters, $C_v(t, n)$ and $C_v(t, n+1)$ are the local **vapor mass concentrations** in the two layers **in kg m^{-3}** , and $D_{eff}(t, n \rightarrow n+1)$ **in $\text{m}^2 \text{s}^{-1}$** is the effective diffusivity of water vapor in the snow at the **interface**. The thicknesses are known from the previous steps of the Crocus model, but the **vapor mass concentrations** and the interfacial diffusivities must be computed.

The effective diffusivity at the **interface** is obtained in two steps: first the effective diffusivities ($D_{eff}(t, n)$ and $D_{eff}(t, n+1)$) in each layer are calculated (Eq. (6)), second, the interfacial diffusivity ($D_{eff}(t, n \rightarrow n+1)$) is computed as their harmonic mean (Eq. (7)). Effective diffusivity can be expressed as a function of the snow density using the relationship proposed by Calonne et al. (2014), for layers with relatively low density. In these circumstances, the compaction occurs by ‘boundary sliding’, meaning that the grains slide on each **other, but that their shape is not modified. It is therefore applicable to our study** where density is always below 600 kg m^{-3} . The equation of Calonne et al. (2014) is based on the numerical analysis of 3D tomographic images of different types of snow. It relates normalized effective diffusivity D_{eff} / D_v to the snow density ρ_{sn} in the layer (Eq. (6)). **D_v is the vapor diffusivity in air and has a value that varies depending on the air pressure and air temperature (Eq. (19) in Johnsen et al., 2000).** ρ_{ice} corresponds to the density of ice **and has a value of 917 kg m^{-3}** .

$$\frac{D_{eff}(t, n)}{D_v} = \frac{3}{2} \left(1 - \frac{\rho_{sn}(t, n)}{\rho_{ice}} \right) - \frac{1}{2} \quad (6)$$

$$D_{eff}(t, n \rightarrow n + 1) = \frac{1}{\frac{1}{D_{eff}(t, n)} + \frac{1}{D_{eff}(t, n+1)}} \quad (7)$$

We assume that vapor is in general at saturation in the snow layers (Neumann et al., 2008; Neumann et al., 2009). The local **mass concentration of vapor C_v in kg m^{-3}** in each layer is given by the Clausius-Clapeyron equation (Eq. (8)):

$$C_v(t, n) = C_{v0} \exp\left(\frac{L_{sub}}{R_v \rho_{ice}} \left(\frac{1}{T_0} - \frac{1}{T(t, n)}\right)\right) \quad (8)$$

where C_{v0} is the **mass concentration of vapor at 273.16 K and is equal to $2.173 \cdot 10^{-3} \text{ kg m}^{-3}$** , L_{sub} is the latent heat of **sublimation and has a value of $2.6 \cdot 10^9 \text{ J m}^{-3}$** , R_v is the vapor constant **and has a value of $462 \text{ J kg}^{-1} \text{ K}^{-1}$** , ρ_{ice} is the density of ice **and has a value of 917 kg m^{-3}** , T_0 is the temperature of the triple point of water **and is equal to 273.16 K** and T is the temperature of the layer.

All layers are treated identically, except the first layer at the top and the last layer at the bottom. For the uppermost layer, the exchange of vapor occurs only at the bottom boundary. **Indeed, exchanges** with the atmosphere are described elsewhere in Crocus **at step 9** where surface energy balance **is realized**. For the lowermost layer, only exchanges taking place at the top boundary are considered, the flux of vapor to/from the underlying medium being set to zero.

For each layer, the **mass concentration of vapor in air** and effective diffusivity are computed within the layer and in the neighboring layers. Fluxes at the top and bottom of each layer are deduced from Fick's law of diffusion (Eq. (5)). They are integrated over the subroutine time **step, and** the new mass of the layer is computed. **It is used** at the beginning of the next subroutine step. **We use a 1 s time step** within the subroutine, **smaller than the main routine time step of 900 s. This ensures** that vapor fluxes remain small relative to the amount of vapor present in the layers.

Note that the temperature profile, which controls the **vapor pressure** profile, is not modified within the subroutine. Physically, temperature values should change as a result of the transfer of sensible heat from one layer to another associated with vapor transport. They should also evolve due to the loss or gain of heat caused by water sublimation or condensation (Albert and McGilvary, 1992; Kaempfer et al., 2005). However, vapor transport is only a small component to heat transfer between layers (Albert and Hardy, 1995; Albert and McGilvary, 1992). **In the absence of ventilation**, with or without vapor diffusion, the steady-state profile for temperature varies by less than 2% (Calonne et al., 2014). **Thus**, the effect can be neglected at first order.

3.1.3 Implementation of water isotopes

In the model, the isotopic composition of snow in each layer is represented by the triplicate ($\delta^{18}\text{O}$, d-excess, ^{17}O -excess). Only the results of $\delta^{18}\text{O}$ are presented and discussed here. For each parameter, two values per layer are considered independently, corresponding to the ‘snow grain center’ and the ‘snow grain surface’, respectively. Water vapor isotopic composition is deduced at each step from the ‘snow grain surface’ isotopic composition. **It is not stored independently to limit the number of prognostic variables. The isotopic compositions are used at step 1, i.e. for snowfall, and after step 5, within the new module of vapor transfer.**

In the snow fall subroutine, a new layer of snow may be added, **depending on the weather, at** the top of the snowpack. At this step of the routine, the snow grains **being** deposited are supposed to be homogenous, i.e. they have the same composition in the “grain surface” compartment and in the “grain center” compartment. Their composition is deduced from the air temperature (see Sect. 3.2).

Within the vapor transport subroutine, **a specific module deals with the isotopic aspects of vapor transport. It** modifies the isotopic compositions in the two snow grain sub-compartments as a result of water vapor transport and recrystallization of snow crystals. It works with four main steps:

- 1) an initiation step where the vapor isotopic compositions are computed, using equilibrium fractionation, from the ones in the grain surface sub-compartment,
- 2) a transport step where vapor moves from one layer to another, with **a kinetic** fractionation associated with diffusion,
- 3) a balance step where the new vapor in the porosity exchanges with the grain surface compartment **by sublimation/condensation. The flux is** determined by the difference between actual **vapor mass concentration** and expected **vapor mass concentration** at saturation,
- and 4) a ‘recrystallization’ step where the grain center and grain surface isotopic compositions are homogenized, leading to an evolution of grain center isotopic composition.

The time step in this module is 1s, the same as the time step of the sub-routine.

The initial vapor isotope composition $R_{vap\ ini}^i$ in a given layer is taken at equilibrium with the ‘grain surface’ isotopic composition $R_{surf\ ini}^i$. Here **i** denotes heavy isotope, and thus stands for ^{18}O , ^{17}O or D. **Equilibrium fractionation is a hypothesis that is correct in layers where vapor has reached equilibrium with ice grains, physically and chemically. This process is limited by the water vapor - snow mass transfer whose associated speed is of the order of 0.09**

m.s-1 (Albert and McGilvary, 1992). In our case, we are dealing with centimetric scale layers thickness and recalculate the isotopic composition every second so that we consider that the speed of the mass transfer is not limiting the equilibrium situation at the water vapor - snow interface. To compute isotopic ratios for water vapor we use the following Eq. (9) and (10):

$$\begin{cases} R_{vap\ ini}^{18} = \alpha_{sub}^{18} \times R_{surf\ ini}^{18} \\ R_{vap\ ini}^{17} = \alpha_{sub}^{17} \times R_{surf\ ini}^{17} \\ R_{vap\ ini}^{18} + R_{vap\ ini}^{17} + 1 = 1/c_{vap\ ini}^{16} \end{cases} \quad (9)$$

$$\begin{cases} R_{vap\ ini}^D = \alpha_{sub}^D \times R_{surf\ ini}^D \\ R_{vap\ ini}^D + 1 = 1/c_{vap\ ini}^{1H} \end{cases} \quad (10)$$

The equilibrium fractionation coefficients (α_{sub}^i) are obtained using the temperature-based parameterization from Ellehoj et al. (2013). **Note that we make a slight approximation here, by replacing molar concentrations by mass concentrations in our mass balance formulas (see Table 1 for symbol definitions).**

The initial **vapor mass concentration in air C_v** has already been computed in the vapor transport subroutine, and the volume of the porosity can be obtained from the snow **density ρ_{sn} and the thickness of the layer dz** . By combining both, we obtain Eq. (11) which gives the initial mass of vapor in the layer $m_{vap\ ini}$.

$$m_{vap\ ini} = C_v \times \left(1 - \frac{\rho_{sn}}{\rho_{ice}}\right) \times dz \quad (11)$$

This mass of vapor should be subtracted from the initial grain surface mass because vapor mass is not tracked outside of **the sub-routine (Fig. 1). The new** grain surface isotope composition, after vapor individualization is given by Eq. (12):

$$c_{surf\ new}^{18} = \frac{m_{surf\ new}^{18}}{m_{surf\ new}} = \frac{m_{surf\ ini}^{18} - m_{vap\ ini} \times c_{vap\ ini}^{18}}{m_{surf\ ini} - m_{vap\ ini}} \quad (12)$$

The diffusion of isotopes follows the same scheme as the water vapor diffusion described above in Sect. 3.1.2. and Eq. (5). In Eq. (13), the gradient of **vapor mass concentrations** is replaced by a gradient of concentration of the studied isotopologue. The **kinetic fractionation during the diffusion** is realized with **the D^i/D term where i stands for ^{18}O or ^{17}O or 2H** (Barkan and Luz, 2007).

$$F^{18}(n+1 \rightarrow n) = \frac{-2 \times D_{eff}(t, n \rightarrow n+1) (C_v(t, n) \times c_{vap\ ini}^{18}(t, n) - C_v(t, n+1) \times c_{vap\ ini}^{18}(t, n+1))}{dz(t, n) + dz(t, n+1)} \times \frac{D^{18}}{D} \quad (13)$$

As done for water molecules transport (Sect. 3.1.2.), the flux is set to zero at the top of the first layer and at the bottom

of the last layer. **When the vapor concentration is the same in two adjacent layers, the total flux of vapor is null. But diffusion along isotopic gradients still occurs if the isotopic gradients are non-zero (Eq. (13)).** Once top and bottom fluxes of each layer have been computed, the new masses of the various isotopes in the vapor are deduced, as well as the new ratios.

After the **exchanges between layers**, the isotopic composition in the vapor has changed. **However, the** vapor isotopic composition is not a prognostic variable outside of the vapor transport subroutine. **To record this change, it** must be transferred to either the ‘grain surface compartment’ or to the ‘grain center compartment’ before leaving the subroutine. First, we consider exchanges of isotopes with the grain surface compartment, which is in direct contact with the vapor. Depending on the net mass balance of the layer, two situations must be considered:

1) If the mass balance is positive, **condensation occurs, so that the** transfer of isotopes takes place from the vapor toward the grain surface. To evaluate the change in the isotope composition in the grain surface, the mass of vapor condensed $\Delta m_{vap,exc}$ must be computed. It is the difference between the mass of vapor expected at saturation and the mass of vapor present in the porosity after vapor transport. **Note that temperature does not evolve in this sub-routine. Nevertheless, the difference** is not exactly equal to the mass of vapor that has entered the layer, **because of layer** porosity change. The excess mass of vapor is given by **Eq. (14)**:

$$\Delta m_{vap,exc} = \left[(\rho_{sn\ new} - \rho_{sn\ ini}) + C_v \times \left[\left(1 - \frac{\rho_{sn\ ini}}{\rho_{ice}} \right) - \left(1 - \frac{\rho_{sn\ new}}{\rho_{ice}} \right) \right] \right] \times dz \quad (14)$$

Since the excess of vapor is positive, the next step is the condensation of the excess vapor. The number of excess water molecules is determined through comparison with the expected number in the water vapor phase for equilibrium state between surface snow and water vapor. Here the condensation of excess vapor occurs without additional fractionation **because (1) there is a permanent isotopic equilibrium between surface snow and interstitial vapor restored at each first step of the sub-routine and (2) kinetic fractionation associated with diffusion is taken into account during diffusion of the different isotopic species along the isotopic gradients.**

2) If the mass balance is negative, the transfer of isotopes takes place from the grain surface toward the vapor without fractionation. Ice from the grain surface sub-compartment is sublimated without fractionation to reach the expected **vapor concentration at saturation**. Note that the absence of fractionation at sublimation is a frequent hypothesis because water molecules move very slowly in ice lattice (Friedman et al., 1991; Neumann et al., 2005;

Ramseier, 1967). **Consequently**, the sublimation removes all the water molecules present at the surface of grains, including the heaviest ones before accessing inner levels. **In reality, there** are evidences for fractionation at sublimation. **It occurs through** kinetic effects associated with sublimation / simultaneous condensation, **or during** equilibrium fractionation at the boundary, especially when invoking the existence of a thin liquid layer at the snow – air interface (Neumann et al., 2008 and references therein; Sokratov and Golubev, 2009; Stichler et al., 2001; Ritter et al., 2016). The new composition in the vapor results from a mixing between the vapor present and the new vapor recently produced. The composition in the ‘grain surface’ ice compartment does not change.

The limit between the surface compartment and the grain center compartment is defined by the mass ratio of the grain surface compartment to the total grain mass i.e. $\tau = m_{surf} / (m_{center} + m_{surf})$, (Fig. 1). This mass ratio can be used to determine the thickness of the ‘grain surface layer’ as a fraction of grain radius, for spherical grains. The surface compartment must be thin, to be able to react to very small changes in mass when vapor is sublimated or condensed.

Our model has a numerical precision of 6 decimals and is run at a 1 s temporal resolution. **Consequently, the isotopic** composition of the surface compartment can change in response to surface fluxes only if its mass is smaller than 10^6 times the mass of the water vapor present in the porosity. **This constrains the maximum value for τ :**

$$m_{surf} < 10^6 m_{vap}, \text{ or } m_{surf} / (m_{center} + m_{surf}) < 10^6 \frac{\Phi \cdot \rho_v \cdot V_{tot}}{\rho_{sn} \cdot V_{tot}}, \text{ i.e. } \tau < \frac{\rho_v \cdot \Phi}{\rho_{sn}} \cdot 10^6. \text{ Considering typical temperatures, snow}$$

densities and layer thicknesses (Table 3) we obtain a maximum value of $3.3 \cdot 10^{-2}$. On the other hand, this compartment must be thick enough to transmit the change in isotopic compositions caused by vapor transport and condensation/sublimation to the grain center. Again, numerical precision imposes that its mass should be no less than 10^{-6} times the mass of the grain center compartment, **and thus we get an additional constraint: $\tau > 10^{-6}$.** Here we use a ratio $\tau = 5 \cdot 10^{-4}$ for the mass of the grain surface relative to the total mass of the layer (Fig. 1). We have run sensitivity tests with smaller and larger ratios (**Sect. 4.3**).

Two types of mixing between grain surface and grain center are implemented in the model. The first one is associated with crystal growth or shrinkage, because of vapor transfer. Mixing is performed at the end of the vapor transfer subroutine, after sublimation/condensation has occurred. During the exchange of water between vapor and grain surface, the excess or default of mass in the water vapor caused by vapor transport has been entirely transferred to the grain surface sub-compartment. Thus, the mass ratio between the grain surface compartment and the grain center compartment deviates from the original one. To bring the ratio τ back to normal value of $5 \cdot 10^{-4}$, mass is transferred

either from the grain surface to the grain center or from the grain center to the grain surface. This happens without fractionation, i.e. if the transfer occurs from the center to the surface, the composition of the center remains constant. The second type of mixing implemented is the grain center translation (Pinzer et al., 2012) which favors mixing between grain center and grain surface in the case of sustained temperature gradient. Pinzer et al. (2012) used the apparent grain displacement to compute vapor fluxes. Here, we reverse this method and use the vapor fluxes computed from Fick's law to estimate the grain center renewal. We could transfer a small proportion of the surface compartment to the grain center every second. Instead, we choose to totally mix the snow grain every few days. The interval $\Delta t_{surf/center}$ between two successive mixings is derived from the vapor flux $F(n+1 \rightarrow n)$ within the layer **using Eq. (15).**

$$\Delta t_{surf/center} = \frac{m_{sn} \times \tau}{F(n+1 \rightarrow n)} \quad (15)$$

The average temperature gradient of 3 °C m⁻¹ **corresponds** to a flux $F(n+1 \rightarrow n)$ of 1.3 10⁻⁹ kg·m⁻²·s⁻¹. The typical mass for the layer m_{sn} **is** 3.3 kg. **Based on these values**, the dilution of the grain surface compartment into the grain center should occur every 15 days. Of course, this is only an average, since layers have varying masses, and since the temperature gradient can be larger or smaller. We will however apply this time constant for all the layers and any temperature gradient (see sensitivity tests **Sect. 4.3**), to **ensure that** the mixing between compartments **occurs** at the same time in all layers.

In terms of magnitude, this process is probably much more efficient for **mixing the solid grain** than grain growth or solid diffusion. It is thus crucial for the modification of the bulk isotopic composition of the snow layer. It makes the link between microscopic processes and macroscopic results.

3.1.4 Model initialization

For model initialization, an initial snowpack is defined, with a fixed number of snow layers, and for each snow layer an initial value of thickness, density, temperature and $\delta^{18}O$. Typically, **processes of oriented vapor transport** such as **thermally induced diffusion** and ventilation occur mainly in the first meters of snow. **Therefore**, the model starts with an initial snowpack of about 12 m.

The choice of the layer thicknesses depends on the annual accumulation. Because the accumulation is much higher at GRIP than at Dome C (Sect. 3.2., Table 2), the second site is used to define the layer thicknesses. **About 10 cm of**

fresh snow are deposited every year (Genthon et al., 2016; Landais et al., 2017). This implies that to keep seasonal information, at least one point every 4 cm is required in the first meter. For the initial profile, we impose maximal thickness of 2 cm for the layers between 0 and 70 cm depth and 4 cm for the layers between 70 cm and 2 meters depth. As the simulation runs, merging is allowed but restricted in the first meter to a maximum thickness of 2.5 cm. Below 2 meters, the thicknesses are set to 40 cm or even 80 cm. Thus, the diffusion process can only be studied in the first 2 m of the model snowpack. In the very first centimeters of the snowpack, thin millimetric layers are used to accommodate low precipitation amounts and surface energy balance. The initial density profiles are defined for each site specifically (see Sect. 3.2). The initial temperature and $\delta^{18}\text{O}$ profiles in the snowpack depend on the simulation considered (see Sect. 3.3).

3.1.5 Model output

A data file containing the spatio-temporal evolution of prognostic variables such as temperature, density, SSA or $\delta^{18}\text{O}$ is produced for each simulation. Here, we present the results for each variable as two-dimensional graphs, with time on the horizontal axis and snow height on the vertical axis. The variations of the considered variable are displayed as color levels. The white color corresponds to an absence of change of the variable. As indicated above, only the first 12 m of the polar snowpack are included in the model. The bottom of this initial snowpack constitutes the vertical reference or ‘zero’ to measure vertical heights h . The height of the top of the snowpack varies with time due to snow accumulation and to snow compaction. In the text, we sometimes refer to the layer depth z instead of its height h . The depth can be computed at any time by subtracting the current height of the considered layer from the current height of the top of the snowpack.

3.2 Studied sites: meteorology and snowpack description

In this study we run the model under conditions encountered at Dome C, Antarctica and GRIP, Greenland. We chose these two sites because they have been well-studied in the recent years through field campaigns and numerical experiments. In particular for Dome C, a large amount of meteorological and isotopic data is available (Casado et al., 2016a; Stenni et al., 2016; Touzeau et al., 2016). Typical values of the main climatic parameters for the two studied sites, GRIP and Dome C, are given in Table 2, as well as typical $\delta^{18}\text{O}$ range. Dome C has lower accumulation rates of

2.7 cm ice equivalent per year (i.e. yr⁻¹) compared to GRIP rates of 23 cm i.e. yr⁻¹ (Table 2), making it more susceptible to be affected by post-deposition processes.

In this study, we also compare the results obtained for GRIP to results from two other Greenland sites, namely NGRIP and NEEM. GRIP is located at the ice-sheet summit, whereas the two other sites are located further north, in lower elevation areas with higher accumulation rates. In detail, NGRIP is located 316 km to the NNW of GRIP ice-drill site (Dahl-Jensen et al., 1997). GRIP and NGRIP have similar temperatures of -31.6 °C and -31.5 °C but different accumulation rates of 23 cm i.e. yr⁻¹ and 19.5 cm i.e. yr⁻¹ respectively. NEEM ice-core site is located some 365 km to the NNW of NGRIP on the same ice-ridge. It has an average temperature of -22 °C and an accumulation rate of 22 cm i.e. yr⁻¹.

The δ¹⁸O value in the precipitation at a given site reflects the entire history of the air mass, including evaporation, transport, distillation, and possible changes in trajectory and sources. However, assuming that these processes are more or less repeatable from one year to the next, it is possible to empirically relate the δ¹⁸O to the local temperature, using measurements from collected samples. Here, using data from one-year snowfall sampling at Dome C (Stenni et al., 2016; Touzeau et al., 2016), we use the following Eq. (16) to link δ¹⁸O in the snowfall to the local temperature T_{air} , in K:

$$\delta^{18}O_{sf} = 0.45 \times (T_{air} - 273.15) - 31.5 \quad (16)$$

We do not provide an equivalent expression for GRIP, Greenland, because the simulations run here (see Sect. 3.1.1) do not include precipitation.

The initial density profile in the snowpack is obtained from fitting density measurements from Greenland and Antarctica (Bréant et al., 2017). Over the first 12 m of snow, we obtain the following evolution (Eq. (17) and Eq. (18)) for GRIP and Dome C respectively:

$$\rho_{sn}(t, n) = 17.2 \cdot z(t = 0, n) + 310.3 \quad (N=22; R^2=0.95) \quad (17)$$

$$\rho_{sn}(t, n) = 12.41 \times z(t = 0, n) + 311.28 \quad (N=293; R^2=0.50) \quad (18)$$

3.3 List of simulations

Table 4 presents the model configuration for the 6 simulations considered here.

3.3.1 Greenland simulations

The first simulation, **listed as number 1 in Table 4**, is dedicated to the study of diffusion **along** isotopic gradients. **It is realized** on a Greenland snowpack with an initial sinusoidal profile of $\delta^{18}\text{O}$ (**see Eq. 19**) and **with** a uniform and constant vertical temperature profile at 241 K. In addition to comparison to $\delta^{18}\text{O}$ profiles for GRIP and other Greenland sites, the aim of the first simulation is to compare results from Crocus model to the models of Johnsen et al. (2000) and Bolzan and Pohjola (2000) run at this site with only diffusion **along** isotopic profiles. To compare our results to theirs, we consider an isothermal snowpack, without meteorological forcing, and we deactivate modules of surface exchanges and heat transfer. The initial seasonal sinusoidal profile at GRIP is set using Eq. (19):

$$\delta^{18}\text{O}(t, n) = -35.5 - 8 \times \sin\left(\frac{2\pi \times z(t, n)}{a \times \rho_{ice} / \rho_{sn}(t, n)}\right) \quad (19)$$

where z is the depth of the layer n , ρ_{sn} is its density, ρ_{ice} is the density of ice **and has a value of 917** kg m^{-3} , a is the average accumulation at GRIP **and is equal to 0.23** m i.e./yr (**Dahl-Jensen et al., 1993**). The **peak to peak** amplitude value of 16 ‰ is close to the back-diffused amplitude at Summit (Sjolte et al., 2011).

The second simulation is run with evolving temperature in the snowpack. **The snow temperature is computed** by the model, using meteorological forcing from ERA-Interim (**see Table 4**). **In** that case, **the transport of isotopes in the vapor phase** results both from diffusion **along** isotopic gradients and from **vapor concentration gradients**. The initial snowpack is the same as in the previous simulation.

In the two GRIP simulations, the modules of wind compaction and weight compaction are inactive. Indeed, as weight compaction is taken to compensate yearly accumulation (**Eq. (3) and (4)**), applying this compaction without precipitation would lead to an unrealistic drop in snow level. The wind compaction was absent from the model of Johnsen et al. (2000) and using this module would make comparisons more difficult.

3.3.2 Dome C simulations

In simulations 3 to 6, we take advantage of the high documentation of the Dome C site to disentangle the different effects on the variations of water isotopic composition. **All the simulations** at Dome C were performed with an evolving temperature **profile. Temperatures in the snow layers were computed using** a modified meteorological forcing from ERA-Interim (Dee et al., 2011; Libois et al., 2014; see details in Table 4), as well as the modules of energy exchange and transfer. In this series of simulations, the $\delta^{18}\text{O}$ values thus evolve as a result of diverging and/or

alternating vapor fluxes. The simulations are ordered by increasing complexity. First, in **Simulation 3**, the modules of homogeneous compaction and wind drift are deactivated, as well as the module of snowfall. **Thus**, the impact of vapor transport forced by temperature gradients **on the snow isotopic compositions** is clearly visible. Then, in **Simulation 4**, the module of compaction and the module of wind drift are activated, to see their impact **on the isotopes**. We use an accumulation rate dm_{sn}/dt for Dome C of 0.001 kg m⁻² per 15 min (see Eq. (3)). Next, in **Simulation 5**, snowfall is added, to assess how new layers **affect snow $\delta^{18}O$ values**. Lastly, in **Simulation 6**, the model is run over 10 years at Dome C, to build up a snowpack with realistic ‘sinusoidal’ variation in $\delta^{18}O$ values.

4 Results

4.1 Greenland

4.1.1 Results of the Crocus simulations (Simulations 1 and 2)

Figure 2 shows the result of **Simulation 1**, where only diffusion **along** isotopic gradients is active, as in Johnsen et al., 2000. As expected **the peak to peak amplitude of $\delta^{18}O$ cycles is reduced** because of diffusion. Over 10 years, **from 2000 to 2009**, the amplitude decreases **by 1.2 ‰** which corresponds **to a 7.3 % variation**.

Figure 3 shows the result of **Simulation 2**, i.e. with varying temperature in the snowpack. **The attenuation is stronger than the one observed in the previous simulation. The minima at 11.46 m increases by 1.03 ‰ over ten years, and the maxima at 11.15 m decreases by 0.84 ‰. Thus, the total attenuation is ~1.9 ‰ or 11.7 % for this height range. Below, the attenuation is smaller, with a total attenuation of only 6 % for heights between 10.54 and 10.85 m. If we compare attenuation for heights 11.46 and 11.56 m in the 1st and 2nd simulation, we note that including temperature gradients leads to an increased attenuation by 50 %.**

Between 11.46 m and 11.56 m, the $\delta^{18}O_{gcenter}$ values increase over ten years by 1 to 4 ‰. This increase is not caused only by attenuation of the original sinusoidal signal. Indeed, at h=11.60 m, the values get higher than the initial maxima which was -36 ‰ at 11.64 m. There is therefore a local accumulation of heavy isotopes in this layer as a result of vapor transport. This maximum corresponds to a local maximum in temperature and is coherent with departure of ^{18}O -depleted water vapor from this layer. Thus, thermally induced vapor transport does not only result into signal attenuation, but can also shift the $\delta^{18}O$ value, regardless of the initial sinusoidal variations.

Lastly, in the first 2-3 cm of the snowpack, **strong** depletion is observed over the period, **with a decrease by 2 to 3 % instead of 0.5 % when the temperature gradients were absent (Simulation 1)**. This depletion probably results from arrival of ^{18}O -depleted water vapor from warmer layers below. **This shows again** the influence of temperature gradients which were absent from the previous simulation. However, **note that in this simulation we neglect precipitation** and exchange of vapor with the atmosphere. **Thus**, the depletion observed here may not occur **in natural settings** when these processes **are active**.

In conclusion, at GRIP, the diffusion of vapor as a result of temperature gradients **has a double impact on isotopic compositions. It increases the attenuation in the first 60 cm of snow, because of higher vapor fluxes. And it also creates local isotopic maxima and minima, in a pattern corresponding to temperature gradients in the snowpack but disconnected from the original $\delta^{18}\text{O}$ sinusoidal signal.**

4.1.2 Comparison with core data

Here, we evaluate the attenuation of the initial seasonal signal in $\delta^{18}\text{O}$ over 10 years **at 2 Greenland ice-core sites**, NEEM and GRIP. **For the first site**, we use 4 shallow cores (NEEM2010S2, NEEM2008S3, NEEM2007S3, NEEM2008S2) published in Steen-Larsen et al., 2011 and in Masson-Delmotte et al., 2015. **For the second site**, we use one shallow core (1989-S1), published in White et al., 1997. **For the GRIP core, only the first 80 meters are considered. Therefore, the data presented corresponds to deposition and densification conditions like the modern ones.** For NEEM the values of the four cores are taken together. For NEEM and GRIP, the **semi-amplitude** is computed along the core. **In the first 10 meters, the maximum value every 30 cm is retained, and deeper in the firn, because of compaction, the maximum value every 20 cm is retained (see also Supp. Material; Fig. 4).** **For this study, we have chosen to estimate attenuation on years with a clearly marked seasonal cycle, a strategy that can be debated but at least documented. Consequently, from this first series of maxima, a second series of maxima is computed, with a larger window of 1 meter. The ‘attenuated amplitudes’ at each level is then defined as the ratio between these 1-meter maxima and the initial 1-meter maxima.** Maximum **semi-amplitudes** every 5 m are also computed **and displayed on Figure 4.** The 2.5 m attenuation is **slightly higher** at **GRIP, leading to a remaining amplitude of 86 %**, than at NEEM where the **remaining amplitude is 90 %** (Fig. 4). The amplitude decreases with depth in parallel for the two cores, with the amplitude at NEEM staying always higher than at GRIP.

For comparison with our model, we estimate attenuation after 10 years, i.e. at a depth of ~5.8 m for NEEM and ~5.65 m for GRIP. The remaining amplitude is 80 % and 72 % at GRIP and NEEM respectively. Our **Simulation 1 produced 7 % of** attenuation only on the same duration, showing that our model, run on an isothermal snowpack, underestimates the attenuation observed in the data.

4.1.3 Comparison with other models

At 2.5 m at NGRIP, Johnsen et al. (2000) simulate remaining amplitude of 77 % (Fig. 4). For a depth of 5.43 m, corresponding to an age of 10 years, the simulated remaining amplitude is 57 %. For Bolzan and Pohjola (2000), at GRIP after 10 years, 70 % of the initial amplitude is still preserved. The slower attenuation for Bolzan and Pohjola (2000) compared to Johnsen et al. (2000) may be due more to the different sites considered than to the different models. Indeed, GRIP has higher accumulation rates that should limit diffusion. Nevertheless, **the attenuation of 30 %** simulated by Bolzan and Pohjola at GRIP is stronger than the attenuation **of 7 %** simulated in our model. Town et al. (2008, Sect. [31]) found attenuations of a few tenth of per mil after several years when implementing only diffusion, a result consistent with ours since **we get a decrease by 1.2 %** after 10 years.

We explore below the reasons for discrepancies between models. The equation for effective diffusivity of vapor in firn used in our study is different from the ones used by Johnsen et al. (2000) or by Bolzan and Pohjola (2000). **Indeed,** we do not consider the tortuosity factor l , nor the adjustable scale factor s of Bolzan and Pohjola. However, using the values given by the previous authors for l and s lead to D_{eff} values ranging from $6.7 \cdot 10^{-6}$ to $9.9 \cdot 10^{-6} \text{ m}^2 \text{ s}^{-1}$ for a density of 350 kg m^{-3} and a temperature of 241 K which is coherent with our value of $8.7 \cdot 10^{-6} \text{ m}^2 \text{ s}^{-1}$. As indicated by Bolzan and Pohjola (2000), the choice of one equation or another has little impact here.

The most probable difference lie in the way diffusion is taken into account. Johnsen et al. (2000) and Bolzan and Pohjola (2000) use a single equation of diffusion to predict the evolution of the isotopic composition of the **layer. In our case, we** specifically compute the fluxes in the vapor each second and at each depth level and deduce the evolution of $\delta^{18}\text{O}$ in the grain center, after sublimation/condensation and recrystallization. Denux (1996) and van der Wel et al. (2015) indicate **that the model developed by Johnsen (1977) and used in Johnsen et al. (2000)** overestimates the attenuation compared to observed values. For Denux (1996), the model **of Johnsen (1977)** should consider the presence of ice crusts, **and maybe also** the temperature gradients in the surface **snow**, to get closer to the real

attenuation at remote Antarctic sites. **Van der Wel et al. (2015) have compared the model results to a spike-layer experiment realized at Summit. Because an artificial snow layer cannot be representative of natural diffusion, they took care to evaluate diffusion based only on the natural layers present above and below the artificial layer.** van der Wel et al. (2015) propose three causes to the discrepancy between Johnsen et al.'s model prediction and actual measured attenuation at GRIP. **They blame either ice crusts, or a bad knowledge and parametrization of the tortuosity in the first meters of snow, and/or a bad description of the isotopic heterogeneity within the ice grain.** In our model, the grain heterogeneity is included. Even if the parameters defining the mixing between the two compartments are not very well constrained (see **Sect. 4.3**), the attenuation is indeed smaller compared to **the Johnsen's model.**

4.2 Dome C (Antarctica)

The aim of the **Simulations 3 to 6, run at Dome C**, is to isolate diffusion from other effects affecting water isotopic composition, i.e. wind-drift and compaction.

4.2.1 Simulation 3: without precipitation, without wind drift, and without homogeneous compaction

Figure 5 presents the results of temperature evolution (a and b) and $\delta^{18}\text{O}$ evolution (c and d) for Simulation 3.

The main changes of $\delta^{18}\text{O}_{\text{gsurf}}$ and $\delta^{18}\text{O}_{\text{gcenter}}$ occur in summer (Fig. 5c and 5d). **On the one hand, the first 20 cm of snow tend to become ^{18}O -enriched by +0.2 ‰ for the grain center compartment.** On the other hand, the **first centimeter becomes depleted by 1.0 ‰ for grain center.** This pattern is coherent with the temperature profiles **for the summer period (Fig. 5a). Indeed, vapor moves out of the warmest layers and toward colder layers where it condensates. This causes an increase in $\delta^{18}\text{O}$ in warm layers and a decrease in colder layers. This pattern is also confirmed by snow density changes (see Fig. S2).**

During winter, the temperature generally decreases toward the surface (Fig. 5a). Vapor transport is thus reversed in the first 20 cm, but this only slightly reduces the dispersion of $\delta^{18}\text{O}_{\text{gcenter}}$ values. On the first of August, the temperature at the surface temporarily increases to 235 K. This warm event strongly modifies the temperature profile in the snowpack, and therefore the pattern of vapor transport. It is associated with an increase of $\delta^{18}\text{O}$ values at the surface, which is particularly visible for the $\delta^{18}\text{O}_{\text{gsurf}}$ values (Fig. 5c).

Thus, vapor transport **can modify $\delta^{18}\text{O}$ values** in surface snow, even in the absence of precipitation or condensation from the atmosphere. This mechanism could explain the parallel evolution of surface snow isotopic composition and

temperature described by Steen-Larsen et al. (2014) and Touzeau et al. (2016) between precipitation events.

4.2.2 Simulation 4: without precipitation, with wind drift, and with homogeneous compaction

Compaction and wind drift are not supposed to modify directly the $\delta^{18}\text{O}$ values. However, the change in densities and layer thicknesses modifies slightly the temperature profile and the diffusivities. These processes thus could have an indirect impact on $\delta^{18}\text{O}$ values. Figure 6 shows $\delta^{18}\text{O}_{\text{gcenter}}$ changes that are reduced compared to the simulation without wind drift and compaction. This is coherent with a decrease in the density changes associated with vapor transport in the case with compaction (see Fig. S5).

4.2.3 Simulation 5: with precipitation, with wind drift, with homogeneous compaction

In Simulation 5, we add precipitation to wind and weight compaction effects. Both snowfall and wind compaction are responsible for irregular changes, respectively positive and negative, of the height of the snowpack (Fig. 7). In the new deposited layers, the $\delta^{18}\text{O}_{\text{gcenter}}$ values reflect the $\delta^{18}\text{O}$ values in the precipitation. They vary as expected from -40 ‰ on the 31th of December to -59 ‰ in July (Fig. 7, Fig. S8). The effect of vapor transport is visible only in ‘old’ layers which were originally homogeneous in terms of $\delta^{18}\text{O}$. These old layers, which were reaching the surface in January, have been buried below the new layers and are found from 11 cm depth downward in December.

4.2.4 Simulations 6: Ten-years simulation at Dome C

Simulations 6 corresponds to a simulation run over 10 years at Dome C, with variable $\delta^{18}\text{O}$ in the precipitation. Over these 10 years, about 1 m of snow is deposited. At the end of the simulation, the vertical profile of $\delta^{18}\text{O}$ in the new layers has an average value of -49.7 ‰, and a semi-amplitude of 4.5 ‰ (Fig. 8). Here we take into account all the maxima and minima at a vertical resolution of 9 cm of fresh snow. Based on the atmospheric temperature variations only, the isotopic composition in the precipitation should vary around an average value of -53.2 ‰, with a semi-amplitude of 8.6 ‰. The main reason for this difference is the precipitation amounts: large precipitation events in winter are associated with relatively high $\delta^{18}\text{O}$ values. The vertical resolution chosen for the model of 2.5 cm may also contribute to the decrease of the semi-amplitude. Indeed, light snowfall events do not result in the production of a new surface layer but are integrated into the old surface layer. As expected, the peak to peak amplitude of $\delta^{18}\text{O}$ variations is then further reduced as a result of the two vapor diffusion processes

and of associated vapor/solid exchanges. The effect of vapor transport is relatively small. To help its visualization, we selected four layers and displayed the evolution of $\delta^{18}\text{O}$ in these layers over the years (Fig. 8d). The selected layers were deposited during winter 2000, and during summer seasons 2002, 2004, and 2006. For the layer deposited during winter 2000, there is an increase in $\delta^{18}\text{O}$ values of about +0.8 ‰ over ten years. The slope is irregular, with the strongest increases occurring during summers, between November and February, when vapor transport is maximal. The slope is also stronger when the layer is still close to the surface, probably because of the stronger temperature gradients in the first centimeters of snow (Fig. 8a). For the layers deposited during the summers, the evolution of $\delta^{18}\text{O}$ values is symmetric to the one observed for winter 2000. Over 10 years, i.e. between 2000 and 2009, the $\delta^{18}\text{O}$ amplitude thus decreases by about 1.6 ‰. This corresponds to a decrease of 18 % relative to the initial amplitude in the snow layers. This is higher than the 7 % attenuation modelled in Greenland for constant temperature, and to the 11.7 % attenuation observed when including diffusion caused by temperature gradients (Sect. 4.1). However, the comparison between the two sites is not straightforward, because of differences in temperature and accumulation counteracting each other. On the one hand, at GRIP, the diffusion is forced by low vertical gradients of $\delta^{18}\text{O}$ of the order of 0.24 ‰ cm⁻¹. These are much smaller than the typical $\delta^{18}\text{O}$ gradients at Dome C which are close to 1.10 ‰ cm⁻¹. On the other hand, the temperature of 241 K at GRIP is higher than the 220 K measured at Dome C, thus favoring diffusion.

4.3 Sensitivity tests for duration of recrystallization

We have shown above that attenuation of the isotopic signal seems too small at least for the GRIP site. In parallel, the parameters τ and $\Delta t_{\text{surf/center}}$ of the model associated to grain renewal could only loosely be estimated leading to uncertainty in the attenuation modeling. In this section, we perform some sensitivity tests to quantify how $\delta^{18}\text{O}$ attenuation can be increased by exploring the uncertainty range on the renewal of the snow grain. Indeed, the assumed values for the ratio between grain surface and the total mass of the grain τ may have been under or over-estimated. The same is true for the periodicity of mixing between these two compartments $\Delta t_{\text{surf/center}}$. The sensitivity tests are first designed for Greenland sites, run for 6 months, with initial amplitude of the sinusoidal $\delta^{18}\text{O}$ signal of 16 ‰, and a fixed temperature of 241 K in all the layers (Fig. 9). First, we use a periodicity of mixing $\Delta t_{\text{surf/center}}$ of 15 days and vary the value for the mass ratio τ : $1 \cdot 10^{-6}$, $5 \cdot 10^{-4}$, $3.3 \cdot 10^{-2}$. In practice, for $\Delta t_{\text{surf/center}}=15$

days, we realize mixing on the second and 16th of each month. Second, we use the usual value of $5 \cdot 10^{-4}$ for τ and change the periodicity of the mixing to 2 days.

- In the first case, where $\tau = 1 \cdot 10^{-6}$, and the mixing occurs every 15 days, the grain surface compartment is very small. Its original sinusoidal $\delta^{18}\text{O}$ profile disappears in less than one day due to exchanges with vapor (not shown). The impact on grain center is then very small with an increase of the first minimum by $\sim 1.0 \cdot 10^{-4} \text{‰}$ over 6 months (Fig. 9a). In this case, the attenuation due to diffusion is even reduced compared to the results displayed above.

- In the second case, where $\tau = 5 \cdot 10^{-4}$, and the mixing occurs every 15 days, the grain surface compartment is larger, and the attenuation is slower. Thus, in the grain surface compartment, half of the original amplitude still remains at the end of the simulation (not shown). The impact on the grain center compartment is clearly visible with an increase of the first minimum by $2.2 \cdot 10^{-2} \text{‰}$ after 6 months (Fig. 9b).

- In the third case, with $\tau = 3.3 \cdot 10^{-2}$, and mixing every 15 days, the attenuation of the sinusoidal signal in the grain surface compartment is only of 1 % because the grain surface compartment is very large. On opposite, attenuation in the grain center is quite large, i.e. the first minimum increases by $4.0 \cdot 10^{-2} \text{‰}$ after 6 months (Fig. 9c).

- In the fourth case, with $\tau = 5 \cdot 10^{-4}$ and mixing every 2 days, the first minimum increases by $4.1 \cdot 10^{-2} \text{‰}$ after 6 months for the grain center compartment (Fig. 9d). It is similar to the attenuation observed in the third case.

The results of these sensitivity tests suggest that the impact of vapor transfer on the grain center isotopic compositions is maximized when the grain surface compartment is large and/or refreshed often. They also show clearly that using a small grain surface compartment such as $\tau = 1 \cdot 10^{-6}$ drastically reduces the impact on the grain center isotopic values. However, our best estimates for τ and $\Delta t_{\text{surf/center}}$ were not chosen randomly (see Sect. 3.1.3). Moreover, the use of $\tau = 3.3 \cdot 10^{-2}$ or $\Delta t_{\text{surf/center}} = 2$ days leads to a near doubling of the $\delta^{18}\text{O}$ attenuation (see above). This is not yet sufficient to explain the gap between our model output for isothermal simulation and the data. However, if this doubling is applicable to the case with temperature gradients, the attenuation obtained might reach the one observed in the data at GRIP.

At Dome C, sensitivity tests show that we can increase the attenuation by a factor of 3 by reducing the mixing time from 15 to 2 days (Figure 10b-c). Similarly, if the ratio τ is put at $3.3 \cdot 10^{-2}$ instead of $5 \cdot 10^{-4}$, attenuation is more than doubled over 3 years (Figure 10d-e). Thus, at Dome C, the values of τ and $\Delta t_{\text{surf/center}}$ seem to affect more strongly the attenuation obtained compared to GRIP. This greater sensitivity at Dome C could result from the influence of

temperature gradients, as well as from steeper $\delta^{18}\text{O}$ gradients caused by the low accumulation. Indeed, the average layer thickness of 2 cm in the first meter corresponds to ~ 4 points per year at Dome C, but 35 points per year at GRIP.

4.4 Additional missing processes

In the previous sections, we have seen that model outputs for GRIP generally lead to smaller attenuation than the one observed in ice-cores. To improve the model compatibility with data, two kinds of approaches are possible. On the one hand, it would be useful to realize simulations adapted to on-site experiments such as the one by van der Wel et al. (2015). This would allow verifying how diffusion can be improved in the model. For instance, previous studies have suggested that water vapor diffusivity within the snow porosity may be underestimated by a factor of 5 (Colbeck, 1983), but this is debated (Calonne et al., 2014). On the other hand, we also believe that other processes should probably be considered to explain the remaining attenuation. Ventilation is an additional process that has already been implemented in the snow water isotopic model of Town et al. (2008) and Neumann (2003). Because of strong porosity and sensitivity to surface wind and relief, ventilation is probably as important as diffusion in the top of the firn, even if diffusion is expected to be more effective at greater depths. Indeed, for the Dome C simulation (Fig. 8), the slope $d(\delta^{18}\text{O})/dz$ decreases slowly, indicating that diffusion remains almost as active at 60 centimeters than at 10 centimeters depth. Neumann (2003) indicates that at Taylor Mouth the diffusion becomes the only process of vapor transport below 2 meters depth. For Dome C, for a temperature gradient of 3°C m^{-1} , we compute an average speed due to diffusion of $3 \cdot 10^{-6} \text{ m s}^{-1}$. This is comparable to air speed due to wind pumping of about $3 \cdot 10^{-6} \text{ m s}^{-1}$ within the top meters of snow at WAIS (Buizert and Severinghaus, 2016). We conclude that, in as much as these results can be applied to Dome C, the two processes would have comparable impact at this site in the first meters of snow. The next step for Crocus-iso development is thus to implement ventilation. Finally, we are also aware that in Antarctic central regions, the wind reworking of the snow has a strong effect in shaping the isotopic signal. A combination of stratigraphic noise and diffusion could indeed be responsible for creating isotopic cycles of non-climatic origin in the firn (Laepplé et al., 2017). Wind reworking may also contribute to attenuation, by mixing together several layers deposited during different seasons.

5. Conclusions and perspectives

Water vapor transport and water isotopes have been implemented in the Crocus snow model enabling depicting the temporal $\delta^{18}\text{O}$ variations in the **top 50 cm** of the snow in response to new precipitation, evolution of temperature gradient in the snow and densification. The main process implemented here to explain post-deposition isotopic variations is diffusion. We have implemented **two types of diffusion in vapor phase: 1) water vapor diffusion along isotopic gradients**, and **2) thermally induced vapor diffusion. The vapor diffusion** between layers **was realized** at the centimetric scale. **The consequences of the two vapor diffusion processes on isotopes in the solid phase were investigated. The solid phase was modelled as snow grains divided in two sub-compartments: (1) a grain surface sub-compartment** in equilibrium with interstitial water vapor and (2) **an** inner grain only exchanging slowly with the surface compartment. We parameterized the speed of diffusion through the renewal time of a snow grain and proportion of the two snow grain compartments.

Our approach based on a detailed snow model makes it possible to investigate at fine **scale various processes** explaining **the variations of density and $\delta^{18}\text{O}$ in the firn. We look specifically at the effect of evolution** of the temperature gradient, new snow accumulation and compaction event linked to wind drift. Over the first 30 cm, the **snow density** variations are mainly driven by compaction events linked to wind drift. Vapor transport and long-term compaction have secondary effects. Below 30 cm, wind drift driven compaction is no more visible. Because of strong temperature gradient and low density, water vapor transport will have a significant effect down to 60 cm. $\delta^{18}\text{O}$ is primary driven by variations in $\delta^{18}\text{O}$ of precipitation as expected. The seasonal variations are then attenuated by water vapor transport and diffusion **along** isotopic gradients, with an increase of these effects at higher **temperatures i.e. during summer periods.**

From 10 years simulations of the Crocus-iso model both at GRIP Greenland and Dome C Antarctica, we have estimated the post-deposition attenuation of the annual $\delta^{18}\text{O}$ signal in the snow **to about 7-18 %** through diffusion. This attenuation is smaller than the one obtained from isotopic data on shallow cores in Greenland suggesting missing processes in the Crocus model when implementing water vapor. It is also significantly smaller than the diffusion implemented by Johnsen et al. (2000) but some studies have suggested that the Johnsen isotopic diffusivity is too strong (Denux, 1996 ; Van der Wel et al., 2015).

We see our study as a first step toward a complete post-deposition modelling of water isotopes variations. Indeed,

several other developments are foreseen in this model. First, wind pumping is currently not implemented in the Crocus model. This effect, implemented in the approach of Neumann (2003) and Town et al. (2008) is expected to have a contribution as large as the effect of diffusion for the post-deposition isotopic variations. Second, in low accumulation sites like Dome C, wind scouring has probably an important effect on the evolution of the $\delta^{18}\text{O}$ signal in depth through a reworking of the top snow layers (Libois et al., 2014). **This effect has not been considered here but could be implemented in the model in the next years.** It could also play a role in the preservation of anomalously strong $\delta^{18}\text{O}$ peaks at Dome C (Denux, 1996).

Other short-term developments concern the implementation of the exchange of water vapor with the atmosphere through hoar deposition. This is particularly timely since many recent studies have studied the parallel evolution of isotopic composition of water vapor and surface snow during summer both in Greenland and Antarctica (Steen-Larsen et al., 2014; Ritter et al., 2016; Casado et al., 2016a; 2016b). **Similarly, implementation of ventilation of the snowpack in the model since this effect is expected to significantly participate to signal attenuation.**

Another aspect is to look at the post-deposition d-excess and ^{17}O -excess variations in snow pits. Indeed, recent studies have shown that the relationship between ^{17}O -excess and $\delta^{18}\text{O}$ is not the same when looking at precipitation samples and snow pits samples in East Antarctica (Touzeau et al., 2016). **This observation** questions the influence of diffusion within the snowpack on second order parameters such as ^{17}O -excess. Indeed, ^{17}O -excess is strongly influenced by kinetic diffusion driven fractionation which may be quantified by the implementation of ^{17}O -excess in our Crocus-iso model.

Code availability

The code used in the manuscript is a **development of the open source code for SURFEX/ISBA-Crocus model based on version V8.0, hosted on an open git repository at CNRM (https://opensource.umr-cnrm.fr/projects/surfex_git2)**. Before downloading the code, you must register as a user at **<https://opensource.umr-cnrm.fr/>**. You can then obtain the code used in the present study by downloading the revision tagged 'Touzeau_jan2018' of the branch touzeau_dev (last access: January 2018). The meteorological forcing required to perform the runs is available as a supplement.

Author contribution

S. Morin wrote the new module of vapor diffusion. A. Touzeau inserted isotopes and isotope transport into the numerical code with help of S. Morin for numerical issues and physics and help from A. Landais for concepts and hypotheses of the theory of isotopes. G. Picard and L. Arnaud provided information and references on snow microstructure and microphysics as well as direct field experience on site meteorology and accumulation conditions. A. Touzeau run the simulations and interpreted the results. A. Touzeau and A. Landais wrote the manuscript. All the authors corrected the manuscript.

Competing interests

The authors declare that they have no conflict of interest.

Acknowledgements

The research leading to these results has received funding from the European Research Council under the European Union's Seventh Framework Programme (FP7/2007-30 2013)/ERC grant agreement no. 306045. We want to acknowledge A. Orsi and M. Casado from LSCE, who contributed to this work through fertile discussions of the model contents and its applications. We are grateful to M. Casado and C. Bréant for providing snow pit temperature and density profiles as well as firm density profiles for model initialization. We would like to thank D. Roche for his advice during model development, as well as on how to make the code available. We are also indebted to J.-Y. Peterschmidt, who provided continual help and useful tutorials on Fortran and Python languages. We thank M. Lafaysse and V. Vionnet at CNRM/CEN for help with the model and meteorological driving data. CNRM/CEN and IGE are part of LabEX OSUG@2020. **We thank three anonymous reviewers for their questions and comments, which helped to improve the present article.**

References

- Albert, M. R. and Hardy, J. P.: Ventilation experiments in seasonal snow cover, IAHS Publications-Series of Proceedings and Reports-Intern Assoc Hydrological Sciences, 228, 41-50, 1995.
- Albert, M. R. and McGilvary, W. R.: Thermal effects due to air flow and vapor transport in dry snow, Journal of

803 Glaciology, 38, 273-281, 1992.

804 Albert, M. R. and Shultz, E. F.: Snow and firn properties and air–snow transport processes at Summit, Greenland,
805 Atmospheric Environment, 36, 2789-2797, 2002.

806 Albert, M. R., Grannas, A. M., Bottenheim, J., Shepson, P. B., and Perron, F. E.: Processes and properties of snow–air
807 transfer in the high Arctic with application to interstitial ozone at Alert, Canada, Atmospheric Environment, 36, 2779-
808 2787, 2002.

809 Altnau, S., Schlosser, E., Isaksson, E., and Divine, D.: Climatic signals from 76 shallow firn cores in Dronning Maud
810 land, East Antarctica, The Cryosphere, 9, 925-944, 2015.

811 Barkan, E. and Luz, B.: Diffusivity fractionations of $\text{H}_2^{16}\text{O}/\text{H}_2^{17}\text{O}$ and $\text{H}_2^{16}\text{O}/\text{H}_2^{18}\text{O}$ in air and their implications for
812 isotope hydrology, Rapid Communications in Mass Spectrometry, 21, 2999-3005, 2007.

813 **Bartelt, P., Buser, O., and Sokratov, S. A.: A nonequilibrium treatment of heat and mass transfer in alpine**
814 **snowcovers, Cold Regions Science and Technology, 39, 219-242, 2004.**

815 Bolzan, J. F. and Pohjola, V. A.: Reconstruction of the undiffused seasonal oxygen isotope signal in central Greenland
816 ice cores, Journal of Geophysical Research: Oceans, 105, 22095-22106, 2000.

817 Bréant, C., Martinerie, P., Orsi, A., Arnaud, L., and Landais, A.: **Modelling firn thickness evolution during the last**
818 **deglaciation: constraints on sensitivity to temperature and impurities, Clim. Past, 13, 833-853, 2017.**

819 Brun, E. and Touvier, F.: Etude expérimentale de la convection thermique dans la neige, Le Journal de Physique
820 Colloques, 48, C1-257-C1-262, 1987.

821 Brun, E., David, P., Sudul, M., and Brunot, G.: A numerical model to simulate snow-cover stratigraphy for operational
822 avalanche forecasting, Journal of Glaciology, 38, 13-22, 1992.

823 Brun, E., Six, D., Picard, G., Vionnet, V., Arnaud, L., Bazile, E., Boone, A., Bouchard, A., Genton, C., and Guidard,
824 V.: Snow/atmosphere coupled simulation at Dome C, Antarctica, Journal of Glaciology, 57, 721-736, 2011.

825 Buizert, C. and Severinghaus, J. P.: Dispersion in deep polar firn driven by synoptic-scale surface pressure variability,
826 The Cryosphere, 10, 2099-2111, 2016.

827 Calonne, N., Geindreau, C., and Flin, F.: Macroscopic modeling for heat and water vapor transfer in dry snow by
828 homogenization, The Journal of Physical Chemistry B, 118, 13393-13403, 2014.

829 Calonne, N., Geindreau, C., and Flin, F.: Macroscopic modeling of heat and water vapor transfer with phase change in

dry snow based on an upscaling method: Influence of air convection, *Journal of Geophysical Research: Earth Surface*, 120, 2476-2497, 2015.

Carmagnola, C. M., Morin, S., Lafaysse, M., Domine, F., Lesaffre, B., Lejeune, Y., Picard, G., and Arnaud, L.: Implementation and evaluation of prognostic representations of the optical diameter of snow in the SURFEX/ISBA-Crocus detailed snowpack model, *The Cryosphere*, 8, 417-437, 2014.

Casado, M., Landais, A., Masson-Delmotte, V., Genthon, C., Kerstel, E., Kassi, S., Arnaud, L., Picard, G., Prié, F., Cattani, O., Steen-Larsen, H. C., Vignon, E., and Cermak, P.: Continuous measurements of isotopic composition of water vapour on the East Antarctic Plateau, *Atmos. Chem. Phys. Discuss.*, 16, 8521-8538, 2016a.

Casado, M., Landais, A., Picard, G., Münch, T., Laepple, T., Stenni, B., Dreossi, G., Ekaykin, A., Arnaud, L., Genthon, C., Touzeau, A., Masson-Delmotte, V., and Jouzel, J.: Archival of the water stable isotope signal in East Antarctic ice cores, *The Cryosphere Discussions*, doi:10.5194/tc-2016-263, 2016b.

Colbeck, S. C.: Theory of metamorphism of dry snow, *Journal of Geophysical Research*, 88, 5475-5482, 1983.

Colbeck, S. C.: Air movement in snow due to wind pumping, *Journal of Glaciology*, 35, 209-213, 1989.

Dahl-Jensen, D., Johnsen, S., Hammer, C., Clausen, H., and Jouzel, J.: Past accumulation rates derived from observed annual layers in the GRIP ice core from Summit, Central Greenland. In: *Ice in the climate system*, Springer, 1993.

Dahl-Jensen, D., Gundestrup, N. S., Keller, K., Johnsen, S. J., Gogineni, S. P., Allen, C. T., Chuah, T. S., Miller, H., Kipstuhl, S., and Waddington, E. D.: A search in north Greenland for a new ice-core drill site, *Journal of glaciology*, 43, 300-306, 1997.

Dee, D. P., Uppala, S. M., Simmons, A. J., Berrisford, P., Poli, P., Kobayashi, S., Andrae, U., Balmaseda, M. A., Balsamo, G., Bauer, P., Bechtold, P., Beljaars, A. C. M., van de Berg, L., Bidlot, J., Bormann, N., Delsol, C., Dragani, R., Fuentes, M., Geer, A. J., Haimberger, L., Healy, S. B., Hersbach, H., Hólm, E. V., Isaksen, I., Kållberg, P., Köhler, M., Matricardi, M., McNally, A. P., Monge-Sanz, B. M., Morcrette, J. J., Park, B. K., Peubey, C., de Rosnay, P., Tavolato, C., Thépaut, J. N., and Vitart, F.: The ERA-Interim reanalysis: configuration and performance of the data assimilation system, *Quarterly Journal of the Royal Meteorological Society*, 137, 553-597, 2011.

Delmotte, M., Masson, V., Jouzel, J., and Morgan, V. I.: A seasonal deuterium excess signal at Law Dome, coastal eastern Antarctica: A Southern Ocean signature, *Journal of Geophysical Research: Atmospheres*, 105, 7187-7197, 2000.

857 Denux, F.: Diffusion du signal isotopique dans le névé et dans la glace. Implication pour l'échantillonnage., PhD,
858 Geosciences, Université Joseph Fourier-Grenoble 1, Grenoble, 243 pp., 1996.

859 Domine, F., Morin, S., Brun, E., Lafaysse, M., and Carmagnola, C. M.: Seasonal evolution of snow permeability under
860 equi-temperature and temperature-gradient conditions, *The Cryosphere*, 7, 1915-1929, 2013.

861 **Ebner, P. P., Schneebeli, M., and Steinfeld, A.: Metamorphism during temperature gradient with**
862 **undersaturated advective airflow in a snow sample, *The Cryosphere*, 10, 791-797, 2016.**

863 **Ebner, P. P., Steen-Larsen, H. C., Stenni, B., Schneebeli, M., and Steinfeld, A.: Experimental observation of**
864 **transient $\delta^{18}\text{O}$ interaction between snow and advective airflow under various temperature gradient conditions,**
865 ***The Cryosphere*, 11, 1733-1743, 2017.**

866 Ekaykin, A., Hondoh, T., Lipenkov, V. Y., and Miyamoto, A.: Post-depositional changes in snow isotope content:
867 preliminary results of laboratory experiments, *Climate of the Past Discussions*, 5, 2239-2267, 2009.

868 Ekaykin, A. A., Kozachek, A. V., Lipenkov, V. Y., and Shibaev, Y. A.: Multiple climate shifts in the Southern
869 hemisphere over the past three centuries based on central Antarctic snow pits and core studies, *Annals of Glaciology*,
870 55, 259-266, 2014.

871 Ellehoj, M. D., Steen-Larsen, H. C., Johnsen, S. J., and Madsen, M. B.: Ice-vapor equilibrium fractionation factor of
872 hydrogen and oxygen isotopes: Experimental investigations and implications for stable water isotope studies, *Rapid*
873 *Communications in Mass Spectrometry*, 27, 2149-2158, 2013.

874 EPICA comm. members: Eight glacial cycles from an Antarctic ice core, *Nature*, 429, 623-628, 2004.

875 EPICA comm. members: One-to-one coupling of glacial climate variability in Greenland and Antarctica, *Nature*, 444,
876 195-198, 2006.

877 Fisher, D. A. and Koerner, R. M.: Signal and noise in four ice-core records from the Agassiz Ice Cap, Ellesmere Island,
878 Canada: details of the last millennium for stable isotopes, melt and solid conductivity, *The Holocene*, 4, 113-120, 1994.

879 Flanner, M. G. and Zender, C. S.: Linking snowpack microphysics and albedo evolution, *Journal of Geophysical*
880 *Research: Atmospheres*, 111, D12208, doi:10.1029/2005JD006834, 2006.

881 Fréville, H., Brun, E., Picard, G., Tatarinova, N., Arnaud, L., Lanconelli, C., Reijmer, C., and van den Broeke, M.:
882 Using MODIS land surface temperatures and the Crocus snow model to understand the warm bias of ERA-Interim
883 reanalyses at the surface in Antarctica, *The Cryosphere*, 8, 1361-1373, 2014.

884 Frezzotti, M., Pourchet, M., Flora, O., Gandolfi, S., Gay, M., Urbini, S., Vincent, C., Becagli, S., Gragnani, R., and
 885 Proposito, M.: Spatial and temporal variability of snow accumulation in East Antarctica from traverse data, *Journal of*
 886 *Glaciology*, 51, 113-124, 2005.

887 Friedman, I., Benson, C., and Gleason, J.: Isotopic changes during snow metamorphism, *Stable isotope geochemistry:*
 888 *a tribute to Samuel Epstein*, 1991. 211-221, 1991.

889 Gay, M., Fily, M., Genthon, C., Frezzotti, M., Oerter, H., and Winther, J.-G.: Snow grain-size measurements in
 890 Antarctica, *Journal of Glaciology*, 48, 527-535, 2002.

891 Genthon, C., Six, D., Gallée, H., Grigioni, P., and Pellegrini, A.: Two years of atmospheric boundary layer observations
 892 on a 45-m tower at Dome C on the Antarctic plateau, *Journal of Geophysical Research: Atmospheres*, 118, 3218-3232,
 893 2013.

894 Genthon, C., Six, D., Scarchilli, C., Ciardini, V., and Frezzotti, M.: Meteorological and snow accumulation gradients
 895 across Dome C, East Antarctic plateau, *International Journal of Climatology*, 36, 455-466, 2016.

896 Gkinis, V., Simonsen, S. B., Buchardt, S. L., White, J. W. C., and Vinther, B. M.: Water isotope diffusion rates from
 897 the NorthGRIP ice core for the last 16,000 years – Glaciological and paleoclimatic implications, *Earth and Planetary*
 898 *Science Letters*, 405, 132-141, 2014.

899 **Goursaud, S., Masson-Delmotte, V., Favier, V., Preunkert, S., Fily, M., Gallée, H., Jourdain, B., Legrand, M.,**
 900 **Magand, O., Minster, B., Werner, M.: A 60-year ice-core record of regional climate from Adélie land, coastal**
 901 **Antarctica, *The Cryosphere*, 11, 343-362, 2017.**

902 Hoshina, Y., Fujita, K., Nakazawa, F., Iizuka, Y., Miyake, T., Hirabayashi, M., Kuramoto, T., Fujita, S., and
 903 Motoyama, H.: Effect of accumulation rate on water stable isotopes of near-surface snow in inland Antarctica, *Journal*
 904 *of Geophysical Research*, 119, 274-283, 2014.

905 Johnsen, S.: Stable isotope homogenization of polar firn and ice, *Isotopes and impurities in snow and ice*, 1, 210-219,
 906 1977.

907 Johnsen, S. J., Dahl-Jensen, D., Dansgaard, W., and Gundestrup, N.: Greenland palaeotemperatures derived from GRIP
 908 bore hole temperature and ice core profiles, *Tellus*, 47B, 624-629, 1995.

909 Johnsen, S. J., Clausen, H. B., Cuffey, K. M., Hoffmann, G., Schwander, J., and Creyts, T.: Diffusion of stable isotopes
 910 in polar firn and ice: the isotope effect in firn diffusion, *Physics of ice core records*, 159, 121-140, 2000.

911 **Jones, T. R., Roberts, W. H. G., Steig, E. J., Cuffey, K. M., Markle, B. R., White, J. W. C.: Southern Hemisphere**
 912 **climate variability forced by Northern Hemisphere ice-sheet topography, *Nature*, 554, doi:10.1038/nature24669,**
 913 **2018.**

914 Jouzel, J., Masson-Delmotte, V., Cattani, O., Dreyfus, G., Falourd, S., Hoffmann, G., Minster, B., Nouet, J., Barnola,
 915 J. M., Chappellaz, J., Fischer, H., Gallet, J. C., Johnsen, S., Leuenberger, M., Loulergue, L., Luethi, D., Oerter, H.,
 916 Parrenin, F., Raisbeck, G., Raynaud, D., Schilt, A., Schwander, J., Selmo, E., Souchez, R., Spahni, R., Stauffer, B.,
 917 Steffensen, J. P., Stenni, B., Stocker, T. F., Tison, J. L., Werner, M., and Wolff, E. W.: Orbital and millennial Antarctic
 918 climate variability over the past 800,000 years, *Science*, 317, 793-796, 2007.

919 Kaempfer, T. U., Schneebeli, M., and Sokratov, S. A.: A microstructural approach to model heat transfer in snow,
 920 *Geophysical Research Letters*, 32, L21503, doi:10.1029/2005GL023873, 2005.

921 Kawamura, K., Parrenin, F., Lisiecki, L., Uemura, R., Vimeux, F., Severinghaus, J. P., Hutterli, M. A., Nakazawa, T.,
 922 Aoki, S., Jouzel, J., Raymo, M. E., Matsumoto, K., Nakata, H., Motoyama, H., Fujita, S., Goto-Azuma, K., Fujii, Y.,
 923 and Watanabe, O.: Northern Hemisphere forcing of climatic cycles in Antarctica over the past 360,000 years, *Nature*,
 924 448, 912-916, 2007.

925 **Krol, Q., and Löwe, H.: Relating optical and microwave grain metrics of snow: the relevance of grain shape,**
 926 ***The Cryosphere*, 10, 2847-2863, 2016.**

927 Laepple, T., Werner, M., and Lohmann, G.: Synchronicity of Antarctic temperatures and local solar insolation on
 928 orbital timescales, *Nature*, 471, 91, 2011.

929 Landais, A., Barkan, E., and Luz, B.: Record of $\delta^{18}\text{O}$ and ^{17}O -excess in ice from Vostok Antarctica during the last
 930 150,000 years, *Geophysical Research Letters*, 35, L02709, 2008.

931 **Landais, A., Casado, C., Prié, F., Magand, O., Arnaud, L., Ekaykin, A., Petit, J.-R., Picard, G., Fily, M., Minster,**
 932 **B., Touzeau, A., Goursaud, S., Masson-Delmotte, V., Jouzel, J., and Orsi, A.: Surface studies of water isotopes**
 933 **in Antarctica for quantitative interpretation of deep ice core data, *Comptes Rendus Géosciences*, 349, 139-150,**
 934 **2017.**

935 **Legagneux, L., and Domine, F.: A mean field model of the decrease of the specific surface area of dry snow**
 936 **during isothermal metamorphism, *Journal of Geophysical Research*, 110, doi:10.1029/2004JF000181, 2005.**

937 Lefebvre, F., Gallée, H., van Ypersele, J.-P., and Greuell, W.: Modeling of snow and ice melt at ETH Camp (West

938 Greenland): A study of surface albedo, *Journal of Geophysical Research: Atmospheres*, 108, D8-4231,
939 doi:10.1029/2001JD001160, 2003.

940 Libois, Q., Picard, G., Arnaud, L., Morin, S., and Brun, E.: Modeling the impact of snow drift on the decameter-scale
941 variability of snow properties on the Antarctic Plateau, *Journal of Geophysical Research: Atmospheres*, 119, 11662-
942 11681, 2014.

943 Libois, Q., Picard, G., Arnaud, L., Dumont, M., Lafaysse, M., Morin, S., and Lefebvre, E.: Summertime evolution of
944 snow specific surface area close to the surface on the Antarctic Plateau, *The Cryosphere*, 9, 2383-2398, 2015.

945 Lorius, C., Jouzel, J., Ritz, C., Merlivat, L., Barkov, N. I., Korotkevich, Y. S., and Kotlyakov, V. M.: A 150,000-year
946 climatic record from Antarctic ice, *Nature*, 316, 591-596, 1985.

947 Lu, G. and DePaolo, D. J.: Lattice Boltzmann simulation of water isotope fractionation during ice crystal growth in
948 clouds, *Geochimica et Cosmochimica Acta*, 180, 271-283, 2016.

949 Mann, M. E. and Jones, P. D.: Global surface temperatures over the past two millennia, *Geophysical Research Letters*,
950 30, 1820, doi:10.1029/2003GL017814, 2003.

951 Masson-Delmotte, V., Landais, A., Stievenard, M., Cattani, O., Falourd, S., Jouzel, J., Johnsen, S. J., Dahl-Jensen, D.,
952 Sveinbjörnsdóttir, A., White, J. W. C., Popp, T., and Fischer, H.: Holocene climatic changes in Greenland: Different
953 deuterium excess signals at Greenland Ice Core Project (GRIP) and NorthGRIP, *Journal of Geophysical Research:*
954 *Atmospheres*, 110, 1-13, 2005.

955 Masson-Delmotte, V., Buiron, D., Ekaykin, A., Frezzotti, M., Gallée, H., Jouzel, J., Krinner, G., Landais, A.,
956 Motoyama, H., Oerter, H., Pol, K., Pollard, D., Ritz, C., Schlosser, Z., Sime, L. C., Sodemann, H., Stenni, B., Uemura,
957 R., and Vimeux, F.: A comparison of the present and last interglacial periods in six Antarctic ice cores, *Clim. Past*, 7,
958 397-423, 2011.

959 Masson-Delmotte, V., Steen-Larsen, H., Ortega, P., Swingedouw, D., Popp, T., Vinther, B., Oerter, H.,
960 Sveinbjörnsdóttir, A., Gudlaugsdóttir, H., and Box, J.: Recent changes in north-west Greenland climate documented
961 by NEEM shallow ice core data and simulations, and implications for past-temperature reconstructions, *The*
962 *Cryosphere* 9, 1481-1504, 2015.

963 Morse, D. L., Waddington, E. D., Marshall, H.-P., Neumann, T. A., Steig, E. J., Dibb, J. E., Winebrenner, D. P., and
964 Arthern, R. J.: Accumulation Rate Measurements at Taylor Dome, East Antarctica: Techniques and Strategies for Mass

965 Balance Measurements in Polar Environments, *Geografiska Annaler: Series A, Physical Geography*, 81, 683-694,
 966 1999.

967 Neumann, T. A.: Effects of firn ventilation on geochemistry of polar snow, PhD, Department of Earth and Space
 968 Sciences, University of Washington, Washington, 223 pp., 2003.

969 Neumann, T. A. and Waddington, E. D.: Effects of firn ventilation on isotopic exchange, *Journal of Glaciology*, 50,
 970 183-194, 2004.

971 Neumann, T. A., Waddington, E. D., Steig, E. J., and Grootes, P. M.: Non-climate influences on stable isotopes at
 972 Taylor Mouth, Antarctica, *Journal of Glaciology*, 51, 248-258, 2005.

973 Neumann, T., Albert, M., Lomonaco, R., Engel, C., Courville, Z., and Perron, F.: Experimental determination of snow
 974 sublimation rate and stable-isotopic exchange, *Annals of Glaciology*, 49, 1-6, 2008.

975 Neumann, T. A., Albert, M. R., Engel, C., Courville, Z., and Perron, F.: Sublimation rate and the mass-transfer
 976 coefficient for snow sublimation, *International Journal of Heat and Mass Transfer*, 52, 309-315, 2009.

977 Petit, J. R., Jouzel, J., Pourchet, M., and Merlivat, L.: A detailed study of snow accumulation and stable isotope content
 978 in Dome C (Antarctica), *Journal of Geophysical Research*, 87, 4301-4308, 1982.

979 Petit, J. R., Jouzel, J., Raynaud, D., Barkov, N. I., Barnola, J. M., Basile, I., Bender, M., Chappellaz, J., Davis, M.,
 980 Delaygue, G., Delmotte, M., Kotlyakov, V. M., Legrand, M., Lipenkov, V. Y., Lorius, C., Pepin, L., Ritz, C., Saltzman,
 981 E., and Stievenard, M.: Climate and atmospheric history of the past 420,000 years from the Vostok ice core, Antarctica,
 982 *Nature*, 399, 429-436, 1999.

983 Pinzer, B. R., Schneebeli, M., and Kaempfer, T. U.: Vapor flux and recrystallization during dry snow metamorphism
 984 under a steady temperature gradient as observed by time-lapse micro-tomography, *The Cryosphere*, 6, 1141-1155,
 985 2012.

986 Ramseier, R. O.: Self-diffusion of tritium in natural and syntehtic ice monocrystals, *Journal of Applied Physics*, 38,
 987 2553-2556, 1967.

988 Ritter, F., Steen-Larsen, H. C., Werner, M., Masson-Delmotte, V., Orsi, A., Behrens, M., Birnbaum, G., Freitag, J.,
 989 Risi, C., and Kipfstuhl, S.: Isotopic exchange on the diurnal scale between near-surface snow and lower atmospheric
 990 water vapor at Kohnen station, East Antarctica, *The Cryosphere Discuss.*, 2016, 1-35, 2016.

991 Schneider, D. P., Steig, E. J., Ommen, T. D. v., Dixon, D. A., Mayewski, P. A., Jones, J. M., and Bitz, C. M.: Antarctic

992 temperatures over the past two centuries from ice cores, *Geophysical Research Letters*, 33, L16707, 2006.
 993 Shaheen, R., Abauanza, M., Jackson, T. L., McCabe, J., Savarino, J., and Thiemens, M. H.: Tales of volcanoes and El-
 994 Niño southern oscillations with the oxygen isotope anomaly of sulfate aerosol, *Proceedings of the National Academy*
 995 *of Sciences*, 110, 17662-17667, 2013.
 996 Shuman, C. A., Alley, R. B., Anandakrishnan, S., White, J. W. C., Grootes, P. M., and Stearns, C. R.: Temperature
 997 and accumulation at the Greenland Summit: Comparison of high-resolution isotope profiles and satellite passive
 998 microwave brightness temperature trends, *Journal of Geophysical Research: Atmospheres*, 100, 9165-9177, 1995.
 999 Shuman, C. A., Steffen, K., Box, J. E., and Stearns, C. R.: A dozen years of temperature observations at the Summit:
 1000 Central Greenland automatic weather stations 1987–99, *Journal of Applied Meteorology*, 40, 741-752, 2001.
 1001 Sime, L. C., Tindall, J. C., Wolff, E. W., Connolley, W. M., and Valdes, P. J.: Antarctic isotopic thermometer during
 1002 a CO₂ forced warming event, *Journal of Geophysical Research*, 113, D24119, 2008.
 1003 Sjolte, J., Hoffmann, G., Johnsen, S. J., Vinther, B. M., Masson-Delmotte, V., and Sturm, C.: Modeling the water
 1004 isotopes in Greenland precipitation 1959–2001 with the meso-scale model REMO-iso, *Journal of Geophysical*
 1005 *Research: Atmospheres*, 116, D18105, doi:10.1029/2010JD015287, 2011.
 1006 Sokratov, S. A. and Golubev, V. N.: Snow isotopic content change by sublimation, *Journal of Glaciology*, 55, 823-
 1007 828, 2009.
 1008 Steen-Larsen, H. C., Masson-Delmotte, V., Sjolte, J., Johnsen, S. J., Vinther, B. M., Bréon, F. M., Clausen, H., Dahl-
 1009 Jensen, D., Falourd, S., and Fettweis, X.: Understanding the climatic signal in the water stable isotope records from
 1010 the NEEM shallow firn/ice cores in northwest Greenland, *Journal of Geophysical Research: Atmospheres*, 116,
 1011 D06108, doi:10.1029/2010JD014311, 2011.
 1012 Steen-Larsen, H., Masson-Delmotte, V., Hirabayashi, M., Winkler, R., Satow, K., Prié, F., Bayou, N., Brun, E., Cuffey,
 1013 K., and Dahl-Jensen, D.: What controls the isotopic composition of Greenland surface snow?, *Climate of the Past*, 10,
 1014 377-392, 2014.
 1015 Steig, E. J.: The south-north connection, *Nature*, 44, 152-153, 2006.
 1016 Stenni, B., Jouzel, J., Masson-Delmotte, V., Röthlisberger, R., Castellano, E., Cattani, O., Falourd, S., Johnsen, S. J.,
 1017 Longinelli, A., Sachs, J. P., Selmo, E., Souchez, R., Steffensen, J. P., and Udisti, R.: A late-glacial high-resolution site
 1018 and source temperature record derived from the EPICA Dome C isotope records (East Antarctica), *Earth and Planetary*

1019 Science Letters, 217, 183-195, 2004.

1020 Stenni, B., Buiron, D., Frezzotti, M., Albani, S., Barbante, C., Bard, E., Barnola, J. M., Baroni, M., Baumgartner, M.,
1021 Bonazza, M., Capron, E., Castellano, E., Chappellaz, J., Delmonte, B., Falourd, S., Genoni, L., Iacumin, P., Jouzel, J.,
1022 Kipfstuhl, S., Landais, A., Lemieux-Dudon, B., Maggi, V., Masson-Delmotte, V., Mazzola, C., Minster, B.,
1023 Montagnat, M., Mulvaney, R., Narcisi, B., Oerter, H., Parrenin, F., Petit, J. R., Ritz, C., Scarchilli, C., Schilt, A.,
1024 Schupbach, S., Schwander, J., Selmo, E., Severi, M., Stocker, T. F., and Udisti, R.: Expression of the bipolar see-saw
1025 in Antarctic climate records during the last deglaciation, *Nature Geosci*, 4, 46-49, 2011.

1026 Stenni, B., Scarchilli, C., Masson-Delmotte, V., Schlosser, E., Ciardini, V., Dreossi, G., Grigioni, P., Bonazza, M.,
1027 Cagnati, A., Karlicek, D., Risi, C., Udisti, R., and Valt, M.: Three-year monitoring of stable isotopes of precipitation
1028 at Concordia Station, East Antarctica, *The Cryosphere*, 10, 2415-2428, 2016.

1029 Stichler, W., Schotterer, U., Fröhlich, K., Ginot, P., Kull, C., Gäggeler, H., and Pouyaud, B.: Influence of sublimation
1030 on stable isotope records recovered from high-altitude glaciers in the tropical Andes, *Journal of Geophysical Research*,
1031 106, 22613-22620, 2001.

1032 Touzeau, A., Landais, A., Stenni, B., Uemura, R., Fukui, K., Fujita, S., Guilbaud, S., Ekaykin, A., Casado, M., and
1033 Barkan, E.: Acquisition of isotopic composition for surface snow in East Antarctica and the links to climatic
1034 parameters, *The Cryosphere*, 10, 837-852, 2016.

1035 Town, M. S., Warren, S. G., Walden, V. P., and Waddington, E. D.: Effect of atmospheric water vapor on modification
1036 of stable isotopes in near-surface snow on ice-sheets, *Journal of Geophysical Research*, 113, D24303, 2008.

1037 **Uemura, R., Landais, A., Motoyama, H., and Stenni, B. : Ranges of moisture-source temperature estimated**
1038 **from Antarctic ice cores stable isotope records over glacial-interglacial cycles, *Climate of the Past*, 8, 1109-1025,**
1039 **2012.**

1040 Urbini, S., Frezzotti, M., Gandolfi, S., Vincent, C., Scarchilli, C., Vittuari, L., and Fily, M.: Historical behaviour of
1041 Dome C and Talos Dome (East Antarctica) as investigated by snow accumulation and ice velocity measurements,
1042 *Global and Planetary Change*, 60, 576-588, 2008.

1043 van de Berg, W. J., van den Broeke, M. R., Reijmer, C. H., and van Meijgaard, E.: Reassessment of the Antarctic
1044 surface mass balance using calibrated output of a regional atmospheric climate model, *Journal of Geophysical*
1045 *Research: Atmospheres*, 111, D11104, doi:10.1029/2005JD006495, 2006.

1046 van der Wel, L., Been, H., Smeets, P., and Meijer, H.: Constraints on the $\delta^2\text{H}$ diffusion rate in firn from field
 1047 measurements at Summit, Greenland, *The Cryosphere*, 9, 1089-1103, 2015.

1048 Vionnet, V., Brun, E., Morin, S., Boone, A., Faroux, S., Le Moigne, P., Martin, E., and Willemet, J.: The detailed
 1049 snowpack scheme Crocus and its implementation in SURFEX v7. 2, *Geoscientific Model Development*, 5, 773-791,
 1050 2012.

1051 Waddington, E. D., Steig, E. J., and Neumann, T. A.: Using characteristic times to assess whether stable isotopes in
 1052 polar snow can be reversibly deposited, *Annals of Glaciology*, 35, 118-124, 2002.

1053 **WAIS Divide Project Members: Onset of deglacial warming in West Antarctica driven by local orbital forcing,**
 1054 ***Nature*, 500, 440-444, 2013.**

1055 White, J.W.C., Barlow, L.K., Fisher, D., Grootes, P., Jouzel, J., Johnsen, S.J., Stuiver, M., and Clausen, H.: The climate
 1056 signal in the stable isotope of Summit, Greenland snow : Results of comparisons with modern climate observations.
 1057 *Journal of Geophysical Research*, 102, C12, 26425 - 26439, 1997.

1058

1059 **Table 1.** Definition of the symbols used.

Symbol	Description
Constants	
T_0	Temperature of the triple point of water (K)
R_v	Vapor constant for water ($J \cdot kg^{-1} K^{-1}$)
L_{sub}	Latent heat of sublimation of water ($J \cdot m^{-3}$)
C_{v0}	Vapor mass concentration at 273.16 K ($kg \cdot m^{-3}$ of air)
D_{ice}	Diffusivity of water molecules in solid ice ($m^2 \cdot s^{-1}$)
D_v	Diffusivity of vapor in air at 263 K ($m^2 \cdot s^{-1}$) (temperature dependency neglected)
ρ_{ice}	Density of ice ($kg \cdot m^{-3}$)
A	Accumulation (m i.e. per year)
R_{moy}	Average snow grain radius (m)
Δt_{sol}	Characteristic time for solid diffusion (s)
$\Delta t_{surf/center}$	Periodicity of the mixing between grain center and grain surface, because of grain center translation (s)
1D-variables	
T	Time (s)
N	Layer number from top of the snowpack
$\delta^{18}O_{sf}(t)$	Isotopic composition of oxygen in the snowfall (‰)
$T_{air}(t)$	Temperature of the air at 2 m (K)
2D-variables	
$h(t, n)$	Height of the center of the snow layer relative to the bottom of the snowpack (m)
$z(t, n)$	Depth of the center of the snow layer (m from surface)
$dz(t, n)$	Thickness of the snow layer (m)
$T(t, n)$	Temperature of the snow layer (K)
$\rho_{sn}(t, n)$	Density of the snow layer ($kg \cdot m^{-3}$)
$m_{sn}(t, n)$	Mass of the snow layer (kg)
$C_v(t, n)$	Vapor mass concentration at saturation in the porosity of the snow layer ($kg \cdot m^{-3}$ of air)
$D_{eff}(t, n)$	Effective diffusivity of vapor in the layer ($m^2 \cdot s^{-1}$)
$\delta^{18}O(t, n)$	Isotopic composition of oxygen in the snow layer (‰)
$F^{18}(n+1 \rightarrow n)$	Flux of the heavy water molecules (^{18}O) from layer $n+1$ to layer n ($kg \cdot m^{-2} \cdot s^{-1}$)
$F(n+1 \rightarrow n)$	Vapor flux from layer $n+1$ to layer n ($kg \cdot m^{-2} \cdot s^{-1}$)
$D_{eff}(t, n \rightarrow n+1)$	Effective interfacial diffusivity between layers n and $n+1$ ($m^2 \cdot s^{-1}$)
$R_{vap\ ini}^i$	Isotopic ratio in the initial vapor (i is either ^{18}O , ^{17}O or D)
$R_{surf\ ini}^i$	Isotopic ratio in the grain surface sub-compartment before vapor individualization
$C_{vap\ ini}^x$	Ratio between the mass of a given isotopologue in the initial vapor (x is ^{18}O, ^{17}O, ^{16}O, 1H or D) and the total mass of vapor (no unit). The mass balance is made separately and independently for H and O (i.e.: $C_{vap\ ini}^{18} + C_{vap\ ini}^{17} + C_{vap\ ini}^{16} = 1$ and $C_{vap\ ini}^{1H} + C_{vap\ ini}^D = 1$).
α_{sub}^i	Fractionation coefficients at equilibrium during sublimation (i is either ^{18}O , ^{17}O or D)
	Fractionation coefficients during condensation (i is either ^{18}O , ^{17}O or D)
α_{cond}^i	No fractionation
$\alpha_{cond\ eff}^i$	Effective (total) fractionation

$\alpha_{cond\ kin}^i$	Kinetic fractionation only
$\alpha_{cond\ eq}^i$	Equilibrium fractionation only
$m_{vap\ ini}$	Initial mass of vapor in the porosity (kg)
$m_{surf\ ini}$	Mass of water in the grain surface sub-compartment before vapor individualization (kg)
$m_{surf\ new}$	Mass of water in the grain surface sub-compartment after vapor individualization (kg)
T	Ratio of between the mass of the grain surface compartment and the mass of total grain
m_{surf}	Mass of grain surface compartment
m_{center}	Mass of grain center compartment
m_{vap}	Mass of vapor in the porosity
V_{tot}	Total volume of the considered layer
Φ	Porosity of the layer
$m_{surf\ ini}^{18}$	Mass of heavy water molecules (^{18}O) in the grain surface before vapor individualization (kg)
$m_{surf\ new}^{18}$	Mass of heavy water molecules (^{18}O) in the grain surface after vapor individualization (kg)
D^{18}/D	Ratio of diffusivities between heavy isotope and light isotope
$\Delta m_{vap,exc}$	Mass of vapor in excess in the porosity after vapor transport (kg)
$\rho_{sn\ ini}$	Density of the snow layer before vapor transport
$\rho_{sn\ new}$	Density of the snow layer after vapor transport
T_{ini}, T_{new}	Temperature of the snow layer before and after vapor transport

1060
1061

GRIP		
Accumulation	23 cm i.e. yr. ⁻¹	Dahl-Jensen et al., 1993
Annual temperature	241 K	Masson-Delmotte et al., 2005
Winter temperature	232 K	(Feb.) Shuman et al., 2001
Summer temperature	261 K	(Aug.) Shuman et al., 2001
Mean $\delta^{18}\text{O}$	-35.2‰	Masson-Delmotte et al., 2005
$\delta^{18}\text{O}$ min	-43 ‰	(2m snow pit) Shuman et al., 1995
$\delta^{18}\text{O}$ max	-27 ‰	(2m snow pit) Shuman et al., 1995
$\delta^{18}\text{O}$ /T slope	0.46 ‰/°C	(2m snow pit) Shuman et al., 1995
DOME C		
Accumulation	2.7 cm i.e. yr. ⁻¹	Frezzotti et al., 2005; Urbini et al., 2008
Annual temperature	221 K	Stenni et al., 2016
Min winter T	199 K	Stenni et al., 2016
Max summer T	248 K	Stenni et al., 2016
Mean $\delta^{18}\text{O}$	-56.4 ‰	Stenni et al., 2016
$\delta^{18}\text{O}$ min winter	-71.8 ‰	Stenni et al., 2016
$\delta^{18}\text{O}$ max summer	-40.2 ‰	Stenni et al., 2016
$\delta^{18}\text{O}$ /T slope	0.49 ‰/°C	Stenni et al., 2016

Table 2. Climate and isotope variability at GRIP (Greenland) and Dome C (Antarctica).

Variable	Equation		Average	Range	
Thickness (m)	dz		$1.2 \cdot 10^{-1}$	$5 \cdot 10^{-4}$	$8 \cdot 10^{-1}$
Density (kg m^{-3})	ρ_{sn}		340	300	460
Temperature (K)	T		225	205	255
Mass (kg)	m_{sn}	$= dz \cdot \rho_{\text{sn}}$	42	0.15	368
Vapor mass concentration ($\text{kg} \cdot \text{m}^{-3}$)	C_v	Eq. (8)	$1.8 \cdot 10^{-5}$	$1.2 \cdot 10^{-6}$	$4.4 \cdot 10^{-4}$
Porosity	Φ	$= 1 - (\rho_{\text{sn}} / \rho_{\text{ice}})$	0.63	0.5	0.67
Vapor mass (kg)	m_{vap}	Eq. (11)	$1.3 \cdot 10^{-6}$	$3 \cdot 10^{-10}$	$2.4 \cdot 10^{-4}$
Minimum ratio	τ_{min}	$= 1/10^6$	$1 \cdot 10^{-6}$	$1 \cdot 10^{-6}$	$1 \cdot 10^{-6}$
Maximum ratio	τ_{max}	$= \frac{C_v \cdot \Phi}{\rho_{\text{sn}}} \cdot 10^6$	$3.3 \cdot 10^{-2}$	$1.3 \cdot 10^{-3}$	1

Table 3. Typical thickness, density, temperature and other parameters of the snow layers in the simulations. The ratio τ is the mass ratio between the grain surface compartment and the grain center compartment. It must be chosen within the interval $[10^{-6} ; 10^6 (C_v \Phi / \rho_{\text{sn}})]$ to allow exchanges between grain surface compartment and grain center compartment, on the one hand; and between grain surface compartment and vapor compartment on the other hand (see text for details).

	GRIP simulation			Dome C simulations		
N°	1	2	3	4	5	6
Section	4.1.1.	4.1.2.	4.2.1.	4.2.2.	4.2.3.	4.2.4.
Figures	Figure 2	Figure 3	Figure 5	Figure 6	Figure 7	Figure 8
Duration	10 years	10 years	1 year	1 year	1 year	10 years
Period	Jan 2000- Dec 2010	Jan 2001- Dec 2011	Jan- Dec 2001	Jan- Dec 2001	Jan- Dec 2001	Jan 2000- Dec 2010
<i>Atmospheric forcing applied</i>						
Air T	-	ERA-Interim (GR)	ERA-Interim	ERA-Interim	ERA-Interim	ERA-Interim
Specific humidity	-	ERA-Interim (GR)	ERA-Interim	ERA-Interim	ERA-Interim	ERA-Interim
Air pressure	-	ERA-Interim (GR)	ERA-Interim	ERA-Interim	ERA-Interim	ERA-Interim
Wind velocity	-	ERA-Interim (GR)	ERA-Interim	ERA-Interim	ERA-Interim	ERA-Interim
Snowfall	NO	NO	NO	NO	YES	YES
$\delta^{18}\text{O}_{\text{sf}}$	-	-	-	-	Function (T)*	Function (T)*
<i>Model configuration</i>						
Initial snow T	Flat profile (241 K)	One-year run initialization (Jan-Dec 2000)	One-year run initialization (Jan-Dec 2000)	One-year run initialization (Jan-Dec 2000)	One-year run initialization (Jan-Dec 2000)	Exponential profile**
Evolution of snow T	Constant	Computed	Computed	Computed	Computed	Computed
Initial snow d18O	Sinusoidal profile***	Sinusoidal profile***	-40 ‰	-40 ‰	-40 ‰	-40 ‰
Wind drift	NO	NO	NO	YES	YES	NO
Homogeneous compaction	NO	NO	NO	YES	YES	NO

Table 4. List of simulations described in the article with the corresponding paragraph number. The external atmospheric forcing used for Dome C is ERA-Interim reanalysis (2000-2013). However, the precipitation amounts from ERA-Interim reanalysis are increased by 1.5 times to account for the dry bias in the reanalysis (as in Libois et al., 2014). For the second simulation at GRIP, Greenland meteorological conditions are derived from the atmospheric forcing of Dome C, but the

1075 temperature is modified ($T_{\text{GRIP}}=T_{\text{DC}}+15$) as well as the longwave down ($\text{LW}_{\text{GRIP}}=0.85 \text{ LW}_{\text{DC}} +60$).

1076 * Using data from one-year snowfall sampling at Dome C (Stenni et al., 2016; Touzeau et al., 2016), we obtained the following [Eq. \(16\)](#) linking $\delta^{18}\text{O}$ in the snowfall

1077 to the local temperature: $\delta^{18}O_{sf} = 0.45 \times (T - 273.15) - 31.5$.

1078 **The exponential profile of temperature used in simulation 6 is defined using [Eq. \(20\)](#):

1079
$$T(z) = T(10m) + \Delta T \times \exp(-z/z_0) + 0.1 \times z \tag{20}$$

1080 with $T(10m)=218 \text{ K}$, $\Delta T=28 \text{ K}$, and $z_0=1.516 \text{ m}$.

1081 It fits well with temperature measurements of midday in January (Casado et al., 2016b).

1082 ***The Greenland snowpack has an initial sinusoidal profile of $\delta^{18}\text{O}$ defined using [Eq. \(19\)](#): $\delta^{18}O = -35.5 - 8 \times \sin\left(\frac{2\pi \times z}{a \times \rho_{ice}/\rho_{sn}}\right)$

1083

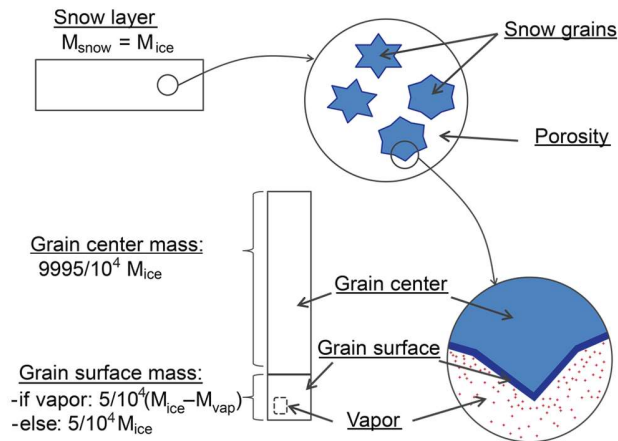
1084

1085

	GRIP sensitivity tests				Dome C sensitivity tests				
N°	1	2	3	4	1	2	3	4	5
Section	4.3.	4.3.	4.3.	4.3.	4.3.	4.3.	4.3.	4.3.	4.3.
Figures	Figure 9	Figure 9	Figure 9	Figure 9	Figure 10	Figure 10	Figure 10	Figure 10	Figure 10
Duration	6 months	6 months	6 months	6 months	3 years	3 years	3 years	3 years	3 years
Period	Jan-Jun 2000	Jan-Jun 2000	Jan-Jun 2000	Jan-Jun 2000	Jan 2000-Dec 2002	Jan 2000-Dec 2002	Jan 2000-Dec 2002	Jan 2001-Dec 2003	Jan 2001-Dec 2003
<i>Atmospheric forcing applied</i>									
Air T	-	-	-	-	-	-	-	ERA-Interim	ERA-Interim
Specific humidity	-	-	-	-	-	-	-	ERA-Interim	ERA-Interim
Air pressure	-	-	-	-	-	-	-	ERA-Interim	ERA-Interim
Wind velocity	-	-	-	-	-	-	-	ERA-Interim	ERA-Interim
Snowfall	NO	NO	NO	NO	NO	NO	NO	NO	NO
$\delta^{18}\text{O}_{\text{sf}}$	-	-	-	-	-	-	-	-	-
<i>Model configuration</i>									
Initial snow T	Flat profile (241 K)	Flat profile (241 K)	Flat profile (241 K)	Flat profile (241 K)	Flat profile (241 K)	Flat profile (220 K)	Flat profile (220 K)	One-year run initialization (Jan-Dec 2000)	One-year run initialization (Jan-Dec 2000)
Evolution of snow T	Constant	Constant	Constant	Constant	Constant	Constant	Constant	Computed	Computed
Initial snow d18O	Sinusoidal profile***	Sinusoidal profile***	Sinusoidal profile***	Sinusoidal profile***	Sinusoidal profile****	Sinusoidal profile****	Sinusoidal profile****	Sinusoidal profile****	Sinusoidal profile****
Wind drift	NO	NO	NO	NO	NO	NO	NO	NO	NO
Homogeneous compaction	NO	NO	NO	NO	NO	NO	NO	NO	NO
Mass ratio τ within the grain	$1 \cdot 10^{-6}$	$5 \cdot 10^{-4}$	$3.3 \cdot 10^{-2}$	$5 \cdot 10^{-4}$	$5 \cdot 10^{-4}$	$5 \cdot 10^{-4}$	$5 \cdot 10^{-4}$	$5 \cdot 10^{-4}$	$3.3 \cdot 10^{-2}$

	Period for recrystallization $\Delta t_{surf/center}$	15 days	15 days	15 days	2 days	15 days	2 days	15 days	15 days	15 days
1086	<hr/>									
1087	Table 5. List of the sensitivity tests performed at GRIP and at Dome C. The external atmospheric forcing used for Dome C is ERA-Interim reanalysis (see Table 4).									
1088	***The Greenland snowpack has an initial sinusoidal profile of $\delta^{18}O$ defined using Eq. (19) :									
1089	$\delta^{18}O = -35.5 - 8 \times \sin\left(\frac{2\pi \times z}{a \times \rho_{ice} / \rho_{sn}}\right)$									
1090	****The Dome C snowpack has an initial sinusoidal profile of $\delta^{18}O$ defined using Eq. (21) :									
1091	$\delta^{18}O = -48.5 - 6.5 \times \sin\left(\frac{2\pi \times z}{a \times \rho_{ice} / \rho_{sn}}\right) \tag{21}$									

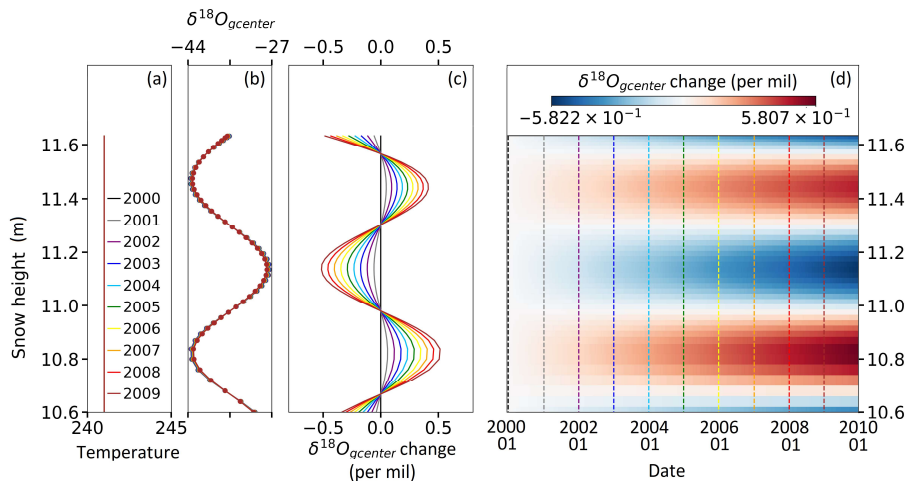
1092



1093
1094
1095
1096
1097

Figure 1. Splitting of the snow layer into two compartments, grain center and grain surface, with a constant mass ratio between them. The vapor compartment is a sub-compartment inside the grain surface compartment and is only defined at specific steps of the model.

1098



1099

1100

1101

1102

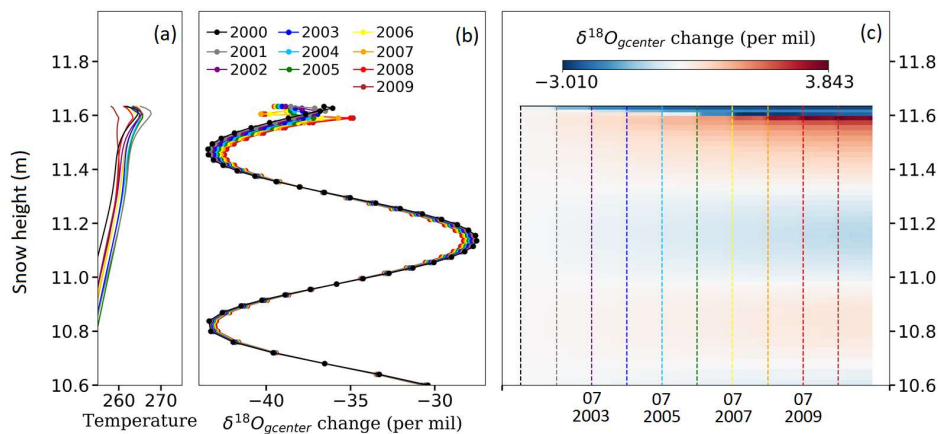
1103

1104

1105

1106

Figure 2. Simulation 1: Attenuation of the seasonal $\delta^{18}O_{gcenter}$ variation caused by diffusion **along** isotopic gradients in vapor phase over 10 years (homogeneous and constant temperature of 241 K, original signal with mean value of -35.5 ‰ and amplitude of 16 ‰). (a) Vertical homogeneous temperature profile; (b) $\delta^{18}O$ profile at the beginning and end of the simulation; (c) Deviation of the $\delta^{18}O$ relative to the original profile, for 10 dates; (d) Evolution of the deviation to the original profile of $\delta^{18}O$.



1107

1108

1109

1110

1111

1112

Figure 3. Simulation 2: Attenuation of the seasonal $\delta^{18}O_{gcenter}$ variation caused by diffusion in vapor phase over 10 years (with temperature evolution, original signal with mean value of -35.5 ‰ and amplitude of 16 ‰). (a) Vertical temperature profile for each summer; (b) $\delta^{18}O_{gcenter}$ profile for each summer; (c) Evolution of the deviation to the original profile of $\delta^{18}O_{gcenter}$. **Note that temperature evolves during the whole year (see Fig. S1).**

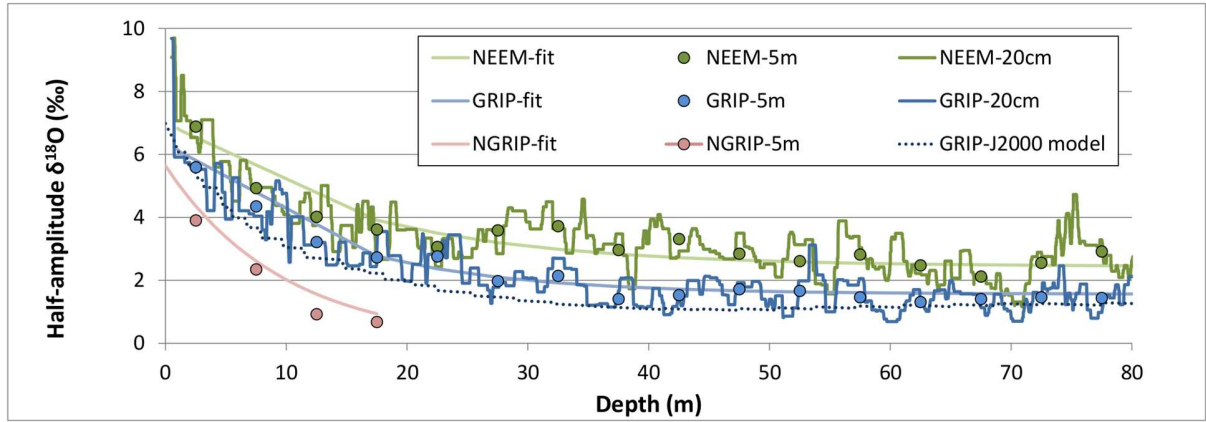


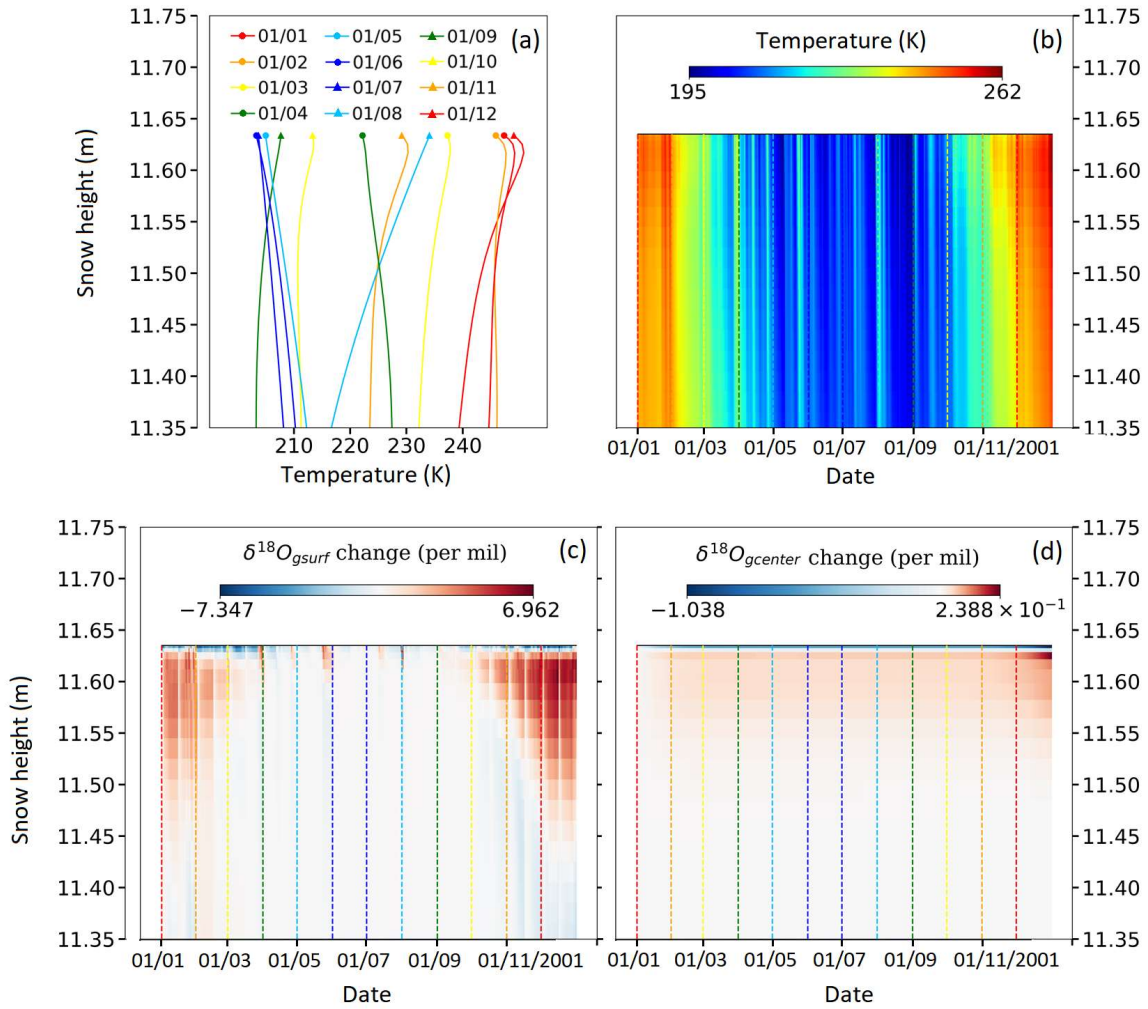
Figure 4. Evolution of the $\delta^{18}\text{O}$ semi-amplitude with depth in shallow cores at NEEM, GRIP and NGRIP (Steen-Larsen et al., 2011 and Masson-Delmotte et al., 2015; White et al., 1997; Johnsen et al., 2000). The attenuation of the semi-amplitude values with depth was fitted using an exponential equation (Eq. (22)):

$$A = A_0 \cdot \exp(-\gamma \cdot z) - b \quad (22)$$

With $A_0=4.976$ ‰; $\gamma=0.08094$; $b=-1.56$ ‰ at GRIP, and $A_0=4.685$ ‰; $\gamma=0.06622$; $b=-2.44$ ‰ at NEEM.

The dotted curve corresponds to the simulated attenuation at GRIP based on the Johnsen et al.'s model (diffusion length σ from their Figure 2, and wavelength λ fitted on the Eurocore core from GRIP, White et al., 1997).

1122
1123



1124
1125 **Figure 5. Simulation 3: Evolution of temperature and $\delta^{18}\text{O}$ values from January to December 2001. (a)**
1126 **Temperature profiles for the first day of each month; (b) Temperature evolution in the snowpack; (c) ‘ $\delta^{18}\text{O}$**
1127 **change’ in the grain surface compartment; (d) ‘ $\delta^{18}\text{O}$ change’ in the grain center compartment. Here, ‘ $\delta^{18}\text{O}$**
1128 **change’ stands for the difference between $\delta^{18}\text{O}$ at t and at the beginning of the simulation for the selected layer.**
1129
1130
1131
1132
1133
1134

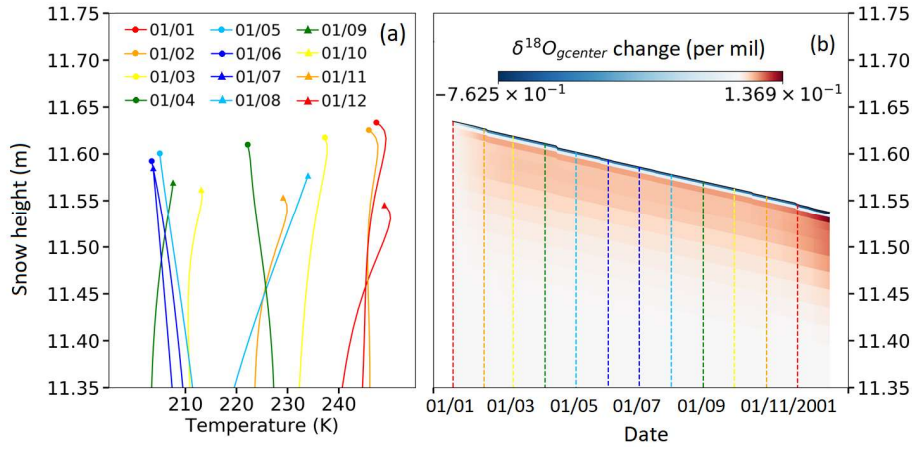


Figure 6. Simulation 4: Cumulative change in $\delta^{18}O_{gcenter}$ values (vapor transport, compaction and wind drift active).

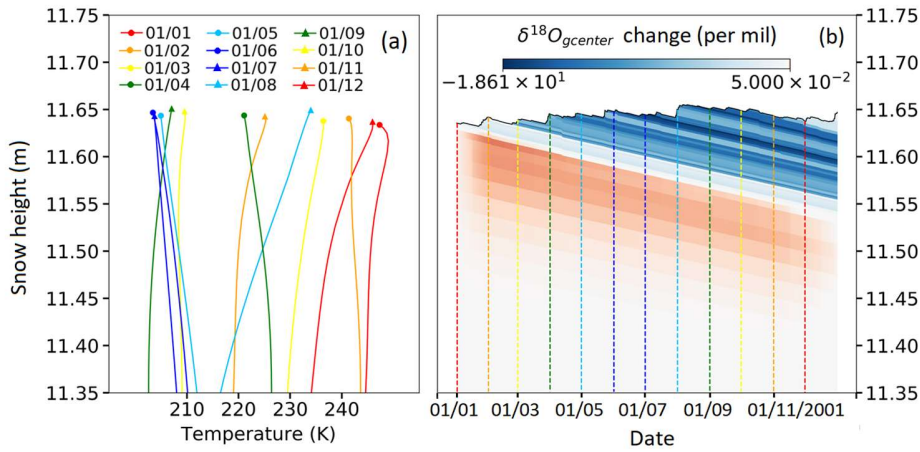


Figure 7. Simulation 5: Cumulative change of $\delta^{18}O$ values at the grain center (relative to t_0) over 6 months. Simulation with snowfall with varying $\delta^{18}O$ (function of T_{air}), vapor transport active, wind and weight compaction active.

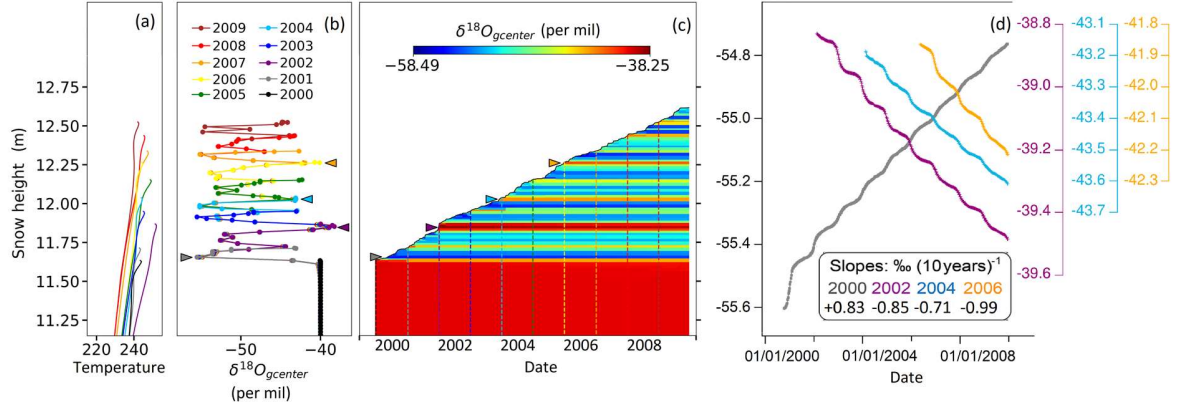


Figure 8. Simulation 6: Evolution of $\delta^{18}\text{O}_{\text{gcenter}}$ values as a result of snowfall and vapor transport over 10 years (compaction is inactive; merging between layers is allowed but limited). (a) Temperature profiles at mid-January for each year. (b) $\delta^{18}\text{O}_{\text{gcenter}}$ profile at mid-January for each year. (c) Repartition of $\delta^{18}\text{O}_{\text{gcenter}}$ values as a function of time and depth. (d) Evolution of $\delta^{18}\text{O}_{\text{gcenter}}$ values after burial for 4 selected layers (deposited in winter 2000, and summer 2002, 2004, 2006). Note that we do not present the evolution of snow composition in the first year after deposition because the thin snow layers resulting from precipitation are getting merged.

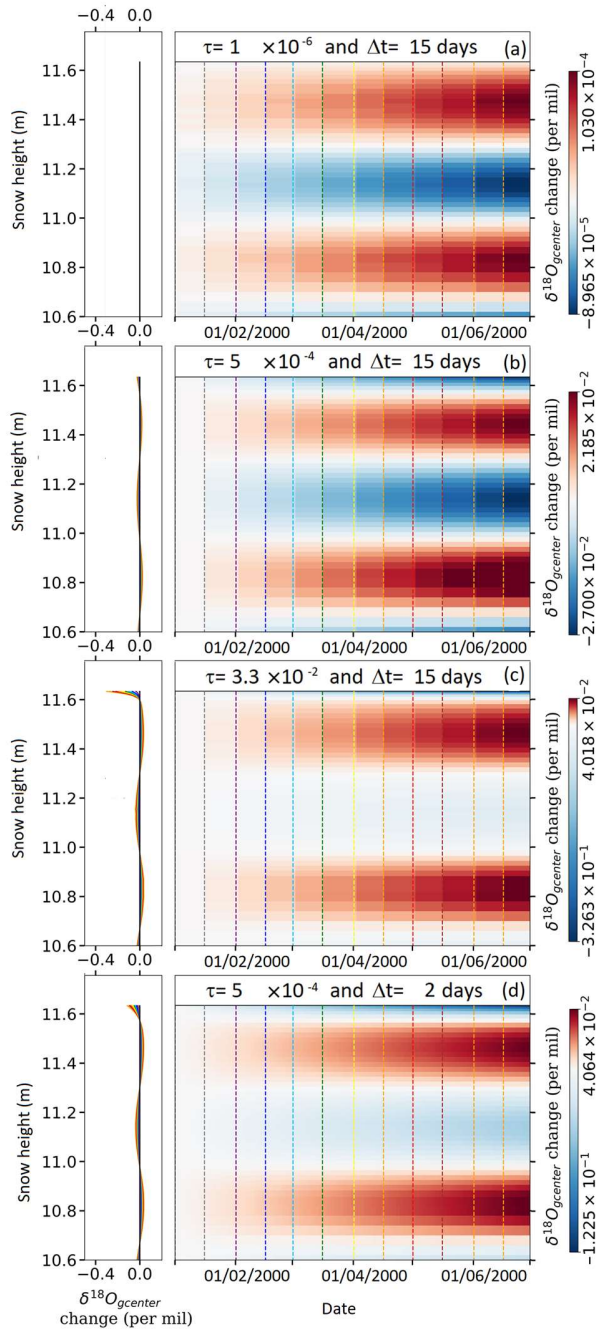


Figure 9. Test of the sensitivity of the model to the ratio of mass between **grain surface compartments** and **total grain** and to the interval of mixing between the two compartments (GRIP).

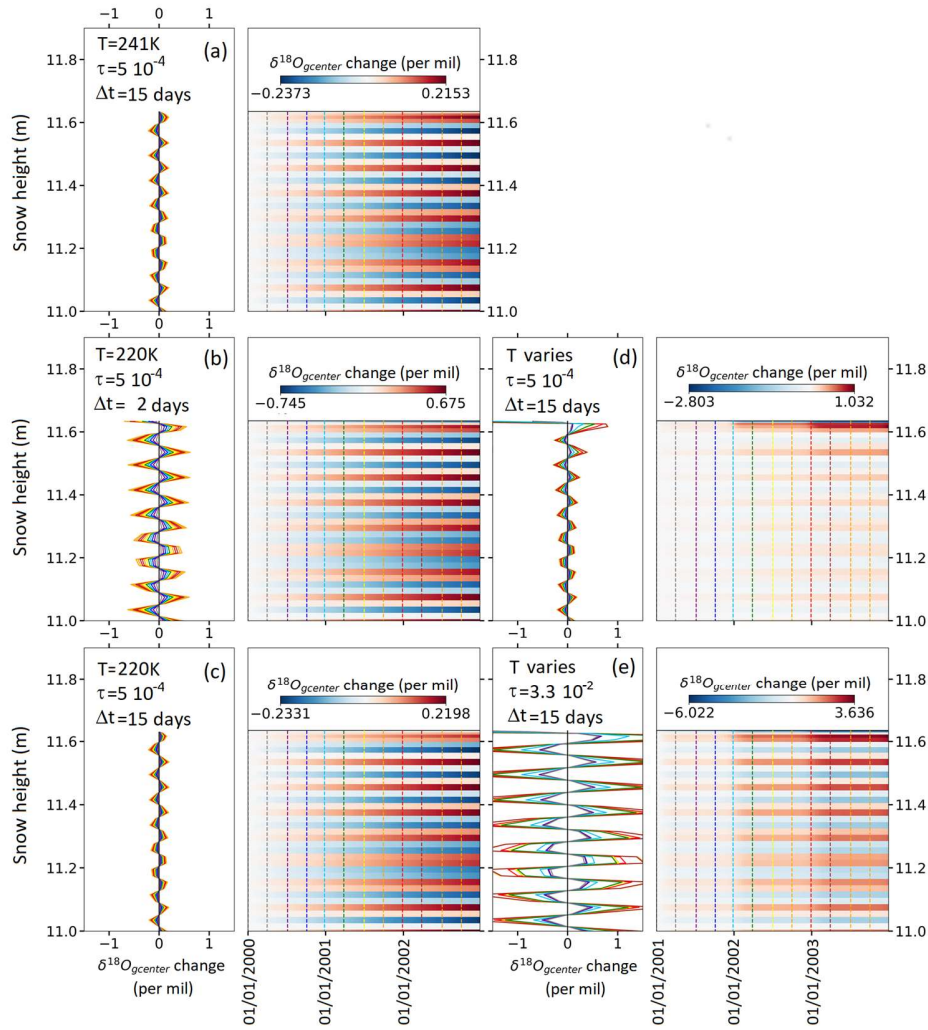


Figure 10. Test of the sensitivity of the model to the ratio of mass between surface and grain center compartments and to the interval of mixing between the two compartments (Dome C).

Numerical experiments on ~~isotope~~vapor diffusion in polar snow and firn ~~and its impact on isotopes~~ using ~~a~~the multi-layer energy balance model Crocus in SURFEX V8.0

Alexandra Touzeau¹, Amaëlle Landais¹, Samuel Morin², Laurent Arnaud³, Ghislain Picard³

¹LSCE, CNRS UMR8212, UVSQ, Université Paris-Saclay, Gif-sur-Yvette, 91191, France

²Météo-France - CNRS, CNRM UMR3589, Centre d'Etudes de la Neige, Grenoble, France

³~~LGGE~~³IGE, CNRS UMR5183, Université Grenoble Alpes, Grenoble, France

Correspondence to: Alexandra Touzeau (alexandra.touzeau@~~lsce~~.ipsl.fr~~uib.no~~)

Abstract

To evaluate the impact of vapor diffusion onto isotopic composition variations in the snow pits and then in ice cores, we introduced water isotopes in the detailed snowpack model Crocus. ~~The isotopes routine is run with a 1-s resolution.~~ At each step and for each snow layer, 1) the initial isotopic composition of vapor is taken at equilibrium with solid phase, 2) ~~a~~ kinetic fractionation is applied during transport, and 3) ~~condensation~~vapor is ~~realized~~condensed or snow is sublimated to compensate deviation to vapor pressure at saturation.

We study the different effects of temperature gradient, compaction, wind compaction and precipitation on the final vertical isotopic profiles. We also run complete simulations of vapor ~~and isotopic diffusion~~diffusion along isotopic ~~gradients and of vapor diffusion driven by temperature gradients~~ at GRIP, Greenland and at Dome C, Antarctica over periods of 1 or 10 years. The vapor diffusion tends to smooth the original seasonal signal, with an attenuation of ~~9.57~~ ~~% to 12~~ % of the original signal over 10 years at GRIP. This is smaller than the observed attenuation in ice cores, indicating that the model ~~underestimates~~attenuation due to diffusion ~~is underestimated~~ or that other processes, such as ventilation, ~~also contribute to the observed~~influence attenuation. At Dome C, the attenuation is stronger (~~14~~18 %), probably because of the lower accumulation and stronger $\delta^{18}\text{O}$ gradients.

~~Because vapor diffusion is not the only process responsible of the signal attenuation, it would be useful to implement in the model ventilation of the snowpack and exchanges with the atmosphere to evaluate~~

~~their contribution.~~

1 Introduction

~~Ice is a key archive for past climate reconstruction, which preserves both the composition of the past atmosphere in bubbles (EPICA comm. members, 2004; Kawamura et al., 2007; Petit et al., 1999; Schilt et al., 2010) and indications relevant to the temperature of formation of the snow precipitation through variations of the~~The isotopic ~~ratioratios~~ of oxygen or deuterium ~~(EPICA comm. measured in ice cores have been used for a long time to reconstruct the evolution of temperature over the Quaternary (EPICA comm. members, 2004; Johnsen et al., 1995; Jones et al., 2018; Jouzel et al., 2007; Kawamura et al., 2007; Lorius et al., 1985; Petit et al., 1999; Schneider et al., 2006; Stenni et al., 2004). This; Stenni et al., 2011; Uemura et al., 2012; WAIS-Divide members, 2013). They are however subject to alteration during post-deposition through various processes. Consequently, even if the link between temperature and isotopic composition of the precipitations is quantitatively determined from measurements and modelling studies (Stenni et al., 2016; Goursaud et al., 2017), it cannot faithfully be applied to reconstruction of past temperature. Nevertheless, ice cores remain a primary climatic archive is particularly useful in the southern hemisphere, for the Southern Hemisphere where continental archives are rare (Mann and Jones, 2003; Mayewski and Goodwin, 1999)). In Antarctica, where meteorological records only started in the 50's1950s (Genthon et al., 2013), these archives are not only a tool for past climate reconstruction, but also a necessary source of 2013), they provide useful information for understanding climate variability (Ekaykin et al., 2014; e.g. EPICA comm. members, 2006; Jouzel et al., 2007; Jouzel et al., 2005; Masson-Delmotte et al., 2003; Shaheen et al., 2013; Steig, 2006; Stenni et al., 2011; Stenni et al., 2004) and recent climate change (e.g. Altnau et al., 2015; Joos and Spahni, 2008; Mann and Jones, 2003; Mayewski and Goodwin, 1999; Schneider et al., 2006).~~

When using ice cores for past climate reconstruction, other parameters than temperature at condensation influence the isotopic compositions and must be considered. Humidity and temperature in the region of evaporation (Landais et al., 2008; Masson-Delmotte et al., 2011; ~~Vimeux et al., 2002~~), or the seasonality of precipitation (Delmotte et al., 2000; Sime et al., 2008; Laepple et al., 2011) should be taken into account. In addition, uneven accumulation in time and space introduces ~~randomness in the core stratigraphy~~ ('stratigraphic ~~noise~~', ~~noise~~ (Ekaykin et al., 2009). Indeed, records from adjacent snow pits have been shown to be markedly different, under the influence of decameter-scale local effects ~~(such as wind redeposition of snow, erosion, compaction, and metamorphism)~~ (~~Casado et al., 2016b~~; (Ekaykin et al., 2014; ~~Ekaykin et al., 2002~~; Petit et al., 1982). These local effects reduce the signal/noise ratio, ~~and then. Then~~ only stacking a series of ~~records from~~ snow pits can eliminate this local variability and yield information relevant to recent climate variations (~~Altnau et al., 2015; Ekaykin et al., 2014; Ekaykin et al., 2002~~; Fisher and Koerner, 1994; Hoshina et al., 2014; Ekaykin et al., 2014); ~~Altnau et al., 2015~~). This concern is particularly significant in central regions of east Antarctica characterized by ~~very low~~-accumulation rates (~~lower than~~ 100 mm ~~w.e. water equivalent~~ per year; ~~(van de Berg et al., 2006) and~~). ~~There~~, strong winds ~~which~~ can scour and erode snow layer over depths larger than the annual accumulation (Frezzotti et al., 2005; ~~Libois et al., 2014~~; Morse et al., 1999; ~~Magand et al., 2004; Epstein and Sharp, 1965; Town et al., 2008; Picard et al., 2016~~ ~~Libois et al., 2014~~). There is thus a strong need to study post-deposition effects in these cold and dry regions.

Additionally to mechanical ~~shuffling~~ ~~reworking~~ of the snow, the isotopic compositions are further modified in the snowpack. First, diffusion ~~against~~ ~~along~~ isotopic gradients can occur within the ~~ice microstructure at~~ ~~snow grains~~ ~~due to~~ solid ~~state~~ ('~~solid diffusion~~', ~~diffusion~~ (Ramseier et al., 1967). Second, within the porosity, the vapor isotopic composition can change due to: 1) diffusion ~~against~~ ~~along~~ isotopic gradients (in gaseous state), ~~oriented~~, 2) ~~thermally induced~~ vapor transport caused by vapor ~~density~~ ~~pressure~~ gradients, 3) ventilation (~~also~~ in gaseous state), or 4) exchanges between the gas phase and the solid phase (~~i.e. sublimation, and condensation~~). ~~The. In the porosity, the~~ combination of diffusion ~~against~~ ~~along~~ isotopic gradients in the vapor and of exchange between vapor and the solid phase has been suggested to be the main explanation to the smoothing of the isotopic signal in the solid phase

(JohnsenEbner et al., 2000, 2016, 2017; Gkinis et al., 2014); Johnsen et al., 2000). The combination of oriented vapor transport caused by vapor density gradients and exchange with isotopic compositions in the solid phase (~~is also modified by 'dry metamorphism', Colbeck et al., 1983), or by snow ventilation and exchange with the solid phase ('forced- and 'ventilation', Town et al., 2008) also modifies~~ but in a less predictable way. In both cases, the vapor transport exerts an influence on the isotopic compositions in the solid phase, ~~but in a less predictable way~~ because of permanent exchanges between solid and vapor. During 'dry metamorphism' (Colbeck et al., 1983), vapor transport is driven by vapor pressure gradients, themselves caused by temperature gradients. During ventilation (Town et al., 2008), vapor moves as part of the air in the porosity, because of pressure variations at the surface. Last, at the top of the snowpack, the isotopic composition of snow may also be modified through direct exchange with atmospheric vapor (Casado et al., 2016b; Ritter et al., 2016).

To elucidate the impact of these various post-deposition processes on the snow isotopic compositions, numerical models are powerful tools, ~~since they. They~~ allow ~~discriminating one to discriminate~~ between processes and test their impact one at a time. Indeed, Johnsen et al. (2000) ~~have been were~~ able to simulate and deconvolute the influence of diffusion ~~against along~~ isotopic gradients in the vapor at two Greenland ice-core sites, GRIP and NGRIP, using a numerical model. To do this, they ~~evaluated~~ define a quantity named 'diffusion length' which is the ~~diffusion length (as a function of depth) using mean displacement of a deformation~~ water molecule during its residence time in the porosity. Using a thinning model and an equation of diffusivity of the water isotopes in snow, ~~This, they compute this~~ diffusion length ~~as a function of depth. It~~ is then used to compute the attenuation ratio $\langle A/A_0 \rangle_z$, and in the end retrieve the original amplitude $\langle A_0 \rangle$. ~~Additionally. Additionally,~~ the effect of forced ventilation was investigated by Neumann (2003) and Town et al. (2008) using similar multi-layer numerical models. In these models, wind-driven ventilation forces atmospheric vapor into snow; ~~there. There,~~ the vapor is condensed especially in layers colder than the atmosphere.

We focus on the ~~impact movement~~ of ~~oriented vapor transport~~ water isotopes in the vapor phase in the porosity, in the absence of macroscopic air movement. In that situation, the movement of vapor molecules

in the porosity is caused by vapor ~~density~~pressure gradients ~~in the snow and recrystallization (i.e. ‘dry metamorphism’)~~ and of, or by diffusion ~~against~~along isotopic gradients. ~~Because the vapor density~~Note that in the first case, the vapor transport is ‘thermally induced’ i.e. the vapor pressure gradients directly result from temperature gradients within the snowpack. Thus, the first prerequisite of our model is to correctly simulate macroscopic energy transfer within the snowpack and energy exchange at the surface.

~~The~~ The transport of vapor molecules will affect the isotopic composition in the solid phase only if exchanges between vapor and solid are also implemented. Thus, the second prerequisite is that the model includes a description of the snow microstructure, ~~because exchanges between vapor and solid grains depend on it and~~and of its evolution in time. Snow microstructure is typically represented by its emerging scalar properties such as density, specific surface area and higher order terms often referred to as “shape parameters” (e.g. Krol and Löwe, 2016). While the concept of “grain” bears ambiguity, it is a widely used term in snow science and glaciology which we here employ as a surrogate for “elementary microstructure element”, without explicit reference to a formal definition, be it crystallographic or geometrical.

Crocus is a unidimensional multi-layer model of snowpack with a typically centimetric resolution initially dedicated to the numerical simulation of snow in temperate regions (Brun et al., 1992). It describes ~~dry snow metamorphism~~ {the evolution of the snow microstructure} driven by temperature and temperature gradients during dry snow metamorphism, using semi-empirical variables and laws. It has been used for ice-sheetsheets conditions in polar regions, both Greenland and Antarctica (Brun et al., 2011; Lefebvre et al., 2003; Fréville et al., 2013; Libois et al., 2014, 2015)-where). In these regions, it gives realistic predictions of density and snow type profiles (Brun et al., 1992; Vionnet et al., 2012), snow temperature profile -(Brun et al., 2011) and snow specific surface area and permeability (Carmagnola et al., 2014; Domine et al., 2013). It has been recently optimized for application to conditions prevailing at Dome C, Antarctica (Libois et al., 2014)). This was necessary to account for specific conditions such as high snow density values at the surface and low precipitation amounts.

The [Crocus model](#) has high vertical spatial resolution ~~of Crocus, its~~ and also includes interactive simulation of snow metamorphism in near-surface snow and firn ~~makes~~. Therefore, it [is](#) a good basis for the study of post-deposition effects in low accumulation regions. For the purpose of this study, we thus implemented vapor transport resulting from temperature gradients and the water ~~isotope~~[isotopes](#) dynamics into the Crocus model. This article presents this double implementation, and a series of sensitivity tests. ~~While a~~ perfect match of observations is not anticipated, in part because not all relevant processes are represented in the model, ~~this~~ [This](#) study represents thus a first step towards better understanding the impact of diffusion driven by temperature gradients on the snow isotopic composition.

2 Physical basis

The isotopic composition of the snow can evolve after deposition due to several processes. Here, we first give a ~~rapid~~ [survey/brief overview](#) of such processes at the macroscopic level ~~{~~ [Section 2.1 thus deals with](#) modification of the isotopic composition of a centimetric/decametric snow layer after exchanges with the other layers~~}~~. Second, we consider the evolution of the isotopic composition at the microscopic level, i.e. at the level of the microstructure. Indeed, the macroscopic change of the isotopic composition results from both large scale and small ~~scale~~ processes. For instance, dry metamorphism includes both vapor transport from one layer to another, and vapor/ice grain exchange inside a layer.

2.1 Evolution of the snow layers composition ~~(at the macroscopic scale)~~

Several studies address the evolution of the isotopic compositions in the snow column after deposition. Here, ~~following~~ [Elkaykin et al., 2009](#), we ~~separate random~~[describe first](#) processes ~~that induce smoothing of the original isotope profile (leading only to~~ attenuation of [the original](#) amplitude~~) without modification of the mean local pluriannual value, from oriented~~ (Sect. 2.1.1). Then we ~~describe~~ processes which ~~affect also the mean local pluriannual value (lead to other types of signal modifications~~ (Sect. 2.1.2). These modifications result from transportation and accumulation of [heavy or light](#) ~~or heavy~~ isotopes in some layers~~, without any link to the original isotopic signal. In some cases, the mean $\delta^{18}\text{O}$ value of the snow deposited can also be modified.~~

2.1.1 Signal attenuation on a vertical profile (~~is~~ smoothing)

~~The smoothing of isotopic compositions with conservation of the mean local pluriannual value is caused by diffusion against~~ In this Section we consider processes leading only to attenuation of the original amplitude of the $\delta^{18}\text{O}$ signal by smoothing. We define the mean local pluriannual value as the average isotopic composition in the precipitation taken over 10 years. The smoothing processes, which act only on signal variability, do not modify this average value. Within the snow layers, the smoothing of isotopic compositions is caused by diffusion along isotopic gradients in vapor phase and in solid phase. The magnitude of smoothing depends on site temperature, and on accumulation. Indeed, higher temperatures correspond to higher vapor ~~densities~~ concentrations, and ~~also~~ higher diffusivities in the vapor and solid phases. Oppositely, high accumulation rates ensure a greater separation between seasonal $\delta^{18}\text{O}$ peaks (Ekaykin et al., 2009; Johnsen et al., 1977) thereby limiting the impact of diffusion. ~~They also result in increased densification rates, and therefore reduced diffusivities (Gkinis et al., 2014).~~ Because sites with high accumulation rates also usually have higher temperatures, the resulting effect on diffusion is still unclear. These two competing effects should be thoroughly investigated and Johnsen et al. (2000) displays the damping amplitude of a periodic signal depending on wavelength and on diffusion length, strongly driven by temperature.

In Greenland, Johnsen et al. (1977) indicate that annual cycles generally disappear at depths shallower than 100 m for sites with accumulation lower than $200 \text{ kg m}^{-2} \text{ yr}^{-1}$. Diffusion ~~against~~ along isotopic gradients exists throughout the entire snow/ice column, ~~but is more intense.~~ It occurs mainly in the vapor phase in the firn, especially in the upper layers with larger porosities. -After pore closure, it takes place mostly in the solid phase, at a much slower rate. Note that in the solid phase, all isotopes have the same diffusion coefficient.

2.1.2 Signal shift caused by ~~oriented~~ processes leading to oriented vapor transport

We consider here the oriented movement of water molecules forced by external variables such as temperature or pressure. We use the term 'oriented' here to describe an overall movement of water molecules that is different from their molecular agitation, and externally forced. Three processes can contribute to oriented vapor transport and hence possible isotopic modification within the snowpack: diffusion, convection, and ventilation (Albert et al., 2002). ~~Convection is not considered here, since~~ Brun et Touvier (1987) have demonstrated that convection of dry air

within the snow ~~as a response to strong temperature gradients cannot occur except~~ occurs only in case of very low snow density (~~~of the order of ~100 kg/m³~~) which. These conditions are generally not encountered in Antarctic snow and therefore convection is not considered here. Bartelt et al. (2004) also indicate that energy transfer by advection is negligible compared to energy transfer by conduction in the first meters of the snowpack. The two other processes, ventilation and diffusion are forced respectively by variations of the surface pressure and surface temperature. In the first case, the interaction between wind and surface roughness is responsible for wind-pumping, i.e. renewal of the air of the porosity through macroscopic air movement (Albert et al., 2002; Colbeck, 1989, Neumann et al., 2004). In the second case, air temperature diurnal or seasonal variations generate vertical temperature gradients within the snow (Albert and McGilvary, 1992; Colbeck, 1983), and consequently. They result into vertical vapor density pressure gradients, responsible for vapor diffusion. These two processes are largely exclusive (Town et al., 2008) because strong ventilation homogenize the air and vapor in the porosity and therefore prevents diffusion. Diffusion as a result of temperature gradients can coexist with ventilation only at very low air velocities (Calonne et al., 2015). It becomes the main process of vapor transport when air is stagnant in the porosity. During diffusion, lighter molecules move more quickly in the porosity, leading to a kinetic fractionation of the various isotopologues.

2.2 Evolution of the isotopic composition at the microscopic scale

2.2.1 Conceptual representation of snow microstructure as spherical grains

The term “snow grain” as used classically is an approximation. In reality, ‘snow grains’ are very diverse in size, shape, degree of metamorphism and may also be made of several snow crystals agglomerated. Moreover, they are often connected to each other, forming an ice matrix (~~‘the snow microstructure’~~). However, several studies addressing snow metamorphism physical processes have relied on spherical ice elements to represent snow grains and snow microstructure (Legagneux and Domine, 2005; Flanner and Zender, 2006). Here, we consider that the snow grains are made of two concentric layers (one internal and one external) with different isotopic compositions. In terms of snow microstructure, this could correspond to inner vs. outer regions of the snow microstructure.

Indeed, the snow grain (or the snow microstructure) is not necessarily homogeneous in terms of isotopic composition. On the one hand, the center/central part of the grain (inner region of the microstructure) is relatively insulated,

and, This central part becomes ~~more-and-even~~ more insulated as the grain grows ~~(, or as the structure gets coarser),~~. On the other hand, outer layers are not necessarily formed at the same time as ~~its center (core of the microstructure), the central part,~~ or in the same environment (Lu and DePaolo, 2016). They are prone to subsequent sublimation or condensation of water molecules, implying that their composition ~~may change more quickly and varies~~ more frequently than ~~in for~~ the inner layers. Of course, only the bulk $\delta^{18}\text{O}$ value of the snow grain can be measured by mass spectrometry, ~~but. But~~ considering the heterogeneity of the grain may be required to get a fine understanding of the processes. In the following, we propose to split the ice grain compartment into two sub-compartments: grain surface and grain center. Thus, the grain surface isotopic composition ~~is allowed to evolve as a result evolves because~~ of exchange with ~~two compartments: 1) with~~ vapor in the porosity ~~(through~~ sublimation or condensation), ~~and also as a result of exchange 2)~~ with grain center ~~(through solid diffusion, or grain center translation, see below),~~. The grain center composition evolves at the time scale of week/month, as opposed to the grain surface, where the composition changes at the time scale of the vapor diffusion, i.e. over minutes.

2.2.2 Solid diffusion within snow grains

The grain center isotopic composition may change either as a result of crystal growth/sublimation or as a result of solid diffusion within the grain. For solid diffusion, ~~water molecules move in the transfer crystal lattice through a vacancy mechanism, in a process of molecules from the grain boundary towards the center of the grain self-diffusion that has no particular direction, and that~~ is very slow. The diffusivity of water molecules in solid ice (D_{ice} in $\text{m}^2\cdot\text{s}^{-1}$) follows Arrhenius law ~~and thus. Thus, it~~ can be expressed as a function of ice temperature ~~(T)~~ (Gkinis et al., 2014; Johnsen et al., 2000; Ramseier, 1967) using Eq. (1):

$$D_{ice} = 9.2 \cdot 10^{-4} \times \exp\left(\frac{-7186}{T}\right) \quad (1)$$

~~Note that all where~~ symbols are listed in Table 1.

Thus at 230 K, the diffusivity is $2.5 \times 10^{-17} \text{ m}^2\cdot\text{s}^{-1}$. ~~Gay et al., which leads to a (2002) indicate that in the first meter at Dome C, a typical snow grain has a radius of 0.1 mm. Across this typical snow grain, the characteristic time for solid~~

diffusion (Δt_{sol}) across a typical ice grain of radius $R_{moy} = 0.1$ mm (typical snow grain radius values in the first meter at Dome C, is Gay et al., 2002) given by Eq. (2):

$$\Delta t_{sol} = \frac{R_{moy}^2}{D_{ice}} = 4.03 \times 10^8 \text{ ss, or } \sim 13 \text{ years} \quad (2)$$

Therefore, the solid diffusion between the surface of within the grain and the inner part of the grain is close to zero at the time scales considered in the model (seconds to months) is close to zero. For Dome C, if we use the average temperature T of 248 K for the summer months at Dome C ($T = 248$ K, from (Dec. to Jan., Table 2), the characteristic time becomes 15 months, which remains quite large compared to our time scale. Thus, within a summer period, the snow grain is only partially refreshed through this process. At Summit the grain size is typically larger (from 0.2 to 0.25 mm in wind-blown and wind pack; and from 0.5 to 2 mm in the depth hoar layer) (Albert and Shultz, 2002), and the summer temperature is also higher (with an average value $T = 259$ K at GRIP Summit from July to Sept., after Shuman et al., (2001), yielding). Using a grain size of 0.25 mm, the resulting characteristic time is of the order of 30 months (for 0.25 mm).

2.2.3 Snow grain recrystallization

During snow metamorphism, the number of snow grains tends to decrease with time, while the snow grain size tends to increase (Colbeck, 1983). Indeed, each grain experiences permanent cycles of continuous recycling through sublimation/condensation, but the small grains are more likely to disappear completely, and then. Then, there is no more nucleus for condensation at the grain initial position. Oppositely, the bigger grains do not disappear and accumulate the vapor released by the smaller ones. Concurrently to this change of grain size, the grain shape also tends to evolve. In conditions of maintained/stable temperature gradient, facets appear at the condensing end of snow grains, while the sublimating end becomes rounded (Colbeck, 1983). In that case, the center of the grain moves toward the warm air region. This migration causes a renewal of the grain center, on a proportion that can be estimated from the apparent grain displacement (Pinzer et al., 2012). Pinzer et al. (2012) use this method to get obtain an estimation of vapor fluxes (since vapor transports water in the porosity from the 'sublimating' end of an ice grain toward the 'condensing' end of another ice grain).

The asymmetric recrystallization of snow grains implies that the surface layer of the snow grain is eroded at one end and buried at the other end. Therefore, the composition of the grain center changes more often than if the surface layer was thickening (through condensation) or thinning (through sublimation) homogeneously over the grain surface. This means ~~in particular~~ that the ‘inner core’ of the grain gets exposed more often. Implementing this process is thus very important to have a real-time evolution of the snow grain center isotopic composition. Here, we reverse the method of Pinzer et al. (2012) ~~and~~. ~~Therefore, we~~ use the fluxes of isotopes in vapor phase computed by the model to assess the renewal of the grain center (Sect. 3.1.3.).

3 Material and Methods

3.1 Description of the model ~~(SURFEX/Crocus revision 4805)~~ V8.0

We first present the model structure and second describe the new module of vapor transport (diffusion forced by temperature gradients). Third, we present the integration of water isotopes in the ~~new version of the model including the vapor transport module~~ model.

3.1.1 Model structure

The Crocus model is a one-dimensional detailed snowpack model, consisting of a series of snow layers with variable and evolving thicknesses. Each layer is characterized by its density, heat content, and by parameters describing snow microstructure ~~(such as sphericity and specific surface area)~~ (Vionnet et al., 2012, Carmagnola et al., 2014). In the model, the profile of temperature evolves with time ~~as a function of the in response to 1)~~ surface temperature and ~~of the 2)~~ energy fluxes at the surface and at the ~~bottom interface (ice or soil)~~ base of the snowpack. To correctly compute energy balance, the model integrates albedo calculation, deduced from surface microstructure and impurity content (Brun et al., 1992, Vionnet et al., 2012).

The successive components of the Crocus model have been described by Vionnet et al. (2012). ~~In this subsection, Here~~ we only list them ~~in order to point out~~ describe those ~~that we~~ modified to include water stable isotopes and water vapor transfer. ~~Our modifications are described in greater detail in the next sub-sections.~~

266 Note that the Crocus model has a typical internal time step of 900 s (15 min), corresponding to the update frequency
 267 of layers properties. We only refer here to processes occurring in dry snow.

268 1) Snow fall: The presence/absence of precipitation at a given time is determined from the atmospheric forcing
 269 inputs. When there is precipitation, a new layer of snow may be formed ~~(its, Its~~ thickness is deduced from the
 270 precipitation amount). ~~This module was modified to include water isotopes (see Sect. 3.1.3).~~

271 2) Update of snow layering: At each step, the model may split one layer into two or merge two layers together
 272 to get closer to a target vertical profile for optimal calculations ~~(. This target profile has~~ high resolution in the first
 273 layers to correctly simulate heat and matter exchanges). ~~The layers that are merged together are the closest in terms~~
 274 of microstructure variables ~~(shape, size). This module was slightly modified to include water isotopes (the~~
 275 ~~new isotopic composition after layer merging is the weighted average of the isotopic compositions of the~~
 276 ~~initial layers).~~

277 3) Metamorphism: The microstructure variables evolution follows empirical laws. These laws describe the
 278 change of grain parameters as a function of temperature, temperature gradient, snow density and liquid water content.
 279 ~~This module was not modified.~~

280 4) Snow compaction: ~~The original compaction scheme in Crocus describes the increase of density and~~
 281 ~~the decrease in the layer~~ Layer thickness decreases, and layer density increases under the burden of the overlying
 282 layers and resulting from metamorphism. ~~SAEW~~In the original module, snow viscosity is parameterized using the layer
 283 density and also using information on the presence of hoar or liquid water. However, this parameterization of the
 284 viscosity was designed for alpine snowpack (Vionnet et al., 2012) and may not be adapted to polar snow packs. ~~Here,~~
 285 ~~we used a simplified compaction scheme, where the compaction rate is constant with time and taken to~~
 286 ~~compensate yearly accumulation (Eq. (3), see Sect. 3.3. for accumulation rates).~~ Moreover, since we are
 287 considering only the first 12 m of the snowpack in the present simulations, the compaction in the considered layers
 288 does not compensate the yearly accumulation, leading to rising snow level with time. To maintain a stable surface level
 289 in our simulations, we used a simplified compaction scheme, where the compaction rate ε is the same for all the layers.

The compaction rate is obtained by dividing the accumulation rate at the site (see Sect. 3.3) by the total mass of the snow column (Eq. 3). It is then applied to all layers to obtain the density change per time step using Eq. 4.

$$\frac{1}{\rho_{sn}(t,n)} \times \frac{\rho_{sn}(t+dt,n) - \rho_{sn}(t,n)}{dt} = \frac{1}{m_{sn}(t,n)} \times \frac{dm_{sn}}{dt} \quad \varepsilon = \frac{dm_{sn}}{dt} / \sum_1^{nmax} (\rho_{sn}(t,n) \times dz(t,n)) \quad (3)$$

Note that symbols ρ_{sn} , m_{sn} and t are defined in Table 1.

$$\frac{\rho_{sn}(t+dt,n) - \rho_{sn}(t,n)}{dt} = \varepsilon \times \rho_{sn}(t,n) \quad (4)$$

5) Wind drift events: They modify the properties of the snow grains which tend to become more rounded, and they also increase the density of the first layers through compaction (higher degree of packing of the grains). An option allows snow to be partially sublimated during these wind drift events (Vionnet et al., 2012). This module was not modified.

6) Snow albedo and transmission of solar radiation: for each layer in the first 3 cm of snow, snow albedo and absorption coefficient are computed from snow microstructure properties and impurity content (computed based on snow age). The average albedo value in three wavelength bands, using the properties of first 3 cm is used to determine the two uppermost snow layers. Incoming part of incoming solar radiation is partly reflected (using albedo value) at the surface. The rest of the radiation penetrates into the snowpack. Then, for each layer starting from the top, incoming radiation is partly absorbed (using absorption coefficient) and partly transmitted to the layer underneath. This module was not modified. is used to describe the rate of decay of the radiation as it is progressively absorbed by the layers downward, following an exponential law.

7) Latent and sensible surface energy and mass fluxes: The sensible heat flux and the latent heat flux are computed using the aerodynamic resistance and the turbulent exchange coefficients. This module was not modified.

8) Vertical snow temperature profile: It is deduced from the heat diffusion equation, using the snow conductivity, as well as the energy balance at the top (radiation, latent heat, sensible heat) and at the bottom of the snowpack. This module was not modified.

9) Snow sublimation and condensation at the surface: The amount of snow sublimated/condensed is deduced from the latent heat flux, and the thickness of the first layer is updated. Other properties of the first layer (such as density, and SSA) are kept constant. This module was not modified.

3.1.2 Implementation of water transfer

The new vapor transport subroutine which has been inserted after the compaction (4) and wind drift (5) modules, and before the solar radiation module (6). In this section, the term 'interface' is used for the horizontal surface of exchange between two consecutive layers. The flux of vapor at the interface between two layers is obtained using the Fick's law of diffusion (Eq. (45)):

$$F(n+1 \rightarrow n) = \frac{-2 D_{eff}(t, n \rightarrow n+1) (\rho_v(t, n) - \rho_v(t, n+1))}{dz(t, n) + dz(t, n+1)} - \frac{2 D_{eff}(t, n \rightarrow n+1) (C_v(t, n) - C_v(t, n+1))}{dz(t, n) + dz(t, n+1)} \quad (45)$$

where $dz(t, n)$ and $dz(t, n+1)$ are the thicknesses of the two layers considered in meters, $\rho_v(t, n)$ and $\rho_v(t, n+1)$ are the local vapor mass concentrations in the two layers (kg m^{-3}), and $D_{eff}(t, n \rightarrow n+1)$ ($\text{m}^2 \text{s}^{-1}$) is the effective diffusivity of water vapor in the snow at the interface. The thicknesses are known from the previous steps of the Crocus model and account for snowfall and snow layering modifications, but the vapor mass concentrations and the interfacial diffusivities must be computed.

The effective diffusivity at the interface is obtained in two steps: first the effective diffusivities ($D_{eff}(t, n)$ and $D_{eff}(t, n+1)$) in each layer are calculated (Eq. (56)), second, the interfacial diffusivity ($D_{eff}(t, n \rightarrow n+1)$) is computed as their harmonic mean (Eq. (67)). Effective diffusivity can be expressed as a function of the snow density using the relationship proposed by Calonne et al. (2014), for layers with relatively low density compacting mostly. In these circumstances, the compaction occurs by 'boundary sliding (sliding', meaning that the grains slide on each other, but do not interpenetrate) modified. It is therefore applicable to our study where density is always below 600 kg m^{-3} . The equation of Calonne et al. (2014) is based on the numerical analysis of 3D tomographic images of different types of snow. It relates normalized effective diffusivity (D_{eff} / D_v) where to the snow density ρ_{sn}

in the layer (Eq. (6)). D_v is the vapor diffusivity in air and has a value of $2.036 \cdot 10^{-5} \text{ m}^2 \text{ s}^{-1}$, ~~Calonne~~ that varies depending on the air pressure and air temperature (Eq. (19) in Johnsen et al., 2014) to the snow density (ρ_{sn}) in the layer. ρ_{ice} corresponds to the density of ice (and has a value of 917 kg m^{-3}). ~~Here we do not take into account the effect of temperature on D_v .~~

$$\frac{D_{eff}(t,n)}{D_v} = \frac{3}{2} \left(1 - \frac{\rho_{sn}(t,n)}{\rho_{ice}} \right) - \frac{1}{2} \quad (56)$$

$$D_{eff}(t, n \rightarrow n+1) = \frac{1}{\frac{1}{D_{eff}(t,n)} + \frac{1}{D_{eff}(t,n+1)}}$$

(67)

We assume that vapor is in general at saturation in the snow layers (Neumann et al., 2008; Neumann et al., 2009). The local mass concentration of vapor density $\rho_v C_v$ (in kg m^{-3}) in each layer is given by the Clausius-Clapeyron equation (Eq. (78)):

$$\rho_v C_v(t, n) = \rho_{v0} C_{v0} \exp \left(\frac{L_{sub}}{R_v \rho_{ice}} \left(\frac{1}{T_0} - \frac{1}{T(t,n)} \right) \right) \quad (78)$$

where, $\rho_{v0} C_{v0}$ is the mass concentration of vapor density at 273.16 K (and is equal to $2.173 \cdot 10^{-3} \text{ kg m}^{-3}$), L_{sub} is the latent heat of sublimation (and has a value of $2.6 \cdot 10^9 \text{ J m}^{-3}$), R_v is the vapor constant (and has a value of $462 \text{ J kg}^{-1} \text{ K}^{-1}$), ρ_{ice} is the density of ice (and has a value of 917 kg m^{-3}), T_0 is the temperature of the triple point of water (and is equal to 273.16 K) and T is the temperature of the layer.

All layers are treated identically, except the first layer at the top and the last layer at the bottom. For the uppermost layer, the exchange of vapor occurs only at the bottom boundary ~~since, Indeed,~~ exchanges with the atmosphere are described elsewhere in Crocus (at step 9, where surface energy balance) ~~is realized~~. For the lowermost layer, only exchanges taking place at the top boundary are considered, the flux of vapor to/from the underlying medium being set to zero.

For each layer, the mass concentration of vapor density in air and effective diffusivity are computed within the layer and in the neighboring layers. Fluxes at the top and bottom of each layer are deduced from Fick's law of diffusion (Eq. 4)-(5)). They are integrated over the subroutine time step ~~(1-s)~~, and the new mass of the layer is computed ~~and, It is~~

used at the beginning of the next subroutine step. ~~The choice of~~ We use a ~~small~~ 1 s time step within the subroutine (the time step in, smaller than the main routine is time step of 900 s). This ensures that vapor fluxes remain small relative to the amount of vapor present in the layers. Note that the temperature profile, which controls the vapor density/pressure profile, is not modified within the subroutine. Physically, temperature values should change as a result of the transfer of sensible heat from one layer to another associated with vapor transport, as well as. They should also evolve due to the loss or gain of heat caused by water sublimation or condensation, respectively, in warm or cold layers, respectively (Albert and McGilvary, 1992; Kaempfer et al., 2005). However, vapor transport is only a small component to heat transfer between layers (Albert and Hardy, 1995; Albert and McGilvary, 1992). WithIn the absence of ventilation, with or without vapor diffusion, the steady-state profile for temperature varies by less than 2% (without ventilation) (Calonne et al., 2014). Thus, the effect can be neglected at first order.

3.1.3 Implementation of water isotopes

~~To enable the Crocus model for isotopes, 1) we introduce a new variable for isotopes, and 2) we compute its value in snowfall, as well as 3) its evolution with time, as a result of layer merging or diffusion. The~~In the model, the isotopic composition of snow in each layer is represented by the triplicate ($\delta^{18}\text{O}$, d-excess, ^{17}O -excess). Only the results of $\delta^{18}\text{O}$ are presented and discussed here. Moreover, ~~for~~For each parameter, two values per layer are considered independently, corresponding to the ‘snow grain center’ and the ‘snow grain surface’, respectively. Water vapor isotopic composition is deduced at each step from the ‘snow grain surface’ isotopic composition, and. It is not stored independently (to limit the number of prognostic variables). ~~To compute the evolution of. The~~ isotopic compositions, ~~we modified the Crocus model~~ are used at step 1 (i.e. for snowfall), and after step 5 (within the new module of vapor transfer ~~described in Section 3.1.2.~~).

In the snow fall subroutine, a new layer of snow may be added (depending on the weather), at the top of the snowpack. At this step of the routine, ~~we suppose that~~ the snow grains ~~that are being~~ deposited are supposed to be homogenous (i.e. they have the same composition in the “grain surface” compartment and in the “grain center” compartment). ~~We~~

deduce their isotopic. Their composition is deduced from the air temperature (see Sect. 3.2-).
 Within the new-vapor transport subroutine, we add a specific module that deals with the isotopic aspects of vapor transport. It modifies the isotopic compositions in the two snow grain sub-compartments as a result of water vapor transport and recrystallization of snow crystals. It works with four main steps:
 1) an initiation step where the vapor isotopic compositions are computed, using equilibrium fractionation, from the ones in the grain surface sub-compartment,
 2) a transport step where vapor moves from one layer to another, with a kinetic fractionation associated with diffusion,
 3) a balance step where the new vapor in the porosity exchanges with the grain surface compartment (by sublimation/condensation) with a. The flux is determined by the difference between actual vapor density/mass concentration and expected vapor density/mass concentration at saturation,
 and 4) a 'recrystallization' step where the grain center and grain surface isotopic compositions are homogenized, leading to an evolution of grain center isotopic composition.
 The time step in this module is 1s, the same as the time step of the sub-routine.
 The initial vapor isotope composition $R_{vap\ ini}^*$ in a given layer is taken at equilibrium with the 'grain surface' isotopic composition $R_{surf\ ini}^*$. Here $*$ denotes heavy isotope, and thus stands for ^{18}O , ^{17}O or D. Equilibrium fractionation is a hypothesis that is correct in layers where the air has been standing still for a long time in the porosity and where vapor has reached equilibrium with ice grains, physically and chemically. This process is limited by the water vapor - snow mass transfer whose associated speed is of the order of 0.09 m.s⁻¹ (Albert and McGilvary, 1992). In our case, we are dealing with centimetric scale layers thickness and recalculate the isotopic composition every second so that we consider that the speed of the mass transfer is not limiting the equilibrium situation at the water vapor - snow interface. To compute isotopic ratios for water vapor we use the following Eq. (89) and (910):

$$\begin{cases} R_{vap\ ini}^{18} = \alpha_{sub}^{18} \times R_{surf\ ini}^{18} \\ R_{vap\ ini}^{17} = \alpha_{sub}^{17} \times R_{surf\ ini}^{17} \\ R_{vap\ ini}^{18} + R_{vap\ ini}^{17} + 1 = 1/c_{vap\ ini}^{16} \end{cases} \quad (89)$$

$$\begin{cases} R_{vap\ ini}^D = \alpha_{sub}^D \times R_{surf\ ini}^D \\ R_{vap\ ini}^D + 1 = 1/c_{vap\ ini}^{1H} \end{cases} \quad (910)$$

The equilibrium fractionation coefficients (α_{sub}^{*i}) are obtained using the temperature-based parameterization from Ellehoj et al. (2013). Note that we make a slight approximation here, by replacing molar concentrations by mass concentrations in our mass balance formulas (see Table 1 for symbol definitions).

The initial vapor density $\rho_{vap ini}$ mass concentration in air C_v has already been computed in the vapor transport subroutine, and the volume of the porosity can be obtained from the snow density (ρ_{sn}) and the thickness of the layer (dz). By combining both, we obtain Eq. (10) which gives the initial mass of vapor in the layer

$$m_{vap ini} = \rho_{vap ini} C_v \times \left(1 - \frac{\rho_{sn}}{\rho_{ice}}\right) \times dz \quad (10)$$

This mass of vapor should be subtracted from the initial grain surface mass (as vapor mass is not tracked outside of the sub-routine, see Fig. 1) so that the new grain surface isotope composition, after vapor individualization is given by Eq. (11):

$$c_{surf new}^{18} = \frac{m_{surf new}^{18}}{m_{surf new}} = \frac{m_{surf ini}^{18} - m_{vap ini} \times c_{vap ini}^{18}}{m_{surf ini} - m_{vap ini}} \quad (11)$$

This mass of vapor should be subtracted from the initial grain surface mass because vapor mass is not tracked outside of the sub-routine (Fig. 1). The new grain surface isotope composition, after vapor individualization is given by Eq. (12):

$$c_{surf new}^{18} = \frac{m_{surf new}^{18}}{m_{surf new}} = \frac{m_{surf ini}^{18} - m_{vap ini} \times c_{vap ini}^{18}}{m_{surf ini} - m_{vap ini}} \quad (12)$$

Refer to Table 1 for the definition of symbols.

The diffusion of isotopes follows the same scheme as the water vapor diffusion described above in Sect. 3.1.2. and Eq. (45). In Eq. (42), the gradient of vapor density mass concentrations is replaced by a gradient of concentration of the studied isotopologue. The kinetic fractionation during the diffusion is realized with the D^*/D term (where $*_i$ stands for ^{18}O or ^{17}O or ^2H ; (Barkan and Luz, 2007).

$$F^{18}(n+1 \rightarrow n) =$$

$$\frac{-2 \times D_{eff,n,n+1} \left(\rho_v(t,n) \times c_{vap,ini}^{18}(t,n) - \rho_v(t,n+1) \times c_{vap,ini}^{18}(t,n+1) \right) - 2 \times D_{eff}(t,n \rightarrow n+1) \left(C_v(t,n) \times c_{vap,ini}^{18}(t,n) - C_v(t,n+1) \times c_{vap,ini}^{18}(t,n+1) \right)}{dz(t,n) + dz(t,n+1)} \times \frac{D^{18}}{D} \quad (1213)$$

Refer to Table 1 for symbol definitions.

As done for water molecules transport (Sect. 3.1.2.), the flux is set to zero at the top of the first layer and at the bottom of the last layer. ~~Note that when~~ When the vapor concentration is the same in two adjacent layers, the total flux of vapor is null ~~(same vapor density in the two adjacent layers), we still have. But diffusion along~~ isotopic diffusion because of gradients still occurs if the isotopic concentration gradients are non-zero (Eq. (12)). In that case, heavy and light molecules cross the boundary in opposite directions, with a null absolute flux of water molecules across the boundary (13)). Once top and bottom fluxes of each layer have been computed, the new masses of the various isotopes in the vapor are deduced, as well as the new ratios.

After the exchanges between layers, the isotopic composition in the vapor has changed. However, ~~because~~ the vapor isotopic composition is not a prognostic variable outside of the vapor transport subroutine. To record this change, it must be transferred to either the 'grain surface compartment' or to the 'grain center compartment' before leaving the subroutine. First, we consider exchanges of isotopes with the grain surface compartment, which is in direct contact with the vapor. Depending on the net mass balance of the layer, two situations must be considered:

1) If the mass balance is positive, condensation occurs, so that the transfer of isotopes takes place from the vapor toward the grain surface ~~(condensation)~~. To evaluate the change in the isotope composition in the grain surface, the mass of vapor condensed ~~($\Delta m_{vap,exc}$)~~ $\Delta m_{vap,exc}$ must be computed. It is the difference between the mass of vapor expected at saturation ~~(note that temperature does not evolve in this subroutine)~~, and the mass of vapor present in the porosity after vapor transport. ~~This~~ Note that temperature does not evolve in this sub-routine. Nevertheless, the difference is not exactly equal to the mass of vapor that has entered the layer, ~~as a consequence~~ because of layer porosity change. The excess mass of vapor is given by Eq. (1314):

$$\Delta m_{vap,exc} = \left[\left(\rho_{sn,new} - \rho_{sn,ini} \right) + \rho_v \times \left[\left(1 - \frac{\rho_{sn,ini}}{\rho_{ice}} \right) - \left(1 - \frac{\rho_{sn,new}}{\rho_{ice}} \right) \right] \right] \left[\left(\rho_{sn,new} - \rho_{sn,ini} \right) + C_v \times \left[\left(1 - \right. \right. \right]$$

$$\left[\frac{\rho_{sn}^{ini}}{\rho_{ice}} - \left(1 - \frac{\rho_{sn}^{new}}{\rho_{ice}} \right) \right] \times dz \quad (14)$$

Refer to Table 1 for the list of symbols.

Since the excess of vapor is positive, the next step is the condensation of the excess vapor. ~~Here the condensation of excess vapor occurs without additional fractionation.~~ The number of excess water molecules is determined through comparison with the expected number in the water vapor phase for equilibrium state between surface snow and water vapor. ~~They are drawn to cold grains and get stuck.~~ Here the condensation of excess vapor occurs without additional fractionation because (1) there is a permanent isotopic equilibrium between surface snow and interstitial vapor restored at each first step of the sub-routine and (2) kinetic fractionation associated with diffusion is taken into account during diffusion of the different isotopic species along the isotopic gradients.

2) If the mass balance is negative, the transfer of isotopes takes place from the grain surface toward the vapor without fractionation. Ice from the grain surface sub-compartment is sublimated without fractionation to reach the expected vapor density-concentration at saturation. Note that the absence of fractionation at sublimation is a frequent hypothesis, because water molecules move very slowly in ice lattice (Friedman et al., 1991; Neumann et al., 2005; Ramseier, 1967), ~~and thus~~. Consequently, the sublimation removes all the water molecules present at the surface of grains, including the heaviest ones before accessing inner levels. ~~Note that in~~ reality, there are evidences for fractionation at sublimation, ~~either~~. It occurs through kinetic effects associated with sublimation / simultaneous condensation, or during equilibrium fractionation at the boundary, especially when invoking the existence of a thin liquid layer at the snow – air interface (Neumann et al., 2008 and references therein; Sokratov and Golubev, 2009; Stichler et al., 2001; Ritter et al., 2016). The new composition in the vapor results from a mixing between the vapor present and the new vapor recently produced. The composition in the ‘grain surface’ ice compartment does not change. The limit between the surface compartment and the grain center compartment is defined by the mass ratio of the grain surface compartment to the total grain mass (i.e. $\tau = m_{surf} / (m_{center} + m_{surf})$, (Fig. 1, ~~symbols listed in Table 1~~). This mass ratio can be used to determine the thickness of the ‘grain surface layer’ as a fraction of grain radius, for spherical grains. The surface compartment must be thin, to be able to react to very small changes in mass when vapor is sublimated or

condensed. ~~Because of the~~ Our model has a numerical precision of ~~our model~~ (6 decimals) and is run at a 1 s temporal resolution. Consequently, the isotopic composition of the surface compartment can change in response to surface fluxes only if its mass is smaller than 10^6 times the mass of the water vapor present in the porosity. This constrains the maximum value for τ : $m_{surf} < 10^6 m_{vap}$, or $m_{surf} / (m_{center} + m_{surf}) \tau < 10^6 \frac{\phi \rho_s V_{tot} \rho_v V_{tot}}{\rho_{sn} V_{tot} \rho_{sn} V_{tot}}$, i.e. $\tau < \frac{\rho_s \phi \rho_v \phi}{\rho_{sn} \rho_{sn}} 10^6$. Here V_{tot} corresponds to the total volume of the. Considering typical temperatures, snow densities and layer ~~whereas ϕ represents its porosity~~ thicknesses (Table 3) we obtain a maximum value of $3.3 \cdot 10^{-4}$. On the other hand, this compartment must be thick enough to transmit the change in isotopic compositions caused by vapor transport and condensation/sublimation to the grain center. Again, numerical precision imposes that its mass should be no less than 10^{-6} times the mass of the grain center compartment ($\tau > 10^{-6}$). Considering typical temperatures, snow densities and layer thicknesses (Table 3) such approach leads to a range for the ratio τ between 10^{-6} (minimum value to influence the grain center) to $1.3 \cdot 10^{-3}$ (maximum value to perceive the influence of exchanges with water vapor), and thus we get an additional constraint: $\tau > 10^{-6}$. Here we use a ratio $\tau = 5 \cdot 10^{-4}$ for the mass of the grain surface relative to the total mass of the layer (Fig. 1). We have run sensitivity tests with smaller and larger ratios (Sect. 4.1.4.3). Here, we implement two types of mixing between grain surface and grain center are implemented in the model. The first one is associated with crystal growth or shrinkage, as a result because of vapor transfer. Mixing is performed at the end of the vapor transfer subroutine, after sublimation/condensation has occurred. During the exchange of water between vapor and grain surface, the excess (or default) of mass in the water vapor caused by vapor transport has been entirely transferred to the grain surface sub-compartment. Thus, the mass ratio between the grain surface compartment and the grain center compartment deviates from the original one. To bring the ratio τ back to normal ($\tau = \text{value of } 5 \cdot 10^{-4}$), mass is transferred either from the grain surface to the grain center or from the grain center to the grain surface. This happens without fractionation, i.e. if the transfer occurs from the center to the surface, the composition of the center remains constant. The second type of mixing implemented is the grain center translation (Pinzer et al., 2012) which favors mixing

between grain center and grain surface in the case of sustained temperature gradient. While Pinzer et al. (2012) used the apparent grain displacement to compute vapor fluxes, here, Here, we reverse this method and use the vapor fluxes computed from Fick's law to estimate the grain center renewal. However, instead of transferring We could transfer a small proportion of the surface compartment to the grain center every second. Instead, we choose to transfer the totality of totally mix the snow grain surface compartment every few days (total mixing of the grain). The interval $\Delta t_{surf/center}$ between two successive mixings is derived from the vapor flux $F(n+1 \rightarrow n)$ within the layer using Eq. (14).

$$\Delta t_{surf/center} = \frac{m_{sn} \times \tau}{F(n+1 \rightarrow n)} \quad (14)$$

$$\text{Using a typical flux } F(n+1 \rightarrow n) \text{ of } 1.3 \cdot 10^{-9} \text{ kg} \cdot \text{m}^{-2} \cdot \text{s}^{-1} \text{ (for the } \Delta t_{surf/center} = \frac{m_{sn} \times \tau}{F(n+1 \rightarrow n)} \text{)} \quad (15)$$

The average temperature gradient of $3 \text{ }^{\circ}\text{C m}^{-1}$ and corresponds to a flux $F(n+1 \rightarrow n)$ of $1.3 \cdot 10^{-9} \text{ kg} \cdot \text{m}^{-2} \cdot \text{s}^{-1}$. The typical mass for the layer of m_{sn} of 3.3 kg (i.e. a mass for the grain surface compartment of $m_{sn} \times \tau$). Based on these values, the dilution of the grain surface compartment into the grain center should occur every 15 days. Of course, this is only an average, since layers have varying masses, and since the temperature gradient can be larger or smaller. We will however apply this time constant for all the layers and any temperature gradient (see sensitivity tests Sect. 4.1.4.1, because it is necessary), to ensure that the mixing between compartments occurs at the same time in all layers.

In terms of magnitude, this process is probably much more efficient for mixing between the two sub-compartments of the solid grain than grain growth or solid diffusion. It is thus crucial for the modification of the bulk isotopic composition of the snow layer. It makes the link between microscopic processes and macroscopic results.

3.1.4 Model initialization

For model initialization, an initial snowpack is defined, with a fixed number of snow layers, and for each snow layer an initial value of thickness, density, temperature and $\delta^{18}\text{O}$. Typically, ~~oriented~~ processes [of oriented vapor transport](#) such as [thermally induced](#) diffusion and ventilation occur mainly in the first meters of snow ~~so that~~. Therefore, the model starts with an initial snowpack of about 12 m.

The choice of the layer thicknesses depends on the annual accumulation. Because the accumulation is much higher at GRIP than at Dome C (Sect. 3.2., Table 2), the second site is used to define the layer thicknesses. About [810](#) cm of fresh snow are deposited every year (Genthon et al., 2016; [PicardLandais et al., 2016; Libois et al., 2014](#)), [which](#)2017). This implies that ~~in order~~ to keep seasonal information, at least one point every 4 cm is required in the first meter. ~~We~~For the initial profile, we impose maximal thickness of 2 cm for the layers between 0 and 70 cm depth and ~~a maximal thickness of~~ 4 cm for the layers between 70 cm and 2 meters depth. [As the simulation runs, merging is allowed but restricted in the first meter to a maximum thickness of 2.5 cm.](#) Below 2 meters, the thicknesses are set to 40 cm or even 80 cm. Thus, the diffusion process can only be studied in the first 2 m of the model snowpack. In the very first centimeters of the snowpack, thin [millimetric](#) layers ~~(mm)~~ are used to accommodate low precipitation amounts, and surface energy balance ~~(radiations...)~~. The initial density profiles are defined for each site specifically (see Sect. 3.2.~~7~~). The initial temperature and $\delta^{18}\text{O}$ profiles in the snowpack depend on the simulation considered (see Sect. 3.3.~~7~~).

3.1.5 Model output

A data file containing the spatio-temporal evolution of prognostic variables such as temperature, density, SSA or $\delta^{18}\text{O}$ is produced for each simulation. Here, we present the results for each variable as two-dimensional graphs, with ~~the~~ time on the horizontal axis and ~~the~~ snow height [ason](#) the vertical axis. The variations of the considered variable are displayed as color levels. [The white color corresponds to an absence of change of the variable.](#) As indicated above, only the first 12 m of the polar snowpack are included in the model. The bottom of this initial snowpack constitutes the vertical reference ~~(zero)~~or 'zero' to measure vertical heights ~~(h)~~. The height of the top of the snowpack varies with

time due to snow accumulation and to snow compaction. In the text, we sometimes refer to the layer depth (z) instead of its height (h). The depth z can be computed at any time by subtracting the current height of the considered layer from the current height of the top of the snowpack.

3.2. Studied sites: meteorology and snowpack description

In this study we run the model under conditions encountered at Dome C, Antarctica and GRIP, Greenland. We chose these two sites because they have been well-studied in the recent years through field campaigns and numerical experiments. In particular, for Dome C, a large amount of meteorological and isotopic data is available (Casado et al., 2016a; Stenni et al., 2016; Touzeau et al., 2016). Typical values of the main climatic parameters for the two studied sites (Summit, GRIP and Dome C), are given in Table 2, as well as typical $\delta^{18}\text{O}$ range. Dome C has lower accumulation rates (of 2.7 cm ice equivalent per year (i.e., Table 2) than Summit (yr^{-1}) compared to GRIP rates of 23 cm i.e. yr^{-1} (Table 2), making it more susceptible to be affected by post-deposition processes.

In this study, we also compare the results obtained for GRIP to results from two other Greenland sites, namely NGRIP and NEEM. GRIP is located at the ice-sheet summit, whereas the two other sites are located further north, in lower elevation areas with higher accumulation rates. In detail, NGRIP is located 316 km to the NNW of GRIP ice-drill site (Dahl-Jensen et al., 1997). GRIP and NGRIP have similar temperatures of -31.6°C and -31.5°C but different accumulation rates of 23 cm i.e. yr^{-1} and 19.5 cm i.e. yr^{-1} respectively. NEEM ice-core site is located some 365 km to the NNW of NGRIP on the same ice-ridge. It has an average temperature of -22°C and an accumulation rate of 22 cm i.e. yr^{-1} .

The $\delta^{18}\text{O}$ value in the precipitation at a given site reflects the entire history of the air mass, including evaporation, transport, distillation, and possible changes in trajectory and sources. However, assuming that these processes are more or less repeatable from one year to the next, it is possible to empirically relate the $\delta^{18}\text{O}$ to the local temperature, using measurements from collected samples. Here, using data from one-year snowfall sampling at Dome C (Stenni et al., 2016; Touzeau et al., 2016), we use the following Eq. (4516) to link $\delta^{18}\text{O}_{sf}$ in the snowfall to the local temperature

(T_{air} , in K):

$$\delta^{18}\text{O}_{sf} = 0.45 \times (T_{air} - 273.15) - 31.5 \quad (4516)$$

We do not provide an equivalent expression for GRIP, Greenland, because the simulations run here (see Sect. 3.1.1) do not include precipitation.

The initial density profile in the snowpack is obtained from fitting density measurements from Greenland and Antarctica (Bréant et al., 2016, 2017). Over the first 12 m of snow, we obtain the following evolution (Eq. (4617) and Eq. (4718)) for NGRIP (in the absence of density measurements at GRIP) and Dome C respectively:

$$\rho_{sn}(t, n) = 17.2 \cdot z(t = 0, n) + 310.3 \quad (N=22; R^2=0.95) \quad (4617)$$

$$\rho_{sn}(t, n) = 12.41 \times z(t = 0, n) + 311.28 \quad (N=293; R^2=0.50) \quad (4718)$$

3.3 List of simulations

Table 4 presents the model configuration for the 6 simulations considered here.

3.3.1 Greenland ~~simulations~~simulations

The first simulation ~~is~~, listed as number 1 in Table 4, is dedicated to the study of diffusion ~~against~~along isotopic gradients, ~~and~~. It is realized on a Greenland snowpack with an initial sinusoidal profile of $\delta^{18}\text{O}$ (see Eq. 4819) and ~~with~~ a uniform and constant vertical temperature profile at 241 K. In addition to comparison to $\delta^{18}\text{O}$ profiles for GRIP and other Greenland sites, the aim of the first simulation is to compare results from Crocus model to the models of Johnsen et al. (2000) and Bolzan and Pohjola (2000) run at this site with only diffusion ~~against~~along isotopic profiles. To compare our results to theirs, we consider an isothermal snowpack, without meteorological forcing, and we deactivate modules of surface exchanges and heat transfer. The initial seasonal sinusoidal profile at GRIP is set using Eq. (4819):

$$\delta^{18}\text{O}(t, n) = -35.5 - 8 \times \sin\left(\frac{2\pi \times z(t, n)}{a \times \rho_{ice} / \rho_{sn}(t, n)}\right) \quad (4819)$$

where z is the depth of the layer n , ρ_{sn} is its density, ρ_{ice} is the density of ice ~~and has a value of~~ 917 kg m⁻³, a is the average accumulation at GRIP ~~and is equal to~~ 0.23 m i.e./yr, ~~Guillevie (Dahl-Jensen et al., 2013, 1993)~~. The ~~peak~~ to peak amplitude value of 16 ‰ is close to the back-diffused amplitude at Summit (Sjolte et al., 2011).

The second simulation is run with evolving temperature in the snowpack ~~The snow temperature is~~ computed by the model, using meteorological forcing from ERA-Interim ~~(see Table 4)~~. In that case, ~~isotopic diffusion~~the transport

of isotopes in the vapor phase results both from diffusion against isotopic gradients and from vapor density/concentration gradients. The initial snowpack is the same as in the previous simulation.

In the two GRIP simulations, the modules of wind compaction and weight compaction are inactive. Indeed, as weight compaction is taken to compensate yearly accumulation (Eq. (3) and (4)), applying this compaction in a case without precipitation would lead to an unrealistic drop in snow level. The wind compaction was absent from the model of Johnsen et al. (2000) and using this module would make comparisons more difficult.

3.3.2 Dome C simulations

In simulations 3 to 6, we take advantage of the high documentation of the Dome C site to disentangle the different effects on the variations of snow density and water isotopic composition, hence with a high number of simulations (4). The All the simulations at Dome C were performed with an evolving temperature profile (simulations 3 to 6). We use Temperatures in the snow layers were computed using a modified meteorological forcing from ERA-Interim (Dee et al., 2011; Libois et al., 2014; see details in Table 4), and as well as the modules of energy exchange and transfer within the snow to compute temperatures in the snow layers. In this series of simulations, the densities and $\delta^{18}\text{O}$ values thus evolve as a result of diverging and/or alternating vapor fluxes. The simulations are ordered by increasing complexity. First, in Simulation 3, the modules of homogeneous compaction and wind drift are deactivated, as well as the module of snowfall (Simulation 3). Thus, the impact of vapor transport forced by temperature gradients on the snow densities/isotopic compositions is clearly visible. Then, in Simulation 4, the module of compaction and the module of wind drift are activated, to see their impact on the snow density and isotopes (Simulation 4). We use an accumulation rate dm_{sn}/dt for Dome C of -0.001 kg m^{-2} per 15 min (dm_{sn}/dt in see Eq. (3)). Next, in Simulation 5, snowfall is added, to assess how new layers affect both snow density and snow $\delta^{18}\text{O}$ values (Simulation 5). Lastly, we, in Simulation 6, the model is run a simulation (6) over 10 years at Dome C, in order to build up a snowpack with realistic 'sinusoidal' variation in $\delta^{18}\text{O}$ values.

3.3.3 Summary of the simulations

Table 4 presents the model configuration for the 6 simulations considered here.

4 Results

4.1 Greenland

4.1.1 Results of the Crocus simulations (Simulations 1 and 2)

Figure 2 shows the result of the first simulation Simulation 1, where only diffusion against a long isotopic gradient is active, as in Johnsen et al., 2000. As expected the maxima and minima peak to peak amplitude of the grain center isotopic composition ($\delta^{18}\text{O}_{\text{center}}$) are $\delta^{18}\text{O}$ cycles is reduced as a result because of diffusion. Over 10 years (from 2000 to 2009), the amplitude decreases by 1.32 ‰ which corresponds to 8 a 7.3 % variation.

Figure 3 shows the result of the second simulation, Simulation 2, i.e. with varying temperature in the snowpack. The results are very similar to the results from the first simulation, except the attenuation is stronger than the one observed in the previous simulation. The minima at 11.46 m increases by 1.03 ‰ over ten years, and the maxima at 11.15 m decreases by 0.84 ‰. Thus, the total attenuation is ~1.9 ‰ or 11.7 % for this height range. Below, the attenuation is smaller, with a total attenuation of only 6 % for heights between 10.54 and 10.85 m. If we compare attenuation for heights 11.46 and 11.56 m in the 1st and 2nd simulation, we note that including temperature gradients leads to an increased attenuation by 50 %.

Between 11.46 m and 11.56 m, the $\delta^{18}\text{O}_{\text{center}}$ values increase over ten years by 1 to 4 ‰. This increase is not caused only by attenuation of the original sinusoidal signal. Indeed, at $h=11.60$ m, the values get higher than the initial maxima which was -36 ‰ at 11.64 m. There is therefore a local accumulation of heavy isotopes in this layer as a result of vapor transport. This maximum corresponds to a local maximum in temperature and is coherent with departure of ^{18}O -depleted water vapor from this layer. Thus, thermally induced vapor transport does not only result into signal attenuation, but can also shift the $\delta^{18}\text{O}$ value, regardless of the initial sinusoidal variations.

Lastly, in the first 2-3 cm, which show a greater of the snowpack, strong depletion is observed over the period

~~(-1.8, with a decrease by 2 to 3 ‰ instead of -0.5 ‰), ‰ when the temperature gradients were absent~~
(Simulation 1). This depletion probably results from arrival of ^{18}O -depleted water vapor from warmer layers
below. ~~The vapor transport here is forced by~~ This shows again the influence of temperature gradients which
were absent from the previous simulation. However, ~~several processes are neglected here (note that in~~
~~this simulation we neglect precipitation, and~~ exchange of vapor with the atmosphere) ~~that could~~
~~counteract this effect in natural conditions and we thus do not focus more on this first layer. In the layers~~
~~below (first meter of snow) the half attenuation is of 0.76 ‰, corresponding to an attenuation of 1.6 ‰,~~
~~and to a relative attenuation of 0.5 % of the initial amplitude. This result is very similar to the one obtained~~
~~in the first, simplified simulation.~~ Thus, the depletion observed here may not occur in natural settings
when these processes are active.

In conclusion, at GRIP, the diffusion of vapor as a result of temperature gradients has ~~only a limited~~ double impact on
isotopic compositions, ~~and most of~~. It increases the simulated attenuation ~~can be attributed to diffusion~~
~~against~~ in the first 60 cm of snow, because of higher vapor fluxes. And it also creates local isotopic maxima and
minima, in a pattern corresponding to temperature gradients, in the snowpack but disconnected from the original $\delta^{18}\text{O}$
sinusoidal signal.

4.1.2 Comparison with core data

Here, we evaluate the attenuation of the initial seasonal signal in $\delta^{18}\text{O}$ over 10 years at ~~NEEM using 2~~ Greenland ice-
core sites, NEEM and GRIP. For the first site, we use 4 shallow cores (NEEM2010S2, NEEM2008S3, NEEM2007S3,
NEEM2008S2) published in Steen-Larsen et al., 2011 and in Masson-Delmotte et al., 2015, ~~and at GRIP using~~. For
the second site, we use one shallow core (1989-S1), published in White et al., 1997. For the GRIP core, only the first
80 meters are considered. Therefore, the data presented corresponds to deposition and densification conditions like the
modern ones. For NEEM the values of the four cores are taken together. For NEEM and GRIP, the half semi-amplitude
is computed along the core. In the first 10 meters, the maximum value every 30 cm is retained, and deeper in the firn,
because of compaction, the maximum value every 20 cm is retained (see also Supp. Material; Fig. 4). For this study,

we have chosen to estimate attenuation on years with a clearly marked seasonal cycle, a strategy that can be debated but at least documented. Consequently, from this first series of maxima, a second series of maxima is computed, with a larger window of 1 meter. The 'attenuated amplitudes' at each level is then defined as the ratio between these 1-meter maxima and the initial 1-meter maxima. Maximum half semi-amplitudes every 5 m are also computed, and displayed on Figure 4. The 2.5 m attenuation is ~~greater~~ slightly higher at GRIP, leading to a remaining amplitude of 86 %, than at NEEM (where the remaining amplitude is 90 %, (Fig. 4): ~~the~~). The amplitude decreases with depth in parallel for the two cores, with the amplitude at NEEM staying always higher than at GRIP. For comparison with our model, we estimate attenuation after 10 years ~~(i.e. at a depth of ~5.8 m deep at for NEEM and ~5.65 m deep at for GRIP)~~; ~~the~~. The remaining amplitude is 80 % and 72 % at GRIP and NEEM respectively. Our ~~simulation~~ Simulation 1 produced 87 % of attenuation only on the same duration, showing that our model ~~(run on an isothermal snowpack)~~, underestimates the attenuation observed in the data.

4.1.3 Comparison with other models

At 2.5 m at NGRIP, Johnsen et al. (2000) simulate remaining amplitude of 77 % (Fig. 4). For a depth of 5.43 m, corresponding to an age of 10 years, the ~~simulated~~ remaining amplitude is 57 %. For Bolzan and Pohjola, (2000), at GRIP after 10 years ~~(1977-1987)~~, 70 % of the initial amplitude is still preserved. The slower attenuation for Bolzan and Pohjola (2000) compared to Johnsen et al. (2000) may be due more to the different sites ~~(NGRIP/GRIP)~~ considered than to the different models. Indeed, GRIP has higher accumulation rates that should limit diffusion. Nevertheless, the attenuation of 30 % simulated by Bolzan and Pohjola at GRIP is stronger than the ~~one~~ attenuation of 7 % simulated in our model ~~(30 % vs 8 %)~~. Town et al. (2008, Sect. [31]) found attenuations of a few tenth of per mil after several years when implementing only diffusion, a result consistent with ours ~~(since we get a decrease by 1.32 % after 10 years)~~.

We explore below the reasons for discrepancies between models. The equation for effective diffusivity of vapor in firm used in our study is different from the ~~one~~ ones used by Johnsen et al. (2000) ~~and from the one used~~ or by Bolzan and Pohjola (2000). ~~Contrary to the previous authors~~ Indeed, we do not consider the ~~impact of temperature on~~

the diffusivity in air (D_a) and we do not take into account the tortuosity factor (l/s), nor the adjustable scale factor (s) of Bolzan and Pohjola. However, using the values given by the previous authors for l and s lead to D_{eff} values ranging from $6.7 \cdot 10^{-6}$ to $9.9 \cdot 10^{-6} \text{ m}^2 \text{ s}^{-1}$ for a density of 350 kg m^{-3} and a temperature of 241 K which is coherent with our value of $8.7 \cdot 10^{-6} \text{ m}^2 \text{ s}^{-1}$. As indicated by Bolzan and Pohjola, (2000), the choice of one equation or another has little impact here.

The most probable difference lie in the way diffusion is taken into account. Johnsen et al. (2000) and Bolzan and Pohjola (2000) use a single equation of diffusion to predict the evolution of the isotopic composition of the layer while, In our case, we specifically compute the fluxes in the vapor, as a result of isotopic gradients, each second and at each depth level and deduce the evolution of $\delta^{18}\text{O}$ in the grain center, after sublimation/condensation and recrystallization. Denux (1996) and van der Wel et al. (2015) indicate that the model developed by Johnsen (1977) and used in Johnsen et al. (2000) overestimates the attenuation compared to observed values. For Denux (1996), the model by Johnsen et al. (2000) should take into account consider the presence of ice crusts, and maybe also the temperature gradients in the surface snow, to get closer to the real attenuation at remote Antarctic sites. For Van der Wel et al. (2015) have compared the model results to a spike-layer experiment realized at Summit. Because an artificial snow layer cannot be representative of natural diffusion, they took care to evaluate diffusion based only on the natural layers present above and below the artificial layer. van der Wel et al. (2015) propose three causes to the discrepancy between Johnsen et al.'s model prediction and actual measured attenuation at GRIP: could have three causes: They blame either ice crusts, or a bad knowledge and parametrization of the tortuosity in the first meters of snow, and/or a bad description of the isotopic heterogeneity within the ice grain. In our model, the grain heterogeneity is included. Even if the parameters defining the mixing between the two compartments are not very well constrained (see Sect. 4.3), the attenuation is indeed smaller compared to Johnsen et al.'s the Johnsen's model.

4.2 Dome C (Antarctica)

4.2.1 Simulation without precipitation, without wind drift, and without homogeneous compaction

The aim of the following simulations Simulations 3 to 6, run at Dome C, is to isolate diffusion, from other effects

affecting ~~snow density as well as~~ water isotopic composition, i.e. wind-drift and compaction.

When only taking into account temperature profiles variations in 4.2.1 Simulation 3: without precipitation, without wind drift, and without homogeneous compaction

Figure 5 presents the firn, the maximum density change occurs in the first layers with an increase results of $+112 \text{ kg m}^{-3}$ over one year (Fig. 5). The additional water comes most probably from the underlying layers which show temperature evolution (a progressive decrease in density of -20.5 kg m^{-3} over one year. This upward flux of vapor in the top millimeters of snow reflects a slightly colder temperature at the top of the snowpack, and this even in summer, due to infrared radiation.

Density changes are very limited during winter. As long as the atmosphere remains cold, vapor moves upward, but in very small quantities, insufficient to make the summer density increase disappear. During short warm events in winter (in particular on the 1st of August) the first layer loses mass, but again the change remains small compared to the change observed in summer. As a conclusion, it seems that temperatures above about 240 K are required to observe a significant change in densities at the seasonal scale.

As observed for the density, the $\delta^{18}\text{O}$ evolution (c and d) for Simulation 3. The main changes of isotopic compositions in the grain surface ($\delta^{18}\text{O}_{\text{gsurf}}$) and grain center ($\delta^{18}\text{O}_{\text{gcenter}}$) compartments occur in summer (Fig. 6). During these periods (5c and 5d). On the one hand, the first 20 cm of snow tend to become ^{18}O -enriched (+by +0.2 ‰), due to vapor departure. However ‰ for the grain center compartment. On the other hand, the first 1–2 cm become centimeter becomes depleted (–1.1 ‰) because of the condensation of water vapor. During winter, by 1.0 ‰ for grain center. This pattern is coherent with the temperature profiles for the summer period (Fig. 5a). Indeed, vapor moves out of the warmest layers and toward colder layers where it condensates. This causes an increase in $\delta^{18}\text{O}$ in warm layers and a decrease in colder layers. This pattern is also confirmed by snow density changes (see Fig. S2).

During winter, the temperature generally decreases toward the surface (Fig. 5a). Vapor transport is thus reversed in the first 20 cm, but this only slightly reduces the dispersion of $\delta^{18}\text{O}_{\text{gcenter}}$ values ~~is only slightly reduced~~. Warm events during winter (1st of August, for instance) cause. On the first of August, the temperature at the surface temporarily increases to 235 K. This warm event strongly modifies the temperature profile in the snowpack, and therefore the pattern of vapor transport. It is associated with an increase of $\delta^{18}\text{O}$ values at the surface, which is particularly visible for the $\delta^{18}\text{O}_{\text{gsurf}}$ values ~~(Fig. 5c)~~. Thus ~~it seems that warm events leave an imprint on $\delta^{18}\text{O}_{\text{gsurf}}$~~ , vapor transport can modify $\delta^{18}\text{O}$ values in surface snow, ~~through vapor transport~~, even in the absence of precipitation or condensation from the atmosphere. This mechanism could explain the parallel evolution of surface snow isotopic composition and temperature described by Steen-Larsen et al. (2014) and Touzeau et al. (2016) between precipitation events.

4.2.2 Simulation 4: without precipitation, with wind drift, and with homogeneous compaction

~~In this simulation, there are three potential sources of density changes: homogeneous snow compaction, wind induced snow compaction and vapor transport.~~

Figure 7 shows the total density change over one year. The total density change reaches $+115 \text{ kg m}^{-3}$ in the first layer. Several events of compaction by wind drift are visible, in particular on the 2nd-3rd of February, the 11th-12th of April, the 23rd-24th of May and on the 3rd-4th of June, on the 18th of October and the 27th of November (see also Fig. S1, density changes per 12 h period). Wind drift events are rare but lead to density changes up to 5 kg m^{-3} per 12 h, while vapor transport occurs every day in summer but never leads to changes larger than 250 g m^{-3} per 12 h. Homogeneous compaction leads to a small density increase of about 3 g m^{-3} per 12 h.

Compaction and wind drift are not supposed to modify directly the $\delta^{18}\text{O}$ values; ~~however~~. However, the change in densities and layer thicknesses modifies slightly the temperature profile and the diffusivities ~~and~~. These processes thus could have an indirect impact on $\delta^{18}\text{O}$ values. Figure 86 shows $\delta^{18}\text{O}_{\text{gcenter}}$ changes that are reduced compared to the

simulation without wind drift and compaction. This is coherent with a decrease in the density changes associated with vapor transport in the case with compaction (see Fig. S2S5).

4.2.3 Simulation 5: with precipitation, with wind drift, with homogeneous compaction

In this simulation Simulation 5, we add precipitation to wind and weight compaction effects. Both snowfall and wind compaction are responsible for irregular changes—(resp., respectively positive and negative), of the height of the snowpack (Fig. 97). In terms of density, the new snow deposited has a small density (304 kg m^{-3}), and therefore snowfall tends to decrease layers, the density $\delta^{18}\text{O}_{\text{center}}$ values reflect the $\delta^{18}\text{O}$ values in the first layer, relative to the original vertical density profile precipitation. They vary as expected from -40 ‰ on the 31th of December to -59 ‰ in July (Fig. 97, Fig. S3aS8). The effect of snowfall is therefore opposite to the one of wind drift and compaction. As a result of these various processes vapor transport is visible only in 'old' layers which were originally homogeneous in terms of $\delta^{18}\text{O}$. These old layers, which were reaching the density in the first layer varies between 304 and 370 kg m^{-3} —surface in January, have been buried below the new layers and are found from 11 cm depth downward in December. When $\delta^{18}\text{O}$ in the precipitation varies with a seasonal cycle, $\delta^{18}\text{O}_{\text{center}}$ in the new layers varies as expected from -40 ‰ (31th of December) to -59 ‰ (July) (Fig. 10, Fig. S4). The effect of vapor transport is visible only in 'old' layers (up to the surface in January; from 11 cm depth downward in December), which were originally homogeneous in terms of $\delta^{18}\text{O}$.

4.2.4 Simulations 6: Ten-years simulation at Dome C

We run Simulations 6 corresponds to a simulation run over 10 years at Dome C, with variable $\delta^{18}\text{O}$ in the precipitation. Over these 10 years, about 1 m of snow is deposited. At the end of the simulation, the vertical profile of $\delta^{18}\text{O}$ in the new layers has an average value of -49.87 ‰, and a half semi-amplitude of 4.5-52 ‰ (Fig. 11). Thus. Here we take into account all the initial signal in maxima and minima at a vertical resolution of 9 cm of fresh snow. Based on the snow is already different from atmospheric temperature variations only, the initial signal isotopic composition in

the precipitation ~~(should vary around an~~ average value of -53.2 ‰, ~~half with a semi-~~amplitude of 8.6 ‰~~), due to ‰.~~

The main reason for this difference is the precipitation intermittency, and also to the amounts: large precipitation events in winter are associated with relatively high $\delta^{18}\text{O}$ values. The vertical resolution chosen for the model (layer thickness ~~~ of~~ 2.5 cm). The values recorded for summer layers (above -45 ‰) reflect ~~may also contribute to~~ the average summer temperatures, whereas decrease of the values recorded for winter layers (below -50 ‰) are biased toward warm events (leading to an increase of +6 ‰ of $\delta^{18}\text{O}$ compared to semi-amplitude. Indeed, light snowfall events do not result in the value production of a new surface layer but are integrated into the old surface layer. As expected ~~with constant precipitation throughout the year),~~ the peak to peak amplitude of $\delta^{18}\text{O}$ variations is then further reduced as a result of the two vapor diffusion processes and of associated vapor/solid exchanges. The effect of vapor transport is relatively small. To help its visualization, we selected four layers and displayed the evolution of $\delta^{18}\text{O}$ in these layers over the years (Fig. 8d). The selected layers were deposited during winter 2000, and during summer seasons 2002, 2004, and 2006.

As expected, the maxima and minima of $\delta^{18}\text{O}$ are further reduced as a result of diffusion driven by temperature gradients. The effect of vapor transport is relatively small so that to help its visualization, we selected three summers (2002, 2004, 2006) and one winter (2000), and followed the evolution of $\delta^{18}\text{O}$ in the layers corresponding to the deposited snow during these seasons (Fig. 11d).

For the layer deposited during winter 2000, there is an increase in $\delta^{18}\text{O}$ values of about +0.8 ‰ over ten years.

The slope is irregular, with the strongest increases occurring during summers ~~(Nov.-Feb.), between~~ November and February, when vapor transport is maximal. The slope is also stronger when the layer is still close to the surface, probably because of the stronger temperature gradients in the first centimeters of snow (Fig. 11a; Sect. 4.3.1.; 8a). For the layers deposited during the summers, the evolution of $\delta^{18}\text{O}$ values is symmetric to the one observed for winter 2000.

Over 10 years ~~(, i.e. between 2000- and 2009),~~ the $\delta^{18}\text{O}$ amplitude thus decreases by about 1.6 ‰ ~~(0.8 ‰ for the half-amplitude), ‰.~~ This corresponds to a decrease of 14.18 % relative to the initial amplitude in the snow layers.

This is higher than the 8.7 % attenuation ~~(or 9.5 % modelled in Greenland for constant temperature, and to the 11.7 %~~
~~attenuation observed~~ when including diffusion caused by temperature gradients ~~modelled in Greenland~~ (Sect.
 4.1.7). However, the comparison between the two sites is not straightforward, because of differences in temperature
 and accumulation counteracting each other. On the one hand, at GRIP, the diffusion is forced by low vertical gradients
 of $\delta^{18}\text{O}$ of the order of 0.24 ‰ cm^{-1} . ~~These are~~ much smaller than the typical $\delta^{18}\text{O}$ gradients at Dome C ~~(110 ‰ m~~
~~which are close to 1) 7.10 ‰ cm⁻¹.~~ On the other hand, the temperature ~~of 241 K~~ at GRIP is higher than ~~the 220 K~~
~~measured~~ at Dome C ~~(241 K instead of 220 K)~~, thus favoring diffusion.

4.3 Sensitivity tests for duration of recrystallization

We have shown above that attenuation of the isotopic signal seems too small at least for the GRIP site. In parallel,
~~some~~ parameters τ and $\Delta t_{\text{surf/center}}$ of the model ~~especially for the parameterization of~~ ~~associated to~~ grain
 renewal, could only loosely be estimated leading to ~~a large~~ uncertainty in the attenuation modeling. In this section,
 we perform some sensitivity tests to quantify how $\delta^{18}\text{O}$ attenuation can be increased by exploring the uncertainty range
 on the renewal of the snow grain. Indeed, the assumed values for the ratio between ~~the mass of~~ grain surface and the
 total mass of the grain ~~(τ), or may have been under or over-estimated. The same is true~~ for the periodicity of mixing
 between these two compartments ~~($\Delta t_{\text{surf/center}}$) may have been under or over-estimated.~~

The sensitivity tests are first designed for Greenland sites, run for 6 months, with initial amplitude of the sinusoidal
 $\delta^{18}\text{O}$ signal of 16 ‰, and a fixed temperature of 241 K in all the layers (Fig. 129). First, we use a periodicity of mixing
 $\Delta t_{\text{surf/center}}$ of 15 days ~~(more precisely, this mixing occurs on the second and 16th of each month)~~ and vary the
 value for the mass ratio ~~between the grain surface compartment and the total mass of the grain (τ):~~ $1 \cdot 10^{-6}$,
 $5 \cdot 10^{-4}$, $3.3 \cdot 10^{-2}$. ~~Then~~ ~~In practice, for $\Delta t_{\text{surf/center}}=15$ days, we realize mixing on the second and 16th of each month.~~
~~Second~~, we use the usual value of $5 \cdot 10^{-4}$ for τ , and change the periodicity of the mixing to 2 days.

- In the first case ~~where $\tau=1 \cdot 10^{-6}$, and the mixing occurs every 15 days, Fig. 12a)~~, the grain surface
 compartment is very small, ~~and its~~ ~~Its~~ original sinusoidal $\delta^{18}\text{O}$ profile disappears in less than one day due to exchanges

with vapor (not shown). The impact on grain center is then very small (attenuation of with an increase of the first minimum by $\sim 1.70 \cdot 10^{-4} \%$ over 6 months (Fig. 9a). In this case, the attenuation due to diffusion is even reduced compared to the results displayed above.

- In the second case, where $\tau = 5 \cdot 10^{-4}$, and the mixing occurs every 15 days, (Fig. 12b), the grain surface compartment is larger, and the attenuation is slower, and. Thus, in the grain surface compartment, half of the original amplitude still remains at the end of the 15 days simulation (not shown). The impact on the grain center compartment is clearly visible (attenuation with an increase of the first minimum by $4.92 \cdot 10^{-2} \%$ after 6 months (Fig. 9b).

- In the third case, with $\tau = 3.3 \cdot 10^{-2}$, and mixing every 15 days, (Fig. 12c), the attenuation of the sinusoidal signal in the grain surface compartment is only of 1 % because the grain surface compartment is very large. On opposite, attenuation in the grain center is quite large, i.e. 7.2 the first minimum increases by $4.0 \cdot 10^{-2} \%$ after 6 months (Fig. 9c).

- In the fourth case, with $\tau = 5 \cdot 10^{-4}$, and mixing every 2 days, (Fig. 12d), the attenuation in first minimum increases by $4.1 \cdot 10^{-2} \%$ after 6 months for the grain center compartment (Fig. 9d). It is similar to the attenuation observed in the third case ($7.5 \cdot 10^{-2} \%$ in 6 months).

The results of these sensitivity tests suggest that the impact of vapor transfer on the grain center isotopic compositions is maximized when the grain surface compartment is large ($\tau = 3.3 \cdot 10^{-2}$) and/or refreshed often ($\Delta t_{\text{surf/center}} = 2 \text{ days}$).

They also show clearly that using a small grain surface compartment (such as $\tau = 1 \cdot 10^{-6}$) drastically reduces the impact on the grain center isotopic values. However, our best estimates for τ and $\Delta t_{\text{surf/center}}$ were not chosen randomly (see Sect. 3.1.3., and moreover). Moreover, the use of $\tau = 3.3 \cdot 10^{-2}$ or $\Delta t_{\text{surf/center}} = 2 \text{ days}$ leads to an increase near doubling of the $\delta^{18}\text{O}$ attenuation by only a third (see above), which does. This is not bridge yet sufficient to explain the gap between our model output for isothermal simulation and the data. However, if this doubling is applicable to the case with temperature gradients, the attenuation obtained might reach the one observed in the data at GRIP.

At Dome C (mean temperature of 220 K in the simulation), sensitivity tests show that we can increase the attenuation by a factor of 3 by reducing the mixing time from 15 to 2 days (Figure 10b-c). Similarly, if the ratio τ is

put at $3.3 \cdot 10^{-2}$ instead of $5 \cdot 10^{-4}$, a maximum attenuation of 4.3 % instead of 0.45 % is attained more than doubled over 63 years. (Figure 10d-c). Thus, at Dome C and in opposite to GRIP, the values of τ and $\Delta t_{\text{surf/center}}$ can seem to affect more strongly the attenuation obtained, compared to GRIP. This greater sensitivity at Dome C could result from the influence of temperature gradients (in Greenland the impact of temperature gradients on attenuation is minor), as well as from steeper $\delta^{18}\text{O}$ gradients caused by the low accumulation. Indeed, the average layer thickness of 2 cm in the first meter corresponds to ~ 4 points per year at Dome C, but 35 points per year at GRIP.

4.4 Additional missing processes

In the previous sections, we have seen that within the uncertainty range of badly constrained parameters, it is difficult to reconcile data and model output for GRIP. We thus believe that other processes should probably be considered to explain the remaining attenuation. First model outputs for GRIP generally lead to smaller attenuation than the one observed in ice-cores. To improve the model compatibility with data, two kinds of approaches are possible. On the one hand, it would be useful to realize simulations adapted to on-site experiments such as the one by van der Wel et al. (2015). This would allow verifying how diffusion can be improved in the model. For instance, previous studies have suggested that water vapor diffusivity within the snow porosity may be underestimated by a factor of 5 (Colbeck, 1983), but this is debated (Calonne et al., 2014). Second, ventilation (2014). On the other hand, we also believe that other processes should probably be considered to explain the remaining attenuation. Ventilation is an additional process that has already been implemented in the snow water isotopic model of Town et al. (2008) and Neumann (2003). Because of strong porosity and sensitivity to surface wind and relief, ventilation is probably as important as diffusion in the top of the firn, even if diffusion is expected to be more effective at greater depths. Indeed, for the Dome C simulation (Fig. 118), the slope $d(\delta^{18}\text{O})/dz$ decreases slowly, indicating that diffusion remains almost as active at 60 centimeters than at 10 centimeters depth. Neumann (2003) indicates that at Taylor Mouth the diffusion becomes the only process of vapor transport below 2 meters depth. For Dome C, for a temperature gradient of 3°C m^{-1} , we compute an average speed due to diffusion of $3 \cdot 10^{-6} \text{ ms}^{-1}$ (for a temperature gradient of 3°C m^{-1}), which is s^{-1} . This is comparable to air speed due to wind pumping of about $3 \cdot 10^{-6} \text{ ms}^{-1}$ within the top meters of snow at

WAIS (Buizert and Severinghaus, 2016). We conclude that, in as much as these results can be applied to Dome C, the two processes would have comparable impact at this site in the first meters of snow. The next step for Crocus-iso development is thus to implement ventilation. [Finally, we are also aware that in Antarctic central regions, the wind reworking of the snow has a strong effect in shaping the isotopic signal. A combination of stratigraphic noise and diffusion could indeed be responsible for creating isotopic cycles of non-climatic origin in the firm \(Laepplé et al., 2017\). Wind reworking may also contribute to attenuation, by mixing together several layers deposited during different seasons.](#)

5. Conclusions and perspectives

Water vapor transport ~~(diffusion)~~ and water isotopes have been implemented in the Crocus snow model enabling depicting the temporal $\delta^{18}\text{O}$ variations in the top ~~10 m~~ [50 cm](#) of the snow in response to new precipitation, evolution of temperature gradient in the snow and densification. [The main process implemented here to explain post-deposition isotopic variations is diffusion.](#) We have implemented ~~water~~ [two types of diffusion in vapor phase: 1\) water vapor diffusion along isotopic gradients, and isotopic 2\) thermally induced vapor diffusion.](#) The vapor diffusion between layers ~~was realized~~ at the centimetric scale ~~taking into account two~~. [The consequences of the two vapor diffusion processes on isotopes in the solid phase were investigated. The solid phase was modelled as snow grains divided in two sub-compartments in the snow: \(1\) a grain \(surface snow sub-compartment in equilibrium with interstitial water vapor and \(2\) an inner grain only exchanging slowly with the surface compartment\).](#) We parameterized the speed of diffusion through the renewal time of a snow grain and proportion of the two snow grain compartments.

Our approach based on a detailed snow model makes it possible to investigate at fine scale ~~the various~~ processes explaining the variations of density and $\delta^{18}\text{O}$ in the firm ~~with~~. [We look specifically at the effect of](#) evolution of the temperature gradient, new snow accumulation and compaction event linked to wind drift. Over the first 30 cm, the [snow](#) density variations are mainly driven by compaction events linked to wind drift. Vapor transport and long-term compaction have secondary effects. Below 30 cm, wind drift driven compaction is no more visible. Because of strong temperature gradient and low density, water vapor transport will have a significant effect down to 60 cm. $\delta^{18}\text{O}$ is

primary driven by variations in $\delta^{18}\text{O}$ of precipitation as expected. The seasonal variations are then attenuated by water vapor transport and diffusion ~~again~~^{along} isotopic gradients, with an increase of these effects at higher ~~temperature~~^{temperatures} i.e. ~~during~~ summer periods).

From 10 years simulations of the Crocus-iso model both at ~~Summit~~^{GRIP} Greenland and Dome C Antarctica, we have estimated the post-deposition attenuation of the annual $\delta^{18}\text{O}$ signal in the snow to about ~~8-147-18~~ % through diffusion. This attenuation is smaller than the one obtained from isotopic data on shallow cores in Greenland suggesting missing processes in the Crocus model when implementing water vapor. It is also significantly smaller than the diffusion implemented by Johnsen et al. (2000) but some studies have suggested that the Johnsen isotopic diffusivity is too strong (Denux, 1996 ; Van der Wel et al., 2015).

We see our study as ~~a~~ first step toward a complete post-deposition modelling of water ~~isotope~~^{isotopes} variations. Indeed, several other developments are foreseen in this model. First, wind pumping is currently not implemented in the Crocus model. This effect, implemented in the approach of Neumann (2003) and Town et al. (2008) is expected to have a contribution as large as the effect of diffusion for the post-deposition isotopic variations. Second, in low accumulation sites like Dome C, wind scouring has probably an important effect on the evolution of the $\delta^{18}\text{O}$ signal in depth through a reworking of the top snow layers (Libois et al., 2014). This effect has not been considered here ~~but~~ ^{could be implemented in the model in the next years}. It could also play a role in the preservation of anomalously strong $\delta^{18}\text{O}$ peaks at Dome C (Denux, 1996).

Other short-term developments concern the implementation of the exchange of water vapor with the atmosphere through hoar deposition. This is particularly timely since many recent studies have studied the parallel evolution of isotopic composition of water vapor and surface snow during summer both in Greenland and Antarctica (Steen-Larsen et al., 2014; Ritter et al., 2016; Casado et al., 2016a; 2016b). ~~Similarly, implementation of ventilation of the snowpack in the model since this effect is expected to significantly participate to signal attenuation.~~

Another aspect is to look at the post-deposition d-excess and ^{17}O -excess variations in snow pits. Indeed, recent studies have shown that the relationship between ^{17}O -excess and $\delta^{18}\text{O}$ is not the same when looking at precipitation samples and snow pits samples in East Antarctica ~~questioning~~^{(Touzeau et al. 2016). This observation questions} the influence of diffusion within the snowpack on second order parameters such as ^{17}O -excess ~~(Touzeau et al., 2016).~~ Indeed, ^{17}O -

excess is strongly influenced by kinetic diffusion driven fractionation which may be quantified by the implementation of ^{17}O -excess in our Crocus-iso model.

Code availability

The code used in the manuscript is a development of the [open source code for SURFEX/ISBA-Crocus model based on version V8.0](https://opensource.umr-cnrm.fr/projects/surfex_git2), hosted [on an open git repository at CNRM/GAME](https://opensource.umr-cnrm.fr/projects/surfex_git2). ~~Both the initial code and~~ [Before downloading the code, you must register as a user at https://opensource.umr-cnrm.fr/](https://opensource.umr-cnrm.fr/projects/surfex_git2). ~~You can then obtain the onecode used in the manuscript are open source and hosted on a svn server at CNRM/GAME. Users may obtain access to~~ [present study by downloading the svn following first the procedure described at: https://opensource.umr-cnrm.fr/projects/snowtools/wiki/Procedure_for_new_users](https://opensource.umr-cnrm.fr/projects/snowtools/wiki/Procedure_for_new_users). ~~The specific version revision tagged 'Touzeau_jan2018' of the code corresponding to the results presented can then be retrieved from the svn branch at: http://svn.cnrm-game-meteo.fr/projets/surfex/branches/touzeau_dev using revision 4805. The climate~~ [\(last access: January 2018\)](https://climate.clermont.fr/). The meteorological forcing required to perform the runs is available as a supplement.

Author contribution

S. Morin wrote the new module of vapor diffusion. A. Touzeau inserted isotopes and isotope transport into the numerical code with help of S. Morin for numerical issues and physics, and help from A. Landais for concepts and hypotheses of the theory of isotopes. G. Picard and L. Arnaud provided information and references on snow microstructure and microphysics as well as direct field experience on site meteorology and accumulation conditions. A. Touzeau run the simulations, and interpreted the results. A. Touzeau and A. Landais wrote the manuscript. All the authors corrected the manuscript.

Competing interests

950 The authors declare that they have no conflict of interest.

951

952 Acknowledgements

953 The research leading to these results has received funding from the European Research Council under the European
954 Union's Seventh Framework Programme (FP7/2007-30 2013)/ERC grant agreement no. 306045. We want to
955 acknowledge A. Orsi and M. Casado from LSCE, who contributed to this work through fertile discussions of the model
956 contents and its applications. We are grateful to M. Casado and C. Bréant for providing snow pit temperature and
957 density profiles as well as firn density profiles for model initialization. We would like to thank D. Roche for his advice
958 during model development, as well as on how to make the code available. We are also indebted to J.-Y. Peterschmidt,
959 who provided continual help and useful tutorials on Fortran and Python languages. We thank M. Lafaysse and V.
960 Vionnet at CNRM/CEN for help with the model and meteorological driving data. CNRM/CEN and IGE are part of
961 LabEX OSUG@2020. [We thank three anonymous reviewers for their questions and comments, which helped to](#)
962 [improve the present article.](#)

963

964 References

965 Albert, M. R. and Hardy, J. P.: Ventilation experiments in seasonal snow cover, IAHS Publications-Series of
966 Proceedings and Reports-Intern Assoc Hydrological Sciences, 228, 41-50, 1995.

967 Albert, M. R. and McGilvary, W. R.: Thermal effects due to air flow and vapor transport in dry snow, Journal of
968 Glaciology, 38, 273-281, 1992.

969 Albert, M. R. and Shultz, E. F.: Snow and firn properties and air-snow transport processes at Summit, Greenland,
970 Atmospheric Environment, 36, 2789-2797, 2002.

971 Albert, M. R., Grannas, A. M., Bottenheim, J., Shepson, P. B., and Perron, F. E.: Processes and properties of snow-air
972 transfer in the high Arctic with application to interstitial ozone at Alert, Canada, Atmospheric Environment, 36, 2779-
973 2787, 2002.

974 Altnau, S., Schlosser, E., Isaksson, E., and Divine, D.: Climatic signals from 76 shallow firn cores in Dronning Maud
975 land, East Antarctica, The Cryosphere, 9, 925-944, 2015.

976 Barkan, E. and Luz, B.: Diffusivity fractionations of $\text{H}_2^{16}\text{O}/\text{H}_2^{17}\text{O}$ and $\text{H}_2^{16}\text{O}/\text{H}_2^{18}\text{O}$ in air and their implications for

977 isotope hydrology, Rapid Communications in Mass Spectrometry, 21, 2999-3005, 2007.

978 [Bartelt, P., Buser, O., and Sokratov, S. A.: A nonequilibrium treatment of heat and mass transfer in alpine snowcovers,](#)

979 [Cold Regions Science and Technology, 39, 219-242, 2004.](#)

980 Bolzan, J. F. and Pohjola, V. A.: Reconstruction of the undiffused seasonal oxygen isotope signal in central Greenland

981 ice cores, Journal of Geophysical Research: Oceans, 105, 22095-22106, 2000.

982 Bréant, C., Martinerie, P., Orsi, A., Arnaud, L., and Landais, A.: Modelling the firn thickness evolution during the last

983 deglaciation: ~~constrains~~[constraints](#) on sensitivity to temperature and impurities, Clim. Past ~~Discuss.~~, 2016, 1-36, 2016,

984 [13, 833-853, 2017.](#)

985 Brun, E. and Touvier, F.: Etude expérimentale de la convection thermique dans la neige, Le Journal de Physique

986 Colloques, 48, C1-257-C1-262, 1987.

987 Brun, E., David, P., Sudul, M., and Brunot, G.: A numerical model to simulate snow-cover stratigraphy for operational

988 avalanche forecasting, Journal of Glaciology, 38, 13-22, 1992.

989 Brun, E., Six, D., Picard, G., Vionnet, V., Arnaud, L., Bazile, E., Boone, A., Bouchard, A., Genthon, C., and Guidard,

990 V.: Snow/atmosphere coupled simulation at Dome C, Antarctica, Journal of Glaciology, 57, 721-736, 2011.

991 Buizert, C. and Severinghaus, J. P.: Dispersion in deep polar firn driven by synoptic-scale surface pressure variability,

992 The Cryosphere, 10, 2099-2111, 2016.

993 Calonne, N., Geindreau, C., and Flin, F.: Macroscopic modeling for heat and water vapor transfer in dry snow by

994 homogenization, The Journal of Physical Chemistry B, 118, 13393-13403, 2014.

995 Calonne, N., Geindreau, C., and Flin, F.: Macroscopic modeling of heat and water vapor transfer with phase change in

996 dry snow based on an upscaling method: Influence of air convection, Journal of Geophysical Research: Earth Surface,

997 120, 2476-2497, 2015.

998 Carmagnola, C. M., Morin, S., Lafaysse, M., Domine, F., Lesaffre, B., Lejeune, Y., Picard, G., and Arnaud, L.:

999 Implementation and evaluation of prognostic representations of the optical diameter of snow in the SURFEX/ISBA-

1000 Crocus detailed snowpack model, The Cryosphere, 8, 417-437, 2014.

1001 Casado, M., Landais, A., Masson-Delmotte, V., Genthon, C., Kerstel, E., Kassi, S., Arnaud, L., Picard, G., Prié, F.,

1002 Cattani, O., Steen-Larsen, H. C., Vignon, E., and Cermak, P.: Continuous measurements of isotopic composition of

1003 water vapour on the East Antarctic Plateau, Atmos. Chem. Phys. Discuss., 16, 8521-8538, 2016a.

1004 Casado, M., Landais, A., Picard, G., Münch, T., Laepple, T., Stenni, B., Dreossi, G., Ekaykin, A., Arnaud, L., Genthon,
1005 C., Touzeau, A., Masson-Delmotte, V., and Jouzel, J.: Archival of the water stable isotope signal in East Antarctic ice
1006 cores, *The Cryosphere Discussions*, doi:10.5194/tc-2016-263, 2016b.

1007 Colbeck, S. C.: Theory of metamorphism of dry snow, *Journal of Geophysical Research*, 88, 5475-5482, 1983.

1008 Colbeck, S. C.: Air movement in snow due to wind pumping, *Journal of Glaciology*, 35, 209-213, 1989.

1009 Dahl-Jensen, D., Johnsen, S., Hammer, C., Clausen, H., and Jouzel, J.: Past accumulation rates derived from observed
1010 annual layers in the GRIP ice core from Summit, Central Greenland. In: *Ice in the climate system*, Springer, 1993.

1011 [Dahl-Jensen, D., Gundestrup, N. S., Keller, K., Johnsen, S. J., Gogineni, S. P., Allen, C. T., Chuah, T. S., Miller, H.,](#)
1012 [Kipstuhl, S., and Waddington, E. D.: A search in north Greenland for a new ice-core drill site, *Journal of glaciology*,](#)
1013 [43, 300-306, 1997.](#)

1014 Dee, D. P., Uppala, S. M., Simmons, A. J., Berrisford, P., Poli, P., Kobayashi, S., Andrae, U., Balmaseda, M. A.,
1015 Balsamo, G., Bauer, P., Bechtold, P., Beljaars, A. C. M., van de Berg, L., Bidlot, J., Bormann, N., Delsol, C., Dragani,
1016 R., Fuentes, M., Geer, A. J., Haimberger, L., Healy, S. B., Hersbach, H., Hólm, E. V., Isaksen, L., Kållberg, P., Köhler,
1017 M., Matricardi, M., McNally, A. P., Monge-Sanz, B. M., Morcrette, J. J., Park, B. K., Peubey, C., de Rosnay, P.,
1018 Tavolato, C., Thépaut, J. N., and Vitart, F.: The ERA-Interim reanalysis: configuration and performance of the data
1019 assimilation system, *Quarterly Journal of the Royal Meteorological Society*, 137, 553-597, 2011.

1020 Delmotte, M., Masson, V., Jouzel, J., and Morgan, V. I.: A seasonal deuterium excess signal at Law Dome, coastal
1021 eastern Antarctica: A Southern Ocean signature, *Journal of Geophysical Research: Atmospheres*, 105, 7187-7197,
1022 2000.

1023 Denux, F.: Diffusion du signal isotopique dans le névé et dans la glace. Implication pour l'échantillonnage., PhD,
1024 Geosciences, Université Joseph Fourier-Grenoble 1, Grenoble, 243 pp., 1996.

1025 Domine, F., [Taillandier, A. S., Cabanes, A., Douglas, T. A., and Sturm, M.: Three examples where the specific surface](#)
1026 [area of snow increased over time, *The Cryosphere*, 3, 31-39, 2009.](#)

1027 [Domine, F.,](#) Morin, S., Brun, E., Lafaysse, M., and Carmagnola, C. M.: Seasonal evolution of snow permeability under
1028 equi-temperature and temperature-gradient conditions, *The Cryosphere*, 7, 1915-1929, 2013.

1029 [Ekaykin, A. A., Lipenkov, V. Y., Barkov, N. I., Petit, J. R., and Masson-Delmotte, V.: Spatial and temporal variability](#)
1030 [in isotope composition of recent snow in the vicinity of Vostok station, Antarctica: implications for ice-core record](#)

1031 [interpretation, *Annals of Glaciology*, 35, 181-186, 2002.](#)

1032 [Ebner, P. P., Schneebeli, M., and Steinfeld, A.: Metamorphism during temperature gradient with undersaturated](#)

1033 [advective airflow in a snow sample, *The Cryosphere*, 10, 791-797, 2016.](#)

1034 [Ebner, P. P., Steen-Larsen, H. C., Stenni, B., Schneebeli, M., and Steinfeld, A.: Experimental observation of transient](#)

1035 [\$\delta^{18}\text{O}\$ interaction between snow and advective airflow under various temperature gradient conditions, *The Cryosphere*,](#)

1036 [11, 1733-1743, 2017.](#)

1037 Ekaykin, A., Hondoh, T., Lipenkov, V. Y., and Miyamoto, A.: Post-depositional changes in snow isotope content:

1038 preliminary results of laboratory experiments, *Climate of the Past Discussions*, 5, 2239-2267, 2009.

1039 Ekaykin, A. A., Kozachek, A. V., Lipenkov, V. Y., and Shibaev, Y. A.: Multiple climate shifts in the Southern

1040 hemisphere over the past three centuries based on central Antarctic snow pits and core studies, *Annals of Glaciology*,

1041 55, 259-266, 2014.

1042 Ellehoj, M. D., Steen-Larsen, H. C., Johnsen, S. J., and Madsen, M. B.: Ice-vapor equilibrium fractionation factor of

1043 hydrogen and oxygen isotopes: Experimental investigations and implications for stable water isotope studies, *Rapid*

1044 *Communications in Mass Spectrometry*, 27, 2149-2158, 2013.

1045 EPICA comm. members: Eight glacial cycles from an Antarctic ice core, *Nature*, 429, 623-628, 2004.

1046 EPICA comm. members: One-to-one coupling of glacial climate variability in Greenland and Antarctica, *Nature*, 444,

1047 195-198, 2006.

1048 Fisher, D. A. and Koerner, R. M.: Signal and noise in four ice-core records from the Agassiz Ice Cap, Ellesmere Island,

1049 Canada: details of the last millennium for stable isotopes, melt and solid conductivity, *The Holocene*, 4, 113-120, 1994.

1050 [Epstein, S. and Sharp, R. P.: Six-year record of oxygen and hydrogen isotope variations in South Pole firn, *Journal of*](#)

1051 [Geophysical Research, 70, 1809-1814, 1965.](#)

1052 Flanner, M. G. and Zender, C. S.: Linking snowpack microphysics and albedo evolution, *Journal of Geophysical*

1053 *Research: Atmospheres*, 111, D12208, doi:10.1029/2005JD006834, 2006.

1054 Fréville, H., Brun, E., Picard, G., Tatarinova, N., Arnaud, L., Lanconelli, C., Reijmer, C., and van den Broeke, M.:

1055 Using MODIS land surface temperatures and the Crocus snow model to understand the warm bias of ERA-Interim

1056 reanalyses at the surface in Antarctica, *The Cryosphere*, 8, 1361-1373, 2014.

1057 Frezzotti, M., Pourchet, M., Flora, O., Gandolfi, S., Gay, M., Urbini, S., Vincent, C., Becagli, S., Gragnani, R., and

Proposito, M.: Spatial and temporal variability of snow accumulation in East Antarctica from traverse data, *Journal of Glaciology*, 51, 113-124, 2005.

Friedman, I., Benson, C., and Gleason, J.: Isotopic changes during snow metamorphism, *Stable isotope geochemistry: a tribute to Samuel Epstein*, 1991. 211-221, 1991.

[Gallet, J.-C., Domine, F., Arnaud, L., Picard, G., and Savarino, J.: Vertical profile of the specific surface area and density of the snow at Dome C and on a transect to Dumont D'Urville, Antarctica-albedo calculations and comparison to remote sensing products, *The Cryosphere*, 5, 631-649, 2011.](#)

Gay, M., Fily, M., Genthon, C., Frezzotti, M., Oerter, H., and Winther, J.-G.: Snow grain-size measurements in Antarctica, *Journal of Glaciology*, 48, 527-535, 2002.

Genthon, C., Six, D., Gallée, H., Grigioni, P., and Pellegrini, A.: Two years of atmospheric boundary layer observations on a 45-m tower at Dome C on the Antarctic plateau, *Journal of Geophysical Research: Atmospheres*, 118, 3218-3232, 2013.

Genthon, C., Six, D., Scarchilli, C., Ciardini, V., and Frezzotti, M.: Meteorological and snow accumulation gradients across Dome C, East Antarctic plateau, *International Journal of Climatology*, 36, 455-466, 2016.

Gkinis, V., Simonsen, S. B., Buchardt, S. L., White, J. W. C., and Vinther, B. M.: Water isotope diffusion rates from the NorthGRIP ice core for the last 16,000 years – Glaciological and paleoclimatic implications, *Earth and Planetary Science Letters*, 405, 132-141, 2014.

[Guillevie, M., Bazin, L., Landais, A., Kindler, Goursaud, S., Masson-Delmotte, V., Favier, V., Preunkert, S., Fily, M., Gallée, H., Jourdain, B., Legrand, M., Magand, O., Minster, B., Werner, M.: A 60-year ice-core record of regional climate from Adélie land, coastal Antarctica, *The Cryosphere*, 11, 343-362, 2017.](#)

[P., Orsi, A., Masson-Delmotte, V., Blunier, T., Buchardt, S., Capron, E., and Leuenberger, M.: Spatial gradients of temperature, accumulation and \$\delta^{18}\text{O}\$ ice in Greenland over a series of Dansgaard-Oeschger events, *Climate of the Past*, 9, 1029-1051, 2013.](#)

Hoshina, Y., Fujita, K., Nakazawa, F., Iizuka, Y., Miyake, T., Hirabayashi, M., Kuramoto, T., Fujita, S., and Motoyama, H.: Effect of accumulation rate on water stable isotopes of near-surface snow in inland Antarctica, *Journal of Geophysical Research*, 119, 274-283, 2014.

Johnsen, S.: Stable isotope homogenization of polar firn and ice, *Isotopes and impurities in snow and ice*, 1, 210-219,

1085 1977.

1086 Johnsen, S. J., Dahl-Jensen, D., Dansgaard, W., and Gundestrup, N.: Greenland palaeotemperatures derived from GRIP
 1087 bore hole temperature and ice core profiles, *Tellus*, 47B, 624-629, 1995.

1088 Johnsen, S. J., Clausen, H. B., Cuffey, K. M., Hoffmann, G., Schwander, J., and Creyts, T.: Diffusion of stable isotopes
 1089 in polar firn and ice: the isotope effect in firn diffusion, *Physics of ice core records*, 159, 121-140, 2000.

1090 ~~Joes, F. and Spahni, Jones, T. R., Roberts, W. H. G., -: Rates of change in natural and anthropogenic radiative forcing
 1091 over the past 20,000 years, *Proceedings of the National Academy of Sciences*, 105, 1425-1430, 2008.~~

1092 ~~Jouzel, Steig, E. J., Masson-Delmotte, V., Stievenard, Cuffey, K. M., Markle, B. R., Landais, A., Vimeux, F., Johnsen,
 1093 S. J., Sveinbjörnsdottir, A. E., and White, J. W. C.: Rapid deuterium-excess changes in Greenland Southern Hemisphere
 1094 climate variability forced by Northern Hemisphere ice cores: a link between the ocean and the atmosphere, *Comptes
 1095 Rendus Geoscience*, 337, 957-969, 2005-sheet topography, *Nature*, 554, doi:10.1038/nature24669, 2018.~~

1096 Jouzel, J., Masson-Delmotte, V., Cattani, O., Dreyfus, G., Falourd, S., Hoffmann, G., Minster, B., Nouet, J., Barnola,
 1097 J. M., Chappellaz, J., Fischer, H., Gallet, J. C., Johnsen, S., Leuenberger, M., Loulergue, L., Luethi, D., Oerter, H.,
 1098 Parrenin, F., Raisbeck, G., Raynaud, D., Schilt, A., Schwander, J., Selmo, E., Souchez, R., Spahni, R., Stauffer, B.,
 1099 Steffensen, J. P., Stenni, B., Stocker, T. F., Tison, J. L., Werner, M., and Wolff, E. W.: Orbital and millennial Antarctic
 1100 climate variability over the past 800,000 years, *Science*, 317, 793-796, 2007.

1101 Kaempfer, T. U., Schneebeli, M., and Sokratov, S. A.: A microstructural approach to model heat transfer in snow,
 1102 *Geophysical Research Letters*, 32, L21503, doi:10.1029/2005GL023873, 2005.

1103 Kawamura, K., Parrenin, F., Lisiecki, L., Uemura, R., Vimeux, F., Severinghaus, J. P., Hutterli, M. A., Nakazawa, T.,
 1104 Aoki, S., Jouzel, J., Raymo, M. E., Matsumoto, K., Nakata, H., Motoyama, H., Fujita, S., Goto-Azuma, K., Fujii, Y.,
 1105 and Watanabe, O.: Northern Hemisphere forcing of climatic cycles in Antarctica over the past 360,000 years, *Nature*,
 1106 448, 912-916, 2007.

1107 ~~Krol, Q., and Löwe, H.: Relating optical and microwave grain metrics of snow: the relevance of grain shape, *The
 1108 Cryosphere*, 10, 2847-2863, 2016.~~

1109 Laepple, T., Werner, M., and Lohmann, G.: Synchronicity of Antarctic temperatures and local solar insolation on
 1110 orbital timescales, *Nature*, 471, 91, 2011.

1111 Landais, A., Barkan, E., and Luz, B.: Record of $\delta^{18}\text{O}$ and ^{17}O -excess in ice from Vostok Antarctica during the last

1112 150,000 years, *Geophysical Research Letters*, 35, L02709, 2008.

1113 [Landais, A., Casado, C., Prié, F., Magand, O., Arnaud, L., Ekaykin, A., Petit, J.-R., Picard, G., Fily, M., Minster, B.,](#)
1114 [Touzeau, A., Goursaud, S., Masson-Delmotte, V., Jouzel, J., and Orsi, A.: Surface studies of water isotopes in](#)
1115 [Antarctica for quantitative interpretation of deep ice core data, *Comptes Rendus Géosciences*, 349, 139-150, 2017.](#)
1116 [Legagneux, L., and Domine, F.: A mean field model of the decrease of the specific surface area of dry snow during](#)
1117 [isothermal metamorphism, *Journal of Geophysical Research*, 110, doi:10.1029/2004JF000181, 2005.](#)

1118 Lefebvre, F., Gallée, H., van Ypersele, J.-P., and Greuell, W.: Modeling of snow and ice melt at ETH Camp (West
1119 Greenland): A study of surface albedo, *Journal of Geophysical Research: Atmospheres*, 108, D8-4231,
1120 doi:10.1029/2001JD001160, 2003.

1121 Libois, Q., Picard, G., Arnaud, L., Morin, S., and Brun, E.: Modeling the impact of snow drift on the decameter-scale
1122 variability of snow properties on the Antarctic Plateau, *Journal of Geophysical Research: Atmospheres*, 119, 11662-
1123 11681, 2014.

1124 Libois, Q., Picard, G., Arnaud, L., Dumont, M., Lafaysse, M., Morin, S., and Lefebvre, E.: Summertime evolution of
1125 snow specific surface area close to the surface on the Antarctic Plateau, *The Cryosphere*, 9, 2383-2398, 2015.

1126 Lorius, C., Jouzel, J., Ritz, C., Merlivat, L., Barkov, N. I., Korotkevich, Y. S., and Kotlyakov, V. M.: A 150,000-year
1127 climatic record from Antarctic ice, *Nature*, 316, 591-596, 1985.

1128 Lu, G. and DePaolo, D. J.: Lattice Boltzmann simulation of water isotope fractionation during ice crystal growth in
1129 clouds, *Geochimica et Cosmochimica Acta*, 180, 271-283, 2016.

1130 ~~Magand, O., Frezzotti, M., Porechet, M., Stenni, B., Genoni, L., and Fily, M.: Climate variability along latitudinal and~~
1131 ~~longitudinal transects in East Antarctica, *Annals of Glaciology*, 39, 351-358, 2004.~~

1132 Mann, M. E. and Jones, P. D.: Global surface temperatures over the past two millennia, *Geophysical Research Letters*,
1133 30, 1820, doi:10.1029/2003GL017814, 2003. ~~Masson-Delmotte, V., Delmotte, M., Morgan, V., Etheridge, D., van~~
1134 ~~Ommen, T., Tartarin, S., and Hoffmann, G.: Recent southern Indian Ocean climate variability inferred from a Law~~
1135 ~~Dome ice core: new insights for the interpretation of coastal Antarctic isotopic records, *Clim Dyn*, 21, 153-166, 2003.~~

1136 Masson-Delmotte, V., Landais, A., Stievenard, M., Cattani, O., Falourd, S., Jouzel, J., Johnsen, S. J., Dahl-Jensen, D.,
1137 Sveinbjörnsdóttir, A., White, J. W. C., Popp, T., and Fischer, H.: Holocene climatic changes in Greenland: Different
1138 deuterium excess signals at Greenland Ice Core Project (GRIP) and NorthGRIP, *Journal of Geophysical Research:*

1139 Atmospheres, 110, 1-13, 2005.

1140 Masson-Delmotte, V., Buiron, D., Ekaykin, A., Frezzotti, M., Gallée, H., Jouzel, J., Krinner, G., Landais, A.,
 1141 motoyama, H., Oerter, H., Pol, K., Pollard, D., Ritz, C., Schlosser, Z., Sime, L. C., Sodemann, H., Stenni, B., Uemura,
 1142 R., and Vimeux, F.: A comparison of the present and last interglacial periods in six Antarctic ice cores, *Clim. Past*, 7,
 1143 397-423, 2011.

1144 Masson-Delmotte, V., Steen-Larsen, H., Ortega, P., Swingedouw, D., Popp, T., Vinther, B., Oerter, H.,
 1145 Sveinbjörnsdóttir, A., Gudlaugsdóttir, H., and Box, J.: Recent changes in north-west Greenland climate documented
 1146 by NEEM shallow ice core data and simulations, and implications for past-temperature reconstructions, *The*
 1147 *Cryosphere Discussions*, 2015, 1481-1504, 2015. Mayewski, P. and Goodwin, L.: *Antarctic's role pursued in global*
 1148 *climate change*, *Eos, Transactions American Geophysical Union*, 80, 398-400, 1999, 1481-1504, 2015.

1149 Morse, D. L., Waddington, E. D., Marshall, H.-P., Neumann, T. A., Steig, E. J., Dibb, J. E., Winebrenner, D. P., and
 1150 Arthern, R. J.: Accumulation Rate Measurements at Taylor Dome, East Antarctica: Techniques and Strategies for Mass
 1151 Balance Measurements in Polar Environments, *Geografiska Annaler: Series A, Physical Geography*, 81, 683-694,
 1152 1999.

1153 Neumann, T. A.: Effects of firn ventilation on geochemistry of polar snow, PhD, Department of Earth and Space
 1154 Sciences, University of Washington, Washington, 223 pp., 2003.

1155 Neumann, T. A. and Waddington, E. D.: Effects of firn ventilation on isotopic exchange, *Journal of Glaciology*, 50,
 1156 183-194, 2004.

1157 Neumann, T. A., Waddington, E. D., Steig, E. J., and Grootes, P. M.: Non-climate influences on stable isotopes at
 1158 Taylor Mouth, Antarctica, *Journal of Glaciology*, 51, 248-258, 2005.

1159 Neumann, T., Albert, M., Lomonaco, R., Engel, C., Courville, Z., and Perron, F.: Experimental determination of snow
 1160 sublimation rate and stable-isotopic exchange, *Annals of Glaciology*, 49, 1-6, 2008.

1161 Neumann, T. A., Albert, M. R., Engel, C., Courville, Z., and Perron, F.: Sublimation rate and the mass-transfer
 1162 coefficient for snow sublimation, *International Journal of Heat and Mass Transfer*, 52, 309-315, 2009.

1163 Petit, J. R., Jouzel, J., Pourchet, M., and Merlivat, L.: A detailed study of snow accumulation and stable isotope content
 1164 in Dome C (Antarctica), *Journal of Geophysical Research*, 87, 4301-4308, 1982.

1165 Petit, J. R., Jouzel, J., Raynaud, D., Barkov, N. I., Barnola, J. M., Basile, I., Bender, M., Chappellaz, J., Davis, M.,

1166 Delaygue, G., Delmotte, M., Kotlyakov, V. M., Legrand, M., Lipenkov, V. Y., Lorius, C., Pepin, L., Ritz, C., Saltzman,
1167 E., and Stievenard, M.: Climate and atmospheric history of the past 420,000 years from the Vostok ice core, Antarctica,
1168 Nature, 399, 429-436, 1999.

1169 [Picard, G., Arnaud, L., Panel, J. M., and Morin, S.: Design of a scanning laser meter for monitoring the spatio-temporal
1170 evolution of snow depth and its application in the Alps and in Antarctica, The Cryosphere, 10, 1495-1511, 2016.](#)

1171 Pinzer, B. R., Schneebeli, M., and Kaempfer, T. U.: Vapor flux and recrystallization during dry snow metamorphism
1172 under a steady temperature gradient as observed by time-lapse micro-tomography, The Cryosphere, 6, 1141-1155,
1173 2012.

1174 Ramseier, R. O.: Self-diffusion of tritium in natural and syntehtic ice monocrystals, Journal of Applied Physics, 38,
1175 2553-2556, 1967.

1176 Ritter, F., Steen-Larsen, H. C., Werner, M., Masson-Delmotte, V., Orsi, A., Behrens, M., Birnbaum, G., Freitag, J.,
1177 Risi, C., and Kipfstuhl, S.: Isotopic exchange on the diurnal scale between near-surface snow and lower atmospheric
1178 water vapor at Kohnen station, East Antarctica, The Cryosphere Discuss., 2016, 1-35, 2016.

1179 [Schilt, A., Baumgartner, M., Blunier, T., Schwander, J., Spahni, R., Fischer, H., and Stocker, T. F.: Glacial-interglacial
1180 and millennial-scale variations in the atmospheric nitrous oxide concentration during the last 8000,000 years,
1181 Quaternary Science Reviews, 29, 182-192, 2010.](#)

1182 Schneider, D. P., Steig, E. J., Ommen, T. D. v., Dixon, D. A., Mayewski, P. A., Jones, J. M., and Bitz, C. M.: Antarctic
1183 temperatures over the past two centuries from ice cores, Geophysical Research Letters, 33, L16707, 2006.

1184 Shaheen, R., Abauanza, M., Jackson, T. L., McCabe, J., Savarino, J., and Thiemens, M. H.: Tales of volcanoes and El-
1185 Niño southern oscillations with the oxygen isotope anomaly of sulfate aerosol, Proceedings of the National Academy
1186 of Sciences, 110, 17662-17667, 2013.

1187 Shuman, C. A., Alley, R. B., Anandakrishnan, S., White, J. W. C., Grootes, P. M., and Stearns, C. R.: Temperature
1188 and accumulation at the Greenland Summit: Comparison of high-resolution isotope profiles and satellite passive
1189 microwave brightness temperature trends, Journal of Geophysical Research: Atmospheres, 100, 9165-9177, 1995.

1190 Shuman, C. A., Steffen, K., Box, J. E., and Stearns, C. R.: A dozen years of temperature observations at the Summit:
1191 Central Greenland automatic weather stations 1987-99, Journal of Applied Meteorology, 40, 741-752, 2001.

1192 Sime, L. C., Tindall, J. C., Wolff, E. W., Connolley, W. M., and Valdes, P. J.: Antarctic isotopic thermometer during

1193 a CO₂ forced warming event, *Journal of Geophysical Research*, 113, D24119, 2008.

1194 Sjolte, J., Hoffmann, G., Johnsen, S. J., Vinther, B. M., Masson-Delmotte, V., and Sturm, C.: Modeling the water
1195 isotopes in Greenland precipitation 1959–2001 with the meso-scale model REMO-iso, *Journal of Geophysical*
1196 *Research: Atmospheres*, 116, D18105, doi:10.1029/2010JD015287, 2011.

1197 Sokratov, S. A. and Golubev, V. N.: Snow isotopic content change by sublimation, *Journal of Glaciology*, 55, 823-
1198 828, 2009.

1199 Steen-Larsen, H. C., Masson-Delmotte, V., Sjolte, J., Johnsen, S. J., Vinther, B. M., Bréon, F. M., Clausen, H., Dahl-
1200 Jensen, D., Falourd, S., and Fettweis, X.: Understanding the climatic signal in the water stable isotope records from
1201 the NEEM shallow firn/ice cores in northwest Greenland, *Journal of Geophysical Research: Atmospheres*, 116,
1202 D06108, doi:10.1029/2010JD014311, 2011.

1203 Steen-Larsen, H., Masson-Delmotte, V., Hirabayashi, M., Winkler, R., Satow, K., Prié, F., Bayou, N., Brun, E., Cuffey,
1204 K., and Dahl-Jensen, D.: What controls the isotopic composition of Greenland surface snow?, *Climate of the Past*, 10,
1205 377-392, 2014.

1206 Steig, E. J.: The south-north connection, *Nature*, 44, 152-153, 2006.

1207 Stenni, B., Jouzel, J., Masson-Delmotte, V., Röthlisberger, R., Castellano, E., Cattani, O., Falourd, S., Johnsen, S. J.,
1208 Longinelli, A., Sachs, J. P., Selmo, E., Souchez, R., Steffensen, J. P., and Udisti, R.: A late-glacial high-resolution site
1209 and source temperature record derived from the EPICA Dome C isotope records (East Antarctica), *Earth and Planetary*
1210 *Science Letters*, 217, 183-195, 2004.

1211 Stenni, B., Buiron, D., Frezzotti, M., Albani, S., Barbante, C., Bard, E., Barnola, J. M., Baroni, M., Baumgartner, M.,
1212 Bonazza, M., Capron, E., Castellano, E., Chappellaz, J., Delmonte, B., Falourd, S., Genoni, L., Iacumin, P., Jouzel, J.,
1213 Kipfstuhl, S., Landais, A., Lemieux-Dudon, B., Maggi, V., Masson-Delmotte, V., Mazzola, C., Minster, B.,
1214 Montagnat, M., Mulvaney, R., Narcisi, B., Oerter, H., Parrenin, F., Petit, J. R., Ritz, C., Scarchilli, C., Schilt, A.,
1215 Schupbach, S., Schwander, J., Selmo, E., Severi, M., Stocker, T. F., and Udisti, R.: Expression of the bipolar see-saw
1216 in Antarctic climate records during the last deglaciation, *Nature Geosci*, 4, 46-49, 2011.

1217 Stenni, B., Scarchilli, C., Masson-Delmotte, V., Schlosser, E., Ciardini, V., Dreossi, G., Grigioni, P., Bonazza, M.,
1218 Cagnati, A., Karlicek, D., Risi, C., Udisti, R., and Valt, M.: Three-year monitoring of stable isotopes of precipitation
1219 at Concordia Station, East Antarctica, *The Cryosphere*, 10, 2415-2428, 2016.

1220 Stichler, W., Schotterer, U., Fröhlich, K., Ginot, P., Kull, C., Gäggeler, H., and Pouyaud, B.: Influence of sublimation
1221 on stable isotope records recovered from high-altitude glaciers in the tropical Andes, *Journal of Geophysical Research*,
1222 106, 22613-22620, 2001.

1223 [Taillandier, A. S., Domine, F., Simpson, W. R., Sturm, M., Douglas, T. A., and Severin, K.: Evolution of the snow
1224 area index of the subarctic snowpack in central Alaska over a whole season. Consequences for the air to snow transfer
1225 of pollutants, *Environmental Science and Technology*, 40, 7521-7527, 2006.](#)

1226 [Taillandier, A. S., Domine, F., Simpson, W. R., Sturm, M., and Douglas, T. A.: Rate of decrease of the specific surface
1227 area of dry snow: Isothermal and temperature gradient conditions, *Journal of Geophysical Research: Earth Surface*,
1228 112, doi:10.1029/2006JF000514, 2007.](#)

1229 Touzeau, A., Landais, A., Stenni, B., Uemura, R., Fukui, K., Fujita, S., Guilbaud, S., Ekaykin, A., Casado, M., and
1230 Barkan, E.: Acquisition of isotopic composition for surface snow in East Antarctica and the links to climatic
1231 parameters, *The Cryosphere*, 10, 837-852, 2016.

1232 Town, M. S., Warren, S. G., Walden, V. P., and Waddington, E. D.: Effect of atmospheric water vapor on modification
1233 of stable isotopes in near-surface snow on ice-sheets, *Journal of Geophysical Research*, 113, D24303, 2008.

1234 [Uemura, R., Landais, A., Motoyama, H., and Stenni, B.: Ranges of moisture-source temperature estimated from
1235 Antarctic ice cores stable isotope records over glacial-interglacial cycles, *Climate of the Past*, 8, 1109-1025, 2012.](#)

1236 Urbini, S., Frezzotti, M., Gandolfi, S., Vincent, C., Sarchilli, C., Vittuari, L., and Fily, M.: Historical behaviour of
1237 Dome C and Talos Dome (East Antarctica) as investigated by snow accumulation and ice velocity measurements,
1238 *Global and Planetary Change*, 60, 576-588, 2008.

1239 van de Berg, W. J., van den Broeke, M. R., Reijmer, C. H., and van Meijgaard, E.: Reassessment of the Antarctic
1240 surface mass balance using calibrated output of a regional atmospheric climate model, *Journal of Geophysical
1241 Research: Atmospheres*, 111, D11104, doi:10.1029/2005JD006495, 2006.

1242 van der Wel, L., Been, H., Smeets, P., and Meijer, H.: Constraints on the $\delta^2\text{H}$ diffusion rate in firn from field
1243 measurements at Summit, Greenland, *The Cryosphere*, 9, 1089-1103, 2015.

1244 [Vimeux, F., Cuffey, K. M., and Jouzel, J.: New insights into Southern Hemisphere temperature changes from Vostok
1245 ice cores using deuterium excess correction, *Earth and Planetary Science Letters*, 203, 829-843, 2002.](#)

1246 Vionnet, V., Brun, E., Morin, S., Boone, A., Faroux, S., Le Moigne, P., Martin, E., and Willemet, J.: The detailed

|

1247 snowpack scheme Crocus and its implementation in SURFEX v7. 2, Geoscientific Model Development, 5, 773-791,
1248 2012.

1249 Waddington, E. D., Steig, E. J., and Neumann, T. A.: Using characteristic times to assess whether stable isotopes in
1250 polar snow can be reversibly deposited, Annals of Glaciology, 35, 118-124, 2002.

1251 [WAIS Divide Project Members: Onset of deglacial warming in West Antarctica driven by local orbital forcing, Nature,](#)
1252 [500, 440-444, 2013.](#)

1253 White, J.W.C., Barlow, L.K., Fisher, D., Grootes, P., Jouzel, J., Johnsen, S.J., Stuiver, M., and Clausen, H.: The climate
1254 signal in the stable isotope of Summit, Greenland snow : Results of comparisons with modern climate observations.
1255 Journal of Geophysical Research, 102, C12, 26425 - 26439, 1997.

1256

|

Table 1. Definition of the symbols used.

Symbol	Description
Constants	
T_0	Temperature of the triple point of water (K)
R_v	Vapor constant for water ($J \cdot kg^{-1} \cdot K^{-1}$)
L_{sub}	Latent heat of sublimation of water ($J \cdot m^{-3}$)
$\rho_v \phi C_{v0}$	Vapor density mass concentration at 273.16 K ($kg \cdot m^{-3}$ of air)
D_{ice}	Diffusivity of water molecules in solid ice ($m^2 \cdot s^{-1}$)
D_v	Diffusivity of vapor in air at 263 K ($m^2 \cdot s^{-1}$) (temperature dependency neglected)
ρ_{ice}	Density of ice ($kg \cdot m^{-3}$)
θA	Accumulation (m i.e. per year)
R_{moy}	Average snow grain radius (m)
Δt_{sol}	Characteristic time for solid diffusion (s)
$\Delta t_{surfcenter}$	Periodicity of the mixing between grain center and grain surface, as a result because of grain center translation (s)
1D-variables	
t	Time (s)
n	Layer number from top of the snowpack
$\delta^{18}O_{sf}(t)$	Isotopic composition of oxygen in the snowfall (‰)
$T_{air}(t)$	Temperature of the air at 2 m (K)
2D-variables	
$h(t, n)$	Height of the center of the snow layer relative to the bottom of the snowpack (m)
$z(t, n)$	Depth of the center of the snow layer (m from surface)
$dz(t, n)$	Thickness of the snow layer (m)
$T(t, n)$	Temperature of the snow layer (K)
$\rho_{sn}(t, n)$	Density of the snow layer ($kg \cdot m^{-3}$)
$m_{sn}(t, n)$	Mass of the snow layer (kg)
$\rho_v \phi C_v(t, n)$	Vapor density mass concentration at saturation in the porosity of the snow layer ($kg \cdot m^{-3}$ of air)
$D_{eff}(t, n)$	Effective diffusivity of vapor in the layer ($m^2 \cdot s^{-1}$)
$\delta^{18}O(t, n)$	Isotopic composition of oxygen in the snow layer (‰)
$F^{18}(n+1 \rightarrow n)$	Flux of the heavy water molecules (^{18}O) from layer $n+1$ to layer n ($kg \cdot m^{-2} \cdot s^{-1}$)
$F(n+1 \rightarrow n)$	Vapor flux from layer $n+1$ to layer n ($kg \cdot m^{-2} \cdot s^{-1}$)
$D_{eff}(t, n \rightarrow n+1)$	Effective interfacial diffusivity between layers n and $n+1$ ($m^2 \cdot s^{-1}$)
$R_{vap ini}^i$	Isotopic ratio in the initial vapor (i is either ^{18}O , ^{17}O or D)
$R_{surf ini}^i$	Isotopic ratio in the grain surface sub-compartment before vapor individualization
$c_{vap ini}^x$	Concentration in heavy or light isotope Ratio between the mass of a given isotopologue in the initial vapor (x is ^{18}O , ^{17}O , ^{16}O , 1H -or D) and the total mass of vapor (no unit). The mass balance is made separately and independently for H and O (i.e.: $c_{vap ini}^{18} + c_{vap ini}^{17} + c_{vap ini}^{16} = 1$ and $c_{vap ini}^{1H} + c_{vap ini}^D = 1$).
α_{sub}^i	Fractionation coefficients at equilibrium during sublimation (i is either ^{18}O , ^{17}O or D)

|

1260
1261

GRIP
Accumulation 23 cm i.e./yr

Dahl-Jensen et al., 1993

Cellules supprimées

|

GRIP

Accumulation	23 cm i.e. yr. ⁻¹	Dahl-Jensen et al., 1993
Annual temperature	241 K	Masson-Delmotte et al., 2005
Winter temperature	232 K	(Feb.) Shuman et al., 2001
Summer temperature	261 K	(Aug.) Shuman et al., 2001
Mean $\delta^{18}\text{O}$	-35.2‰	Masson-Delmotte et al., 2005
$\delta^{18}\text{O}$ min	-43 ‰	(2m snowpit snow pit) Shuman et al., 1995
$\delta^{18}\text{O}$ max	-27 ‰	(2m snowpit snow pit) Shuman et al., 1995
$\delta^{18}\text{O}/T_{\text{air}}T$ slope	0.46 ‰/°C	(2m snowpit snow pit) Shuman et al., 1995

DOME C

Accumulation	2.7 cm i.e. yr. ⁻¹	Frezzotti et al., 2005; Urbini et al., 2008
Annual temperature	221 K	Stenni et al., 2016
Min winter $T_{\text{air}}T$	199 K	Stenni et al., 2016
Max summer $T_{\text{air}}T$	248 K	Stenni et al., 2016
Mean $\delta^{18}\text{O}$	-56.4 ‰	Stenni et al., 2016
$\delta^{18}\text{O}$ min winter	-71.8 ‰	Stenni et al., 2016
$\delta^{18}\text{O}$ max summer	-40.2 ‰	Stenni et al., 2016
$\delta^{18}\text{O}/T_{\text{air}}T$ slope	0.49 ‰/°C	Stenni et al., 2016

Table 2. Climate and isotope variability at GRIP (Greenland) and Dome C (Antarctica).

Variable	Equation	Average	Range	
Thickness (m)	dz	$1.2 \cdot 10^{-1}$	$5 \cdot 10^{-4}$	$8 \cdot 10^{-1}$
Density (kg m^{-3})	ρ_{sn}	340	300	460
Temperature (K)	T	225	205	255
Mass (kg)	$m_{\text{sn}} = dz \cdot \rho_{\text{sn}}$	42	0.15	368
Vapor density mass concentration (kg m^{-3})	$\rho_v C_v$ Eq. (78)	$1.8 \cdot 10^{-5}$	$1.2 \cdot 10^{-6}$	$4.4 \cdot 10^{-4}$
Porosity	$\Phi = 1 - (\rho_{\text{sn}} / \rho_i \rho_{\text{ice}})$	0.63	0.5	0.67
Vapor mass (kg)	m_{vap} Eq. (4011)	$1.3 \cdot 10^{-6}$	$3 \cdot 10^{-10}$	$2.4 \cdot 10^{-4}$
Minimum ratio	$\tau_{\text{min}} = 1/10^6$	$1 \cdot 10^{-6}$	$1 \cdot 10^{-6}$	$1 \cdot 10^{-6}$
Maximum ratio	$\tau_{\text{max}} = \frac{\rho_v \Phi C_v \Phi}{\rho_{\text{sn}} \rho_{\text{sn}}} \cdot 10^6$	$3.3 \cdot 10^{-2}$	$1.3 \cdot 10^{-3}$	1

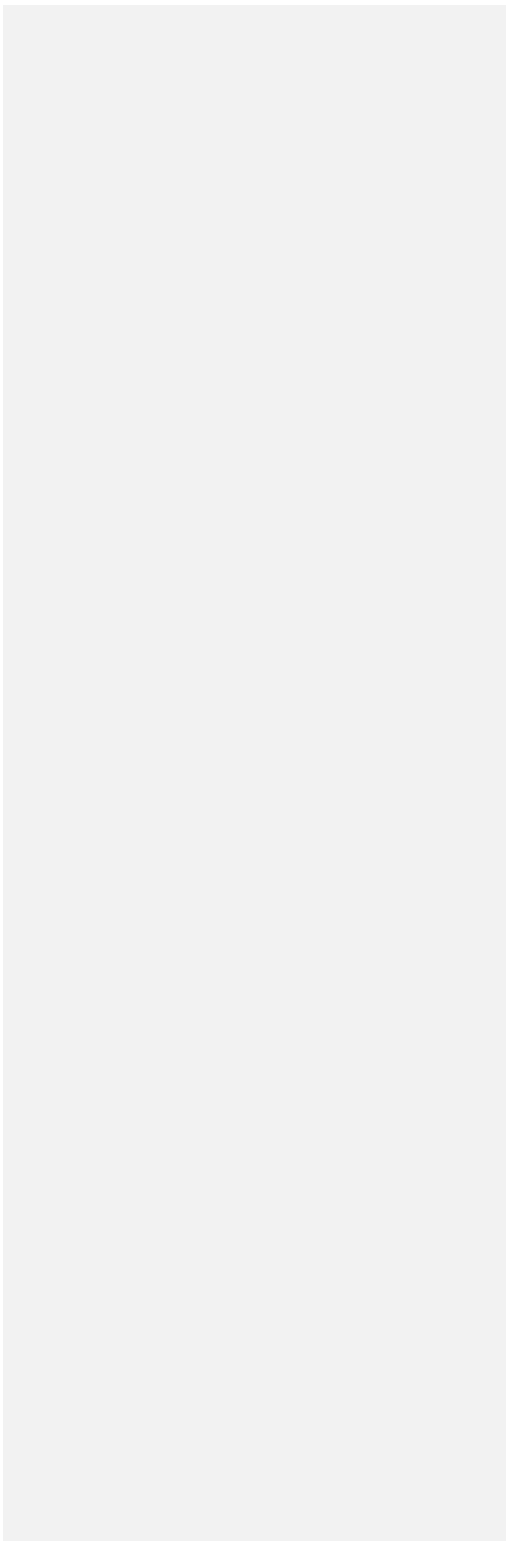
Table 3. Typical thickness, density, temperature and other parameters of the snow layers in the simulations. ~~The definitions of symbols are given in Table 1.~~ The ratio τ is the mass ratio between the grain surface compartment and the grain center compartment. It must be chosen within the interval $[10^{-6}; 10^6 \cdot (\rho_v (C_v \Phi) / \rho_{\text{sn}})]$ to allow exchanges between grain surface compartment and grain center compartment, on the one hand; and between grain surface compartment and vapor compartment on the other hand (see text for details).

|

1272

|

|



	GRIP simulation			Dome C simulations		
N°	1	2	3	4	5	6
Section	4.1.1 ₂	4.1.2 ₂	4.2.1 ₂	4.2.2 ₂	4.2.3 ₂	4.2.4 ₂
Figures	Figure 2	Figure 3	Figure 5 & 6	Figure 7 & 86	Figure 9 & 107	Figure 118
Duration	10 years	10 years	1 year	1 year	1 year	10 years
Period	Jan 2000- Dec 2010	Jan 2001- Dec 2011	Jan- Dec 2001	Jan- Dec 2001	Jan- Dec 2001	Jan 2000- Dec 2010
<i>Atmospheric forcing applied</i>						
Air T	-	ERA-Interim (GR)	ERA-Interim	ERA-Interim	ERA-Interim	ERA-Interim
Specific humidity	-	ERA-Interim (GR)	ERA-Interim	ERA-Interim	ERA-Interim	ERA-Interim
Air pressure	-	ERA-Interim (GR)	ERA-Interim	ERA-Interim	ERA-Interim	ERA-Interim
Wind velocity	-	ERA-Interim (GR)	ERA-Interim	ERA-Interim	ERA-Interim	ERA-Interim
Snowfall	NO	NO	NO	NO	YES	YES
$\delta^{18}\text{O}_{\text{sf}}$	-	-	-	-	Function (T)*	Function (T)*
<i>Model configuration</i>						
Initial snow T	Flat profile (241 K)	One-year run initialization (Jan-Dec 2000)	One-year run initialization (Jan-Dec 2000)	One-year run initialization (Jan-Dec 2000)	One-year run initialization (Jan-Dec 2000)	Exponential profile**
Evolution of snow T	Constant	Computed	Computed	Computed	Computed	Computed
Initial snow d18O	Sinusoidal profile***	Sinusoidal profile***	-40 ‰	-40 ‰	-40 ‰	-40 ‰
Wind drift	NO	NO	NO	YES	YES	NO
Homogeneous compaction	NO	NO	NO	YES	YES	NO

Table 4. List of simulations described in the article with the corresponding paragraph number. The external atmospheric forcing used for Dome C is ERA-Interim reanalysis (2000-2013). However, the precipitation amounts from ERA-Interim reanalysis are increased by 1.5 times to account for the dry bias in the reanalysis

1276 (as in Libois et al., 2014). For the second simulation at GRIP, Greenland meteorological conditions are derived from the atmospheric forcing of Dome C, but the
 1277 temperature is modified ($T_{\text{GRIP}} = T_{\text{DC}} + 15$) as well as the longwave down ($\text{LW}_{\text{GRIP}} = 0.85 \text{ LW}_{\text{DC}} + 60$).

1278 * Using data from one-year snowfall sampling at Dome C (Stenni et al., 2016; Touzeau et al., 2016), we obtained the following Eq. (1516) linking $\delta^{18}\text{O}_{\text{sf}}$ in
 1279 the snowfall to the local temperature T_{air} : $\delta^{18}\text{O}_{\text{sf}} = 0.45 \times (T_{\text{air}} - T - 273.15) - 31.5$.

1280 **The exponential profile of temperature used in simulation 6 is defined using Eq. (1920):

1281
$$T(z) = T(10\text{m}) + \Delta T \times \exp(-z/z_0) + 0.1 \times z \quad (19)$$

1282 with $T(10\text{m}) = 218$ K, $\Delta T = 28$ K, and $z_0 = 1.516$ m.

1283 It fits well with temperature measurements of midday in January (Casado et al., 2016b).

1284 ***The Greenland snowpack has an initial sinusoidal profile of $\delta^{18}\text{O}$ defined using Eq. (19): $\delta^{18}\text{O} = -35.5 - 8 \times \sin\left(\frac{2\pi \times z}{a \times \rho_{\text{ice}} / \rho_{\text{sn}}}\right)$ (18):

1285
$$\delta^{18}\text{O} = -$$

1286
 1287
$$-35.5 - 8 \times \sin\left(\frac{2\pi \times z}{a \times \rho_{\text{ice}} / \rho_{\text{sn}}}\right) \quad (18)$$

1288 (see Table 1 for symbols).

1289

	GRIP sensitivity tests				Dome C sensitivity tests				
N°	1	2	3	4	1	2	3	4	5
Section	4.3_	4.3_	4.3_	4.3_	4.3_	4.3_	4.3_	4.3_	4.3_
Figures	Figure 129	Figure 129	Figure 129	Figure 129	Figure 1310	Figure 1310	Figure 1310	Figure 1310	Figure 1310
Duration	6 months	6 months	6 months	6 months	63 years	63 years	63 years	63 years	63 years
Period	Jan- Jun 2000	Jan- Jun 2000	Jan- Jun 2000	Jan- Jun 2000	Jan 2000- Dec 20052002	Jan 2000- Dec 20052002	Jan 2000- Dec 20052002	Jan 2001- Dec 20062003	Jan 2001- Dec 20062003
<i>Atmospheric forcing applied</i>									
Air T	-	-	-	-	-	-	-	ERA-Interim	ERA-Interim
Specific humidity	-	-	-	-	-	-	-	ERA-Interim	ERA-Interim
Air pressure	-	-	-	-	-	-	-	ERA-Interim	ERA-Interim
Wind velocity	-	-	-	-	-	-	-	ERA-Interim	ERA-Interim
Snowfall	NO	NO	NO	NO	NO	NO	NO	NO	NO
$\delta^{18}\text{O}_{\text{sf}}$	-	-	-	-	-	-	-	-	-
<i>Model configuration</i>									
Initial snow T	Flat profile (241 K)	Flat profile (241 K)	Flat profile (241 K)	Flat profile (241 K)	Flat profile (241 K)	Flat profile (220 K)	Flat profile (220 K)	One-year run init-initialization (Jan-Dec 2000)	One-year run init-initialization (Jan-Dec 2000)
Evolution of snow T	CstConstant Sinusoid	CstConstant Sinusoid	CstConstant Sinusoid	CstConstant Sinusoid	CstConstant Sinusoid	CstConstant Sinusoid	CstConstant Sinusoid	Computed Sinusoid	Computed Sinusoid
Initial snow d18O	Sinusoidal profile ***	Sinusoidal profile ***	Sinusoidal profile ***	Sinusoidal profile ***	Sinusoidal profile ****	Sinusoidal profile ****	Sinusoidal profile ****	Sinusoidal profile ****	Sinusoidal profile ****

Wind drift	NO	NO	NO	NO	NO	NO	NO	NO	NO
Homog.									
Homogeneous compaction	NO	NO	NO	NO	NO	NO	NO	NO	NO
Mass ratio τ <u>within the grain</u>	$1 \cdot 10^{-6}$	$5 \cdot 10^{-4}$	$3.3 \cdot 10^{-2}$	$5 \cdot 10^{-4}$	$5 \cdot 10^{-4}$	$5 \cdot 10^{-4}$	$5 \cdot 10^{-4}$	$5 \cdot 10^{-4}$	$3.3 \cdot 10^{-2}$
<u>Period for recrystallization</u>									
$\Delta t_{surf/center}$	15 days	15 days	15 days	2 days	215 days	2 days	15 days	15 days	15 days

Table 5. List of the sensitivity tests performed at GRIP and at Dome C. The external atmospheric forcing used for Dome C is ERA-Interim reanalysis (see Table 4).

~~***The Greenland snowpack has an initial sinusoidal profile of $\delta^{18}O$ defined using Eq. [Cst: constant \(19\)](#):~~

~~***The Greenland snowpack has an initial sinusoidal profile of $\delta^{18}O$ defined using Eq. [\(18\)](#):~~

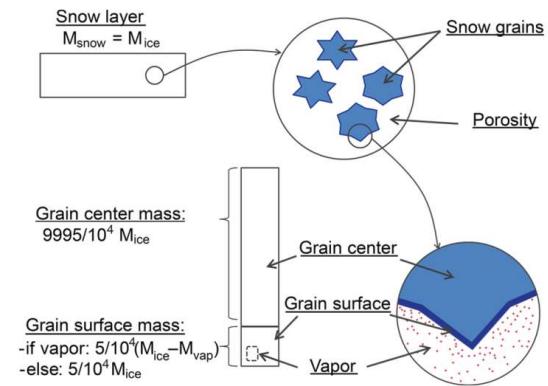
$$\delta^{18}O = -35.5 - 8 \times \sin\left(\frac{2\pi \times z}{a \times \rho_{ice}/\rho_{sn}}\right) \quad (18)$$

****The Dome C snowpack has an initial sinusoidal profile of $\delta^{18}O$ defined using Eq. [\(20\)](#):

$$\delta^{18}O = -48.5 - 6.5 \times \sin\left(\frac{2\pi \times z}{a \times \rho_{ice}/\rho_{sn}}\right) \quad (20)$$

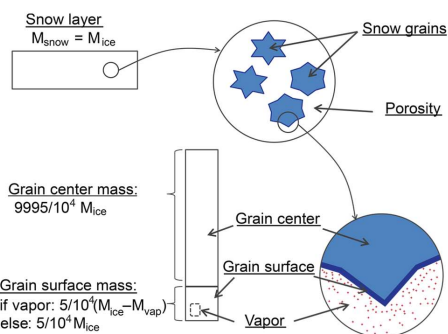
~~[Refer to Table 1 for a list of symbols.](#)~~

1299
1300



(21)

1301



1302

1303

1304

1305

1306

Figure 1. Splitting of the snow layer into two compartments, grain center and grain surface, with a constant mass ratio between them. The vapor compartment is a sub-compartment inside the grain surface compartment, and is only defined at specific steps of the model.

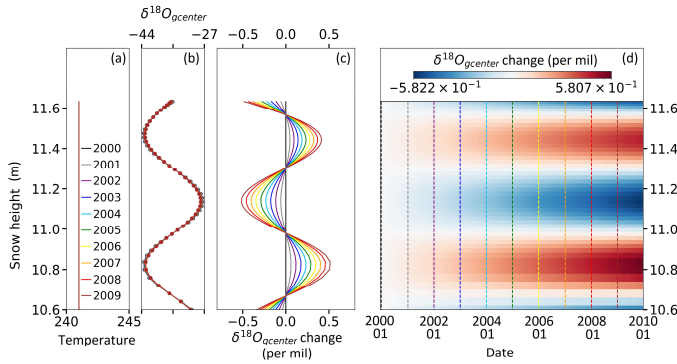
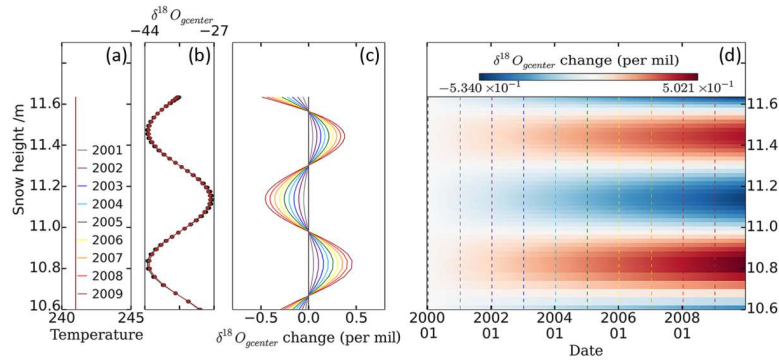


Figure 2. Simulation of the attenuation of the seasonal $\delta^{18}\text{O}_{\text{gcenter}}$ variation caused by diffusion against along isotopic gradients in vapor phase over 10 years (homogeneous and constant temperature of 241 K, original signal with mean value of -35.5 ‰ and amplitude of 16 ‰). (a) Vertical homogeneous temperature profile; (b) $\delta^{18}\text{O}$ profile at the beginning and end of the simulation; (c) Deviation of the $\delta^{18}\text{O}$ relative to the original profile, for 10 dates; (d) Evolution of the deviation to the original profile of $\delta^{18}\text{O}$.

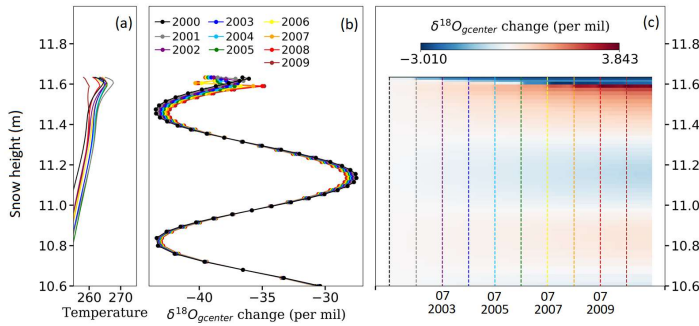
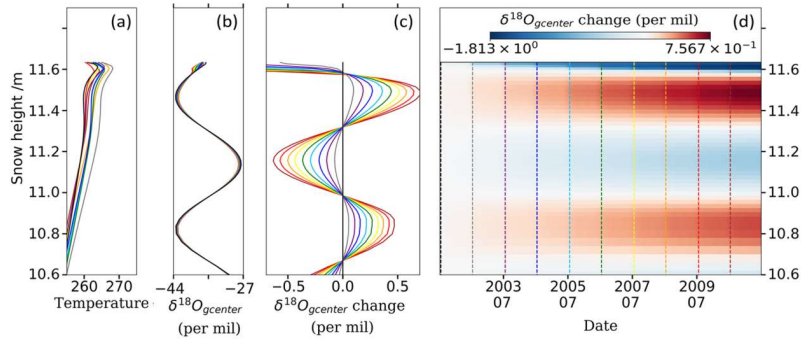


Figure 3. Simulation of the attenuation2: Attenuation of the seasonal $\delta^{18}\text{O}_{\text{gcenter}}$ variation caused by diffusion in vapor phase over 10 years (with temperature evolution, original signal with mean value of -35.5‰ and amplitude of 16‰). (a) Vertical temperature profile for each summer; (b) $\delta^{18}\text{O}_{\text{gcenter}}$ profile for each summer; (c) Deviation of the $\delta^{18}\text{O}_{\text{gcenter}}$ relative to the original profile, for each summer; (d) Evolution of the deviation to the original profile of $\delta^{18}\text{O}_{\text{gcenter}}$. Note that temperature evolves during the whole year (see Fig. S1).

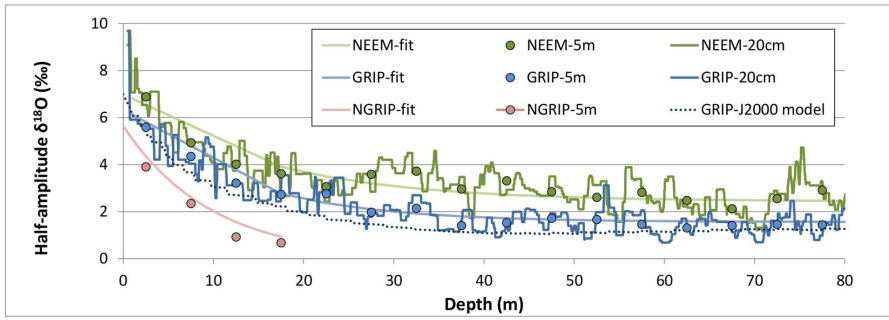
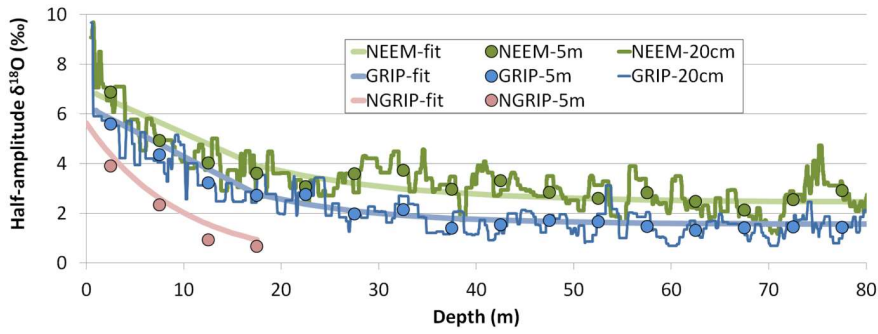
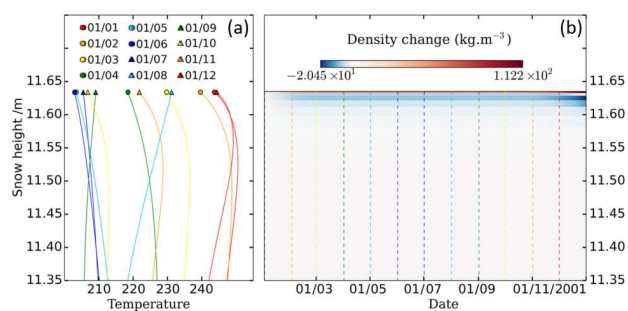


Figure 4. Evolution of the $\delta^{18}\text{O}$ half-amplitude with depth in shallow cores at NEEM, GRIP and NGRIP (Steen-Larsen et al., 2011 and Masson-Delmotte et al., 2015; White et al., 1997; Johnsen et al., 2000). The attenuation of the half-amplitude values with depth was fitted using an exponential equation (Eq. 24)-(22)):

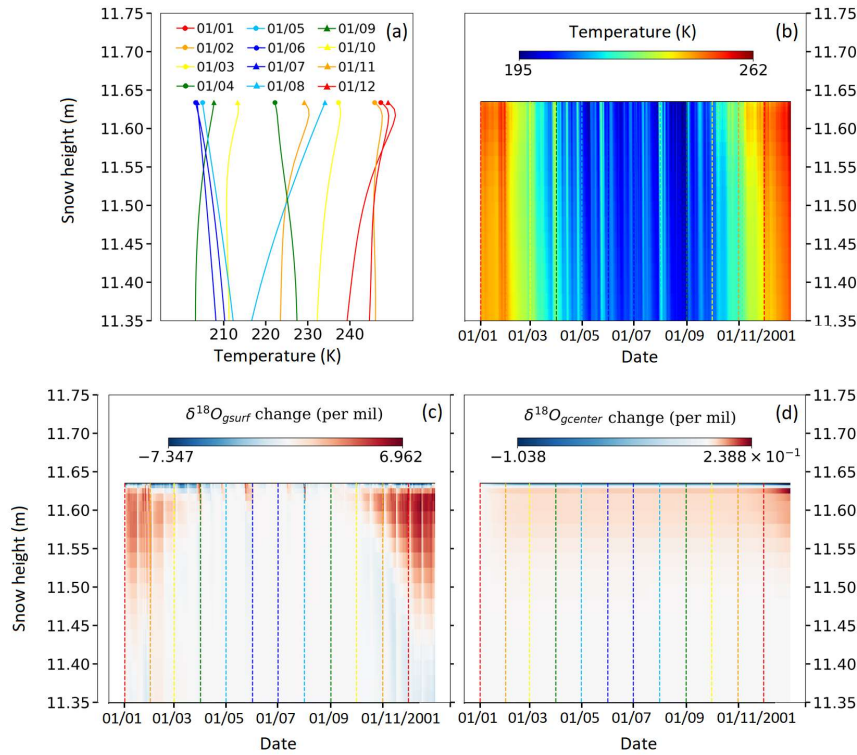
$$A = A_0 \cdot \exp(-\gamma \cdot z) - b \quad (2422)$$

With $A_0=4.976 \text{ ‰}$; $\gamma=0.08094$; $b=-1.56 \text{ ‰}$ at GRIP, and $A_0=4.685 \text{ ‰}$; $\gamma=0.06622$; $b=-2.44 \text{ ‰}$ at NEEM.



The dotted curve corresponds to the simulated attenuation at GRIP based on the Johnsen et al.'s model (diffusion length σ from their Figure 2, and wavelength λ fitted on the Eurocore core from GRIP, White et al., 1997).

1337
1338



1339
1340 Figure 5. Change in snow density caused by vapor transfer over one year (cumulative). (a) Temperature profile on
1341 the first day of each month, around 8 pm. The 1st of August corresponds to a short term warm event within winter.
1342 (b) Evolution of the snow densities. During summer, the first layer is gaining water whereas the layers immediately
1343 below (11.58 to 11.63 m) are losing water. Thus the vapor departure region is not exactly at the top of the
1344 snowpack in this simulation. Further down, layers are once again gaining water. During winter, temperature
1345 gradients are generally reversed, but the amount of vapor is too small to visibly affect the layer densities (for
1346 instance, the warming of Aug., 1st leads to a density loss of only 0.2 kg/m³ in the first layer).
1347

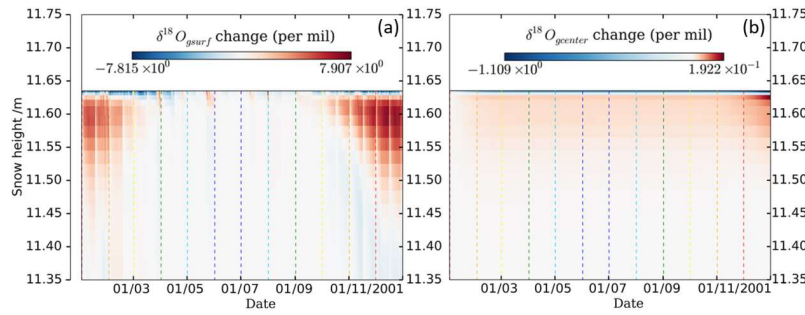


Figure 6. Evolution of temperature and $\delta^{18}\text{O}$ values from January to December 2001. (a) Temperature profiles for the first day of each month; (b) Temperature evolution in the snowpack; (c) ' $\delta^{18}\text{O}$ change' in the grain surface compartment; (d) ' $\delta^{18}\text{O}$ change' in the grain center compartment. Here, ' $\delta^{18}\text{O}$ change' stands for the difference between $\delta^{18}\text{O}$ at t and at the beginning of the simulation for the selected layer.

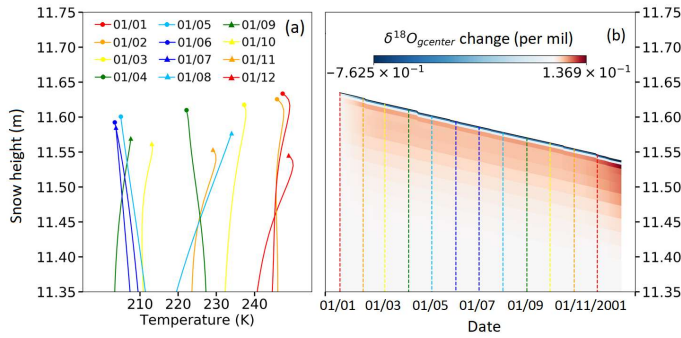


Figure 6. Change of $\delta^{18}\text{O}$ values caused by vapor transfer from January to December 2000. (a) grain surface; (b) grain center. For both grain compartments: $\delta^{18}\text{O}$ values change as a result of vapor transport and therefore maximum change occurs during summer. The first layer that receives water has $\delta^{18}\text{O}$ values that decrease during summer, whereas $\delta^{18}\text{O}$ values increase in the layers immediately below (zone of water export). Further down (around 11.35 m) the $\delta^{18}\text{O}$ values decrease (arrival of ^{18}O -depleted vapor). During the winter, short-lived warm events (like the one on the 1st of August) lead to small changes in the $\delta^{18}\text{O}$ values (the first layer $\delta^{18}\text{O}$ increases). This is more visible for grain surface than for grain center.

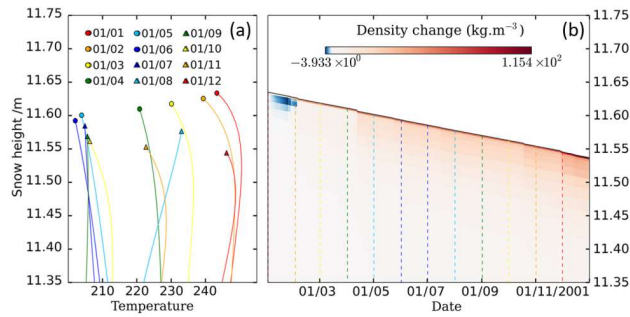


Figure 7. Evolution of the snow density over one year in a case with homogeneous compaction and wind drift, but without precipitation. The density change is taken as the difference relative to the first day for each layer (layer 1 is compared to layer 1, layer 5 to layer 5 etc...), even if they are not at the same height; thus density change may be overestimated compared to "horizontal" density change).

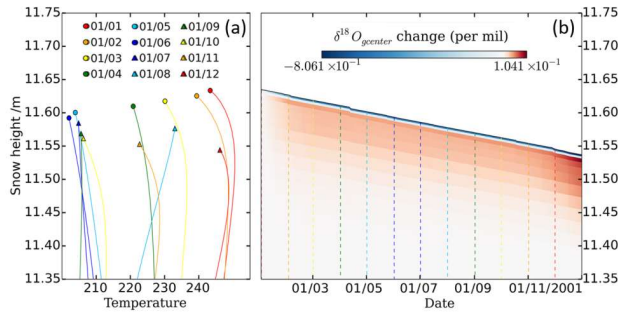


Figure 8. Simulation 4: Cumulative change in $\delta^{18}O_{gcenter}$ values (vapor transport, compaction and wind drift active).

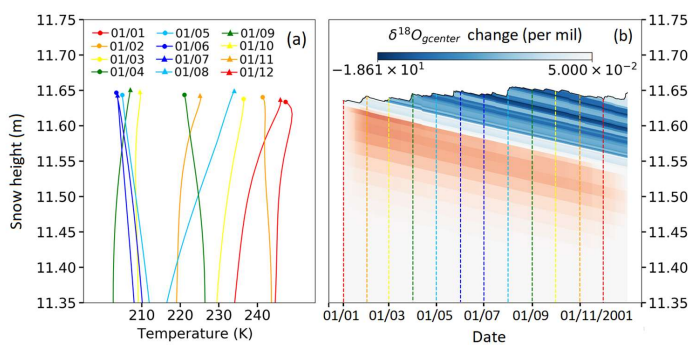
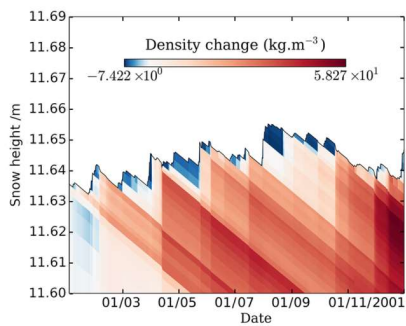


Figure 7. Snow density change (relative to original density profile at t_0) over one year: precipitation (snowfall) active, compaction (wind and weight) active, vapor transfer active.

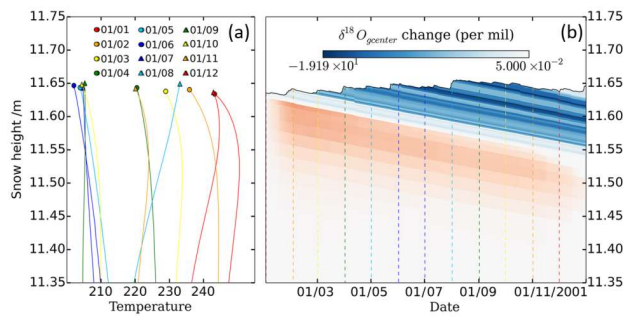


Figure 10- Simulation 5: Cumulative change of $\delta^{18}\text{O}$ values at the grain center (relative to t_0) over 6 months. Simulation with snowfall with varying $\delta^{18}\text{O}$ (function of T_{air}), vapor transport active, wind and weight compaction active.

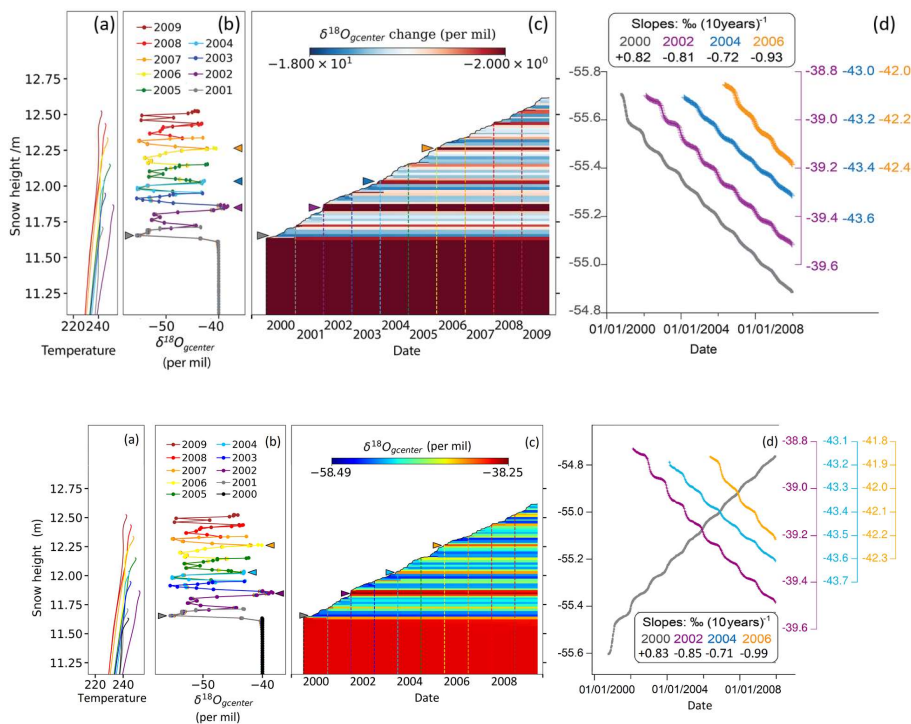
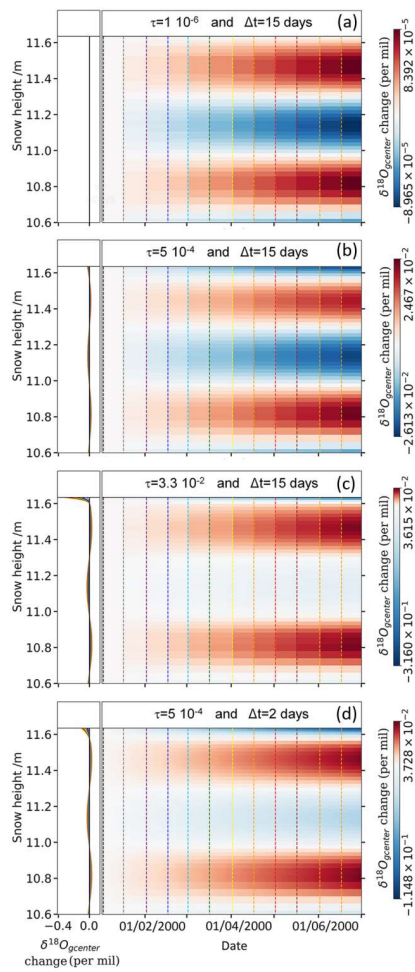


Figure 8. Simulation 6: Evolution of $\delta^{18}\text{O}_{\text{gcenter}}$ values as a result of snowfall and vapor transport over 10 years (compaction is inactive; merging between layers is allowed but limited). (a) Temperature profiles at mid-January for each year. (b) $\delta^{18}\text{O}_{\text{gcenter}}$ profile at mid-January for each year. (c) Repartition of $\delta^{18}\text{O}_{\text{gcenter}}$ values (expressed relative to -40‰) as a function of time and depth. (d) Evolution of $\delta^{18}\text{O}_{\text{gcenter}}$ values after burial for 4 selected layers (deposited in winter 2000, and summer 2002, 2004, 2006). Note that we do not present the evolution of snow composition in the first year after deposition because the thin snow layers resulting from precipitation are getting merged.



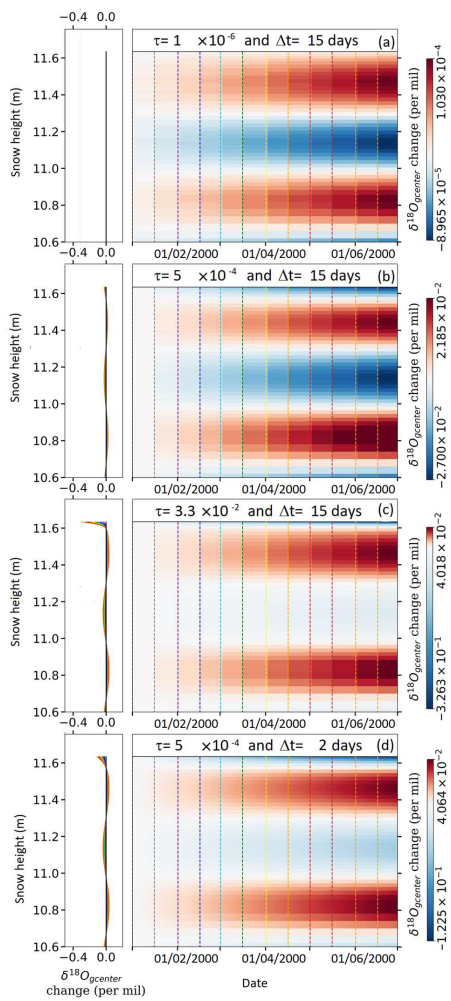
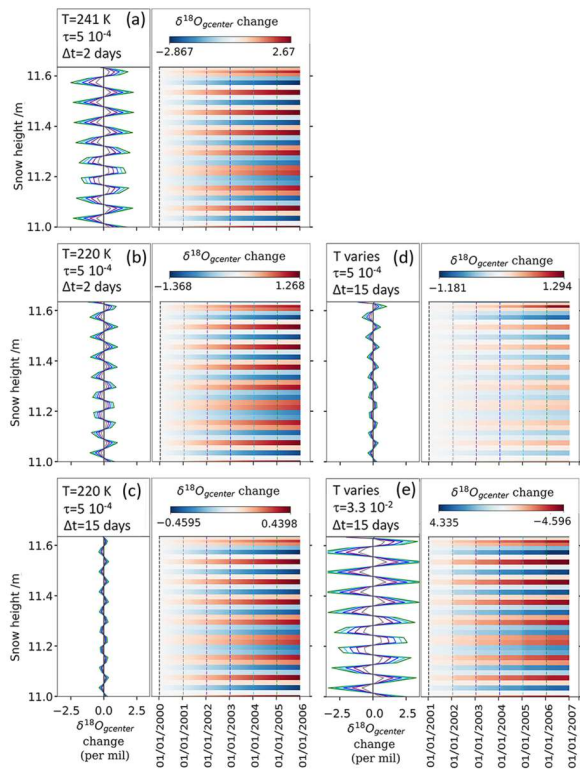


Figure 9. Test of the sensitivity of the model to the ratio of mass between grain surface and grain-center compartments and total grain and to the interval of mixing between the two compartments (GRIP).



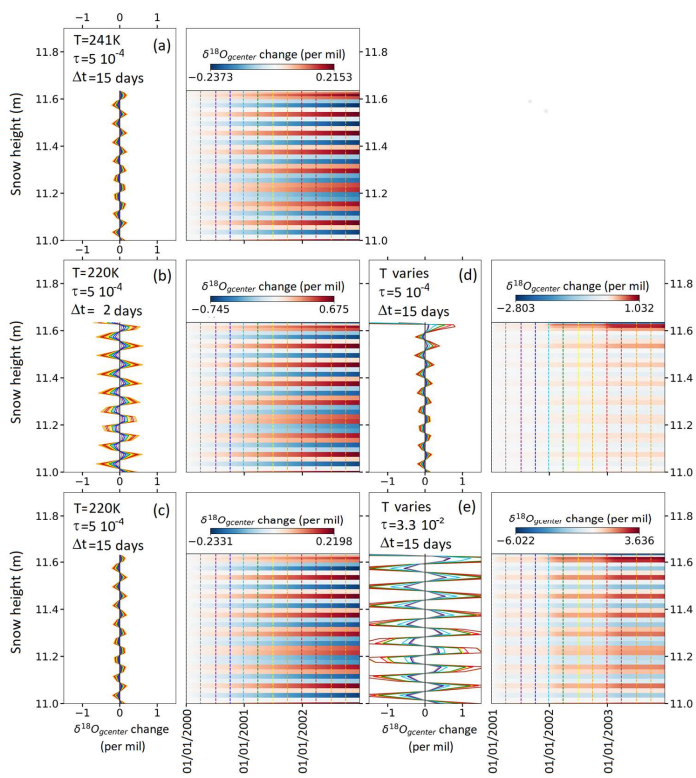


Figure 10. Test of the sensitivity of the model to the ratio of mass between surface and grain center compartments and to the interval of mixing between the two compartments (Dome C).